Estimating Subsidence Induced by Groundwater Abstraction in A Tropical Coastal Alluvium Aquifer

Idham Effendi

A thesis submitted in partial fulfilment of the requirements for the degree of Doctor of Philosophy

The University of Sheffield
Faculty of Engineering
School of Mechanical, Aerospace and Civil Engineering

March 2025

ACKNOWLEDGEMENTS

Alhamdulillah, praise be to Allah, The All-Knowing and The All-Powerful, for granting me the opportunity to explore the remarkable world of science. None of my achievements would have been possible without His Will, Guidance, and Permission.

I would like to express my sincere appreciation to several exceptional individuals and organizations whose knowledge, time, and support have been instrumental in completing this thesis. Foremost among them is my first supervisor, Dr Domenico Bau, whose expertise and continuous guidance have been invaluable throughout this research. I am equally grateful to my second supervisor, Professor Steve Thornton, for his insightful feedback and unwavering support.

I would also like to extend my gratitude to the Centre for Groundwater and Environmental Geology, Ministry of Energy and Mineral Resources, for providing the opportunity to conduct this study, as well as to LPDP for the financial support that made this research possible.

A special thank you goes to my exceptional team: Husna and Ryan for their outstanding data processing skills; Nofi, Acep, Akbar, Joko, Rubedo, Rakim, Febri, Rudi, and Prapto for their dedication and hard work in the field; Firdaus and Afid for their valuable assistance with the *SWAT* analysis; and Argo for his expertise in land use and *InSAR* analysis. Each of you has played an essential role in bringing this work to fruition, and I am deeply grateful.

I am also thankful to my Indonesian friends in Sheffield, especially the Bapak-Bapak Broomhall crew, for making this place feel like home and providing endless laughter and unforgettable memories.

Finally, to my beloved wife, Juliafara Feisal, and our son, Kumara Faiq Musthofa—your unwavering love, support, and patience have been my greatest source of strength. This thesis would not have been possible without you both.

Idham Effendi

Abstract

The coastal areas of Indonesia, especially along the northern coast of Java, are experiencing increasing land subsidence as a result of excessive groundwater abstraction, driven by population growth and economic development. Groundwater extraction from coastal aquifers has been associated with soil compaction, leading to subsidence and worsening flood risks due to rising sea levels. Pekalongan, a rapidly growing urban area, highlights these issues, with groundwater levels reportedly falling below safe limits. This study investigates the relationship between groundwater withdrawal and land subsidence, aiming to inform sustainable water management practices and mitigation strategies.

The research combines MODFLOW-2005, three-dimensional groundwater flow model with Subsidence (SUB) package to simulate groundwater dynamic and subsidence in the study area. Findings indicate that groundwater abstraction significantly contributes to land subsidence, with compaction concentrated in clay-rich areas at certain depths. Additionally, the study highlights the compounded effects of land use change and climate change on groundwater recharge, although these factors did not show a significant impact on subsidence within the study area.

Model projections suggest that, in the absence of intervention, subsidence will continue, further exacerbating flood risks. To mitigate these risks, the study proposes a comprehensive strategy focused on controlling groundwater abstraction, transitioning toward increased reliance on surface water, and implementing regional policies tailored to the unique characteristics of local aquifers. Furthermore, the research emphasizes the importance of integrated approaches that combine numerical modelling and remote sensing techniques to enhance the management of coastal aquifers and protect vulnerable regions from the adverse impacts of subsidence.

Keywords: groundwater, abstraction, land subsidence, climate change, coastal

Table of Contents

List of Tables

List of Figures

DECLARATION

I, the author, confirm that the Thesis is my own work. I am aware of the University's Guidance on the Use of Unfair Means (www.sheffield.ac.uk/ssid/unfair-means). This work has not previously been presented for an award at this, or any other, university.

Abbreviations

AMSL	: Above mean sea level
ASTM	: American Society for Testing and Materials
BMKG	: Badan Meteorologi, Klimatologi dan Geofisika
BPS	: Badan Pusat Statistik
DEM	: Digital Elevation Model
GIS	: Geographic Information System
GPS	: Global Positioning System
HRU	: Hydrologic Response Unit
IDW	: Inverse Distance Weighting
InSAR	: Interferometric Synthetic Aperture Radar
LPF	: Layer Property Flow
PDAM	: Perusahaan Daerah Air Minum
PEST	: Parameter Estimation
PGB	: Pekalongan Groundwater Basin
QGIS	: Quantum Geographic Information System
RMSE	: Root Mean Square Error
SAR	: Synthetic Aperture Radar
SBAS	: Small Baseline Subset
SIMS	: System for Integrated Monitoring of Subsidence
SRTM	: Shuttle Radar Topography Mission
SUB	: Subsidence Package
SWAT	: Soil and Water Assessment Tool

CHAPTER 1
General Introduction

1.1 Background of the study

Groundwater has historically served as a reliable source of freshwater, underpinning domestic, commercial, agricultural, industrial, and ecological needs. Demand for groundwater is increasing rapidly; in some countries, its abstraction has reached critical levels due to rising industrial demands, population growth, and the effects of climate change (Velis et al., 2017). Globally, groundwater supplies at least 50% of potable water, 40% of industrial water demands, and 30% of irrigated agricultural needs (Foster, 2006). In Indonesia, groundwater remains the primary source of household water, meeting over 65% of this demand (BPS, 2020). While precise statistical data regarding industrial and agricultural water use is limited, estimates indicate that groundwater accounts for at least 50% of the country's overall water needs.

As a vast archipelagic country composed predominantly of small islands, Indonesia hosts diverse coastal ecosystems alongside critical economic infrastructure. Notably, it also boasts the second-longest coastline in the world (Carpenter, 1998). The country's coastal regions have experienced rapid population growth and development, with nearly 39.3 million people residing in these areas, approximately 19% of the national population (Neumann et al., 2015). This is particularly evident along the northern coast of Java, home to many of Indonesia's major cities, including Jakarta, the nation's capital, as well as Surabaya and Semarang, the provincial capitals of East Java and Central Java, respectively. As illustrated in Figure 1.1, Java exhibits the highest population density compared to other Indonesian islands. A more detailed examination further reveals that the highest population concentration on the island is located along its northern coastline.

This demographic concentration has significantly increased the demand for essential resources, particularly freshwater, to support various societal activities

such as agriculture, industry, and domestic needs. Coastal regions are inherently rich in groundwater resources, given that most coastal aquifers, composed of young, unconsolidated deposits, serve as critical water sources, providing fresh water to over two billion people globally (Ferguson & Gleeson, 2012). However, in Indonesia's coastal cities, the heavy reliance on groundwater is becoming increasingly problematic due to the fragile nature of coastal ecosystems, posing threats to the quality of these water resources. Coastal zones are particularly vulnerable to sea level rise, a challenge further aggravated by global climate change and human activities (Balica et al., 2012).

Figure 1.1 Map of Indonesia showing the population density

One of the primary challenges posed by intensive groundwater extraction is land subsidence—a gradual sinking of the ground surface caused by the compaction of aquifer materials as groundwater is pumped out. This phenomenon, exacerbated by factors such as sea level rise and climate change, has significant impacts on several coastal regions in Indonesia. A clear manifestation of the effects of land subsidence in these areas is the increasing extent of inundation during flooding events, whether due to heavy rainfall or tidal flooding (known as *rob*). Excessive groundwater abstraction has significant consequences, including the compaction of vulnerable aquifers, directly contributing to land subsidence (Guzy & Malinowska, 2020). Among the various natural and anthropogenic factors, groundwater abstraction-induced subsidence is one of the most well-documented and understood (Galloway & Burbey, 2011). Land subsidence is arguably the most prevalent and hazardous geomechanically impact of groundwater abstraction (Gambolati & Teatini, 2021). In Indonesia, subsidence linked to groundwater withdrawal has been extensively documented in coastal aquifers, particularly along Java Island's northern coastline (Abidin et al., 2011; Beek et al., 2019; Marfai & King, 2007). The combined effects of land subsidence and rising sea levels exacerbate the vulnerability of coastal regions (Wang et al., 2012).

The relationship between groundwater abstraction and land subsidence is well understood from a theoretical perspective based on Terzaghi's soil consolidation theory. According to this theory, groundwater withdrawal causes the reduction of soil porosity, resulting in a reduction in soil volume and a subsequent lowering of the ground surface. An important insight from this theory is the necessity for sustainable groundwater management in areas susceptible to land subsidence. In regions such as Pekalongan, with significant land subsidence and frequent flooding, the need to study and model the impacts of groundwater extraction in a more comprehensive manner is urgent. A detailed understanding of these mechanisms is essential for developing science-based recommendations that can protect coastal communities from future environmental and infrastructural challenges.

This study aims to contribute to this critical area of research by developing a detailed groundwater level subsidence model through numerical simulations, which will be compared with remote sensing data. Using the MODFLOW groundwater

modelling platform, this study assesses the impact of current and projected groundwater abstraction on subsidence rates. This approach will facilitate the examination of various adaptation and mitigation scenarios, such as optimized groundwater withdrawal, adjustments in land-use planning, and flood risk management strategies. This study will provide actionable insights for local policymakers, water resource managers, and stakeholders to make informed decisions regarding sustainable groundwater use by simulating different scenarios.

1.2 Problem statements

The rapid and unregulated extraction of groundwater in urban areas, particularly in Pekalongan, has led to significant land subsidence, which poses a serious threat to the environmental stability, infrastructure, and socio-economic conditions of the region. Excessive groundwater abstraction is widely acknowledged as a primary driver of land subsidence on the north coast of Java Island, as observed in urban centres such as Jakarta (Abidin et al., 2011; Andreas et al., 2018; Lubis & Delinom, 2010) and Semarang (Andreas et al., 2019; Marfai & King, 2007; Sarah et al., 2011). This subsidence phenomenon exacerbates flood risks, accelerates soil degradation, and causes damage to buildings and other structures.

The selection of Pekalongan as the research location is driven by several factors. Pekalongan is a rapidly developing coastal city characterized by high urbanization and a growing industrial sector. The city also heavily relies on groundwater, making it increasingly vulnerable to the adverse effects of groundwater extraction. These factors make Pekalongan an ideal location for studying the impacts of groundwater extraction on groundwater level subsidence. The findings of this study could have broad implications for sustainable water management practices in similar coastal urban areas.

In 2019 alone, tidal flooding affected 1,057 hectares in Pekalongan, representing 23.36% of the city's total area. In June 2020, tidal floods inundated 11 villages across four sub-districts, including some previously unaffected areas (Lutfitiana et al., 2022). The extent of water inundation is illustrated in Figure 1.2, which shows a photo taken during data collection in November 2021 Through InSAR analysis using ALOS SAR images from 2007 to 2009, Chaussuard (2013) reported an average land

subsidence rate of 3 cm per year in Pekalongan and its surrounding areas, suggesting that groundwater abstraction for agricultural needs is a likely contributor to this phenomenon. Andreas (2017)) further projects that, with an annual subsidence rate of 3 cm and rising sea levels, the extent of tidal flooding in Pekalongan will continue to expand, posing a growing threat to local communities. Despite these growing concerns, limited research has been conducted to understand the long-term impacts of groundwater extraction on subsidence in Pekalongan, a coastal city heavily reliant on groundwater for industrial, agricultural, and domestic use.

Figure 1.2 Photos showing water inundation in Pekalongan
(taken during fieldwork on October - November 2021)

A long-term study of land subsidence is essential for accurately assessing the extent and progression of subsidence over time. In regions like Pekalongan, where subsidence is exacerbated by ongoing groundwater extraction, short-term studies often fail to capture the cumulative effects of years of groundwater depletion. These studies do not provide sufficient data to inform sustainable management practices or to predict future trends accurately. A long-term perspective, on the other hand, will allow for a more comprehensive understanding of subsidence dynamics and

provide valuable insights to inform effective mitigation strategies aimed at reducing subsidence and its associated risks.

Long-term studies on land subsidence are essential for accurately assessing its progression over time, as subsidence is a gradual process that often becomes evident only after an extended period (S. Ahmed et al., 2024). Due to its slow nature, the effects of subsidence may not be immediately observable, yet they can have profound implications once they accumulate over time. Precise measurements are critical, as subsidence rates typically range from only a few centimetres to millimetres per year. A comprehensive investigation is also necessary to identify the primary drivers of subsidence, facilitating the development of targeted mitigation strategies to slow or prevent further subsidence.

Moreover, continuous long-term monitoring enables the development of predictive models that can project future subsidence trends under various scenarios. By integrating historical subsidence data with records of groundwater extraction, climate patterns, and land use changes, these models can help anticipate future risks and inform proactive decision-making. Such predictive tools are invaluable for researchers and policymakers in designing resilient infrastructure, regulating groundwater use effectively, and implementing early warning systems to mitigate subsidence-related damage (Yang et al., 2024). Therefore, sustained investment in long-term research and monitoring is crucial to ensuring the sustainability and stability of affected regions, ultimately reducing the long-term social and economic consequences of land subsidence.

Testing the effectiveness of mitigation processes also takes considerable time. Tokyo's efforts to address land subsidence and declining groundwater levels have been ongoing since 1970, when the city reduced groundwater pumping by approximately 75% (Sato et al., 2006). By 2006, it was recorded that groundwater levels had risen to -6 meters below the ground surface, compared to -58 meters in 1970, showing a rebound of approximately 52 meters over 26 years. In terms of subsidence, the rate of subsidence was 24 cm per year in 1970 but significantly slowed to less than 1 cm per year between 2001 and 2006. This is an example of a long-term study conducted to understand and address the issue of subsidence.

To support this research, several available datasets have been integrated. These include the report *"Groundwater Conservation in Pekalongan Groundwater Basin"* published by the Regional Government of Central Java, which outlines areas designated for groundwater conservation and provides insights into the spatial distribution of groundwater abstraction. Additionally, various investigation reports containing lithological data with varying levels of precision for the study area are readily available. These reports are part of routine activities conducted by the Center for Groundwater and Environmental Geology, the Geological Agency, and the local government of Central Java Province. Remote sensing data, such as high-resolution satellite imagery, provides valuable information on land elevation changes and surface displacement, while meteorological and climate data, including historical rainfall and temperature trends, offer context for understanding the influence of climate on subsidence.

For this study, specific datasets have been collected to further enhance the analysis. These datasets primarily include aquifer parameter data derived from pumping tests and groundwater level measurements in observation wells, which serve as the basis for calibrating the transient model. A detailed explanation of the fieldwork and the datasets obtained is provided in the chapter *"General Methodology."* By integrating these diverse datasets, this study aims to develop a comprehensive understanding of the relationship between groundwater abstraction and land subsidence, ultimately contributing to more sustainable groundwater management practices and subsidence mitigation strategies in the study area.

1.3 Aim and objectives

The aim of this study is to evaluate the impact of groundwater withdrawal on land subsidence by integrating results from a numerical model with remote sensing data. This approach is tailored to support both scientific research and management strategies within the study area.

To address the research questions, the study has the following specific objectives:

1. To apply remote sensing techniques to accurately quantify land subsidence in the study area.

2. To develop and refine a integrated groundwater flow and subsidence model for the study area, ensuring it incorporates up-to-date and relevant data.
3. To use the model to assess various adaptation scenarios, particularly in response to projected changes in land use and climate and the growth of groundwater withdrawal.
4. To identify and evaluate mitigation strategies by simulating increased groundwater withdrawal, aiming to manage abstraction rates without exacerbating land subsidence.

1.4 Thesis structure

This thesis is organized as follows:

- *Chapter 1: General Introduction*

  This chapter provides a comprehensive overview of the primary background of the study, focusing on the impact of groundwater extraction on land subsidence in tropical coastal aquifers. It outlines the objectives, significance, and research questions that underpin the investigation.

- *Chapter 2: Literature Review*

  The literature review explores various previous studies on the mechanisms of land subsidence, measurement methods, and numerical modelling approaches. It specifically highlights the importance of lithological references as a foundation for groundwater-related research. This chapter also discusses how land subsidence predictions are influenced by scenarios involving increased groundwater abstraction, climate change, and land-use alterations.

- *Chapter 3: General Methodology*

  This chapter explains the methodologies employed, including data acquisition, processing, and the development of integrated groundwater flow and land subsidence models using MODFLOW and the Subsidence (SUB) package. It also addresses effective calibration techniques to ensure accurate outputs. Additionally, general information about the study area is introduced.

- *Chapter 4: Lithological Modelling and Aquifer Parameter Estimation*

  This chapter focuses on developing a geological model and estimating aquifer parameters such as hydraulic conductivity and compressibility. It underscores the role of lithology in land subsidence modelling and hydrogeological interpretation.

- *Chapter 5: Implementation of 3-D Groundwater Flow Modelling*

  This chapter details the development and application of the MODFLOW-2005 groundwater model for Pekalongan. It discusses conceptual modelling, grid design, and transient modelling results, including calibration and sensitivity analyses.

- *Chapter 6: Land Subsidence Analysis and Future Projections*

  This chapter examines the impacts of groundwater extraction, land use, and climate change on land subsidence rates, utilizing the SUB package in MODFLOW along with remote sensing data (InSAR) and subsidence measurements from GPS. Future scenarios are projected in this chapter, with the primary aim of evaluating subsidence risks and formulating mitigation strategies.

- *Chapter 7: Conclusion*

  The final chapter summarizes the research findings, discusses their implications for sustainable groundwater management, and reflects on the strengths and limitations of the study. It provides recommendations for policymakers and outlines directions for future research.

CHAPTER 2
Literature Review

2.1 Introduction

Land subsidence refers to the downward movement of the Earth's surface, usually caused by insufficient support from beneath, an increase in surface weight, or a combination of both factors (Marker, 2013). Recognized as a damaging phenomenon and classified as a natural hazard, land subsidence has been the subject of extensive research and study. Researchers have continually advanced methods to both measure subsidence rates and analyse the underlying processes and causes, with the ultimate goal of developing effective mitigation strategies to slow or prevent further subsidence.

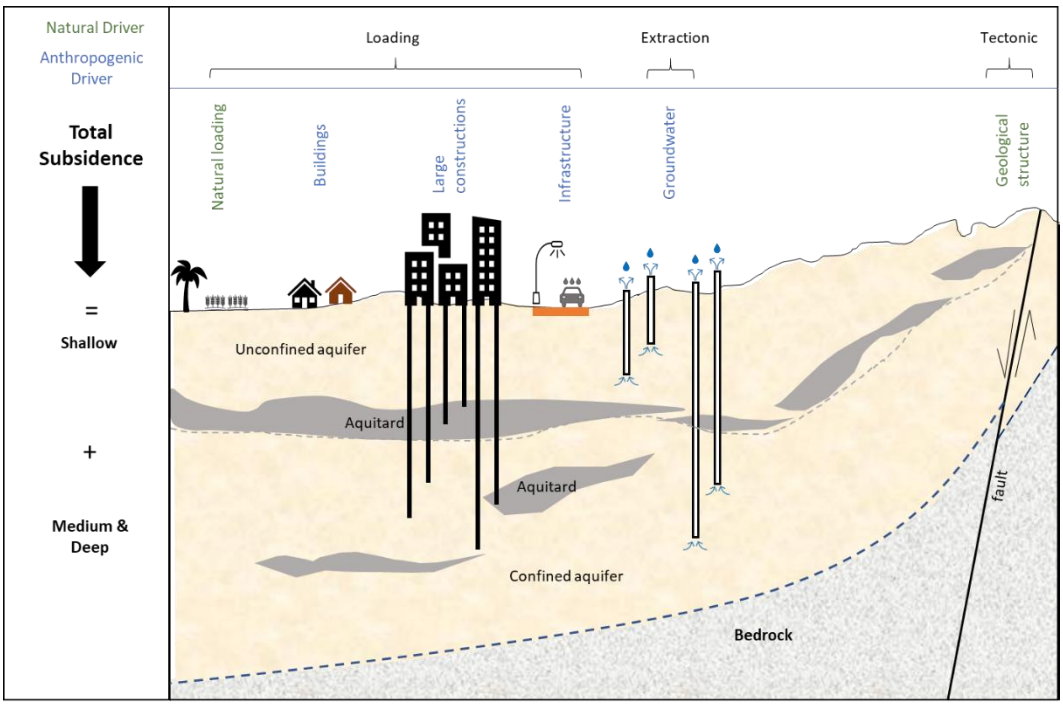

Figure 2.1 Schematic overview of subsidence driver in lowland coastal area (modified from Minderhoud, 2015)

2.2 Processes governing land subsidence

Numerous studies have explored the factors responsible for land subsidence in various cities worldwide, whether due to natural or human-induced processes. The human-induced subsidence can be caused by several factors such as extraction of

hydrocarbons (Chan et al., 2017), taking groundwater for drinking purposes (Chaussard et al., 2013) and lowering of groundwater due to massive construction activities (Wang et al., 2018). On the other hand, natural subsidence can be attributed to processes such as oxidation of peat (Pronger et al., 2014), compaction of soft clay soil (Zhang & Zhang, 2014), natural consolidation of Holocene deposits (Kooi, 2000),and geological activities such as faults (Brunori et al., 2015). A diagram illustrating the causes of subsidence can be found in Figure 2.1.

Many scientific papers have revealed that land subsidence in an area is usually caused by multiple factors. However, subsidence in many major cities is mainly associated with groundwater extraction. An illustration of the factors that can cause subsidence in the coastal area can be seen in Figure 2.1, which has been modified from Minderhoud's work (2015). He divided subsidence causes into shallow and medium-deep drivers and processes. The shallow group has several contributing factors, especially soil consolidation, while in the medium-deep group, the dominant factor is groundwater or fluids extraction causing consolidation.

2.2.1 Subsidence in coastal areas

Coastal cities are the most affected by land subsidence issues due to their similar geological and geographical conditions. These cities have plain morphology consisting of relatively young unconsolidated deposits and abundant groundwater aquifers. This makes them ideal for rapid development, but also means that they rely heavily on groundwater, which exacerbates the issue (Ferguson & Gleeson, 2012). Due to the relatively flat groundwater gradient in coastal areas, the effects of overexploitation on the groundwater system are more pronounced (Cherubini et al., 2023).

Some of the major Southeast Asian coastal cities facing this problem are Jakarta (Abidin et al., 2011), Semarang (Yastika et al., 2019), Bangkok (Phien-wej et al., 2006), Manila (Eco et al., 2018), and Ho Chi Minh City (Thoang & Giao, 2015). Despite similar conditions, these cities experience varying degrees of subsidence, as shown in Table 2.1, according to data from The Sinking Cities which compiles various studies. In his paper, Rahmawan et al. (2016) stated that Demak, one of the small cities on the North Coast of Java, also experienced land subsidence at a speed of -83.76 mm/year.

This subsidence rate is a reasonably high value, considering that Demak is an undeveloped area with less population and less intensive groundwater use. Another study conducted by Sarah et al. (Sarah et al., 2020) stated that natural compaction in the Demak plain reaches 22 mm/year and contributes to land subsidence.

Table 2.1 Subsidence rate of some Asian cities

	Mean cumulative subsidence 1900-2013 (mm)	Mean current subsidence rate (mm/year)	Maximum subsidence rate (mm/year)
Bangkok	1250	20-30	120
Ho Chi Minh City	300	Up to 80	80
Jakarta	2000	75 – 100	179
Manila	1500	Up to 45	45
Tokyo	4250	Around 0	239

Teatini (2011) stated that land subsidence in the Po River Delta is mainly caused by the consolidation of young deposits. Meanwhile, Stanley & Clemente (2014) found that continued land subsidence in the low-elevation region of the North Nile Delta Plain is primarily due to high clay concentration in young sediment layers. According to Mordhorst et al. (2020), natural compaction or consolidation, which is characterised by a clay-enriched layer in young deposits, also significantly contributes to land subsidence in coastal plain areas. This is despite intensive groundwater abstraction. The thickness and distribution of this layer vary in coastal plain areas with young alluvium deposits.

2.2.2 Impact of groundwater abstraction on subsidence

Galloway et al. (1999) stated that over 80% of subsidence in the United States is associated with groundwater abstraction. Various studies have been conducted on land subsidence, especially in large cities where there is intensive groundwater abstraction. This confirms that groundwater abstraction is a significant factor contributing to the land subsidence hazard in many cases. Furthermore, data suggests that groundwater extraction increases as the demand for water grows for various purposes.

A cone of depression indicates intensive groundwater withdrawal in these areas, and then in some cases, it will be characterised by subsidence in the surface, as

shown in Figure 2.2. According to Terzaghi (1975), land subsidence is a reduction in surface elevation due to loss of subsurface supports and the application of the principle of effective stress and the theory of hydrodynamic consolidation. Intensive groundwater abstraction in an area will cause the aquifer system's compaction due to the consolidation of aquitards in the aquifer system, shown as land subsidence on Earth's surface. While aquifers themselves undergo minimal deformation due to their greater stiffness compared to aquitards, they still experience stress changes at least as significant as those occurring in the intervening aquitards. In aquifer systems comprising aquifers and aquitards usually found in young unconsolidated alluvial, aquifer-system compaction could induce significant land subsidence.

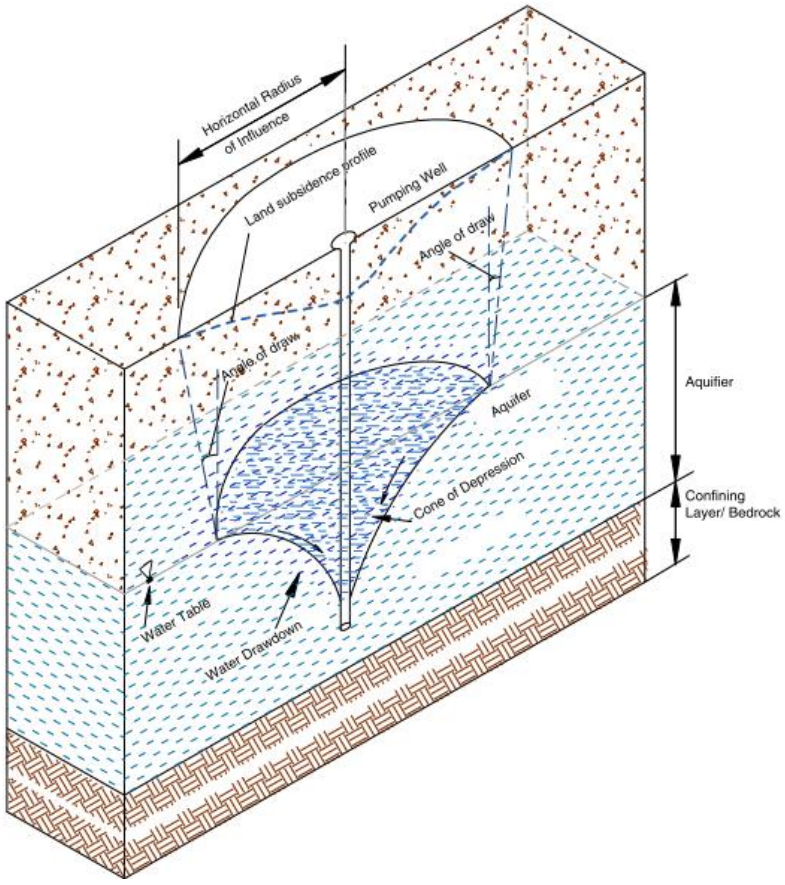

Figure 2.2 The relationship of groundwater cone depression and land subsidence in an aquifer system

2.3 Subsidence measurement and modelling

Researchers worldwide have developed various methods to calculate subsidence rates, primarily based on measuring changes in ground surface elevation. Each method possesses distinct advantages and limitations, often necessitating

combining approaches to obtain more comprehensive temporal and spatial information.

In his study, Teatini et al. (2005) employed a multi-method approach for monitoring and measurement in the city of Venice, known as SIMS (System for Integrated Monitoring of Subsidence). SIMS integrates SAR-based data with site-specific GPS and levelling measurements to produce precise maps of land subsidence and uplift. This system provided unparalleled spatial coverage and accuracy, revealing that while the central area of Venice remains stable, the northern and southern coastal regions are experiencing subsidence rates ranging from 5 to 15 mm/year. As a critical tool for continuous monitoring of land subsidence, SIMS supports authorities in effectively managing and forecasting future subsidence-related changes.

2.3.1 Direct measurement

Historically, the initial approaches to subsidence measurement relied on direct techniques involving the repeated surveying of geodetic benchmarks to assess elevation changes (Galloway & Burbey, 2011) This method quantified land subsidence through the re-surveying of benchmark markers anchored to stable reference points. However, direct subsidence measurement within aquifer systems is technically complex and spatially constrained (Erban et al., 2014). This approach tends to be costly and is typically feasible only at a limited number of specific locations. While traditional methods provide high accuracy, they are inherently point-based, requiring substantial effort and resources to scale up measurements. Additionally, these methods are impractical for capturing deformation across extensive regions.

Another direct measurement technique involves using extensometers, which monitor vertical compaction and expansion within specific depths of the aquifer system. An extensometer device is embedded to a borehole to continuously monitor changes in vertical distance between the ground surface and a "subsurface benchmark" or reference point.

More recently, Global Positioning System (GPS) technology has been employed to measure elevation changes to determine land subsidence in specific areas. GPS

technology is highly effective for positioning and mapping, providing reasonable accuracy (Zainal Abidin, 1999). It is designed to deliver three-dimensional positional and velocity data and continuous time information, making it suitable for applications requiring precise position data. For subsidence measurement, GPS observations must be conducted repeatedly at designated points, requiring approximately 10-12 hours of satellite observation. An illustration of the direct measurement of land subsidence can be found in Figure 2.3.

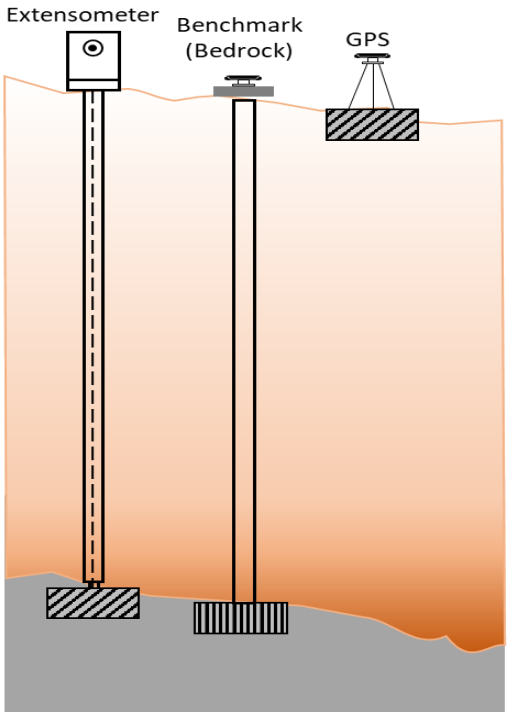

Figure 2.3 The illustration showing direct measurement of land subsidence

However, these land subsidence measurement methods share a common limitation: they capture data only at specific points, depending on the number of instruments deployed. Although increasing the number of instruments enhances the spatial coverage of measurements, generating comprehensive spatial data or land subsidence maps remains challenging without extensive equipment deployment. As shown in Figure 2.4, the frequency distribution of various land subsidence estimation methods applied to subsidence cases worldwide can be observed.

2.3.2 Remote sensing applications

The subsidence measurement using remote sensing has advanced significantly over the past decade. According to a review by Bagheri-Gavkosh et al., (2021), remote

sensing has become the most widely utilized method for subsidence measurement across 290 locations since the 1980s, surpassing traditional land surveys using theodolites or geodetic methods that dominated until the 1990s.

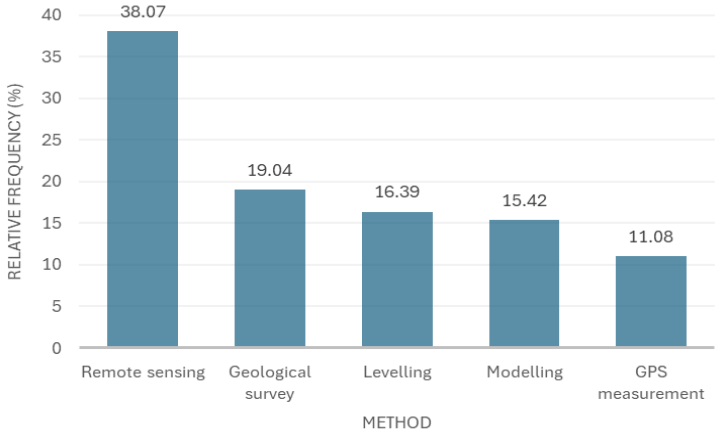

Figure 2.4 Method frequency applied to estimate subsidence rate

Remote sensing is the science and art of obtaining information about an object, area, or phenomenon by analyzing data collected by a device that does not make direct contact with the subject (Lillesand et al., 2004). This approach offers numerous advantages, rendering it a preferred method for measuring subsidence without necessitating costly and time-consuming field investigations. For instance, Castellazzi et al. (2016) utilized InSAR—one of the primary methods for measuring surface changes—for long-term subsidence monitoring in several Mexican cities. Synthetic Aperture Radar (SAR) is an active sensor capable of collecting measurements at any time of day or season.

As a robust technique, InSAR measures ground surface deformation by comparing radar signals obtained at different times (Sneed et al., 2003). InSAR can capture one component of surface displacement with spatial resolutions ranging from meters to tens of meters and precision in the millimeter to centimeter range over extensive areas, potentially covering thousands of square kilometers. The technology offers significant advantages, including large-scale coverage, low cost, and high precision, effectively addressing many limitations associated with traditional measurement methods (Rongrong et al., 2020)

However, using InSAR and direct measurement methods in subsidence measurement often raises questions about the underlying causes of land

subsidence. Researchers typically correlate spatial data to infer possible contributing factors. For example, Du et al., (2018) correlated InSAR subsidence data with land use, finding that high subsidence rates in Bandung, Indonesia, were associated with residential, industrial, and agricultural activities. However, this study did not analyze why these areas experienced higher subsidence rates than regions with different land uses. This limitation has prompted the development of subsidence models that integrate various modules, particularly those related to groundwater extraction.

2.3.3 Groundwater flow and subsidence modelling

An effective approach to determining subsidence rates is through numerical modelling, which simulates land subsidence dynamics by accounting for a range of influencing factors. The first mathematical model addressing subsidence was introduced in 1974 by Gambolati in a study focused on Venice, Italy, laying a foundational precedent for the integration of field data into hydrogeological modelling efforts (Gambolati et al., 1974). Since then, the development of subsidence models has advanced significantly, drawing on extensive field investigations to refine and enhance predictive accuracy.

2.3.3.1 Subsidence package

A variety of studies have applied numerical modelling in subsidence research, with MODFLOW recognized globally as the standard for three-dimensional, finite-difference groundwater flow modelling (McDonald & Harbaugh, 1988). MODFLOW's modular structure supports a suite of extensions, including the Subsidence and Aquifer-System Compaction Package (SUB), which has become integral in analysing subsidence due to groundwater extraction (Hoffmann et al., 2003). The SUB package is especially relevant for cases requiring close coupling of groundwater flow and land subsidence simulations, as demonstrated by its use in research worldwide.

For instance, Deng et al. (2018) applied the SUB package in MODFLOW-2005 to examine the impacts of groundwater withdrawal for drinking water on land subsidence in Tianjin, China. Their work highlighted the application of modelling to estimate subsidence under varied extraction scenarios, providing critical insights

for developing policies on groundwater usage based on model forecasts. Similarly, Zangeneh et al. (Zangeneh et al., 2023) utilized the MODFLOW model with the SUB package to simulate both aquifer dynamics and subsidence rates in Iran's Varamin Plain. By integrating these results with other regulatory criteria, the study contributed valuable data for policy initiatives targeting both groundwater sustainability and subsidence mitigation.

Another significant application is seen in the work of Jafari et al. (Jafari et al., 2016), who employed a integrated groundwater flow and subsidence model in the Saveh Basin, Iran. Their simulations indicated that without regulatory controls, subsidence could intensify to rates exceeding 70 cm annually, particularly in clay-rich areas. Luo (Luo et al., 2016) similarly evaluated groundwater and subsidence coupling models in loose sedimentary regions, observing that the accuracy of the model depended heavily on parameter completeness—highlighting the challenges in modelling diverse hydrogeological conditions.

The SUB package in MODFLOW offers unique capabilities for simulating the complex interplay of drainage, groundwater storage changes, and aquifer compaction (Deng et al., 2018). By simulating the compaction of aquifers, interbeds, and confining units, the SUB package can account for time-dependent factors such as delayed aquifer-system compaction and storage release from interbeds. However, the package requires accurate field data inputs, which are often challenging to acquire due to cost constraints and logistical limitations. As a result, model calibration remains essential, allowing for the adjustment of model outputs to align closely with limited observational data on groundwater levels and subsidence trends.

2.3.3.2 The importance of lithology for aquifer characteristics.

Grasping the geological conditions of a locality is vital, especially regarding the lithological variations shaped by geological history and depositional environments. Knowledge of local geology, especially lithology, is essential for any subsurface modelling application (Brandenburg, 2020). Lithology refers to the physical characteristics and composition of sediments or rocks, encompassing properties such as grain size and hardness. A thorough understanding of lithology is essential

in various geoscience disciplines, particularly hydrogeology, as it directly influences aquifer behaviour (Mohammed et al., 2023).

Table 2.2 Range of hydraulic conductivity and permeability values for different lithologies

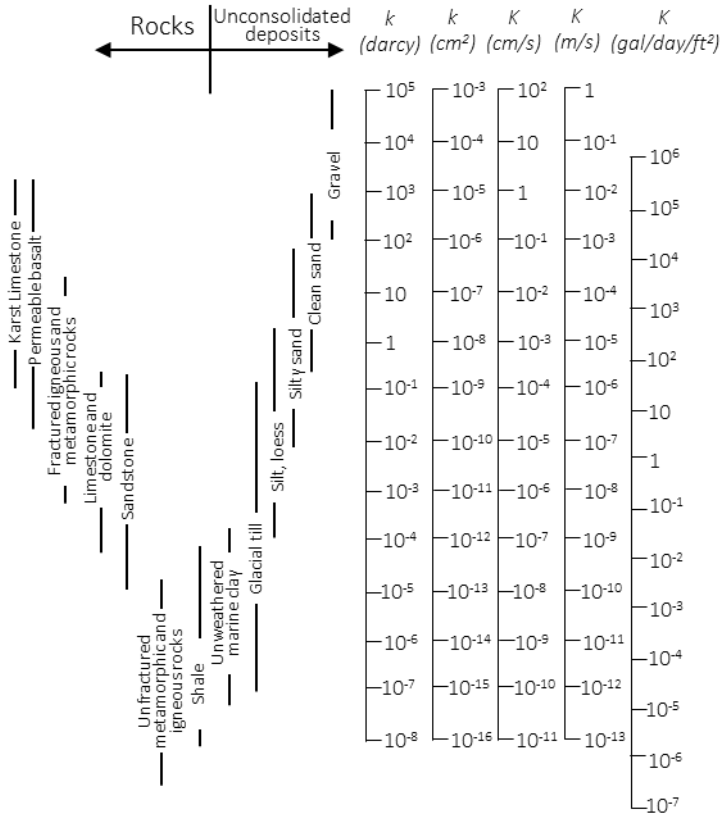

The parameters of aquifers are critical for modelling a conceptual groundwater system (A. A. Ahmed, 2009). These parameters often display spatial variability and anisotropy, which necessitates simplifications in the conceptualization of numerical models (Lunati et al., 2001). In addition to the inherent complexity and variability of aquifer parameters, simplification is justified due to the incomplete understanding of hydrogeological formations. Therefore, thorough analysis of field data is essential to connect aquifer characterization with numerical modelling. Each region, characterized by distinct geological conditions, possesses unique aquifer characteristics that demand localized expertise.

Sedimentary deposits, the primary constituents of most coastal aquifers, exhibit highly heterogeneous physical characteristics, marked by significant lithological variations both horizontally and, especially, vertically (Griffioen et al., 2012). In the case of volcanic rocks, the practice of hydrogeology, including groundwater

modelling, requires detailed data on lithological variations that may differ significantly (Baud et al., 2024). In his book *Applied Hydrogeology*, Fetter (2014) specifically highlights instances of complex stratigraphy and advises hydrogeologists to remain vigilant about such conditions in the field, given their diverse hydrogeological implications.

The physical properties of each lithology are also vital for establishing a preliminary understanding of aquifer parameters within a region. Hydraulic conductivity values can generally be correlated with geological or lithological types, which also reflect the characteristics of an area's aquifer. Hydrogeologists have conducted numerous studies and experiments on the determination of hydraulic conductivity values. For instance, Davis (1969) conducted extensive experiments across various lithological types in different regions, as summarized in Table 2.2 (Freeze, R.A.; Cherry, 1979).

2.4 Subsidence prediction and mitigation

Like other natural disasters, subsidence requires thorough investigation, particularly to understand its primary causes and potential preventive measures. By assessing changes in contributing parameters, accurate subsidence predictions can be developed, creating a critical foundation for effective mitigation efforts. Such informed planning is essential to reduce both the severity of damage and associated losses.

2.4.1 The significance of land-use and climate change on land subsidence

The coastal area, characterized by high utilization, is highly susceptible to environmental degradation from human activities. Uncontrolled land-use change poses a threat to the carrying capacity and sustainability of coastal resources. Land-use in any given area is closely tied to population growth and associated activities. As population and activities intensify, the rate of land-use change often accelerates.

Climate change impacts vary broadly but are anticipated to escalate in the future, significantly affecting hydrological systems and making water resources more vulnerable (Reay et al., 2007). Climate change can be associated with rising temperatures, changing rainfall patterns, and more frequent extreme weather events, including heatwaves, droughts, and heavy rainfall. Global climate change

(climate change) currently ranges from 0.5–0.8°C in 100 years (Lubis & Delinom, 2010). Based on BMKG observations in 1981-2020, the temperature in Indonesia has increased by 0.2 0C and climate-related changes such as increased rainfall intensity in shorter periods over the last 30 years and longer dry seasons; however, the annual average precipitation shows no significant change ((BMKG, 2020).

Climate variability, especially variability in precipitation, can have substantial effects on recharge and groundwater levels. Groundwater recharge is affected by climate changes and changes in land-use (Van Huijgevoort et al., 2020). The increasing rainfall intensity in shorter periods will increase surface run-off; this is indicated by floods that occur more frequently, including in Indonesia. Leterme & Mallants (2012) concluded that land-use and climate change significantly influence the hydrological cycle. It is essential to consider the impacts of climate change and land-use change on a particular strategic area like coastal cities because sustainable management of groundwater in this area is crucial.

As one of the essential components in the hydrological cycle, groundwater recharge is influenced by several climatic parameters such as temperature and rainfall (Dey et al., 2020). Furthermore, rainfall intensity can influence groundwater recharge in those regions, but the recharge largely depends on geology, topography, land-use, and land pattern (Silva, 2015). Land-use conversions will affect the atmosphere-vegetation-soil water balance pattern, thus changing evapotranspiration and groundwater recharge (Cui et al., 2014). As groundwater recharge is identified as the vertical downward water movement across the groundwater table, water movement varies per land-use type, especially vertical flow (van Eekelen et al., 2015). When land-use changes occur, hydrological processes, infiltration, evaporation, and especially groundwater recharge are also affected.

In summary, climate change involves shifts in temperature and rainfall patterns. However, despite fluctuations over the past 30 years, average annual precipitation shows no significant long-term change, leaving future climate scenarios uncertain. Conversely, land-use changes directly influence how land interacts with the hydrological cycle. The decline in groundwater recharge due to extensive land-use change poses challenges in many regions, leading to decreased groundwater

availability, lowered groundwater levels, and heightened potential for land subsidence. Additionally, land-use change can exacerbate subsidence through mechanisms like lowering the phreatic water table and adding surface loads from infrastructure.

2.4.2 Controlling groundwater abstraction for subsidence mitigation

Amongst many significant triggering factors, subsidence accompanying groundwater extraction is perhaps the best understood and identified (Galloway & Burbey, 2011). Groundwater abstraction is also a factor causing land subsidence which tends to be controlled, compared to other factors, including natural compaction. At the same time, controlling groundwater abstraction is critical to ensure that groundwater decline does not occur continuously. Khaliq (2021) applies groundwater modelling and simulates the increasing groundwater extraction in Faisalabad city, Pakistan, for urban water supply availability. So that there will be no excessive groundwater decline considering that groundwater is the city's primary water source.

In coastal areas, regulation of groundwater extraction is also necessary to avoid or minimise the impact of seawater intrusion. Studies on coastal groundwater management to reduce the risk of seawater intrusion have been carried out widely. Simulation and optimisation modelling was studied by (Singh, 2015) as a method for regulating groundwater in coastal areas, considering many unplanned groundwater withdrawals in coastal areas to fulfil the growing freshwater needs.

The development of numerical modelling methods for land subsidence applications is significant to address the relationship between groundwater abstraction and land subsidence hazard. This method's application is also vital for predicting subsidence, especially concerning increased groundwater use, and related to land-use and climate change. Land subsidence modelling and prediction should be followed up with mitigation policies to reduce land subsidence disasters in the future, especially related to groundwater use which is expected to continue to increase along with population growth.

2.5 Research questions and hypothesis

From the practical application of research into the literature gaps, a set of research questions (RQ) and hypotheses (H) arise to conduct the research. The text below summarises three groups of research questions.

RQ-1: *How does groundwater abstraction affect land subsidence rate and spatial distribution in coastal regions, particularly in the study area?*

H-1: The research hypothesis to be tested is that increased groundwater abstraction in coastal regions, particularly in the study area, significantly accelerates the rate and changes the spatial distribution of land subsidence.

The modelling results describing groundwater drawdown can be found in Chapter 5, Section 5.8. Meanwhile, the explanation of the relationship between groundwater abstraction and land subsidence in the study area is provided in Section 6.2.1.1 of Chapter 6.

RQ-2: *What roles do remote sensing and numerical modelling play in accurately estimating land subsidence due to groundwater withdrawal in the study area?*

H-2: The research hypothesis to be tested is that integrating remote sensing with numerical modelling provides a reliable approach to estimate land subsidence's spatial and temporal patterns in response to groundwater withdrawal rates in the study area.

The explanation for RQ-2 is provided in Section 6.2.2, “Subsidence of InSAR and GPS Measurement.” Section 6.3 covers the comparison between subsidence results derived from numerical modelling and remote sensing methods.

RQ-3: *How does land-use change affect land subsidence in coastal tropical areas compared to climate change?*

H-3: The research hypothesis to be tested is that land-use change has a more pronounced effect on land subsidence than climate change due to its impact on the dynamics of groundwater recharge.

The explanation regarding the comparison of the impacts of land use change and climate change on land subsidence is presented in Chapter 6, Section 6.4.1, titled "Land Use and Climate Change Scenarios."

RQ-4: *Which groundwater management and adaptation strategies could effectively mitigate land subsidence while supporting sustainable water resources in the study area?*

H-4: The research hypothesis to be tested is that applying managed groundwater abstraction limits and targeted adaptation strategies will significantly reduce land subsidence rates and support sustainable water resources for coastal communities in the study are

The answer and explanation for RQ-4, or the mitigation strategy for controlling subsidence in the study area, is provided in Section 6.5, titled "Mitigation Strategy to Control Subsidence Through Groundwater Management."

CHAPTER 3
General Methodology

3.1 Introduction

This chapter outlines the methodology employed to investigate land subsidence in the study area which is the Pekalongan Groundwater Basin (PGB), focusing on the development and application of an integrated groundwater flow and land subsidence model. The methodology is designed to identify key aspects of subsidence caused by groundwater extraction and environmental changes, as well as to explore management strategies to mitigate subsidence.

The approach integrates several key components, including geological and hydrogeological data, as well as climate, land-use, and remote sensing data for subsidence measurements. These elements are processed and modelled to understand subsidence patterns and predict future changes under various scenarios.

The chapter begins with a description of the study area, followed by a detailed explanation of data acquisition from existing sources and field measurements. It then discusses the methods used to prepare and process these datasets for model construction, including groundwater model calibration. Finally, the chapter outlines how the processed data will be applied in subsequent chapters to explore various subsidence scenarios and assess the effectiveness of mitigation strategies.

3.2 Research methodology

The research methodology is structured around the following components:

1. **Data acquisition and processing:** This section covers the collection and preparation of key datasets, including:
    - Geological and hydrogeological data for building a conceptual model.
    - Land subsidence data obtained from remote sensing (*InSAR*) and direct field measurements.

- Climate change scenarios, land-use data, and projected increases in groundwater abstraction for model projections.

2. **Model construction and calibration:** The development of a numerical groundwater flow and land subsidence model using MODFLOW and the SUB package forms the core of this research. The groundwater model will be calibrated using field data and automatic parameter estimation (PEST) to ensure the accuracy of flow patterns and water levels compared with groundwater measurement data. The subsidence model from the SUB package will be compared with subsidence measurements obtained from *InSAR* and GPS over a one-year period.

3. **Scenario analysis and mitigation strategies:** This methodology also includes simulations of various scenarios related to climate change, land-use changes, and, most importantly, groundwater abstraction. These simulations aim to project future land subsidence rates and develop effective mitigation strategies to minimise subsidence without compromising groundwater availability.

3.3 Study area

3.3.1 Location and geological setting

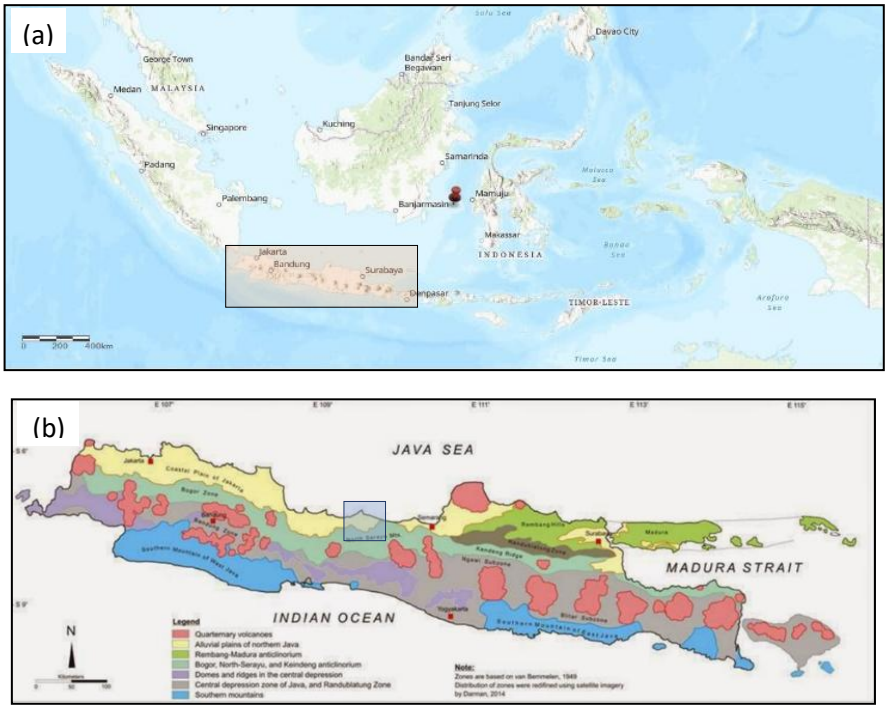

Figure 3.1 Maps showing location of the research area.
(a) map of Indonesia and (b) physiographic map of Java Island

Pekalongan Groundwater Basin is situated on the North Coast of Java Island, a rapidly growing region that connects many major cities in Java. This includes Jakarta, the largest city in the country, located to the west, and Surabaya, the second largest city, to the east, with Pekalongan positioned in the middle. Geographically, the research area is located between longitudes 6.7860 to 7.0530 E and latitudes 109.3250 to 109.7690 S, and administratively it is part of Central Java Province. A more detailed representation of the Pekalongan Groundwater Basin as the study area is provided in Figure 3.1.

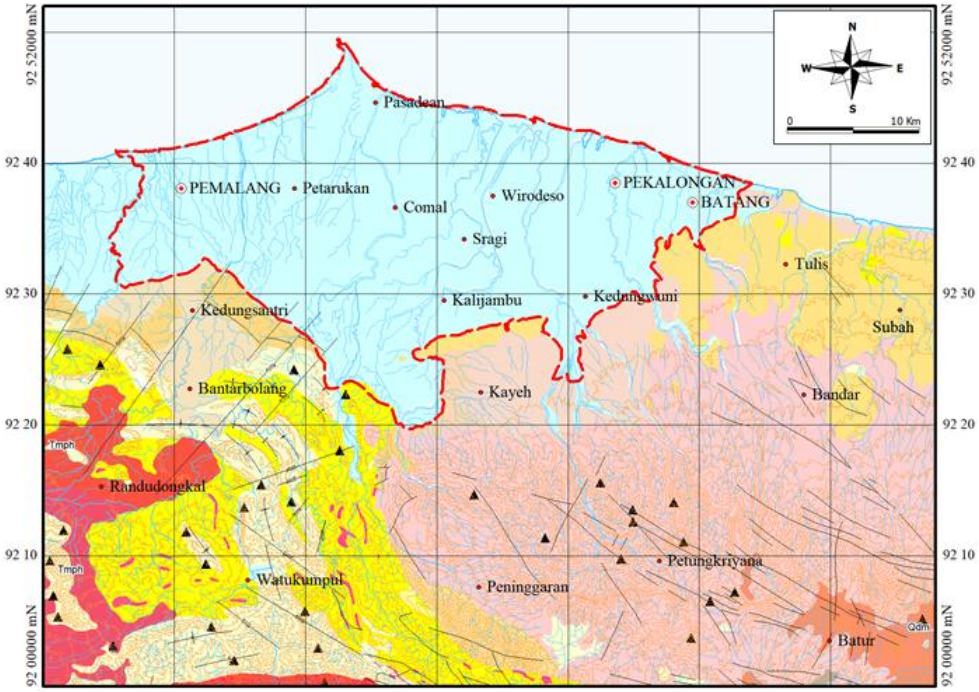

Period	Epoch	Surficial Deposits & Sedimentary Rocks	Volcanic Rocks	Explanation
Quaternary	Holocene	Qa; Qla; Qf		**(Qa) Alluvium** Pebbles, sands, silts, and clay, and swamp deposits. Thickness up to 150 m **(Qf) Alluvial fan** Mainly volcanic debri; dissected **(Qla) Alluvial and Lake Deposits** Sands, silts, muds, and clay; tuffaceous, locally
	Pleistocene	Qt; QTd; QTlb	Qjya / Qjyf; Qjma / Qjmf; Qjm; Qjo	**(Qj) Jembangan Volcanic** Andesitic lava and volcaniclastics. Predominantly, augite-hypersthene andesite containing hornblende in places, as well as olivine basalt. Present as lava flow, flow and pyroclastic breccia, lahar and alluvium (Qjo and Qjm); lahar and alluvium consisting of volcanic debris, lava flow and breccia (Qjya and Qjma) deposited in a gentle slope, and slightly far from eruption centre compared to Qjyf and Qjmf comprising lava flow and breccia, and pyroclastic breccia and lahar **(Qt) Terrace Deposits** Sands, silts, tuff, conglomerate, tuffaceous sandstone, and tuffaceous breccia. Distributed specially along Serayu valley. **(QTd) Damar Formation** Tuffaceous claystone, volcanic breccia, sandstone, tuff, and conglomerate; lahar deposit, in places. Volcanic breccia and tuff are andesitic in composition, whereas, conglomerate is basaltic and locally compact. Mollusc is found, locally Depositional environment was non-marine. **(QTlb) Breccia Member of Ligung Formation** Andesitic volcanic breccia (agglomerate), hornblende andesitic lava, and tuff; forming upper sequence of the Ligung Formation

Figure 3.2 Geological map of Pekalongan Groundwater Basin and surroundings (redrawn from Condon, 1996)

PGB is part of the Great Alluvial Plains of Northern Java, formed during the Quaternary age (Darman, 2000). It is primarily composed of alluvial deposits, but in some places, it includes young volcanic and lake deposits (Condon, 1996). These alluvium deposits, formed in river and coastal swamp environments, consist of loose materials such as gravel, sand, silt, and clay derived from the weathering of older rocks. Larger material, ranging from pebbles to gravel, is found locally, particularly around the estuaries of the Comal River, Rambut River, and other large rivers. Beneath the alluvial deposits lie volcanic rocks resulting from Quaternary volcanic activities, comprising volcanic breccia, agglomerates, and tuff. The geological map of the study area and its surroundings is presented in Figure 3.2.

3.3.2 Land use

As part of the Great Alluvial Plains of Northern Java, the research area features a flat to very gently undulating topography with elevations less than 50 meters above mean sea level and slopes less than 5 degrees (*DEMNAS*, 2020). The area is traversed by several major rivers, including the Comal River, Sragi River, and Pekalongan River, which typically exhibit an anastomotic flow with some meandering sections. These rivers have been utilized for various agricultural purposes, with irrigation channels constructed through several of them.

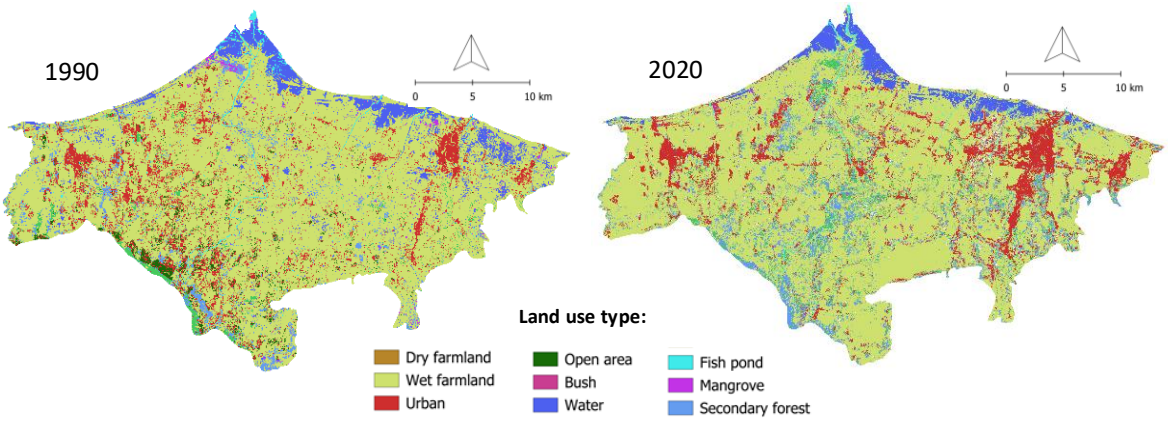

Figure 3.3 Land use of study area of 1990 and 2020

Land use in the research area is generally dominated by aquaculture and mangrove forests in the coastal zone and rice fields in the middle section (Geospatial Information Agency, 2010). Over the past decade, residential areas, including industrial and office zones, have expanded significantly, particularly in Pekalongan

City (Marfai, 2011). This urbanization has been accompanied by a denser and expanding road network that enhances connectivity between settlements, cities, and rapidly growing urban areas.

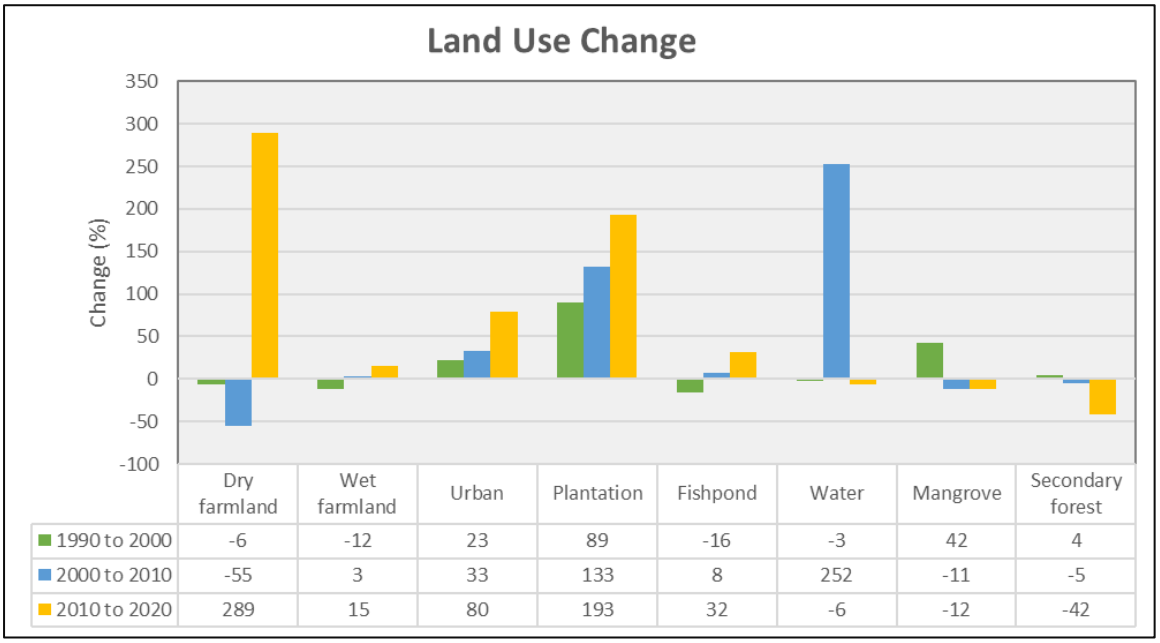

	Dry farmland	Wet farmland	Urban	Plantation	Fishpond	Water	Mangrove	Secondary forest
1990 to 2000	-6	-12	23	89	-16	-3	42	4
2000 to 2010	-55	3	33	133	8	252	-11	-5
2010 to 2020	289	15	80	193	32	-6	-12	-42

Figure 3.4 The graph showing the change of land use type from 1990 to 2020

Based on the analysis of land use development from 1990 to 2020, there has been a substantial increase in residential areas within the study region, with the most rapid development occurring from 2010 to 2020, reaching 80%. The expansion of these built-up areas, encompassing both residential and industrial zones, will inevitably lead to an increased demand for water, including a rise in groundwater abstraction. In contrast, secondary forests experienced a significant reduction, decreasing by 42%, with most of this land being converted into agricultural areas. Based on the analysis of land use development from 1990 to 2020, there has been a substantial increase in residential areas within the study region, with the most rapid development occurring from 2010 to 2020, reaching 80%. The expansion of these built-up areas, encompassing both residential and industrial zones, will inevitably lead to an increased demand for water, including a rise in groundwater abstraction. In contrast, secondary forests experienced a significant reduction, decreasing by 42%, with most of this land being converted into agricultural areas. Figure 3.3 illustrates the land use distribution in 1990 and 2020, while Figure 3.4 presents the land use changes within the study area over this period.

3.3.3 Climate settings

The research area selected for conducting the research has a typical tropical climate (Peel et al., 2007). Tropical climate areas are defined by Köppen classification as the equatorial region, which received very high annual rainfall (exceeds 1.500 mm). As shown in Figure 3.5, the annual rainfall in 2020 in the research area is approximately 2.720 mm (https://dataonline.bmkg.go.id). The average temperature of the area in 2020 is 28.66^0 Celsius (C). The average minimum temperature is 25.13^0 C, and the maximum temperature is 32.18^0 C, as shown in Figure 3.6. Based on these temperature variations, the research area is classified as tropical rainforest (Peel et al., 2007).

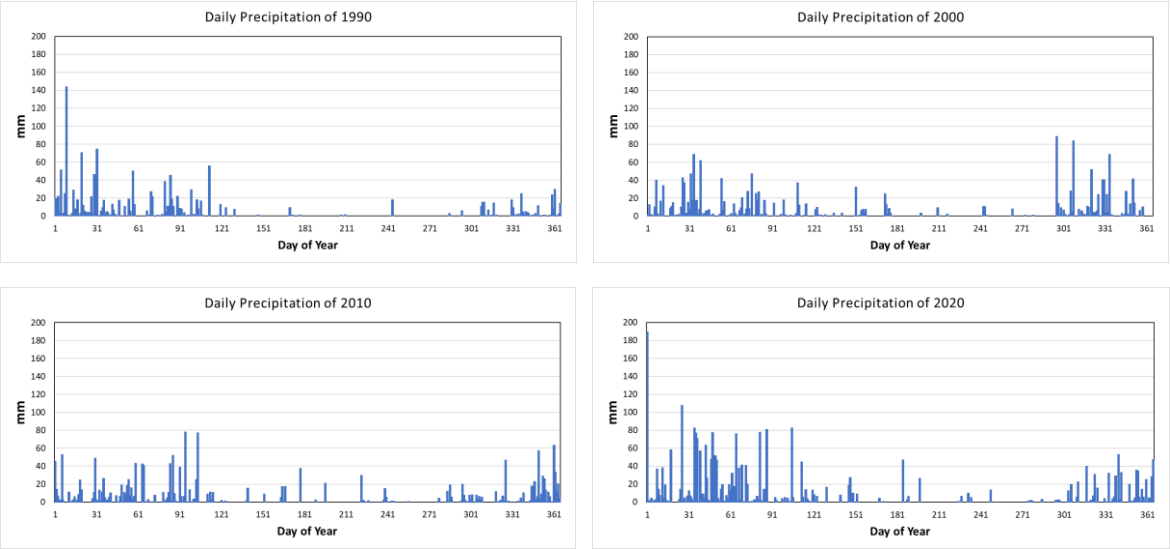

Figure 3.5 The daily precipitation in a year in 1990, 2000, 2010 and 2020

As shown in Figure 3.7, the rainfall pattern in the research area is relatively consistent. Dry months, characterized by rainfall of less than 100 mm per month, occur from May to September. Conversely, the region experiences higher rainfall from October to March, with monthly totals exceeding 100 mm. Several instances of extreme daily rainfall have been recorded even during the dry months, with intensities exceeding 100 mm/day. This phenomenon serves as evidence of the ongoing impacts of climate change (Tabari, 2020).

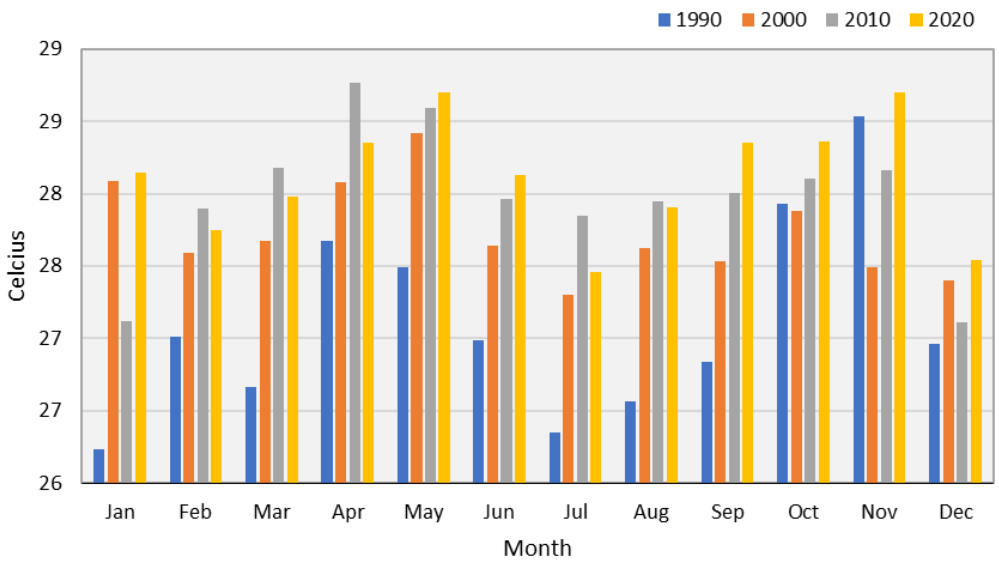

Figure 3.6 Monthly average temperature in 1990, 2000, 2010 and 2020 in different colours

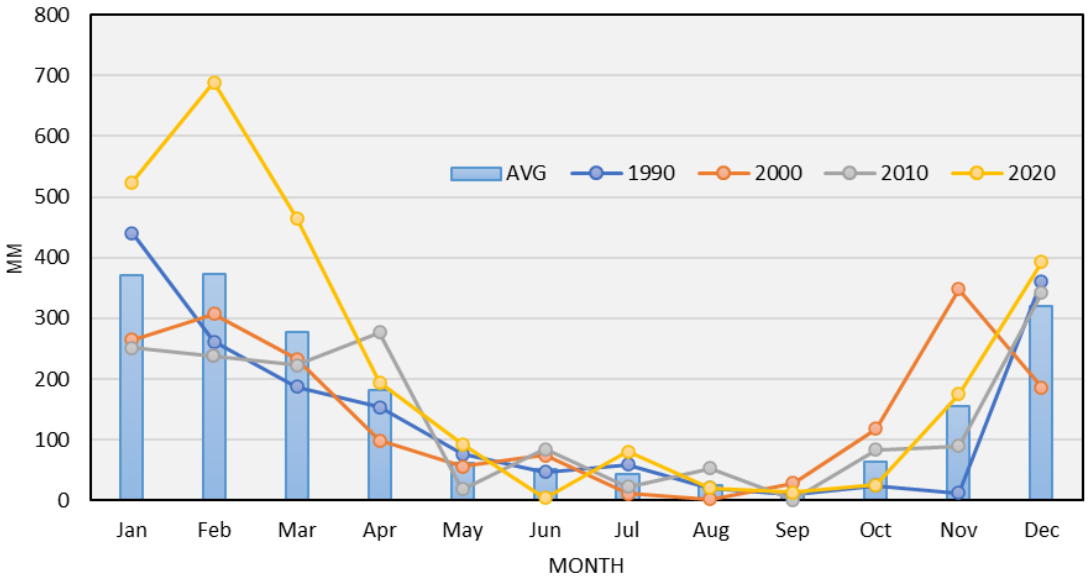

Figure 3.7 Monthly precipitation in 1990, 2000, 2010, and 2020, along with the average monthly precipitation values

3.3.4 Well data

Well data is a critical component in hydrogeological studies. It serves multiple purposes, particularly in determining subsurface conditions that can be more accurately understood through well data. Subsurface data obtained via geophysical analysis or remote sensing must be validated and reinforced with well data. Such data may include the depth and diameter of the well, lithological descriptions, and other information, such as vertical geophysical data within the borehole. This information is typically gathered during exploration drilling operations prior to the establishment of the well for production or monitoring purposes.

Table 3.1 Number of wells in the research area from 1970 to 2020

Year	No of Wells
1970	34
1974	38
1977	44
1982	47
1988	53
1990	55
1992	63
1994	81
1996	85
1998	104
2000	107
2010	182
2020	269

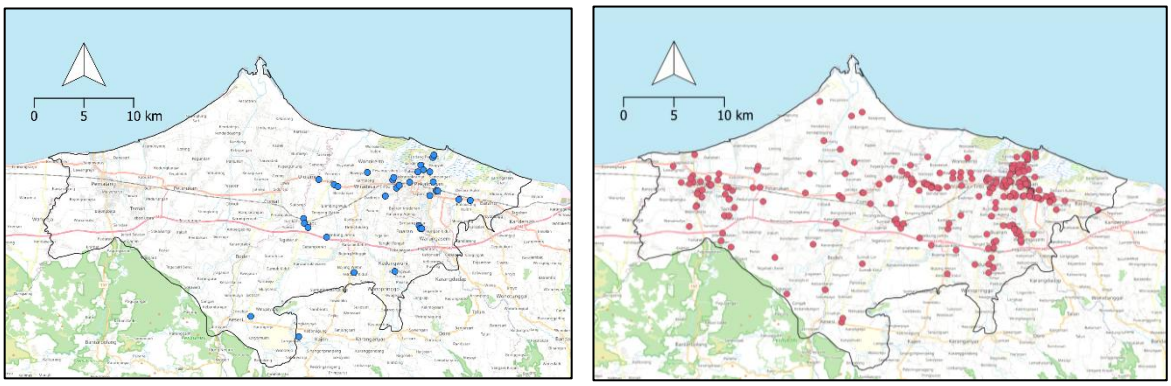

Figure 3.8 Distribution of abstraction wells in 1970 and 2020

The growth of groundwater abstraction is evidenced by an increase in the number of drilled wells, which correlates directly with the rise in industrial activities. Deep groundwater abstraction and the distribution of drilled wells are concentrated in Pekalongan City and Pemalang City, the two primary cities within the study area, with some wells situated in industrial zones dispersed throughout the region. Historical records indicate groundwater drilling commenced in 1866, with 34 drilled wells documented by 1971. By 2020, the number of drilled wells had increased to approximately 274 (Figure 3.8). The detailed growth of groundwater abstraction wells can be seen in Table 3.1. This well data was obtained from reports by the Central Java Provincial Department of Energy and Mineral Resources, conducted by various consulting firms (PT. Giri Awas, 2012; Sudadi, 2004), as well as from licensing data not included in the reports.

Some of these extraction wells have complete technical data, including depth, well diameter, and screen depth, with most wells having depths ranging from 100 to 120 metres below the ground surface and screens positioned at depths of 40 to 100 metres. However, the majority of the extraction wells lack comprehensive technical data, with some wells only having location information available. To ensure consistency in the model, this study assumes that all wells have a depth of 120 metres, with screens positioned below 40 metres, aligning with the general trend observed in wells with available technical data.

3.4 Data Acquisition

3.4.1 The previous data availability

Numerous data were obtained from previous studies and unpublished reports, particularly from the Geological Agency and the Central Java Provincial Office. Most of these data are in the form of hard copies or printed reports, and some require re-verification due to unclear information. The analyses from these data will inform the next stage, including planning further data acquisition to fill any gaps. The available data can be classified into two main types: geotechnical drilling and groundwater drilling, with the distribution of locations shown in Figure 3.9.

1. Geotechnical drilling

This data is the result of an investigation conducted by the Centre for Groundwater and Environmental Geology – Geological Agency in 2015 (Tulus Pramudyo & Wafid, 2015) and 2021 (Raflyndo Pratama, 2021). The drilling method is used for various purposes, including obtaining technical data for land subsidence calculations. Generally, this work is divided into two phases: in-situ testing and laboratory testing, with consolidation test results available in the appendix of this report.

- **In-situ testing** is performed directly on-site and includes:
    - *Core drilling with HQ diameter*: This involves core drilling with a 6-inch diameter to obtain intact samples of rock or soil for detailed description by depth. The core box containing the drill samples is stored in the Geological Agency's sample storage facility.

- *Standard Penetration Test (SPT).* This test assesses the strength or relative density of soil layers at specified depths. The test is conducted following ASTM D1586-67 standards.

- **Laboratory testing** aims to obtain engineering soil parameters to support geotechnical analysis according to ASTM standards. This includes:
  - Basic properties testing, which comprises:
    - Water content (ASTM D2217-71)
    - Specific gravity (ASTM D854-72)
    - Bulk density (ASTM D4718)
  - Index properties testing, which includes:
    - Atterberg limits (ASTM D4318)
    - Grain size analysis (ASTM D422-72)
  - Engineering properties testing, which includes:
    - Triaxial (ASTM D2850)
    - Consolidation (ASTM D2435)

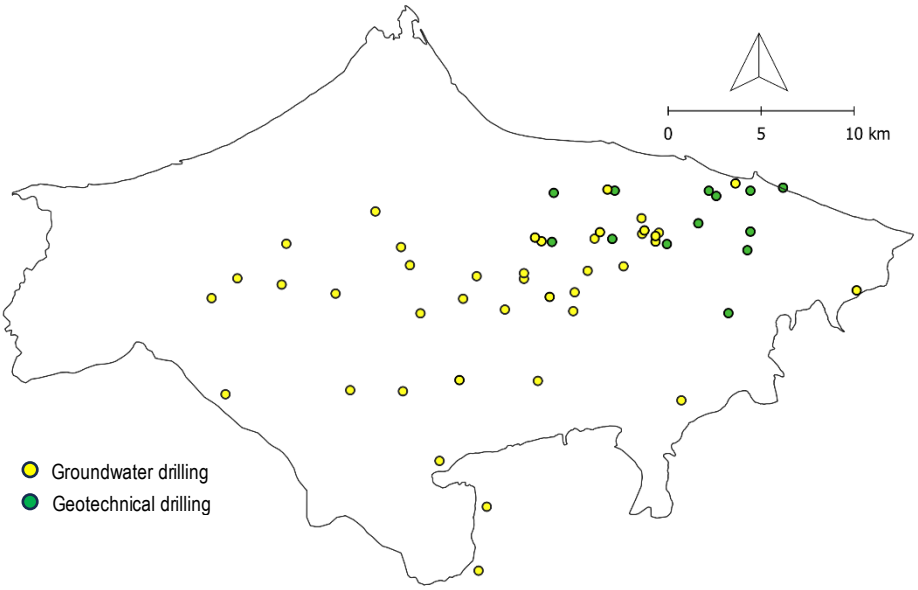

Figure 3.9 Distribution of geotechnical and groundwater drilling in the study area

2. Groundwater Drilling

This data is part of the report on the project *'Exploration and Provision of Clean Water through Groundwater Drilling*,' carried out by the Centre for Groundwater

and Environmental Geology – Geological Agency in collaboration with several consulting firms, in the Regency of Pekalongan (Catur Karsa, 2016a, 2016c, 2016b; Geokarsa, 2018a; Ramapratama, 2014; Tirta Jaya, 2013, 2015b, 2018a, 2018c; Tirta Mandiri, 2019a, 2019d, 2019e) and Pemalang (Catur Karsa, 2011, 2017; Geokarsa, 2018b, 2018c, 2018d; Ramapratama, 2013; Tirta Jaya, 2014, 2015a, 2018b; Tirta Mandiri, 2019b, 2019c, 2019f, 2019g, 2019h).

The drilling work is conducted to create production wells for groundwater extraction. An open-hole drilling method is used, allowing rock/soil descriptions from drill cuttings. The sample descriptions provide a vertical lithological profile, helping identify the aquifer location for screen placement in the well construction pipe. These groundwater wells vary in depth, with most extending to around 120 metres.

3.4.2 Fieldwork

Effective planning is essential for fieldwork to ensure the collection of high-quality data. With data obtained from previous studies and research, fieldwork can be planned more effectively and efficiently, even though it is still conducted within the available time and budget constraints. The fieldwork methods implemented are as follows:

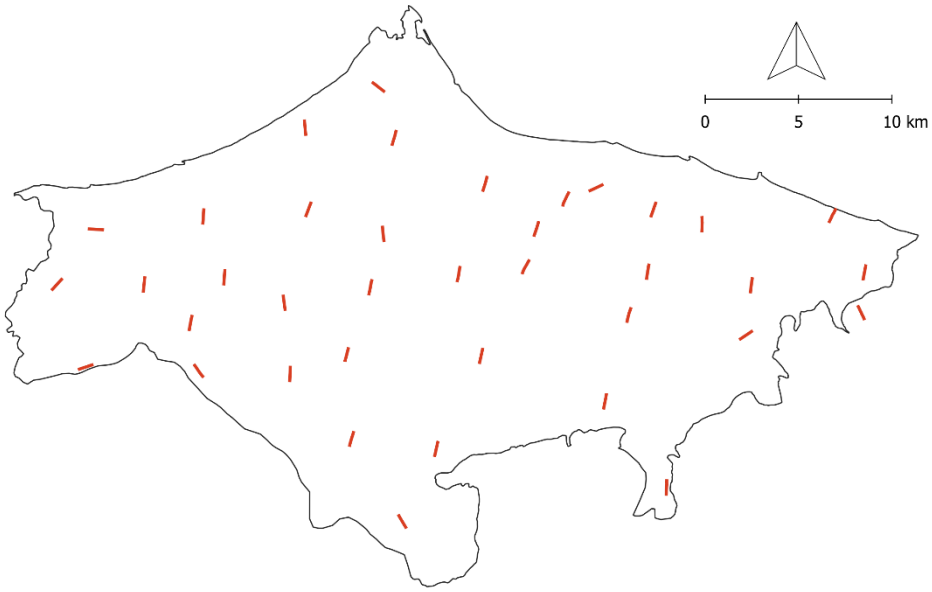

Figure 3.10. Location of geoelectrical measurement

1. Geoelectrical measurement

Based on drilling data from previous studies, many areas remain uncovered. Therefore, it was decided to conduct geoelectrical surveys to obtain lithological interpretation information, particularly in the unexamined areas. Figure 3.10 presents the geoelectric measurement points, while Figure 3.11 displays photographs of the measurement process.

Figure 3.11 Geoelectric measurement activities in the study area

The measurement utilizes the resistivity method with the Vertical Electrical Sounding (VES) technique, following the Schlumberger electrode configuration rules. It employs the multichannel electrode resistivity (2D geoelectrical method) with a penetration depth of up to 200 meters.

In principle, this test is based on the physical properties of rocks against electric currents. The physical properties of rocks to electric currents depend on the rock's porosity, water content, grain size, and compactness. The measurement is executed by flowing a direct electric current into the ground through two electrodes, currents A and B. The difference in the types of rock layers the current passes

through will produce a potential difference measured on the surface through the two potential electrodes, M and N, as shown in Figure 3.12.

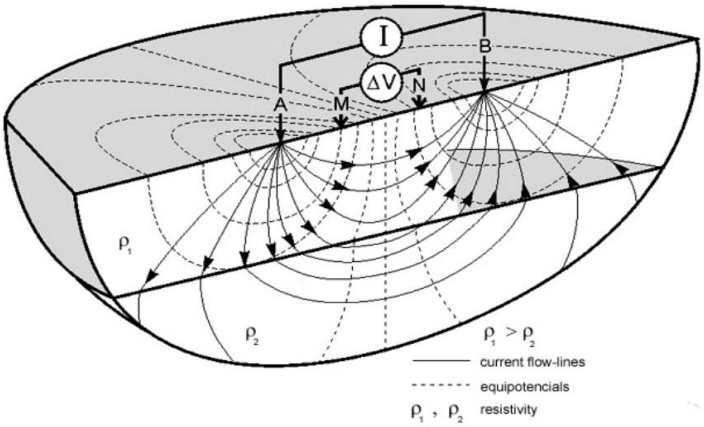

Figure 3.12 The arrangement of the electrodes according to Schlumberger Rules

2. Pumping test

The pumping test or also known as the aquifer test, is a method of evaluating the aquifer by stimulating the aquifer by pumping groundwater from the pumping well and observing the aquifer response in the observation well. Pumping tests are the primary method frequently employed in hydrogeological research to determine aquifer parameters, particularly hydraulic conductivity values.

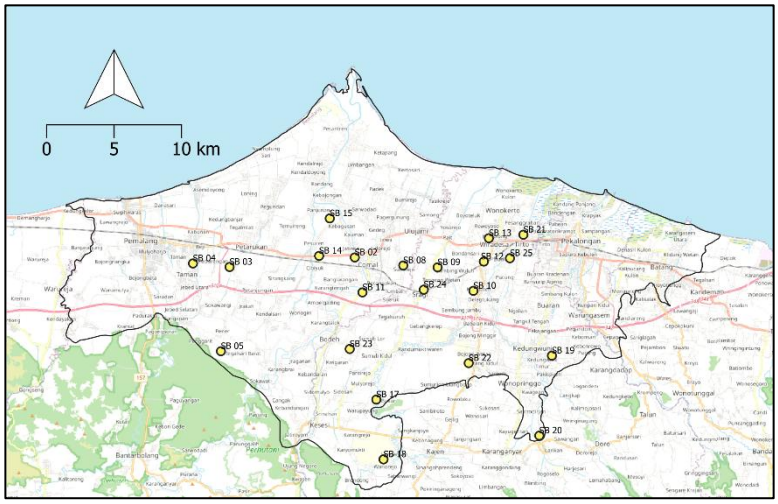

Figure 3.13 Locations of pumping tests conducted on wells meeting the required criteria, resulting in uneven distribution

Pumping tests were conducted at 21 locations, with an uneven distribution across the research area (Figure 3.13). These tests were performed exclusively in wells that met specific criteria, particularly the availability of well data such as lithology, well

depth, and screen location. Additionally, accessibility for testing, considering both the physical location and the necessary permits, was a crucial factor. Consequently, the test locations were not evenly distributed throughout the research area. The aquifer characteristics obtained through this test include transmittivity and hydraulic conductivity. Figure 14 shows the execution of the pumping test and the measurement of groundwater levels in observation wells.

Figure 3.14 Pumping test and groundwater level measurement activities during fieldwork

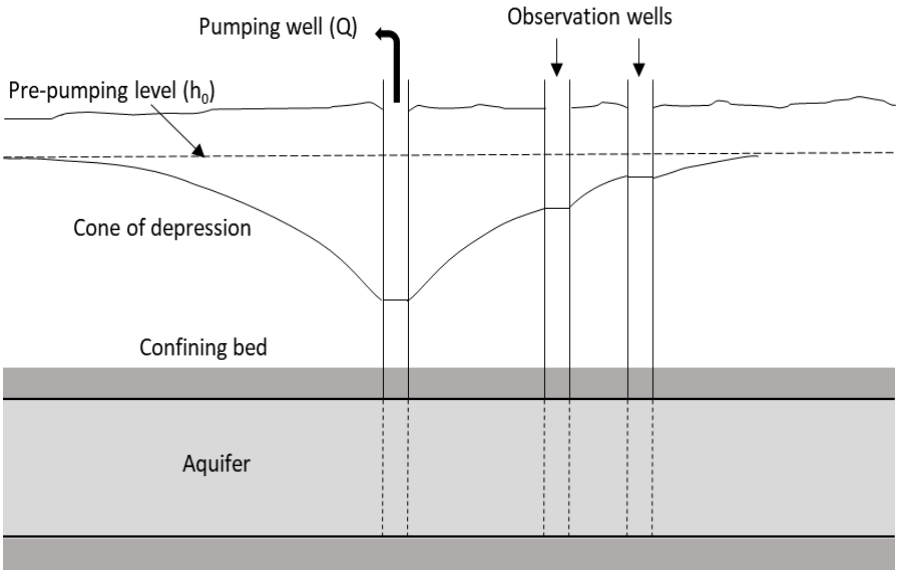

Figure 3.15 Groundwater pumping in a confined aquifer using two observation wells

Before the test is started, the water level in the observation well is measured to determine the pre-pumping or static water level (h0), which represents the hydraulic head at time zero. The test begins by pumping at a specific rate (Q). After pumping starts, the water level is periodically measured through the observation well. This test typically requires one pumping well and one or more observation

wells. The illustration of the theoretical implementation of the pumping test can be seen in Figure 3.15. However, in this study, the pumping tests were conducted using the single-well method, where both pumping and observation occur in the same well. This approach was necessitated by the need to find locations that meet the criteria for conducting pumping tests using two separate wells or an observation well distinct from the test well.

3.4.3 Images acquisition

For the *InSAR* method, remote sensing images are the primary data needed. Due to its numerous advantages, Sentinel-1A will be utilized for *InSAR* processing. Sentinel-1A consists of two satellites created by the European Commission and ESA for the Copernicus Global Earth Observation Project satellite constellation, mainly used for marine environment monitoring and surface deformation observation. The table below provides the specifications of Sentinel-1A, and the data can be freely downloaded from https://scihub.copernicus.eu/.

Table 3.2 Sentinel 1A specification

Satellite	Sentinel-1A
Acquisition mode	Wide Swath
Minimum revisit period (days)	12
Wavelength (λ) (cm)	5.55
Polarization	VV
Orbit	Descending
Incidence angle of the area of interest	$36.47^0 – 41.85^0$
Launch Date	3 April 2014

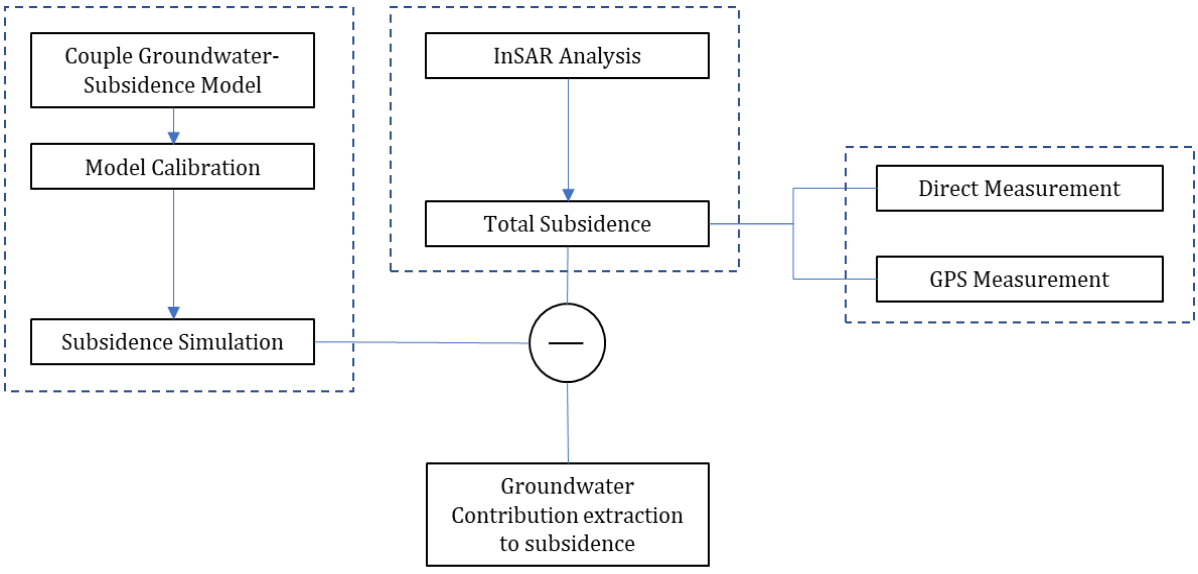

Figure 3.16 Flowchart showing the research method

3.5 Data processing and modelling

The research method is schematically illustrated in Figure 3.16, with numerical simulation being the primary approach. The subsidence simulation results will be compared to total subsidence obtained from *InSAR*, which is the chosen remote sensing application method. Prior to this comparison, the *InSAR* results will be verified with direct measurements.

3.5.1 InSAR processing

SBAS (Small Baseline Subset) technology is a recent advancement in *InSAR* processing that will be utilized in this research. This method, first proposed by Berardino et al. (2002), aims to address limitations of earlier methods, including atmospheric signal delay and temporal and spatial decorrelation. The data processing process is depicted in Figure 3.17.

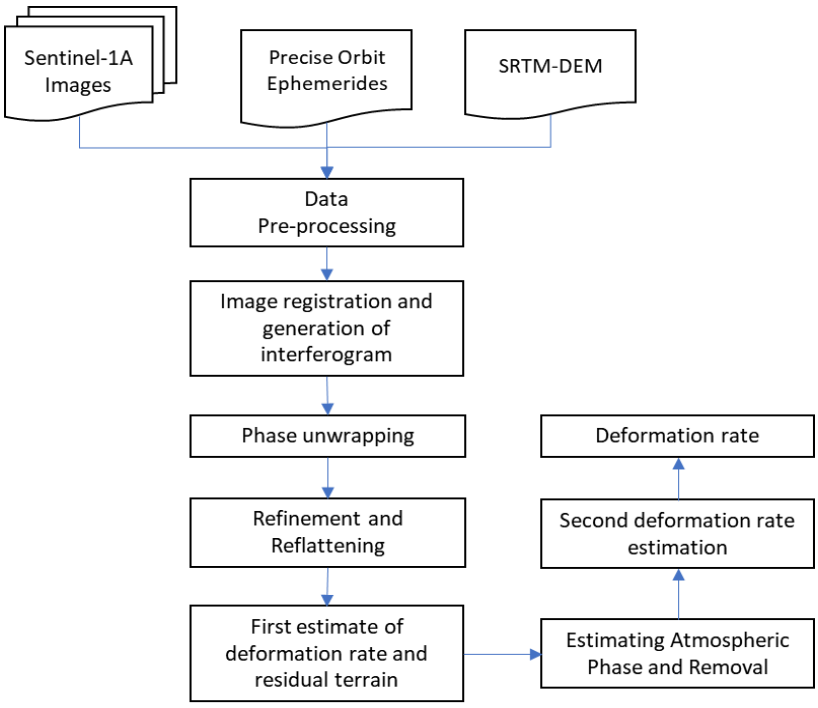

Figure 3.17 Flowchart of *SBAS-InSAR* processing

After processing, the vertical deformation rates for the entire study area during the measurement period will be derived using SBAS-InSAR. These rates provide a comprehensive assessment of subsidence patterns across the region. For simplification, Line-of-Sight (LoS) displacement is assumed to represent vertical displacement or subsidence, based on the assumption that horizontal movement is

minimal or negligible. This assumption allows for a more straightforward interpretation of the results, focusing on the dominant vertical component of ground deformation.

The decision to utilise InSAR data for a single year is justified to ensure consistency, accuracy, and reliability in the analysis. By focusing on a single-year dataset, this study maintains uniform data quality, minimising potential errors arising from multi-year observations with varying technical specifications. Moreover, selecting a specific time frame enables a direct and precise comparison with ground-based measurements, particularly GPS observations available within the study period. This approach enhances the reliability of validation efforts by ensuring that discrepancies between InSAR and in situ measurements reflect actual subsidence patterns rather than inconsistencies in data acquisition or processing techniques.

While long-term datasets offer valuable insights into broader subsidence trends, their feasibility is constrained by computational, and processing demands (Zhang et al., 2024). Extensive multi-year analyses require substantial computational resources for atmospheric corrections, phase coherence assessments, and advanced error filtering. Thus, a single-year approach is a more pragmatic choice given the available resources. By focusing on a well-defined period, this study prioritises data integrity and methodological robustness, ultimately leading to more precise and interpretable results.

3.5.2 Numerical simulation

A numerical model mathematically represents groundwater flow systems by solving partial differential equations that govern subsurface hydrodynamics using numerical discretization methods, such as the finite difference or finite element method (Anderson et al., 2015). A numerical simulation, the primary method in this research, will use MODFLOW-2005, a version of MODFLOW developed by the US Geological Survey.

MODFLOW is a three-dimensional finite-difference groundwater model simulated using a block-centred finite-difference approach (Techniques, 2005). Meanwhile, MODFLOW-2005 itself is a version that is still being developed to date and has

advantages over other versions, including easy to understand, use, refine and modify.

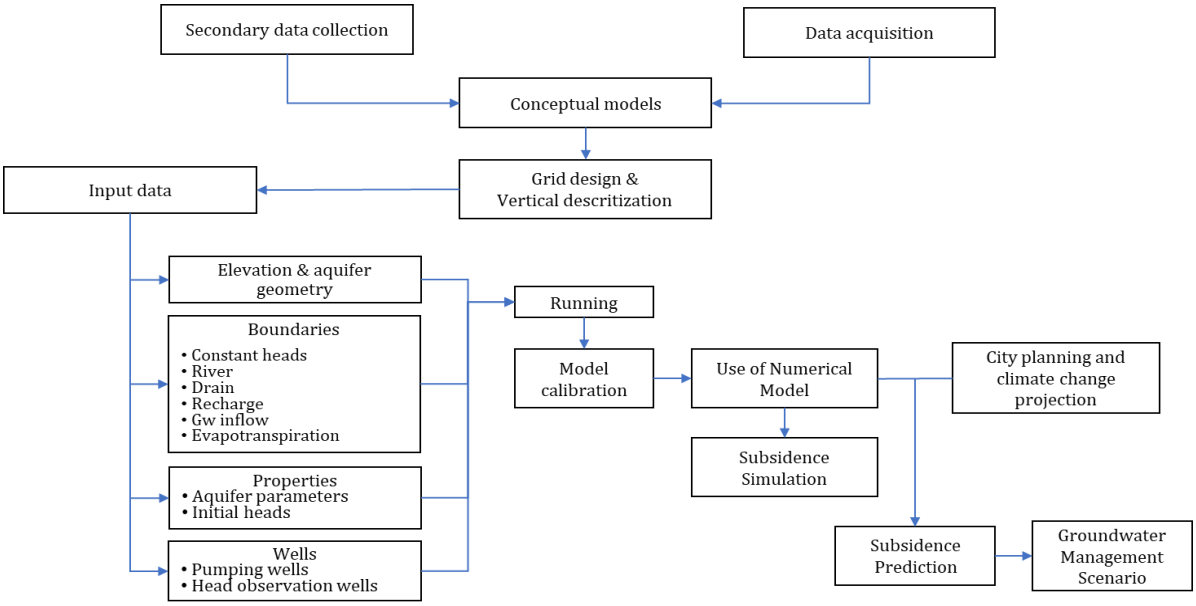

Figure 3.18 Schematic diagram for the modelling procedure

3.5.2.1 Groundwater flow and subsidence package

For MODFLOW-2005 processing, ModelMuse (Winston, 2009) the graphical user interface developed by the USGS, was selected. It has a good ability in dealing with the modelling process in MODFLOW. ModelMuse provides efficient tools for generating and editing the model grid, along with a range of interpolation methods and geographic functions that facilitate the representation of spatial variability within the model.

Table 3.3 Basic datasets for groundwater flow and subsidence model

Data Type	Model Input	Source
Topographic Data	Top model	DEM (Demnas)
Aquifer parameter	Hydraulic Conductivity	Pumping test result
	Storage Coefficients	Laboratory result and analysis
Geological Data	Boundary Conditions	Drilling log and geoelectrical analysis
	Thickness of aquifer layers	
Water level data	Observation data	Field measurement
Groundwater Recharge	Soil and Land Use Data	Landsat analysis
	Climate Data	BMKG
Abstraction Well Data	Well location	Government report
	Abstraction rate	

In general, the stages in the numerical simulation can be seen in Figure 3.18. The first stage is data collection from previous works and data collection to complement existing data to develop the conceptual model. These data are also crucial as input for the processing model. The reliability of the model is primarily determined by the quantity and the quality of input data.

One of the packages in MODFLOW-2005 is a one-dimensional soil consolidation model or the Subsidence and Aquifer-System Compaction package (SUB Package). SUB Package is a modified version of the existing packages in the previous MODFLOW versions, namely IBS1 and IBS2. It simulates elastic (recoverable) compaction and inelastic (permanent) compaction of compressible fine-grained layers in the aquifer system (Hoffmann et al., 2003). The basic datasets available for constructing the model are presented in Table 3.3.

3.5.2.2 Concepts of groundwater flow modelling

According to Anderson and Woessner (1992), a model is designed to represent the mathematical equations of groundwater flow occurring within a system, constrained by groundwater flow boundaries. Groundwater flow in a saturated, homogeneous, and isotropic medium is generally divided into two categories: steady-state and transient (or unsteady-state) flow conditions. The equation for steady-state groundwater flow in a homogeneous isotropic medium assumes that the groundwater head at every point within the model domain remains constant over time. This condition can be expressed mathematically as follows:

$$\frac{\partial^2 h}{\partial x^2} + \frac{\partial^2 h}{\partial y^2} = 0 \qquad \textit{Eq 3.1}$$

In steady-state conditions, the amount of groundwater inflow (recharge) equals the amount of groundwater outflow (discharge). Simulating under these conditions aims to approximate the model area to real-world conditions. Conversely, in transient conditions, the groundwater head varies over time at each point within the model domain due to either a reduction (sink) or addition (source) of groundwater, and this is analytically expressed as follows.

$$\frac{\partial^2 h}{\partial x^2} + \frac{\partial^2 h}{\partial y^2} = \frac{S}{T}\frac{\partial h}{\partial t} \pm \frac{R}{T} \qquad \textit{Eq 3.2}$$

In transient conditions, the groundwater inflow does not equal the outflow, suggesting a disturbance to the natural groundwater flow system. An example of this is excessive groundwater abstraction, where withdrawal exceeds the groundwater recharge, leading to a decline in the water table—a commonly observed phenomenon in natural systems.

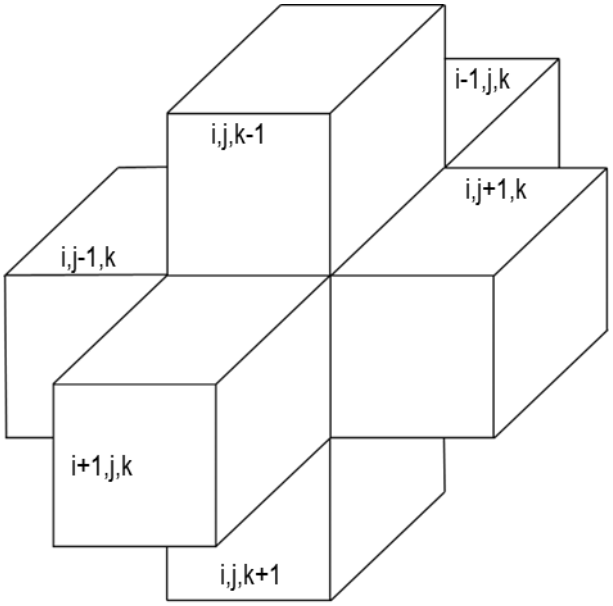

Figure 3.19 Indices for the six adjacent cells surrounding cell i, j, k (Harbaugh, 2005).

The concept of 3D groundwater flow modelling is based on the mathematical representation of groundwater movement through porous media under various conditions (Harbaugh, 2005). The governing equation is a partial differential equation (PDE) that accounts for hydraulic conductivity *(K_{xx}, K_{yy}, K_{zz})* along the principal axes, potentiometric head *(h),* specific storage *(Ss),* and a source or sink term *(W)* representing external water interactions. The PDE describes flow under transient and steady-state conditions within heterogeneous and anisotropic systems. The three-dimensional groundwater flow equation for porous media with constant density is expressed as:

$$S_s \frac{\partial h}{\partial t} = \frac{\partial}{\partial x}\left(K_{xx}\frac{\partial h}{\partial x}\right) + \frac{\partial}{\partial y}\left(K_{yy}\frac{\partial h}{\partial y}\right) + \frac{\partial}{\partial z}\left(K_{zz}\frac{\partial h}{\partial z}\right) + W \qquad Eq\ 3.3$$

Where:

Ss = Specific storage (L^{-1})

H = Hydraulic head (L)

K_{xx}, K_{yy}, K_{zz} = Hydraulic conductivities along x, y, and z axes (L/T)

W = Volumetric flux per unit volume representing sources/sinks (T^{-1})

T = Time (T).

Due to the complexity of real-world systems, numerical methods such as the finite difference method (FDM) are commonly used to approximate solutions. In this approach, the aquifer system is discretized into a grid of cells, each represented by rows, columns, and layers. Nodes at the centre of each cell are the points where pressure is calculated. The finite difference form of the groundwater flow equation is derived by discretizing both space and time. The continuity equation is expressed for a cell as:

$$\sum Q_i = SS \frac{\Delta h}{\Delta t} \Delta V \qquad \textit{Eq 3.4}$$

Where:

Q_i = flow rate into the cell (L^3T^{-1})

SS = specific storage in the finite-difference formulation; its definition is equivalent to that of Ss in Equation 5.3 (L^{-1})

ΔV = the volume of the cell (L^3)

Δh = the change in head over a time interval of length Δt.

Figure 5.1 presents a schematic representation of six aquifer cells that are adjacent to the designated cell at coordinates (i,j,k). The neighbouring cells are defined as follows: i-1, j, k; i+1, j, k; i, j-1, k; i, j+1, k; i, j, k-1; i, j, k+1. In the subsequent analysis, flows are treated as positive when they enter the cell at i, j, k. This convention simplifies the discussion by omitting the negative sign that is typically associated with Darcy's law throughout all relevant terms. The flow towards cell i, j, k in the row direction from cell $i, j-1, k$ (Figure 3.20), as described by Darcy's law, is represented as follows:

$$q_{i,j-1/2,k} = KR_{i,j-1/2,k} \Delta c_i \Delta V_k \frac{(h_{i,j-1,k} - h_{i,j,k})}{\Delta r_{j-1/2}} \qquad \textit{Eq 3.5}$$

Where $h_{i,j,k}$ represents the head at node i,j,k and $h_{i,j-1,k}$ denotes the head at node i,j−1,k; $q_{i,j-1/2,k}$ is the volumetric flow rate through the face between cells i,j,k and i,j−1,k (in units of L^3T^{-1}); $KR_{i,j-1/2,k}$ refers to the hydraulic conductivity along the row between nodes i,j,k and i,j−1,k (in units of LT^{-1}); $\Delta c_i \Delta V_k$ is the area of the cell faces

perpendicular to the row direction; and $\Delta r_{j-1/2}$ is the distance between nodes i,j,k and i,j−1,k (in units of L).

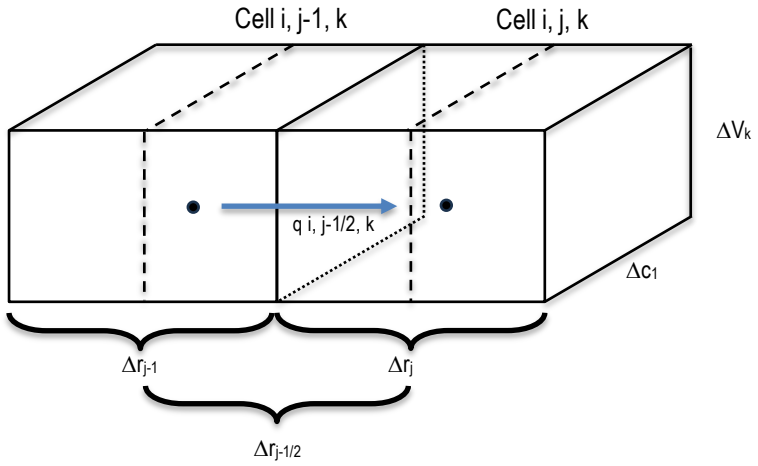

Figure 3.20 Flow into cell i,j,k from cell i,j-1,k (Harbaugh, 2005).

Equation 5.5 represents the exact flow in a one-dimensional steady-state scenario through an aquifer block extending from node i, j−1, k to node i, j, k, with a cross-sectional area of $\Delta c_i \Delta V_k$. $KR_{i,\ j-1/2,\ k}$ is the hydraulic conductivity of the material between nodes i,j,k and i,j−1,k, which reflects the effective conductivity for the entire region between these nodes.

The finite-difference method is commonly used for 3D groundwater flow modelling, forming the foundation for tools like MODFLOW. These models are essential for simulating complex groundwater systems. They play a critical role in analysing groundwater dynamics, assessing environmental impacts, and managing water resources under various hydrological conditions and human activities.

3.5.2.3 Model calibration

Calibration is one of the most critical and challenging processes in the modelling process. In some cases, hydrogeological complexities, and the lack of field data, either temporal or spatial, lead to uncertainty in the model. All input data parameters such as hydraulic conductivity, specific storage, and recharge rate are considered uncertain parameters so that the calibration process can be carried out on these parameters.

Instead of manual calibration, automatic calibration of the model parameters will be performed using a model-independent parameter estimator, PEST. To some extent, manual calibration is subjective and highly time-consuming. Methods of automatic calibration can improve these drawbacks.

PEST is a nonlinear parameter estimation and optimization tool designed to work with various models independently (Doherty, 2015). It determines the optimal parameter values by minimizing the sum of squared differences between observed and simulated results. PEST adjusts parameter values within predefined upper and lower bounds, systematically refining them until the model-generated hydraulic heads closely match observed values. This iterative optimization process enhances the accuracy and reliability of the groundwater model, ensuring a better fit between simulated and measured data.

MODFLOW requires the specification of numerous model parameters during setup, which are typically derived from field data, including aquifer hydraulic properties, groundwater recharge rates, and pumping data. However, comprehensive field data are often limited, making it challenging to define all parameters with high confidence. PEST is employed to optimize parameter estimation by identifying the best combination of selected parameters through sensitivity analysis. Nevertheless, a thorough understanding of the hydrogeological conditions of the study area is crucial to ensure that the estimated parameters remain realistic and consistent with field conditions. Beyond parameter specification, executing PEST involves a series of essential steps, including the following:

1. **Define Parameters and observational Data**

   In model calibration, it is essential to determine which parameters will be calibrated. These calibrated parameters are input parameters considered the most critical and sensitive within the model. Before executing PEST, key model parameters that influence groundwater flow are identified and selected for calibration. These parameters are chosen based on their relevance to groundwater dynamics and their sensitivity to model performance.

   Hydraulic conductivity is the primary parameter targeted for calibration in this model. It is arguably the most critical hydrogeological parameter, as it governs

fluid movement and the spread of contaminants below the ground surface, particularly in soils and aquifers (Peiyue Li, 2014). This assumption is based on the premise that hydraulic conductivity is more sensitive compared to other parameters, as demonstrated in numerous studies, including those by Alizadeh et al (2024), Albers et al (2020), and Slooten et al (2010).

Observational datasets, specifically groundwater level measurements from monitoring wells, are incorporated as reference points for calibration. These data serve as benchmarks for assessing the accuracy of the simulated groundwater flow.

2. **Sensitivity analysis**

PEST conducts a sensitivity analysis to determine which parameters exert the most significant influence on model outputs. Identifying these parameters helps prioritize adjustments, ensuring an efficient and effective calibration process.

Sensitivity analysis offers users of mathematical and simulation models a way to understand how changes in model inputs influence the model outputs (looss & Saltelli, 2016). Key benefits of well-conducted sensitivity analysis include:

- **Identify Key Influential Parameters.** Sensitivity analysis can help determine the parameters that most influence the model outcomes. This information is valuable for improving model accuracy by focusing on the most critical parameters.
- **Enhance Model Calibration.** Sensitivity analysis assists in model calibration by identifying which parameters require refinement. Focusing on the most sensitive parameters can help ensure that model predictions align with field observations.

3. **Optimization Iterations and Validation**

PEST systematically refines the selected parameters by executing multiple model runs, modifying parameter values within predefined ranges. The optimization process aims to minimize the objective function by reducing discrepancies between simulated and observed groundwater levels.

Once the calibration error falls within an acceptable threshold, the final set of optimized parameters is obtained. The calibrated model is then validated by comparing its outputs against an independent groundwater level dataset, ensuring its reliability before application in predictive scenarios.

The purpose of calibration is to minimise the objective function (Φ) as the sum of the weighted squared deviations between the calculated (X_{calc}) and observed (X_{obs}) system responses and is ultimately a function of the defined Parameters (p_j). The difference between the calculated and observed values is indicated as a residual and shown in the following equation:

$$r_i = X_{calc} - X_{obs} \qquad \textit{Eq 3.6}$$

The objective function is obtained using the following equation:

$$\Phi = \sum_i^n \min (r_i) = f(p_j) \qquad \textit{Eq 3.7}$$

3.5.2.4 Subsidence package and the governing equations

The next step involves simulating land subsidence by activating the subsidence module (SUB) in MODFLOW-2005. This module is specifically designed to model land subsidence resulting from the compaction of aquifer systems due to groundwater withdrawal. The simulation process is based on the principle of effective stress and the theory of porous media consolidation, which describe how reductions in pore water pressure lead to gradual compaction of compressible subsurface materials.

The following section provides a detailed explanation of the equations governing land subsidence modeling in the SUB module, outlining the mathematical framework used to quantify subsidence processes within the study area.

Settlement occurs when the effective stress in the soil increases due to a reduction in pore pressure (air pressure) in an aquifer system (Shen & Xu, 2011). The effective stress principle can be expressed as:

$$\sigma' = \sigma - \gamma_w H \qquad \textit{Eq. 3.8}$$

Where:

- σ′ is the effective stress.

- σ is the total stress
- γ_w is the unit weight of water
- H is hydraulic head

When the groundwater level decreases, σ' will change along with the hydraulic head.

$$d\sigma' = d\sigma - \gamma_w dH \qquad \textit{Eq. 3.9}$$

Based on Terzaghi's 1D consolidation theory, during the withdrawal and (or) recharge of groundwater from the aquifer, the total vertical **stress** is constant and thus:

$$d\sigma' = -\gamma_w dH \qquad \textit{Eq. 3.10}$$

The relationship between stress increase and strain increase is expressed as

$$d\varepsilon = -m_v d\sigma' \qquad \textit{Eq. 3.11}$$

where mv is the oedometric compressibility coefficient of the soil.

Combining eqs. [3] and [4], the following relationship between strain change and change of hydraulic head with time is obtained:

$$\frac{\partial \varepsilon}{\partial t} = \gamma_w m_v \frac{\partial H}{\partial t} \qquad \textit{Eq. 3.12}$$

As these equations illustrate, groundwater withdrawal causes a drop in the aquifer pressure head, a decrease in hydraulic head, and an increase in effective stress. This process causes soil consolidation, which, when transmitted to the surface, leads to land subsidence.

3.5.3 Application of the numerical model

The application of the model is focused on predicting a calibrated flow model into several scenarios, such as projections related to climate change and urban development, including changes in land use and increased groundwater abstraction.

3.5.3.1 Recharge estimation based on land-use and climate change

Based on the explanation in the literature review, land-use changes will directly impact groundwater recharge. So, it is necessary to carry out the scenario of land-use change prediction to calculate groundwater recharge, which is the primary input in the integrate (groundwater flow and subsidence) modelling.

The Soil Water and Assessment Tool (SWAT) is a proper modelling tool that can be used to analyse the effects of land-use change on groundwater recharge (Arnold & Fohrer, 2005). SWAT simulates the physical characteristics and processes related to land-use and groundwater recharge and can estimate groundwater recharge rates over an extensive range of scales.

SWAT is applied to predict changes in groundwater recharge based on scenarios of land-use and temperature change. These changes in groundwater recharge serve as the primary input for the subsidence model, allowing for an assessment of their impact on subsidence rates in the study area.

1. Scenario I

   The first scenario relates to climate change. The scenario plans used in this research are based on temperature changes from the Special Report on Emission Scenarios (SRES) A1F1 and B1 issued by the IPCC (Reay et al., 2007) for Southeast Asian countries. The A1F1 scenario represents the highest emissions, characterised by intensive fossil fuel use, while the B1 scenario represents the lowest emissions, based on clean and efficient technology. The temperature change patterns in these scenarios will be used in the calculation of evapotranspiration in the research area, enabling an estimation of groundwater recharge potential.

Table 3.4 Scenario of climate change in 2025 based on IPCC (2007)

Month	Changes of T (^{0}C)	
	Scenario A1F1	Scenario B1
December-January-February	0.86	0.72
March-April-May	0.92	0.8
June-July-August	0.83	0.74
September-October-November	0.85	0.75

2. Scenario II

   The second scenario is the 'Business as Usual' (BAU) of land use change. The change scenarios are compiled based on the percentage change in land cover from the last 20 years (Tanika et al., 2013). The pattern of changes produced in each land type will be the basis for determining land changes in the coming year.

3.5.3.2 Simulating the increasing groundwater abstraction

This simulation aims to assess the potential for land subsidence by estimating the growth of groundwater abstraction. Groundwater use through the construction of production wells across various sectors in the study area remains high, due to the limited coverage of piped water services managed by local authorities. As a result, predicting the growth of groundwater abstraction in the study area, as well as in other parts of Indonesia, presents a challenge. Groundwater abstraction growth scenarios are based on current regulations adopted by the Indonesian government, as well as predictive scenarios derived from abstraction volume increases observed in previous years.

3.5.4 Mitigation strategy to control subsidence

Mitigation encompasses actions to reduce or eliminate the severity of environmental and societal impacts associated with a particular phenomenon (Vilá et al., 2022). In the case of land subsidence, mitigation involves a series of strategic measures to prevent further subsidence and to manage its effects on the environment, infrastructure, and communities (Ye et al., 2016). Erkens and Stouthamer (2020) emphasize the “6M” framework as a fundamental approach to understanding and managing land subsidence, as summarized in Figure 3.21.

One component of the 6M framework is "Measures," which represents the implementation phase of mitigation efforts. The importance of predictive modeling is also highlighted in this context, as it provides projections of future subsidence patterns, facilitating the development of targeted prevention scenarios.

According to the main hypothesis and the findings of previous studies, intensive groundwater abstraction is a primary cause of subsidence in the Pekalongan area. However, other minor factors, such as natural compaction, contribute, particularly along the coastal regions. Enhanced groundwater management, integrated with stringent regulatory controls, can be integrated into the model through various scenarios to evaluate the effectiveness of the planned mitigation strategies.

Several mitigation models for controlling subsidence rates have been implemented in cities worldwide, most of which focus on improving water resource management,

particularly groundwater. Tokyo successfully reduced its subsidence rate from 24 cm/year to less than 1 cm/year over several decades through strict groundwater extraction regulation (Sato et al., 2006). In Thailand, the government aims to manage groundwater damage and slow subsidence rates by implementing groundwater pricing policies, expanding tap water networks, and strictly enforcing groundwater laws against violations (Phien-wej et al., 2006). While some mitigation efforts have proven highly effective, others have yet to achieve optimal outcomes in controlling subsidence.

Figure 3.21 The 6M approach to land subsidence (Bagheri-Gavkosh et al., 2021)

Additionally, Artificial Fluid Injection into geological formations represents a straightforward strategy to mitigate land subsidence by increasing pore pressure and decreasing effective stress, with the goal of halting subsidence and potentially causing land rebound or uplift (Gambolati & Teatini, 2021). A notable application of this method has been demonstrated in Venice, Italy, where seawater injection into geological formations was employed as a strategy to mitigate land subsidence and flooding (Gambolati & Teatini, 2013). Utilizing a hydrogeological model informed by comprehensive geological and lithostratigraphic analyses of the Venice Lagoon, P.

Teatini et al. (2011) projected that the injection of seawater into deep sandy formations (650–1000 m) through 12 wells could achieve a uniform uplift of 25–30 cm within a decade following the initiation of the injection process.

In the field of water resource management, Managed Aquifer Recharge (MAR) is a well-established strategy, particularly utilized in coastal regions susceptible to subsidence-related hazards. Teatini et al (2020) highlights MAR as an effective approach for addressing water resource depletion in the pre-Alpine aquifers—a productive unconfined aquifer system in the northern coastal region of Italy, characterized by multilayered Quaternary formations, allowing for the subsurface storage of approximately one cubic millimetre of water annually.

CHAPTER 4
Lithological Model and Aquifer Parameter Estimation

4.1 Introduction

This chapter presents the development of a comprehensive lithological data integration framework to construct a lithological model of the study area and estimate key aquifer parameters, specifically hydraulic conductivity and compressibility. Additionally, it explores the relationship between the lithological model and aquifer parameters. These elements are essential for groundwater flow and subsidence modeling, serving as critical input data for analyzing aquifer behavior and assessing the potential for land subsidence in the study area.

The lithological model is the foundation for constructing a conceptual hydrogeological model, generated using data from various sources such as geotechnical drilling, groundwater boreholes, and geoelectrical measurements. The established lithological model estimates hydraulic conductivity values, which is crucial for predicting groundwater movement through different aquifer layers. This chapter also explores the compressibility of each lithotype, a key parameter for assessing subsidence potential. Compressibility is estimated through laboratory testing of soil samples, with the results integrated into the model to enhance the accuracy of subsidence predictions.

4.2 Lithological data integration

The stages of lithological data integration are illustrated in Figure 4.1. These stages are each critical to developing a comprehensive and accurate lithological model, which forms the foundation for understanding the geological characteristics of the study area. Each step ensures that the lithological data is properly utilized and contributes to the overall reliability of the model.

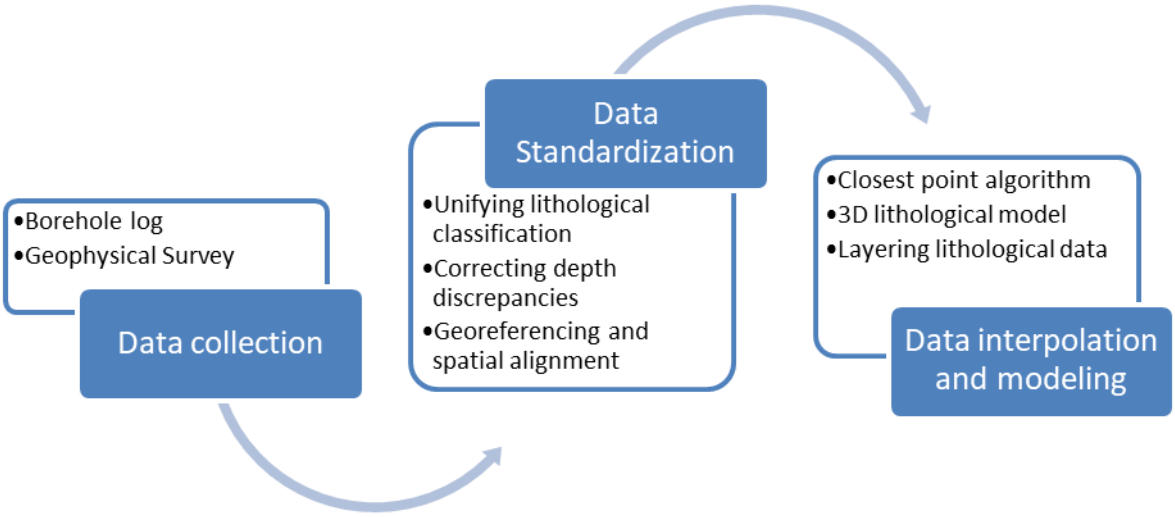

Figure 4.1 Illustration of the stages in lithological data integration

4.2.1 Data collection

Integrating lithological data from diverse sources is essential for accurately capturing subsurface conditions in the groundwater model. The process begins with data collection from multiple sources, including field measurements and existing studies, ensuring a comprehensive and reliable dataset for model development.

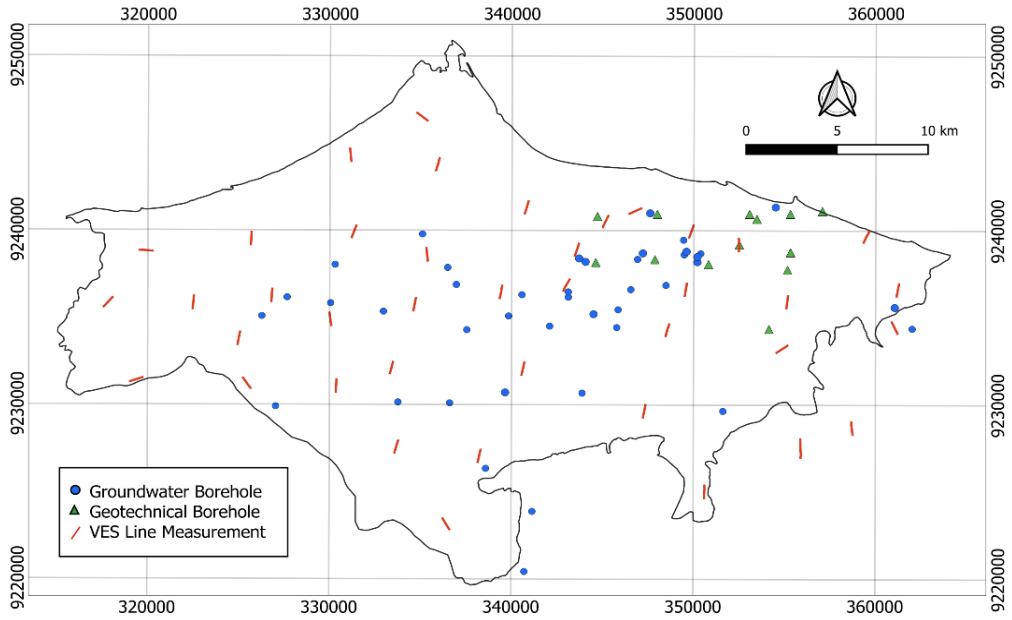

Figure 4.2 Map showing the distribution of locations of previously available data

- Geotechnical drilling

This drilling is conducted using the coring method to a maximum depth of 130 meters to obtain core samples that can be accurately described according to depth. Undisturbed samples are also taken at selected depths for laboratory testing of soil parameters.

- Groundwater boreholes

The primary objective of this drilling is to provide clean water from groundwater sources. The drilling is performed using the open hole method, which produces cutting samples that are then described to determine the lithology type. Naturally, the accuracy of lithological descriptions from this drilling is not as high as that from geotechnical drilling. Figure 4.3 shows the strip log of borehole lithology from both groundwater drilling and geotechnical drilling.

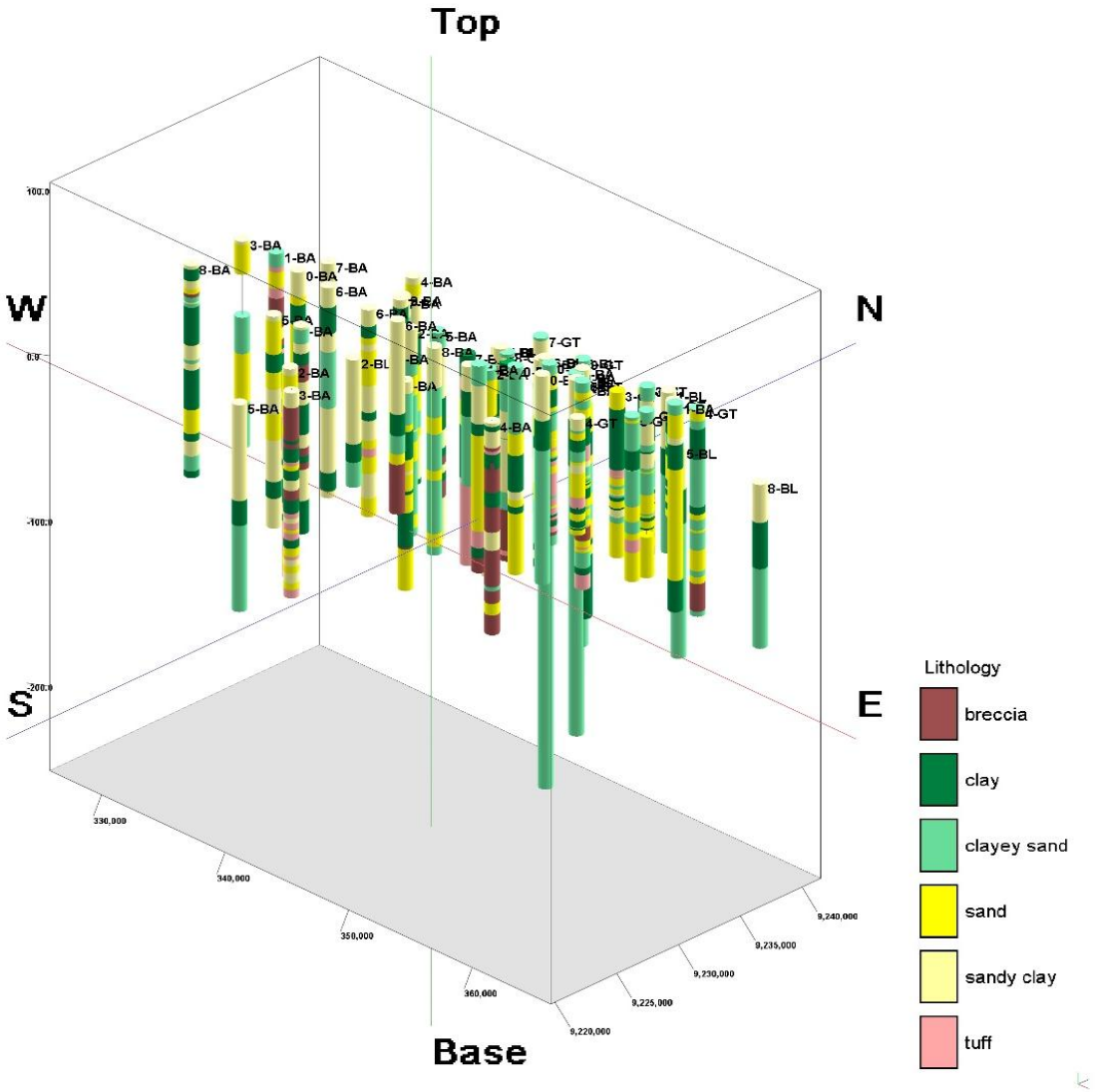

Figure 4.3 3D strip-log of borehole lithology in the study area

- Geoelectrical measurement

This measurement method generates several resistivity cross-sections within the study area, with lithological data interpreted from the resistivity results. The fence diagram of resistivity cross-sections derived from the geoelectrical measurements is presented in Figure 4.4. Iso-resistivity maps for each depth can be found in Appendix 1 at the end of this thesis.

Based on the lithological data from all sources, the layers in the research area vary widely with varying thicknesses, typically of alluvial of the lowland coastal area. Although it is dominated by sand and clay layers and a combination of those two, there is also a lithological volcanic layer, such as tuff and breccias, which appears in several boreholes and is also the result of resistivity interpretation.

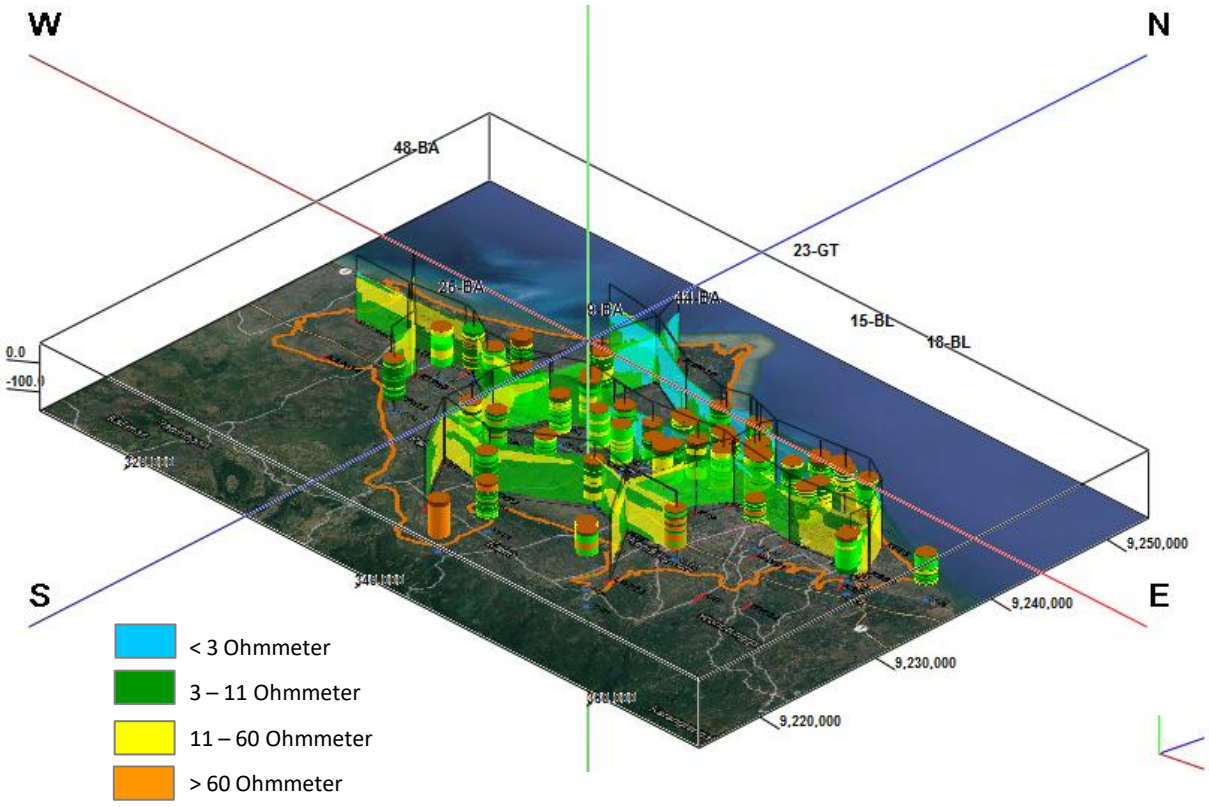

Figure 4.4 A fence diagram illustrating resistivity values derived from geoelectrical measurements alongside the distribution of borehole lithology represented in strip logs

4.2.2 Data standardization

Standardizing lithological data is a crucial step in ensuring consistency and accuracy when integrating information from diverse sources. Rock sample descriptions—

whether obtained from groundwater drilling, geotechnical borings, or geophysical resistivity interpretations—often follow different classification schemes and formats. Therefore, data alignment is necessary before conducting correlation, interpolation, and extrapolation to achieve a reliable subsurface representation.

The process begins with unifying lithological classifications, standardizing various terminologies based on grain size to ensure consistency across datasets. Additionally, borehole depth measurements must be corrected and aligned with Digital Elevation Model (DEM) data to account for surface elevation variations, ensuring an accurate representation of subsurface layer depths. Furthermore, geospatial information must be properly georeferenced, assigning precise coordinates to each borehole location and geophysical measurement point. By meticulously standardizing these parameters, the integration process minimizes errors and enhances the reliability of the resulting 3D geological model, ensuring an accurate representation of subsurface conditions.

4.2.3 Data interpolation and modelling

An interpolation method capable of producing a reliable model is required to obtain a lithological model. Lithological modelling relies on data interpolation to accurately represent the spatial distribution (Guartán & Emery, 2021). *RockWorks* was selected software due to its user-friendly interface, its capabilities in managing borehole and well log data, and its ability to provide various methods for gridding and interpolating borehole data to construct a three-dimensional spatial model.

Several interpolation methods are commonly used in earth science, including kriging, inverse distance weighting (IDW), closest point (or nearest neighbours), and triangulation. The method suitable for lithology interpolation is the closest point algorithm, a straightforward algorithm that assigns the value of the nearest data point to unsampled locations. This method does not create smooth transitions between points but maintains sharp boundaries, which is desirable for categorical data such as lithological units (Fuentes et al., 2020). The resolution of the resulting grid model is 10x10 meters with a depth of 130 meters, matching the maximum depth of the borehole data.

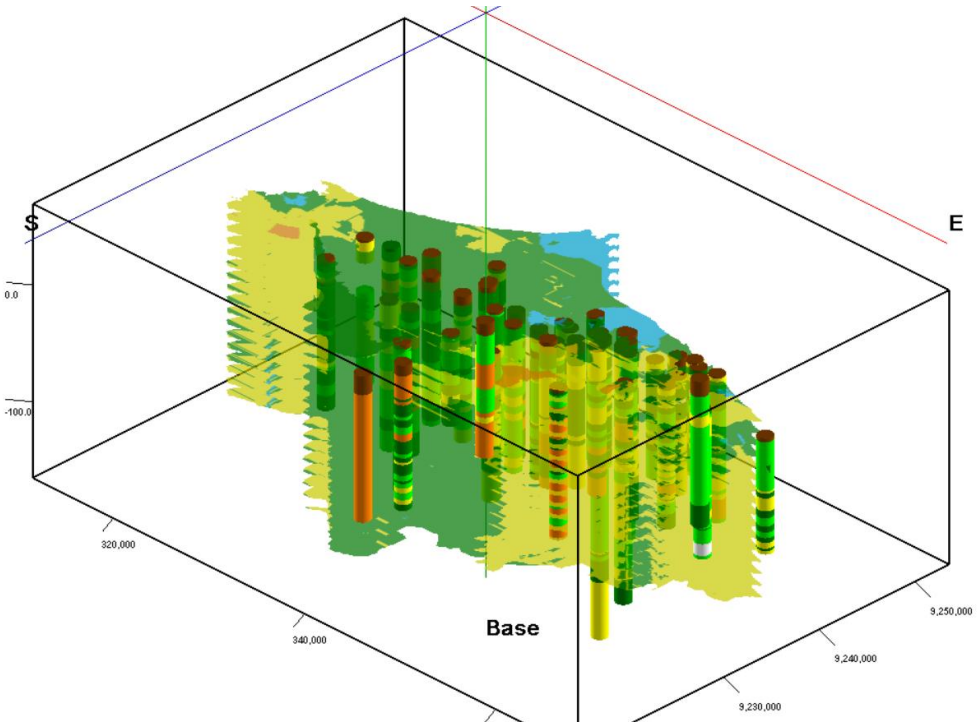

Figure 4.5. An illustration of 13 layers with a resolution of 10x10 meters, generated from the lithology model

The lithological model is the first step in the development of the hydrogeological conceptual model. This work is carried out based on lithological data obtained from previous data. More detailed data is needed to complete the hydrogeological conceptual model, especially aquifer parameter data, which is the primary basis for hydrogeological analysis.

4.3 Hydraulic conductivity estimation

4.3.1 Hydraulic conductivity of pumping test results

As explained in the previous chapter, the pumping test is the primary data collection method for obtaining hydraulic conductivity values in the study area. Testing was conducted at 21 locations throughout the study area, with the location map provided in Figure 3.13 in Section 3.4.2. The data and analysis for all wells can be found in the appendix, while the result of pumping test is shown in Table 4.1.

The results of the pumping test were analysed using the Cooper-Jacob straight-line method, a simplification of the Theis solution (Halford & Kuniansky, 2002).This method was developed to be applicable to a single test well. In the Cooper-Jacob straight-line method, drawdown is represented on the y-axis with an arithmetic

scale, while time is displayed on the x-axis with a logarithmic scale. Transmissivity (T) is calculated based on the pumping rate (Q) and the change in drawdown for each logarithmic cycle (Δs), from the following equation:

$$T = \frac{2.3Q}{4\pi\Delta s} \qquad \textit{Eq 4.1}$$

Meanwhile, the hydraulic conductivity value is obtained using the formula:

$$K = \frac{T}{b} \qquad \textit{Eq 4.2}$$

where b is the aquifer thickness.

Table 4.1 Transmissivity and hydraulic conductivity values derived from pumping test analysis

No	Well Location	X	Y	Parameter Results	
				T	K
				m²/day	m/day
1	SB 02 Desa Ujung Gede	109.52434	-6.90144	65.96	0.94
2	SB 03 Desa Serang	109.44015	-6.90785	62.25	0.76
3	SB 05 Pedurungan	109.41558	-6.90547	42.74	1.10
4	SB 06 Desa Tegalsari Barat	109.43436	-6.96436	5.02	0.08
5	SB 08 Desa Sukorejo	109.55690	-6.90681	32.52	0.82
6	SB 09 TengengWetan	109.57997	-6.90810	21.37	0.30
7	SB 10 Desa Kadipaten	109.60402	-6.92386	79.90	1.77
8	SB 11 Pendowo	109.52948	-6.92491	3.99	0.06
9	SB 12 Kampil	109.61106	-6.90419	85.47	1.13
10	SB 13 Kauman	109.61443	-6.88852	28.80	0.40
11	SB 14 PT. Candimekar	109.50034	-6.90039	566.71	7.62
12	SB 16 Sidokare	109.50750	-6.87525	2.51	0.03
13	SB 17 Desa Kradon	109.53878	-6.99685	195.10	2.35
14	SB 18 Desa Sangkanjoyo	109.56183	-7.01919	69.68	1.95
15	SB 19 Desa Kedungwuni Timur	109.65679	-6.96735	37.16	0.94
16	SB 20 Harjosari	109.65777	-7.03758	7.25	0.10
17	SB 21 Desa Bener	109.63765	-6.88619	42.74	1.10
18	SB 22 Desa Wonosari	109.60608	-7.00181	25.08	0.52
19	SB 23 Desa Bulaksari	109.52092	-6.96289	31.59	0.67
20	SB 24 Sragi	109.57069	-6.92308	139.35	1.83
21	SB 25 Dadirejo	109.62856	-6.90198	41.81	0.55

4.3.2 Hydraulic conductivity on lithotype

Based on the analysis of the lithological model, there are six lithotypes in the study area: (1) clay, (2) sandy clay, (3) clayey sand, (4) sand, (5) breccia, and (6) tuff. The block model reveals a relatively thick clay layer in the northeastern part, particularly at depths of 30-50 meters below mean sea level, which gradually thins out and

disappears towards the west. Thirteen maps displaying the distribution of lithotypes, ranging from layer 1 (0-10 m) to layer 13 (120-130 m), have been generated, as illustrated in Figure 4.5.

The primary assumption of this study is that each lithotype in this groundwater basin possesses uniform properties and characteristics. Consequently, each lithotype is assigned a single value for each aquifer parameter. The distribution and variation of lithotypes also reflect the distribution and variation of aquifer parameters. Identifying the lithotype is crucial to clearly determining the distribution of values for hydraulic conductivity (K) and compressibility (mv), which are the key parameters in this study. The availability of lithological information in the pumping test well is crucial for analysing the relationship between the hydraulic conductivity (K) derived from pumping test and the lithology of each well.

In this study, each lithology is assumed to represent a distinct lithotype with uniform characteristics, allowing a single hydraulic conductivity (K) value and consistent parameter values to be assigned to each lithotype. The lithological composition of each pumping test well is detailed in Table 4.2. The pumping test analysis focuses on lithologies located below a depth of 40 meters. This assumption is based on well construction data from the study area, which indicates that well screens are typically installed at depths of 40–100 meters, while the upper 0–40 meters are sealed or not utilized for groundwater extraction

Table 4.2 Lithological composition in thickness (m) of each pumping test well

Lithotype	Symbol	1	2	3	4	5	6	7	8	9	10	11	12	13	14	15	16	17	18	19	20	21
sand	W1	17	23	19	8	17	15	24	17	23	25	54	9	25	35	21	10	25	19	17	32	14
clay	W2	32	23	32	34	24	32	23	37	32	19	12	43	19	14	12	34	34	13	27	34	24
clayey sand	W3	19	13	19	21	11	11	3	11	13	6	3	13	34	17	3	21	13	19	11	23	2
sandy clay	W4	23	3	12	13	14	18	34	7	28	16	7	19	9	17	15	12	15	10	12	0	15
breccia	W5	0	8	8	0	15	4	12	0	0	0	0	0	0	0	24	0	0	0	13	0	26
tuff	W6	12	0	0	0	0	0	13	10	8	0	0	0	14	23	7	0	0	23	0	0	0

With six categories of lithotype and 21 wells, the hydraulic conductivity (K) values for each lithotype are calculated using a least-square regression method. The matrix for this calculation is as follows:

$$\begin{bmatrix} W_{11} & \cdots & W_{1n} \\ \vdots & \ddots & \vdots \\ W_{nw1} & \cdots & W_{nwn} \end{bmatrix} \begin{bmatrix} K_1 \\ \vdots \\ K_n \end{bmatrix} = \begin{bmatrix} \overline{K}_1 \\ \vdots \\ \overline{K}_{nw} \end{bmatrix} \qquad \textit{Eq 4.3}$$

By applying matrix multiplication in MATLAB, the hydraulic conductivity (K) values for each of the six lithotypes were obtained, as shown in Table 4.3.

As observed in the K values for the lithotypes above, there are negative values for clay and sandy clay. To address this, lower and upper bounds for each lithotype are necessary to ensure that the K values obtained remain within the acceptable range for each lithology (Table 4.4).

Table 4.3 Single K Value of lithotypes (unbounded version)

Lithotype	K (unbounded) (m/day)
sand	0.033246
clay	-0.001395
clayed sand	0.009586
sandy clay	-0.014191
breccia	0.016283
tuff	0.019954

The range of K values for each lithology or lithotype is derived from the book *Applied Hydrogeology* by Fetter (2014). The experiments for determining intrinsic permeability and hydraulic conductivity in this book were conducted on samples of unconsolidated sediments from alluvial deposit locations, which are similar to the study area type.

Table 4.4 Lower and upper bound for each lithotype

Lithotype	m/day	
	Lower Bound	Upper Bound
sand	7.78E-02	5.18E+02
clay	8.64E-05	1.06E-03
clayed sand	1.73E-02	1.73E+01
sandy clay	8.64E-04	1.73E+00
breccia	6.91E-04	2.59E+01
tufa	1.73E-02	4.32E+01

By applying Equation 4.3 and incorporating the lower and upper bounds for each lithotype as shown in Table 4.4, the hydraulic conductivity (K) values for each lithotype were obtained, as presented in Table 4.5.

Table 4.5 Single K Value of lithotypes (bounded version)

Lithotype	Kx
	m/day
Sand	1.05E-01
Clay	1.81E-03
Clayey sand	4.17E-02
Sandy clay	6.22E-03
Breccia	7.99E-02

With the hydraulic conductivity (K) values for each lithotype in the study area now established, these values are systematically integrated into the lithological model to ensure consistency in the groundwater flow simulation. This process involves assigning specific K values to each lithological unit within the model layers, accurately reflecting the hydraulic properties of the aquifer materials.

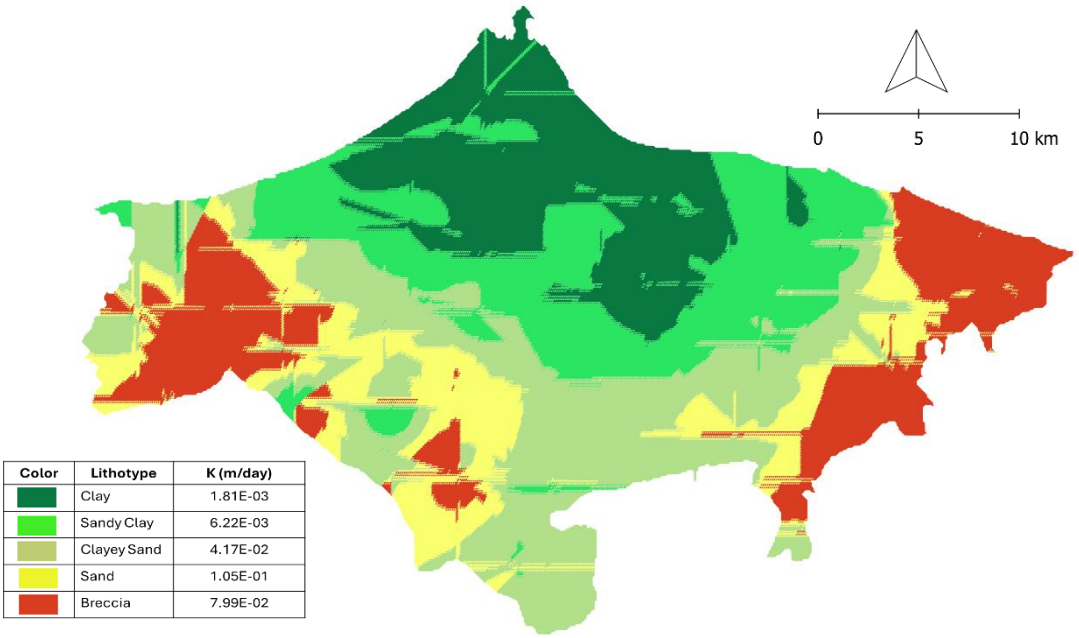

Figure 4.6. Map of lithotype and K distribution of layer 8, in 10x10 m resolution

The binding process begins by classifying each grid cell in the lithological model according to its corresponding lithotype. Once these units are identified, predefined K values are assigned to each lithological type. This step ensures that spatial variations in hydraulic conductivity are properly represented across all model layers, maintaining the integrity of the groundwater flow simulation. To implement this in a GIS environment, QGIS is used to generate 13 spatial maps, each depicting the distribution of K values at specific depth intervals, ranging from layer 1 (0–10 m) to layer 13 (120–130 m), as illustrated in Figure 4.5. Additionally, Figure 4.6 highlights

the K value distribution for layer 8 (70–80 m depth), providing a more detailed assessment of spatial variations in hydraulic conductivity at a critical depth interval.

By systematically integrating K values into the lithological model, this approach ensures a realistic and spatially coherent representation of hydraulic conductivity distributions. This integration is essential for improving the accuracy and reliability of MODFLOW simulations, allowing for more precise modelling of groundwater flow and subsidence processes in the study area.

4.4 Compressibility and specific storage calculations

4.4.1 Compressibility estimation

As discussed in the previous section, the Geological Agency of Indonesia has conducted a series of geotechnical drilling operations at several locations within the Pekalongan Groundwater Basin. The physical and mechanical properties of the soil samples, representing different depths, were subsequently analyzed in the laboratory. These analyses included *Particle Size Distribution Tests* and *Consolidation Tests*. The results from these laboratory tests provide essential data for understanding the soil characteristics and are available in the appendices of this thesis.

The proportion of clay and sand within each sample was determined through Particle Size Distribution Analysis, allowing for a detailed breakdown of the soil's textural composition. Consolidation Tests provided data on the soil's compressibility, with the coefficient of volume compressibility (mv) measured in cm^2/kg. This parameter offers understandings into how much a specific soil layer will compact under the load of overlying strata and the increase of effective stress due to aquifer over-exploitation.

Table 4.6 summarizes the compressibility and size distribution values for each sample, derived from the detailed results of these tests. These two parameters are essential for calculating the compressibility value for each lithotype. Additionally, Table 4.6 shows that the available compressibility data extends only to a maximum depth of 50 meters. Therefore, a modeling approach is necessary to estimate values beyond this depth using the available data, as explained in the following section.

Table 4.6 Data of compressibility (mv) and size distribution of selected samples

Well No	Depth		Compressibility		Size Distribution	
	From	To			Sand	Clay
	(m)		cm/kg2	pa-1	%	
SPPT-01	11.00	11.50	0.037802	3.85E-07	18.97	81.03
	17.00	17.50	0.04194	4.28E-07	22.34	77.66
	25.00	25.50	0.015393	1.57E-07	34.25	65.75
	37.00	37.50	0.017181	1.75E-07	21.00	79.00
	43.00	43.50	0.016461	1.68E-07	12.42	87.58
	49.00	49.50	0.026755	2.73E-07	45.47	54.53
SPPT-02	7.00	7.50	0.013067	1.33E-07	58.91	41.09
	13.00	13.50	0.020348	2.07E-07	13.49	86.51
	23.00	23.50	0.036774	3.75E-07	18.66	81.34
	31.00	31.50	0.028505	2.91E-07	21.65	78.35
	39.00	39.50	0.01748	1.78E-07	16.71	83.29
	45.00	45.50	0.020103	2.05E-07	27.82	72.18
SPPT-03	11.00	11.50	0.041599	4.24E-07	15.50	84.50
	15.00	15.50	0.076642	7.82E-07	12.89	87.11
	27.00	27.50	0.026559	2.71E-07	29.40	70.60
	33.00	33.50	0.013186	1.34E-07	17.36	82.64
	41.00	41.50	0.02593	2.64E-07	37.11	62.89
	49.00	49.50	0.022974	2.34E-07	30.97	69.03
SPPT-07	7.00	7.50	0.033121	3.38E-07	19.74	80.26
	15.00	15.50	0.037833	3.86E-07	26.88	73.12
	23.00	23.50	0.020312	2.07E-07	13.82	86.18
	31.00	31.50	0.025075	2.56E-07	34.32	65.68
	39.00	39.50	0.024109	2.46E-07	26.13	73.87
	49.00	49.50	0.009811	1E-07	92.45	7.55
SPPT-05	3.00	3.55	0.030115	3.07E-07	41.79	58.21
	13.00	13.55	0.031003	3.16E-07	26.65	73.35
	21.00	21.55	0.030425	3.1E-07	21.60	78.40
	33.00	33.55	0.019296	1.97E-07	28.91	71.09
	41.00	41.55	0.036935	3.77E-07	21.51	78.49
	49.50	50.00	0.015258	1.56E-07	24.57	75.43
SPPT-06	3.00	3.50	0.038166	3.89E-07	18.53	81.47
	19.00	19.50	0.049484	5.05E-07	9.46	90.54
	23.00	23.50	0.016066	1.64E-07	26.85	73.15
	35.00	35.50	0.019427	1.98E-07	29.55	70.45
	43.00	43.50	0.023436	2.39E-07	18.07	81.93
	49.00	49.50	0.017657	1.8E-07	23.65	76.35

The compressibility is a weighted average of compressibility of sand and clay material while the weights are the percentage of mass of the two components of the sample, the illustration can be seen in Figure 4.7.

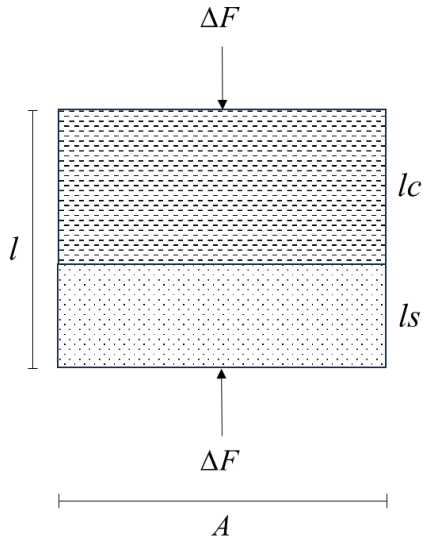

Figure 4.7 The illustration of compressibility in sand and clay layer

From the above illustration, we know that $l = l_c + l_s$ dan $\Delta l = \Delta l_c + \Delta l_s$ and $\Delta\sigma = \frac{\Delta F}{A}$, so the compressibility (mv) can be calculated as $mv_c = \frac{\Delta l_c}{l_c\,\Delta\sigma}\, mv_s$, $\frac{\Delta l_s}{l_s\,\Delta\sigma}$ and $mv = \frac{\Delta l}{l\Delta\sigma}$

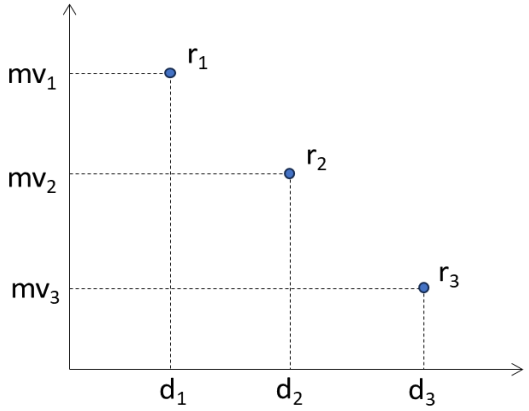

Figure 4.8. The illustration of mv data for samples in a different depth

If $r = \frac{l_s}{l}$, then $l_s = r.l$ and $l_c = (1-r).l$, so the values of mv_c dan mv_s are:

$$mv_c = \frac{\Delta l_c}{(1-r)\,l\,\Delta\sigma} \qquad \textit{Eq 4.4}$$

$$mv_s = \frac{\Delta l_s}{r\,l\,\Delta\sigma} \qquad \textit{Eq 4.5}$$

$$\text{and } mv = (1-r).mv_c + r.mv_s \qquad \textit{Eq 4.6}$$

Assuming we have a set of compressibility (mv) data from samples taken at various depths (d) and with different ratios (r), as illustrated in Figure 4.8, we will have the equation as follows:

$$mv(d,r) = (1-r)mv_c(d) + r.mv_s(d) \qquad \textit{Eq 4.7}$$

The separation between mv_c and mv_s from mv is not known for each data point. With one equation and two unknowns, the solution can be infinite. Therefore, we need to formulate the problem using non-linear least squares regression.

Assuming that mv_c and mv_s are exponential functions, they can be described with the following equations:

$$mv_c = a_c \cdot e^{-z/bc} \qquad \textit{Eq 4.8}$$

$$mv_s = a_s \cdot e^{-z/bs} \qquad \textit{Eq 4.9}$$

Where:

- mv_c is the compressibility for the clay component,
- mv_s is the compressibility for the sand component,
- a_c and a_s are compressibility coefficients derived of clay and sand model, respectively,
- b_c and b_s are the decay constants for clay and sand, respectively,
- z is the depth.

With the conditions:

$$\log mv_c = \log a_c - \frac{z}{b_c} = A_c - B_c.z \quad A_c, B_c > 0 \qquad \textit{Eq 4.10}$$

$$\log mv_s = \log a_s - \frac{z}{b_s} = A_s - B_s.z \quad A_s, B_s > 0 \qquad \textit{Eq 4.11}$$

To find the best-fit parameters (*ac, bc, as, and bs*), we minimize the residual sum of squares (R^2):

$$R = \sum_{i=1}^{n} \log mv_i - \log\left[(1-r_i).a_c.e^{-\frac{z_i}{bc}} + r_i.a_s.e^{-\frac{z_i}{bs}}\right] \qquad \textit{Eq 4.12}$$

$$R^2 = \sum_{i=1}^{n} \left\{ \frac{mv_i - \left[(1-r_i).a_c.e^{-\frac{z_i}{bc}} + r_i.a_s.e^{-\frac{z_i}{bs}}\right]}{mv_i} \right\}^2 \qquad \textit{Eq 4.13}$$

Based on the available data with a sample size of n, an exponential model has been derived, as shown in Figure 4.9.

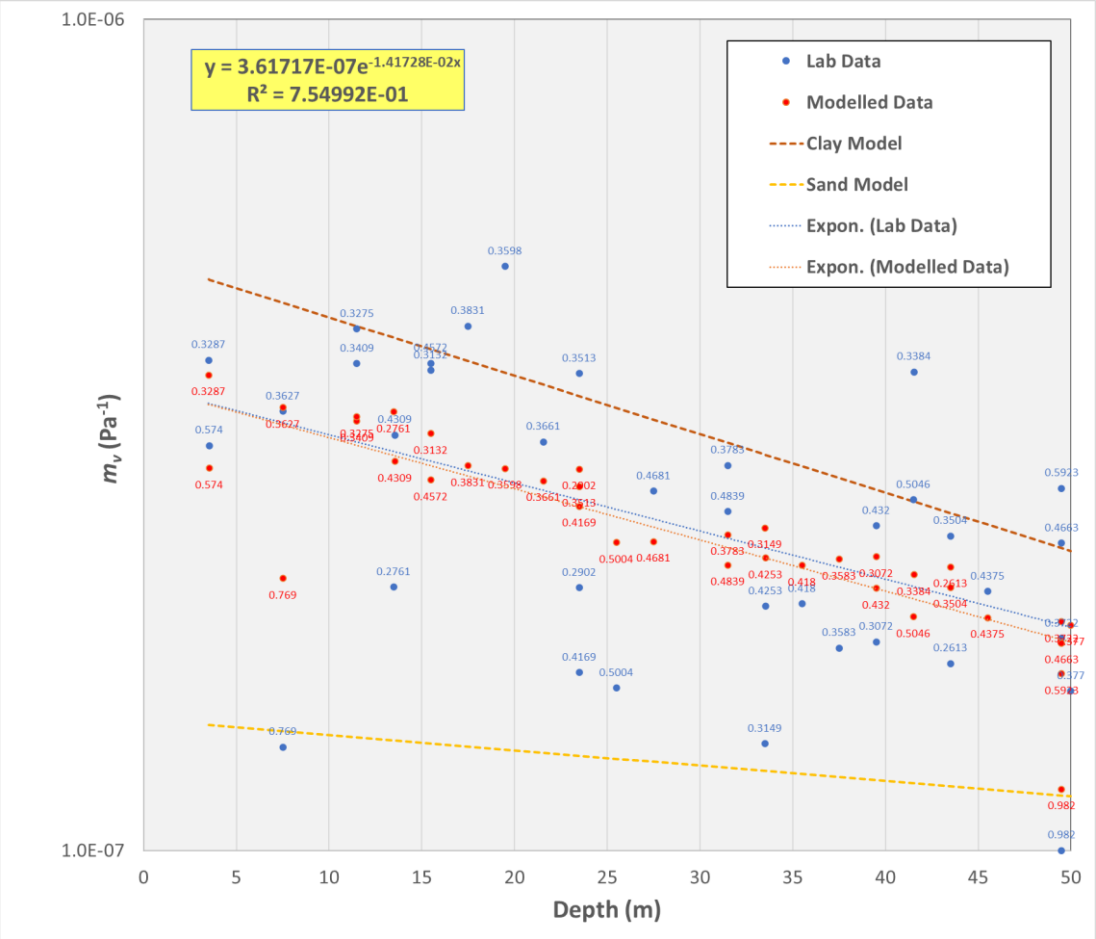

Figure 4.9 Data plotting dan exponential function model

By fitting the model to the data using exponential function regression, we can estimate the parameters include a_c, b_c, a_s, and b_s, also log (As), log (Ac), log (As), log (Bs) (Table 4.7)

Table 4.7 The exponential function model parameters

Parameter	Value	Parameter	Value
ac	5.15E-07	as	1.44E-07
bc	6.18E+01	bs	2.35E+02
log(ac)	-6.2880	log(as)	-6.8425
log(bc)	1.7908	log(as)	2.3715

From the parameters above and using equation 4.8 and 4.9, we obtain the equations to calculate mv_c and mv_s:

$$mv_c = 5.15 \cdot 10^{-7} \cdot e^{\frac{-z}{61.8}} \qquad \textit{Eq 4.14}$$

$$mv_s = 1.44 \cdot 10^{-7} \cdot e^{\frac{-z}{235.25}} \qquad \textit{Eq 4.15}$$

Assuming the sand ratio (r) for each lithotype as shown in Table 4.8, the mv values for each lithotype and layer can be calculated as presented in Table 4.9.

Table 4.8 Sand ratio (r) of each lithotype

Lithotype	Ratio (r)
sand	1.00
clayey sand	0.75
sandy clay	0.25
clay	0.00

Table 4.9 Calculated mv of each lithotype and layer

Layer	Lithotype	mv pa-1	Layer	Lithotype	mv pa-1	Layer	Lithotype	mv pa-1
1	sand	1.3775E-07	5	sand	1.1621E-07	9	sand	9.8035E-08
	clayey sand	2.1286E-07		clayey sand	1.4449E-07		clayey sand	1.0353E-07
	sandy clay	3.6309E-07		sandy clay	2.0105E-07		sandy clay	1.1452E-07
	clay	4.3820E-07		clay	2.2933E-07		clay	1.2002E-07
2	sand	1.3201E-07	6	sand	1.1137E-07	10	sand	9.3954E-08
	clayey sand	1.9219E-07		clayey sand	1.3229E-07		clayey sand	9.5986E-08
	sandy clay	3.1254E-07		sandy clay	1.7413E-07		sandy clay	1.0005E-07
	clay	3.7271E-07		clay	1.9506E-07		clay	1.0208E-07
3	sand	1.2652E-07	7	sand	1.0673E-07	11	sand	9.0044E-08
	clayey sand	1.7414E-07		clayey sand	1.2153E-07		clayey sand	8.9239E-08
	sandy clay	2.6939E-07		sandy clay	1.5111E-07		sandy clay	8.7630E-08
	clay	3.1701E-07		clay	1.6590E-07		clay	8.6825E-08
4	sand	1.2125E-07	8	sand	1.0229E-07	12	sand	8.6296E-08
	clayey sand	1.5835E-07		clayey sand	1.1200E-07		clayey sand	8.3184E-08
	sandy clay	2.3253E-07		sandy clay	1.3140E-07		sandy clay	7.6961E-08
	clay	2.6963E-07		clay	1.4111E-07		clay	7.3849E-08
						13	sand	8.2705E-08
							clayey sand	7.7731E-08
							sandy clay	6.7785E-08
							clay	6.2812E-08

After determining the compressibility values, the subsequent step involves calculating the specific storage values for each lithotype at different depths. This calculation facilitates the identification of the spatial distribution of specific storage, which serves as a crucial input for the model.

4.4.2 Specific storage calculation

Like hydraulic conductivity values, specific storage is calculated for each lithotype unit identified from the lithological model. Additionally, compressibility is the critical parameter used to calculate specific storage (Woessner & Poeter, 2023), following the formula:

$$Ss = \rho g(\alpha + n\beta) \qquad Eq\ 4.16$$

Where:

- ρ is the mass density of water (= 1000 kg/m³),
- g is gravitational acceleration (= 9.8 m/sec²) [L/T²],
- α is the compressibility of the aquifer's solid structure (m sec²/kg or Pa^{-1}) also referred to in the previous formula as mv
- n is the effective porosity [dimensionless], and
- β is the compressibility of water (= 4.4×10^{-10} m sec²/kg or Pa^{-1}).

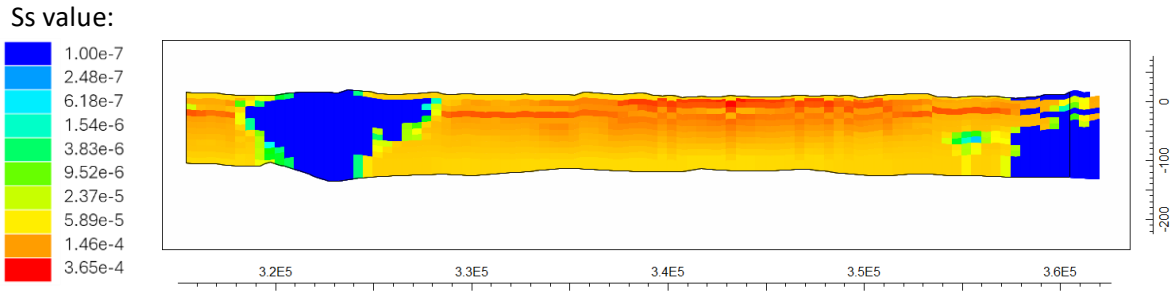

Figure 4.10 Vertical profile of specific storage in model area

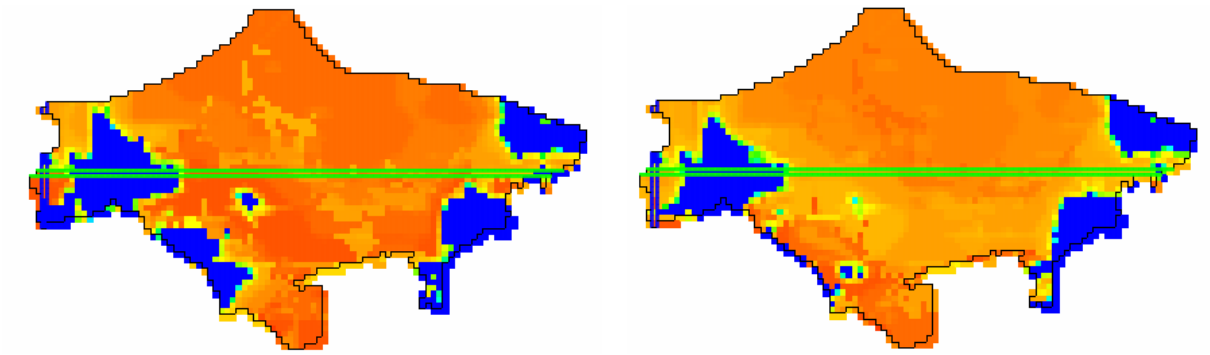

Figure 4.11 Specific storage of layer 6 and 7

The porosity values were obtained from referenced literature, supplemented by the average porosity measurements derived from laboratory testing of soil samples collected from various drilling locations. Using Equation 4.16, specific storage (Ss) was calculated for each layer of every lithotype. This process resulted in the spatial distribution of specific storage dengan profile vertical untuk row 29 (West-East) , as depicted in Figure 4.10. In addition, the specific storage values for layers 6 and 7 are presented in Figure 4.11.

4.5 Conclusion

This chapter applies a detailed lithological framework and groundwater flow parameters needed for groundwater flow and subsidence modelling for the study area. The lithological model comprises different input data (geotechnical drilling, ground water boreholes, geoelectrical measurements). Consequently, it could be deemed as a good basis for understanding the spatial distribution of subsurface materials. It is believed that major lithological variations throughout the model, like the clay-dominated northeast section of the model, will primarily control the results of the subsidence analysis.

The hydraulic conductivity and compressibility parameters obtained from field data collection and laboratory testing are integrated with the lithological model to assign values to each lithotype within the study area. As these parameters are critical for the accuracy of groundwater flow and subsidence models, meticulous calculation is essential. Moreover, defining hydraulic conductivity values for each lithotype significantly streamlines the calibration process.

CHAPTER 5

Implementation of A 3-D Groundwater Flow Model in A Tropical Coastal Region Using MODFLOW

5.1 Introduction

This chapter details the development and application of a 3-D groundwater flow model in the tropical coastal region of northern Java Island, Indonesia. The model is based on MODFLOW-2005, a numerical simulation tool developed by the US Geological Survey and employs Model Muse as the graphical user interface. Its primary focus is to simulate and predict groundwater flow.

The key components of this study include the construction of a conceptual hydrogeological model, the estimation of the aquifer and basement geometry, and the integration of boundary conditions into the numerical model. This chapter also covers the model calibration using transient conditions, utilising automated calibration techniques to optimise key parameters such as hydraulic conductivity. Furthermore, it discusses the use of SWAT modelling to estimate groundwater recharge, a crucial component in groundwater modelling.

The overall objective of this modelling is to provide insight into groundwater flow patterns, assess the potential for groundwater resource management, and predict the impact of land-use changes and groundwater abstraction on the region's water table. The results will help inform decisions on sustainable groundwater use, particularly in an area facing rapid industrial development and urbanization.

5.2 Hydrogeological conceptual model of the study area

The hydrogeological conceptual model is a fundamental tool for understanding the hydrogeological conditions of a region derived from collecting data from various sources within the study area. This model illustrates the key components of the hydrogeological system, including the types of geological layers, aquifer properties, water flow, and the interactions between these components. The conceptual model is the foundation for developing a more detailed numerical model, which will be applied to simulate and predict groundwater systems in specific locations.

Additionally, a well-developed hydrogeological conceptual model can serve as a basis for water resource planning and management, as well as for evaluating groundwater potential and assessing risks such as groundwater contamination and subsidence.

5.2.1 Top model

Topographic height data from DEM (Digital Elevation Model) data from SRTM (Shuttle Radar and Topography Mission) images with a resolution of 30 m are used for the Top Model in the grid design (Figure 5.1). Topographical elevation or land surface elevation with sea level as the data level controls various activities above and below the surface.

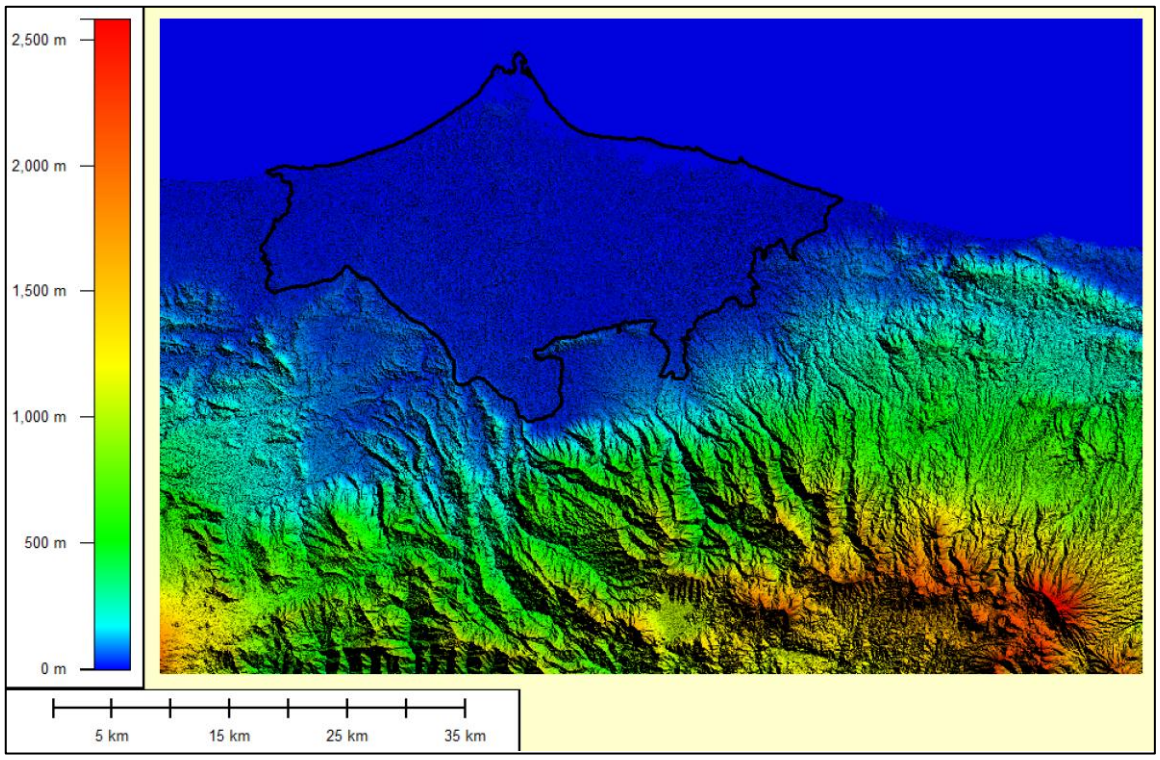

Figure 5.1 Digital Elevation Model (DEM) of the Study Area and surrounding region, which also serves as the Top Model for numerical modelling

As described in the chapter on the study area, the research site is a lowland region located along the northern coast of Java Island, with an elevation ranging from 0 metres above sea level at the coastline to 110 metres in the southern part. In general, the topography of this plain slopes gradually towards the north, with an average gradient of less than 5%. Several major rivers, such as the Comal, Sragi, and Pekalongan, exhibit a meandering flow pattern. Some of these rivers, particularly in

the central part of the plain, have been utilised for agricultural purposes through the construction of irrigation channels that intersect the rivers.

5.2.2 Basement and aquifer system geometry

As discussed in the previous chapter, the study area is an alluvial coastal region composed of young sediment deposits with five lithotypes. As is typical of coastal alluvial deposits, the aquifer in the study area consists of layers of young sediments with highly variable thicknesses, making distinguishing boundaries between different lithological types challenging.

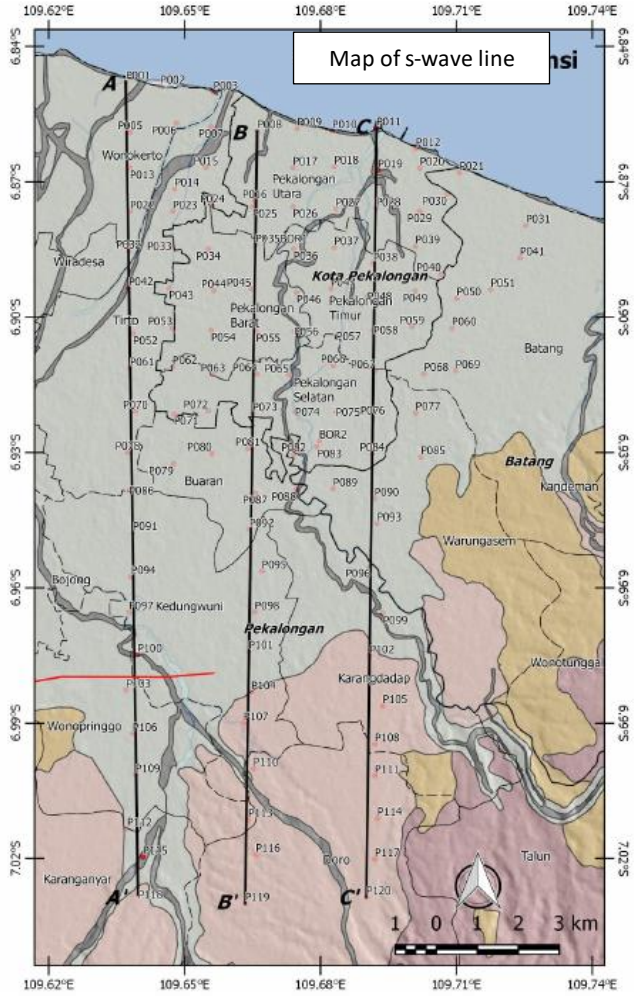

Figure 5.2 Map of S-Wave line measurement. The measurement path is located only in the eastern part of the study area.

Based on soil classification data derived from S-wave velocity measurements in part of the study area, the thickness of the soft layer has been determined, although only for the eastern portion of the study area (Figure 5.2). The interpretation of the soil

profile based on Shear Wave Velocity values can be seen in Table 5.1, with the results of the interpretation for the three measurement sections shown in Figure 5.3. Therefore, an estimation of the thickness distribution across the entire model area needs to be conducted through extrapolation, using the existing data and elevation data as a basis.

Table 5.1 Soil classification based on Vs30 Value (NEHRP)

Site Class	Soil Profile Name	Soil Shear Wave Velocity (Vs30)
		Meters/second
A	Hard Rock	Vs > 1500
B	Rock	760 < Vs ≤ 1500
C	Very dense soil and soft rock	360 < Vs ≤ 760
D	Stiff soil	180 < Vs ≤ 360
E	Soft Soil	Vs < 180

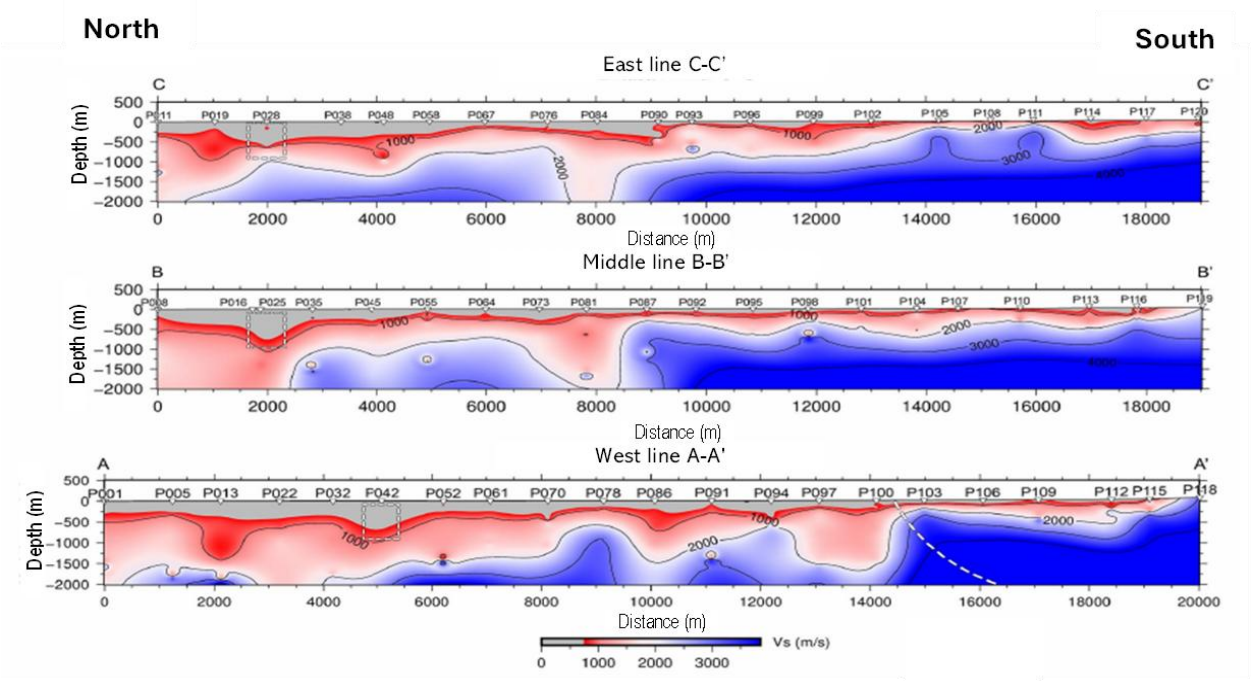

Figure 5.3 Profile of S wave velocity, interpreted from HSVR inversion

The next step involves extrapolating basement depth data across the study area to establish a comprehensive representation of subsurface conditions. Given the limited availability of direct data from deep boreholes or geophysical surveys, basement geometry must be extrapolated over a significant portion of the model domain. This extrapolation is essential for defining the lower boundary of the model, particularly in regions where subsurface data are sparse.

The process begins by generating additional, regularly spaced points in previously data-deficient areas, as shown in Figure 5.4.. The depth values at these points are estimated based on available shear wave measurement data, providing a structured approach to fill data gaps. Extrapolation is then performed using the nearest point interpolation method, also known as the nearest neighbor method, which assigns depth values to unmeasured areas based on the nearest available data points. This approach systematically extends discrete basement depth measurements across the study area, resulting in a spatial basement depth map, as shown in Figure 5.5. This map is a critical component of the hydrogeological conceptual model, as it defines the lower boundary of the aquifer system used in MODFLOW.

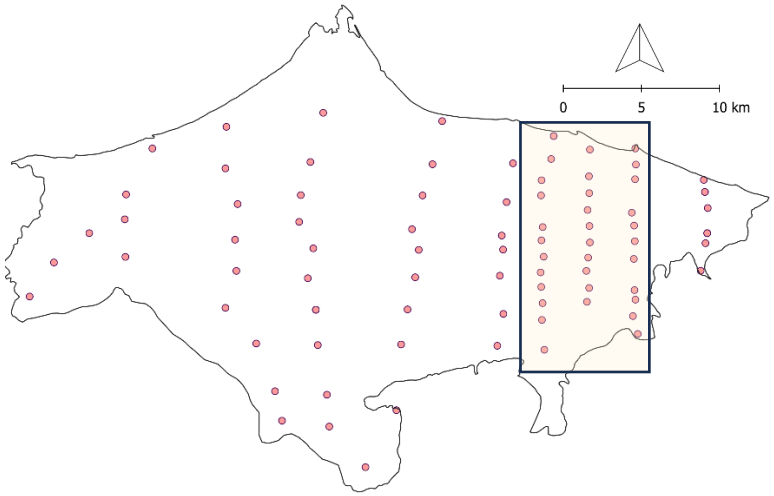

Figure 5.4 New additional points for extrapolating basement data and the available share wave of basement data in the yellow box

However, the reliance on extrapolation over large areas introduces uncertainties, particularly in regions with fewer control points, which may affect the accuracy of basement depth and geometry. These uncertainties can have significant implications for groundwater flow and subsidence models. If basement depth is overestimated or underestimated, it may alter hydraulic gradients and influence overall flow dynamics, potentially impacting model reliability and predictive accuracy.

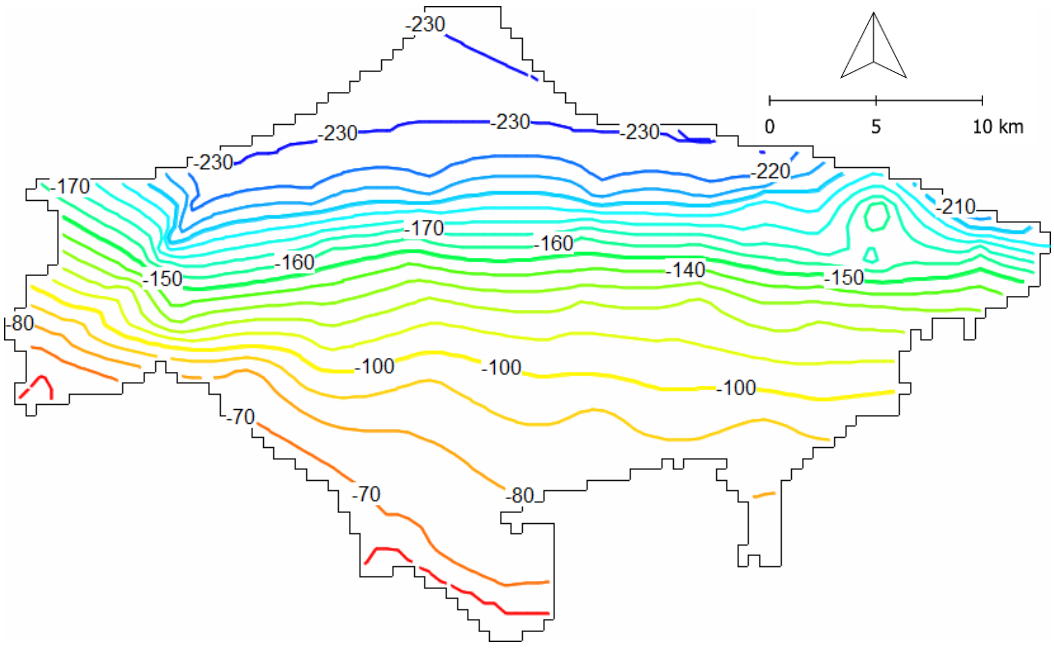

Figure 5.5 Contour map of basement of model area

5.2.3 Hydrogeological boundary conditions

Based on the analysis of various data sources, including geological maps, borehole lithology data, and geoelectric interpretation, the model area boundaries are defined by three types of boundaries as shown in Figure 5.6.

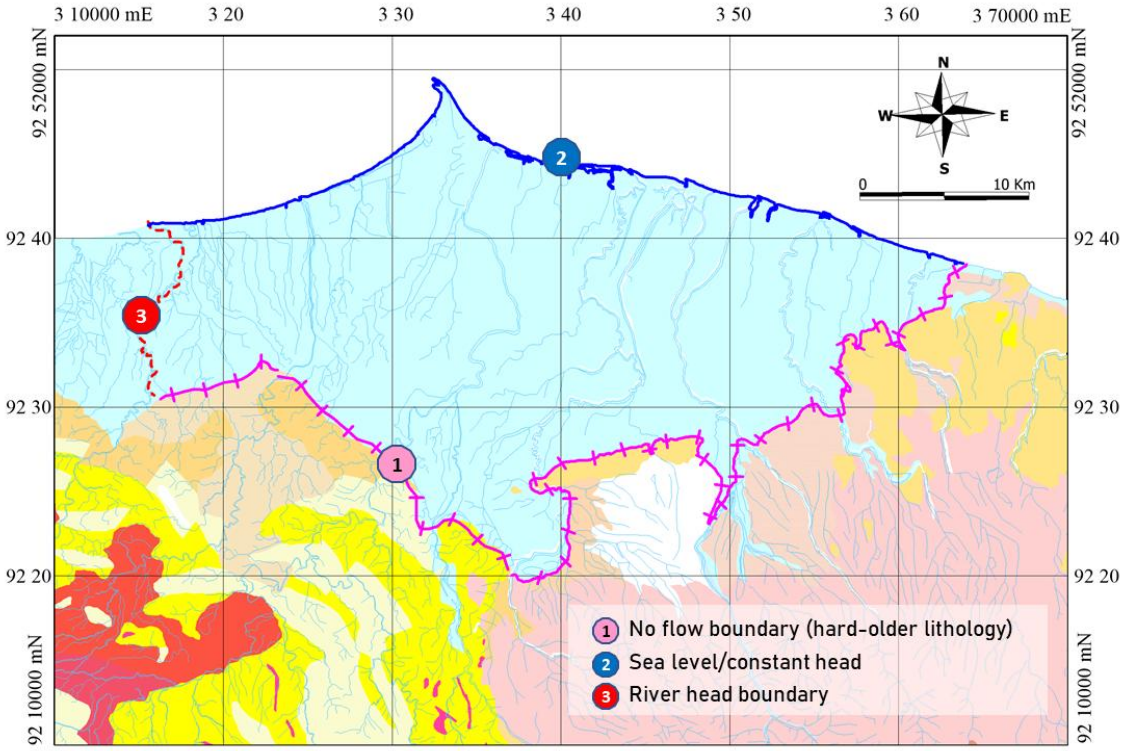

Figure 5.6 Types of hydrogeological boundary condition in the study area

- No flow boundary

  In the model area, the zero-flow boundary is the contact between the aquifer system and the basement aquifer to the south of the model area.
- Sea level

  This boundary is defined as the lateral boundary of the northern groundwater basin, namely the Java Sea coastline.
- River head boundary

  The river that define the model boundary are the primary rivers with permanent flow, characterized by a flow direction that is relatively perpendicular to the coastline.

5.2.4 Grid model design

The purpose of making a grid model design is to help solve groundwater problems more systematically with a mathematical approach. In constructing the model grid, several factors need to be considered, namely:

- the type of problem to be solved
- the accuracy of the results to be achieved
- the form of aquifers
- data availability
- the shape of the model boundary
- the number of cells (nodal cells) planned

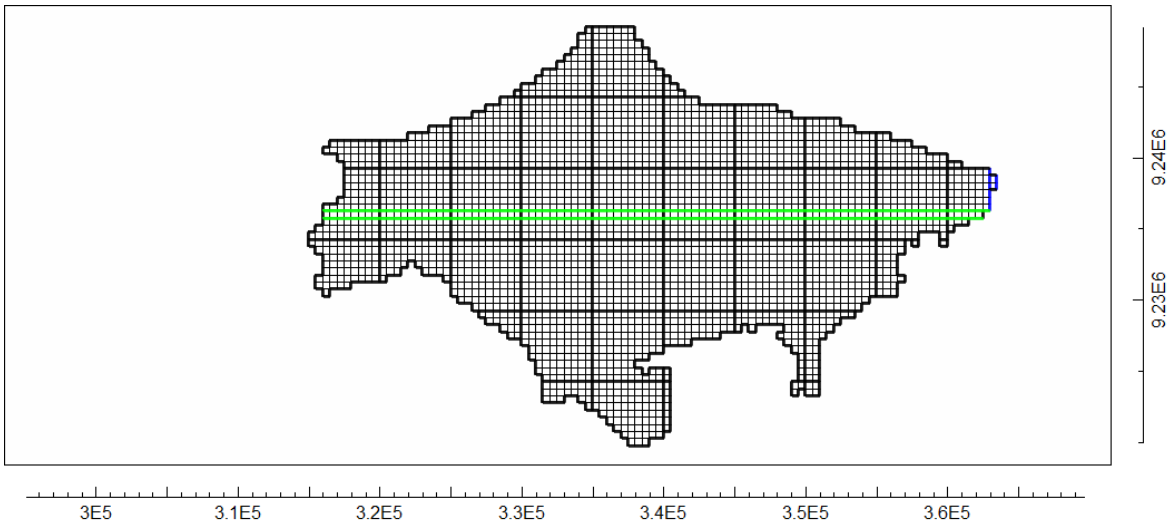

Figure 5.7 Grid model design of the research area

The grid model ranges from 315,055 to 364,045 metres in UTM coordinates in the west-east direction and from 9,219,606 to 9,249,606 metres in the north-south direction, with a grid size (grid spacing) of 500 metres. A 500x500 m grid provides sufficient resolution to capture regional variations in groundwater flow and subsidence patterns while minimising computational demands, which is crucial for running complex, time-dependent models. This grid size also aligns with the available data resolution; a smaller grid size would likely require more data than is available, potentially leading to uncertainties. With this grid size, the study area is divided into 60 rows and 95 columns. The grid model design is shown in Figure 5.7.

The system's layering is defined by depth intervals of 10 meters, rather than lithology, based on the established geological model, as shown in Figure 5.8. This figure presents the vertical profile for row 32 (West-East), indicated by the green line in Figure 5.9. This approach was chosen due to the complexity of lithological variations, which makes delineating precise lithologic boundaries across the entire study area challenging. By using uniform depth intervals, the model minimizes additional assumptions about lithologic transitions. Furthermore, since a key objective of the model is to analyze subsidence, maintaining consistent depth intervals enables more systematic tracking of vertical deformation patterns across layers.

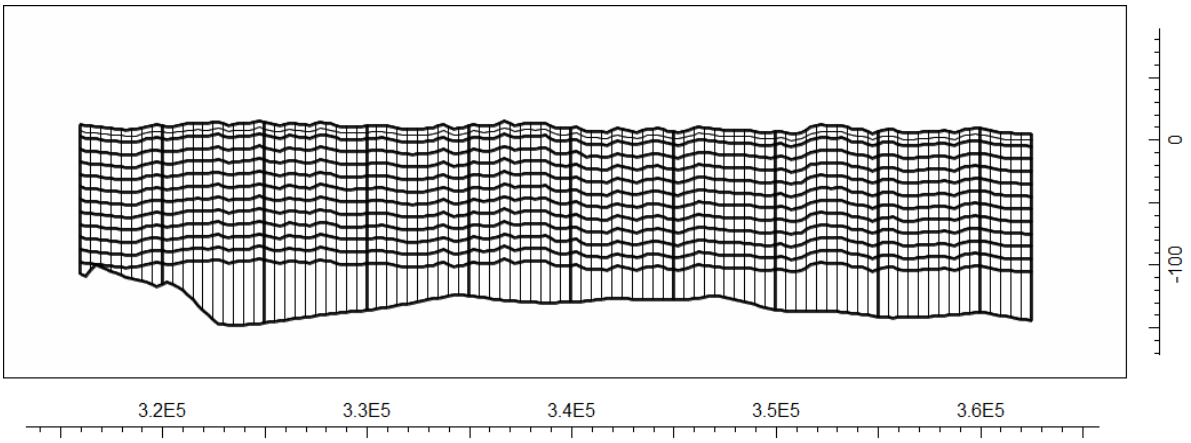

Figure 5.8 Layer of system geometry

According to the data obtained, lithological information in the study area is available only up to a depth of 130 meters, which is the maximum depth of the existing drilling data. Given the lack of lithological data beyond 130 meters, it is assumed that the

lithology from 130 meters to the bedrock is consistent with that of the last known layer.

5.2.5 Boundary conditions

One of the steps in numerical modelling is determining the boundary of the model area. The boundary condition is a mathematical statement that specifies the condition or dependent variable in the form of a head or derivative of the dependent variable in the form of flux in the model area's boundaries (model domain).

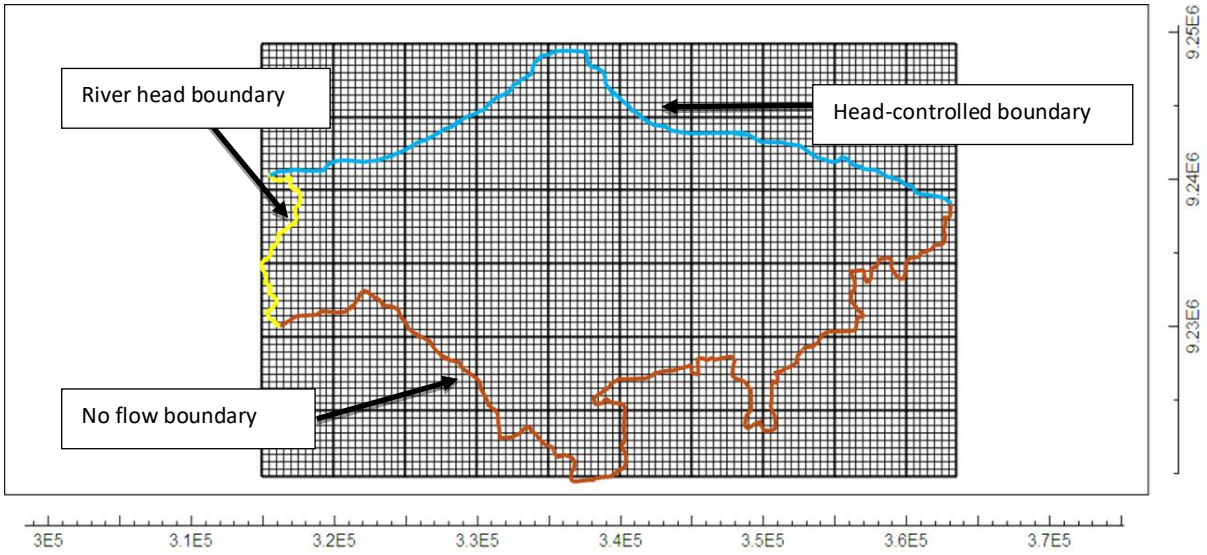

Figure 5.9 Boundary conditions of model design

The boundary condition of the model is based on the defined hydrogeological boundary conditions, which are then translated into the boundary model according to the package in the model with the following types (Figure 5.9):

- no flow boundary

  This boundary indicates no groundwater flow, or no significant inflow/outflow compared to flows in the main aquifer system.
- head-controlled boundary

  In the model area, this type of boundary the external head-controlled boundary which is sea level.
- river head boundary

  The river that define the model boundary are the primary rivers with permanent flow, characterized by a flow direction that is relatively perpendicular to the coastline.

5.3 SWAT modelling for estimating groundwater recharge

Groundwater recharge estimation in this study was conducted using SWAT modelling. In addition to providing temporal data on groundwater recharge, SWAT also generates spatial distribution data, which serves as an important input for groundwater modelling. SWAT operates by simulating the physical characteristics and processes related to land use and groundwater recharge, allowing for the estimation of groundwater recharge rates across a wide range of scales (Arnold & Fohrer, 2005).

SWAT automatically generates sub-basins, each containing a Hydrological Response Unit, based on input data such as geological conditions, land-use characteristics (land-use maps), and elevation and slope data, both of which can be derived from DEM (Digital Elevation Model) data and also climate data. SWAT is a highly versatile model capable of processing various types of data, including measurement point data and remote sensing data. It can be operated using Q-GIS or other GIS processing software, making it adaptable to a wide range of applications.

Table 5.2 Data for SWAT analysis

No	Data	Characteristics	Source
1	Digital Elevation Model (DEM)	10 M resolution	DEMNAS (indonesia.go.id)
2	Land use	Raster analysis	Google Earth Engine Analysis
3	Soil Map	Shapefile	Ina-Geoportal | Penayang Peta (indonesia.go.id)
4	River network	Shapefile	Ina-Geoportal | Penayang Peta (indonesia.go.id)
5	Climate	1990 - 2000	BMKG Climatologi Station

The rainfall and climatological data required for SWAT modelling, such as solar radiation, air temperature, relative humidity, and wind speed, were obtained from the only observation station in the study area. Given that the study area is a relatively small lowland region, it is assumed that the meteorological conditions across the entire area are uniform.

The study area is divided into 122 sub-basins, determined by sub-watershed boundaries based on surface topography, as seen in Figure 5.10. Each sub-basin has specific characteristics, represented by what is known as a Hydrologic Response Unit (HRU). Each HRU will produce different outputs, depending on the specific input data assigned to it.

Figure 5.10 Subbasin in the study area

5.3.1 SWAT Model Components and Equations

The core governing equation in SWAT is the water balance equation, which serves as the foundation for hydrological simulations (Gyamfi et al., 2017):

$$Sw_t = Sw_o + \sum_{i=1}^{t}(R_{day} - Q_{surf} - E_a - W_{seep} - Q_{gw}) \qquad Eq\ 5.1$$

where:

- Sw_t is the final soil water content (mm),
- SW_o is the initial soil water content on day i (mm),
- t is time in days,
- R_{day} is the precipitation on day i (mm),
- Q_{surf} is surface runoff on day i (mm),
- E_a is evapotranspiration on day i (mm),
- W_{seep} is the volume of water percolating into the vadose zone on day i (mm), and
- Q_{gw} is the return flow on day i (mm).

Each of these components is simulated through different sub-models within SWAT.

1. Surface runoff estimation (curve number method)

   Surface runoff, which represents the overland flow of excess water after infiltration and depression storage are satisfied, is estimated using the Soil Conservation Service (SCS) Curve Number (CN) method (Psomiadis et al.,

2020) . This approach accounts for land cover, soil type, and antecedent moisture conditions, and is defined as:

$$Q_{surf} = \begin{cases} \frac{(R_{day}-0.2S)^2}{(R_{day}+0.8S)} , R_{day} > 0.2S, \end{cases} \quad \textit{Eq 5.2}$$

where:

- Q_{surf} is the runoff depth (mm),
- R_{day} is daily rainfall (mm), and
- S is the retention parameter (mm), calculated as:

$$S = 25.4 \left(\frac{1000}{CN} - 10\right) \quad \textit{Eq 5.3}$$

The curve number (CN) is determined based on soil permeability, antecedent moisture conditions, and land use. Standard CN values can be obtained from tables available in the literature, which classify CN based on watershed characteristics.

2. Evapotranspiration and groundwater recharge estimation

SWAT estimates evapotranspiration (ET) using the Penman-Monteith equation, which incorporates factors such as solar radiation, temperature, wind speed, and humidity:

$$ET = \frac{0.408\,(R_n - G_0) + \gamma \frac{900}{T+273} u_2 (e_s - e_a)}{\Delta + \gamma(1 + 0.34 u_2)} \quad \textit{Eq 5.4}$$

where:

- ET is reference evapotranspiration (mm/day),
- Δ is the slope of the saturation vapor pressure curve (kPa/°C),
- R_n is net radiation (MJ/m²/day),
- G_0 is soil heat flux density (MJ/m²/day),
- e_s and e_a are saturation and actual vapor pressures (kPa), respectively,
- γ is the psychrometric constant (kPa/°C),
- $e_s - e_a$ represents the vapor pressure deficit (kPa),
- u_2 is wind speed (m/s), and
- T is the mean daily temperature (°C).

Groundwater recharge is estimated based on percolation and aquifer properties. The recharge process is modelled using an exponential decay function, as proposed by Venetis (1969) (Gyamfi et al., 2017):

$$GW_{rch,i} = \left\{W_{seep} \cdot \left(1 - exp\left[\frac{-1}{\delta_{gw}}\right]\right) + GW_{rch,i-1} \cdot exp\,\frac{-1}{\delta_{gw}}\right\} \qquad \textit{Eq 5.5}$$

where:

- $GW_{rch,i}$ is the recharge entering the aquifer on day iii (mm),
- δ_{gw} is the delay or drainage time of the overlying geological formations (days),
- W_{seep} is the water percolating from the soil profile on day iii (mm), and
- $GW_{rch,i-1}$ is the recharge from the previous day (mm).

5.3.2 SWAT evapotranspiration of study area

In addition to groundwater recharge, the primary output of the SWAT modelling is evapotranspiration. SWAT accommodates three methods for estimating potential evapotranspiration: the Penman-Monteith method, the Priestley-Taylor method, and the Hargreaves method. For this study, the Penman-Monteith method was selected due to the availability of comprehensive data. The Penman-Monteith method, which requires the most data for calculating potential evapotranspiration, utilises solar radiation, air temperature, relative humidity, and wind speed.

Alongside rainfall and runoff, evapotranspiration is crucial in controlling water availability at the Earth's surface. It is also a significant component of the hydrological cycle, second only to precipitation (Brutsaert, 2023). Approximately 62% of the precipitation that reaches the Earth's surface is lost to evapotranspiration, making it generally greater than runoff across nearly all river basins except Antarctica (Dingman, 1994, as cited in S.L. Neitsch, 2011).

Figure 5.11 illustrates the values and distribution of evapotranspiration from 1990 to 2020, representing the annual average for each year. The data for 2000 reflect the annual average from 1991 to 2000, for 2010 from 2001 to 2010, and for 2020 from 2011 to 2020. The figure shows that the highest evapotranspiration values occurred in 2000, followed by a gradual decline in 2010, with a more pronounced drop in 2020. Despite changes in rainfall patterns over the last decade, the total annual

rainfall intensity has not changed significantly. Therefore, the sharp decrease in evapotranspiration is primarily attributed to significant land-use changes, particularly between 2010 and 2020, as shown in Figure 3.4 of Chapter 3.

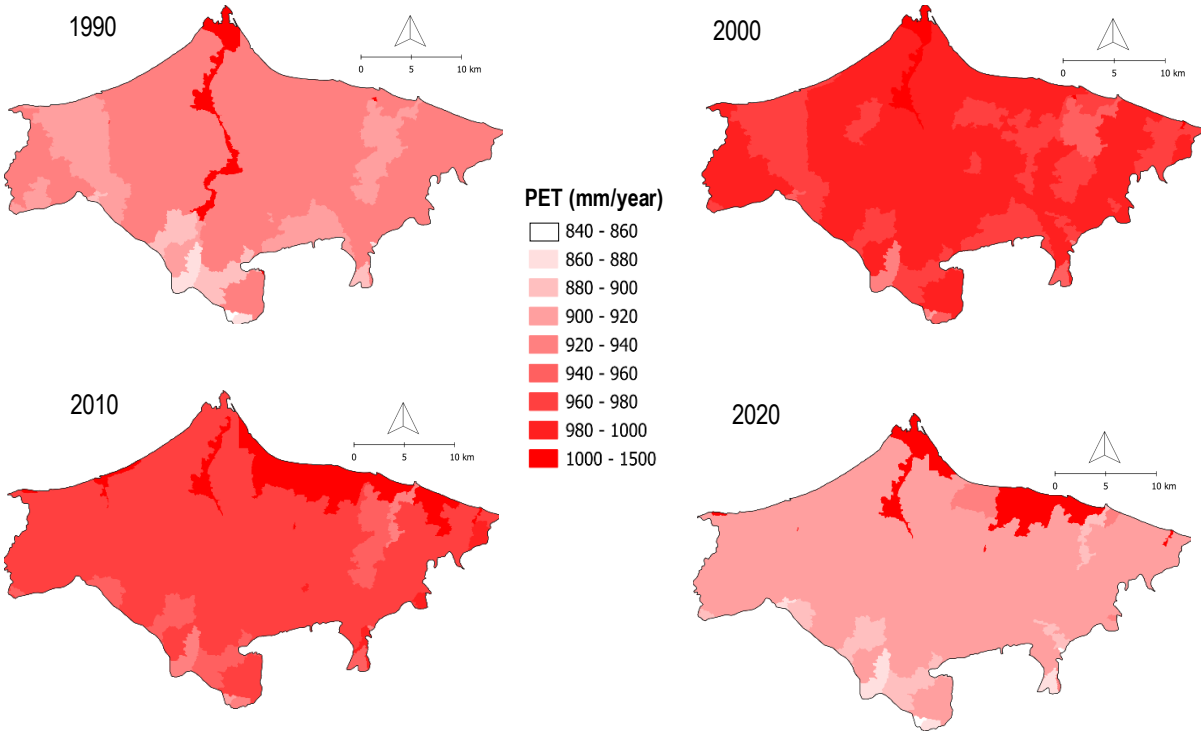

Figure 5.11 Evapotranspiration of SWAT analysis 1990 - 2020

5.3.3 Groundwater recharge of the study area

Pekalongan is one of the cities experiencing significant population growth, accompanied by a rapid expansion of industries across various sectors. This trend is further supported by changes in land use patterns over the years, which indicate an increasing extent of built-up areas, including residential, commercial, and industrial zones. Generally, the expansion of these developed areas has led to an increase in impermeable surfaces within the study region, thereby reducing the potential for groundwater recharge.

Based on Figure 5.12, groundwater recharge in 1990 shows a higher distribution of values compared to the calculations in subsequent years. The decline in groundwater recharge rates is significantly influenced by the ongoing reduction of secondary forests and plantations, which have been replaced by built-up areas, including residential and industrial zones within the study area. This land-use change, particularly the expansion of impermeable surfaces, has reduced the

infiltration capacity of the soil, thereby limiting the natural replenishment of groundwater.

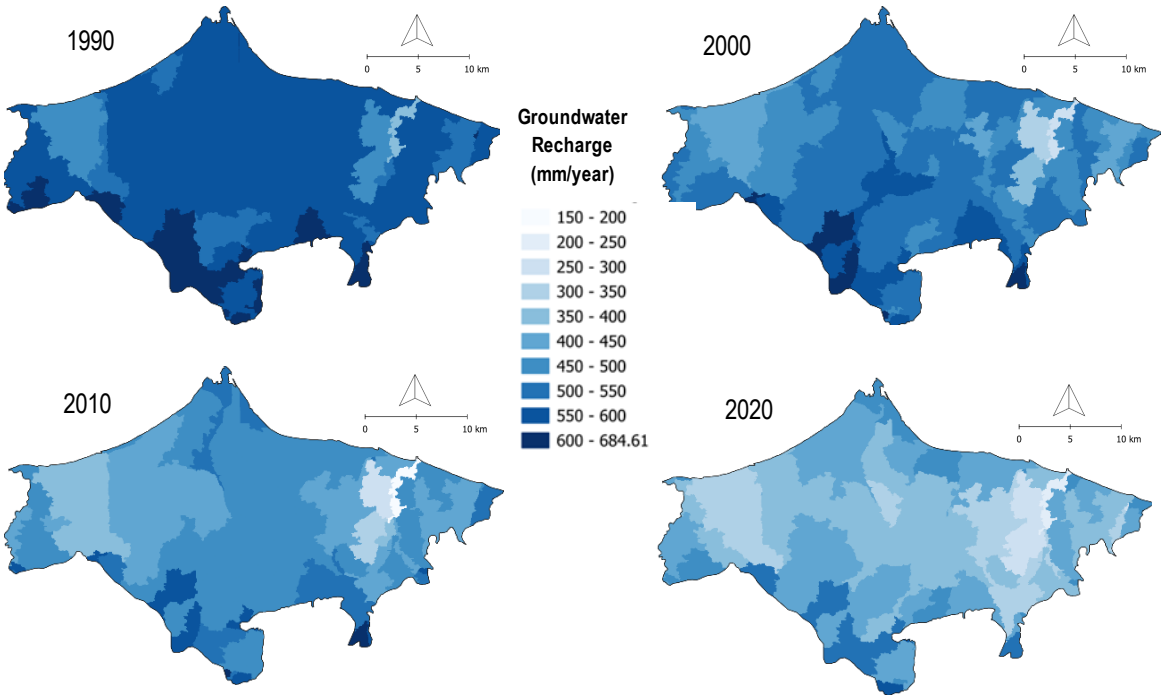

Figure 5.12 Annual groundwater recharge of SWAT analysis 1990 - 2020

5.4 Layer property flow and multiplier hydraulic conductivity

Hydraulic conductivity is a critical parameter in groundwater modelling, necessitating detailed discussion as provided in Chapter 4. Determining K values and estimating their spatial distribution demands accurate analysis to ensure the results are both reliable and representative of actual field conditions. The data analysis presented in Chapter 4 has yielded initial K-values for each lithotype, as shown in Table 5.3

The Layer Property Flow (LPF) package is one of several options in MODFLOW that can be used to simulate flow in the saturated zone. In this package, for the input of hydraulic conductivity, there is an option for an HK multiplier (horizontal conductivity), which accounts for the percentage of a single K value for each lithotype within a model cell. Based on the lithotypes in the study area, a single 500x500 m model cell contains five lithotypes, each with varying percentages according to the lithological model that has already been developed.

Table 5.3 Initial K values of each lithotype

Lithotype	Initial K (m/sec)
Clay	2.10E-08
Sandy Clay	7.20E-08
Clayey Sand	4.83E-07
Sand	1.21E-06
Breccia	9.32E-07

The first step involved calculating the percentage of each lithotype within every cell across the entire model area. These calculations were applied in QGIS for each layer. Figure 5.13 shows the percentage and distribution of each lithotype at depths of 70–80 m and 80–90 m, which represent the main aquifers in this region. White colours indicate a value of 0, meaning that the lithotype is absent in that particular cell and layer. The black colour on each map indicates a value of 1, meaning that the cell is 100% composed of a single lithotype. The grey colours (light grey to dark grey) on the layers represent values between 0 and 1, indicating that a single cell contains more than one lithotype.

The calculation of the K value for each cell in the model layer, as described in the previous sub-chapter on K value calculation, involves considering the percentage of each lithotype with the corresponding single K value obtained earlier. The formula used in Mudflow to calculate the K value for each layer is:

$$K = (w_1 * K_1) + (w_2 * K_2) + (w_3 * K_3) + (w_4 * K_4) + (w_5 * K_5) \qquad Eq\ 5.6$$

Where:

- $w_1 = \frac{\%L_1}{100}$, $w_2 = \frac{\%L_2}{100}$, $w_3 = \frac{\%L_3}{100}$, $w_4 = \frac{\%L_4}{100}$, $and\ w_5 = \frac{\%L_5}{100}$,
- $\%L_1$, $\%L_2$, $\%L_3$, $\%L_4$, $\%L_5$ represent the percentages of clay, sandy clay, clayey sand, sand, and breccia, respectively
- $w_1 + w_2 + w_3 + w_4 + w_5 = 1$
- *K1, K2, K3, K4, and K5* are the K values for clay, sandy clay, clayey sand, sand, and breccia.

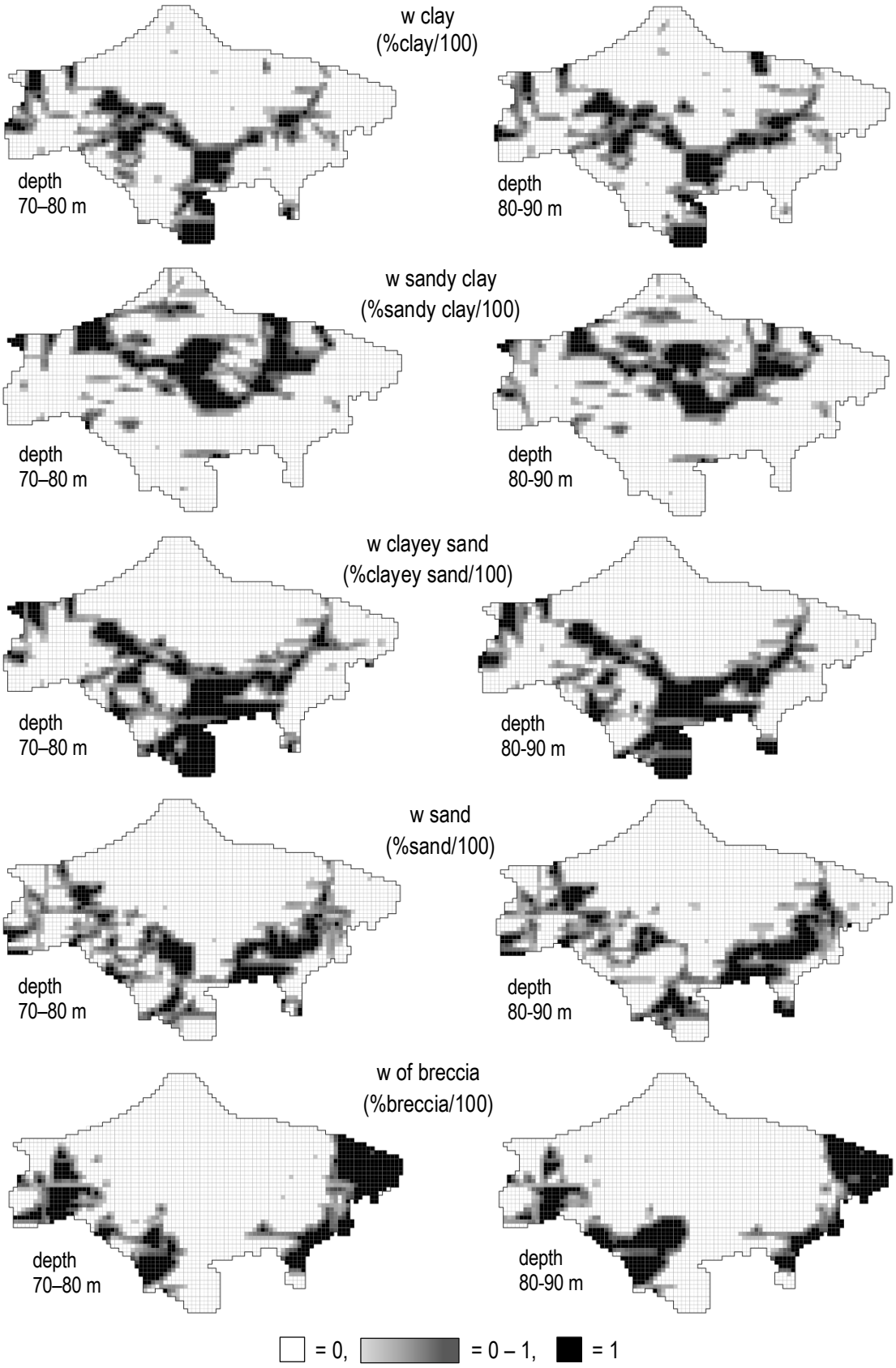

Figure 5.13 Distribution and w value of lithotypes at depths of 70–80 m and 80–90 m.
The w value is calculated as the percentage of each lithotype within a cell divided by 100, ensuring the total w value for each cell equals 1

The values and distribution of K can be seen in Figure 5.14. In this figure, (a) shows the vertical distribution of K values of row 23 (West-East), while (b) and (c) show the K distribution in layers 6 and 7.

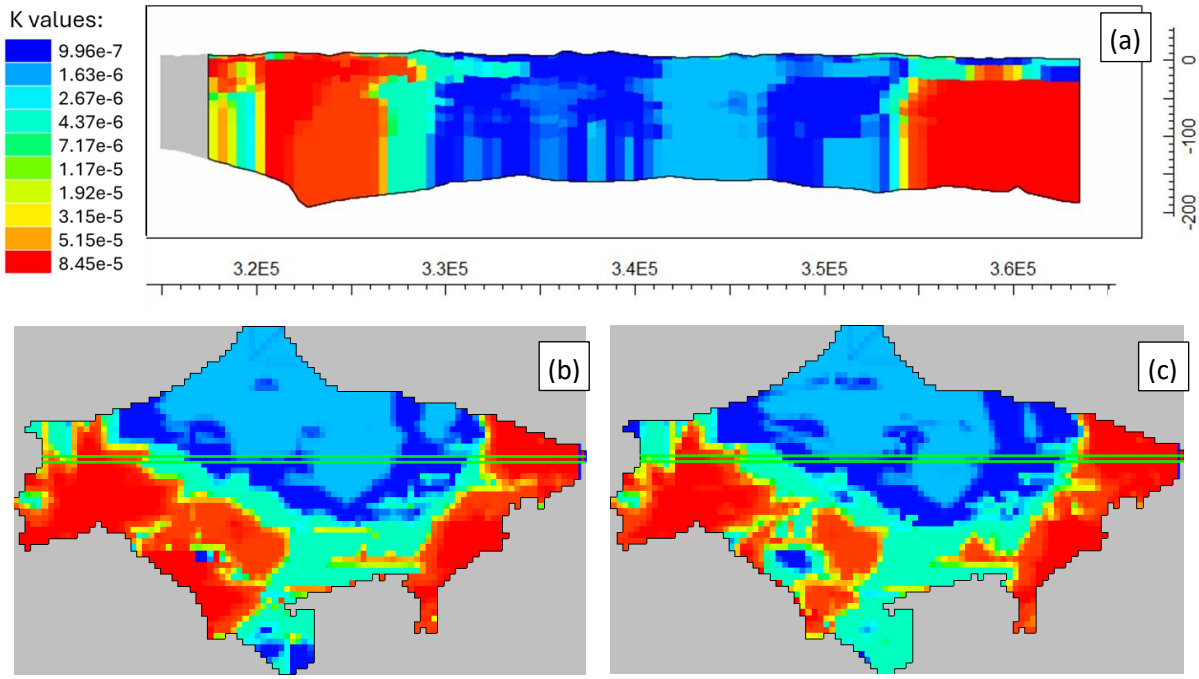

Figure 5.14 (a) Vertical distribution of K values and (b) and (c) spatial distribution of K at depths of 50-60 m and 60-70 m

5.5 Well abstraction

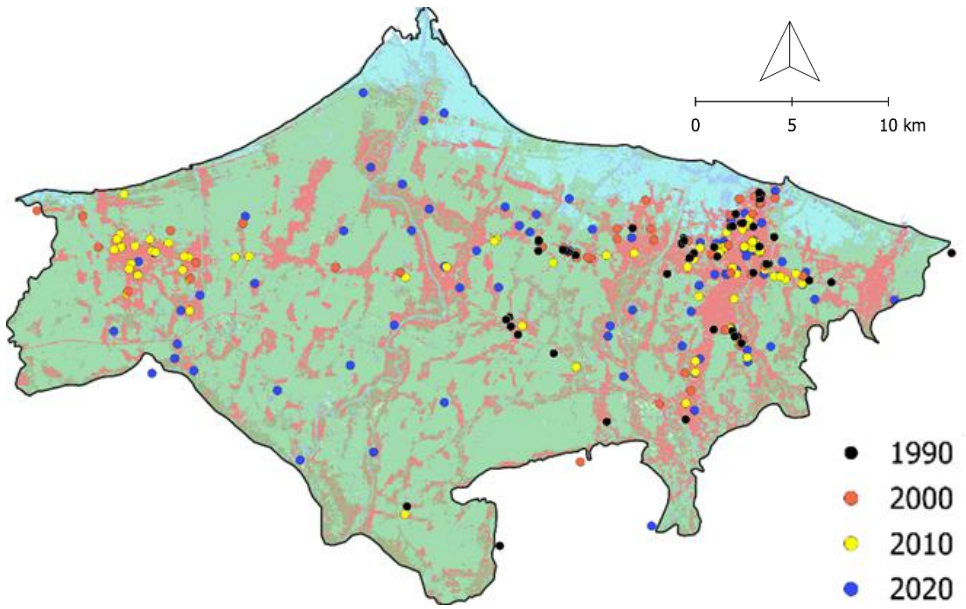

Figure 5.15 Groundwater Well Distribution. Each colour represents the year of well construction. The map indicates that a significant number of wells are in urban areas (highlighted as red zones).

As explained in Chapter 4, the total number of groundwater abstraction wells recorded up until 2020 is 272 wells. In Figure 5.15, we can see the well distribution from 1990, 2000, 2010, and 2020. These wells vary in depth, with an average depth of 100–120 meters. The abstraction volumes also vary, but most wells have a discharge rate of 0.001 m³/second. For Municipal Water Supply Company (PDAM) wells, the abstraction volume is larger, reaching up to 0.003 m³/second.

The wells in the study area are unevenly distributed, but most are located in residential areas (red zones), as well as office and industrial zones, as shown in Figure 5.17.

5.6 Transient model

Under transient conditions, the head distribution throughout the flow system, at times corresponding to past hydrological conditions in the aquifer system, represents the initial hydrogeological conditions for the flow model. The selected periods for the transient flow simulations start in 1990 and continue until 2020, with a stress period every 10 years. The total groundwater abstraction and recharge change throughout the simulation period. However, comparison and calibration will only be done for the year 2020, as groundwater level observations are only available for that year.

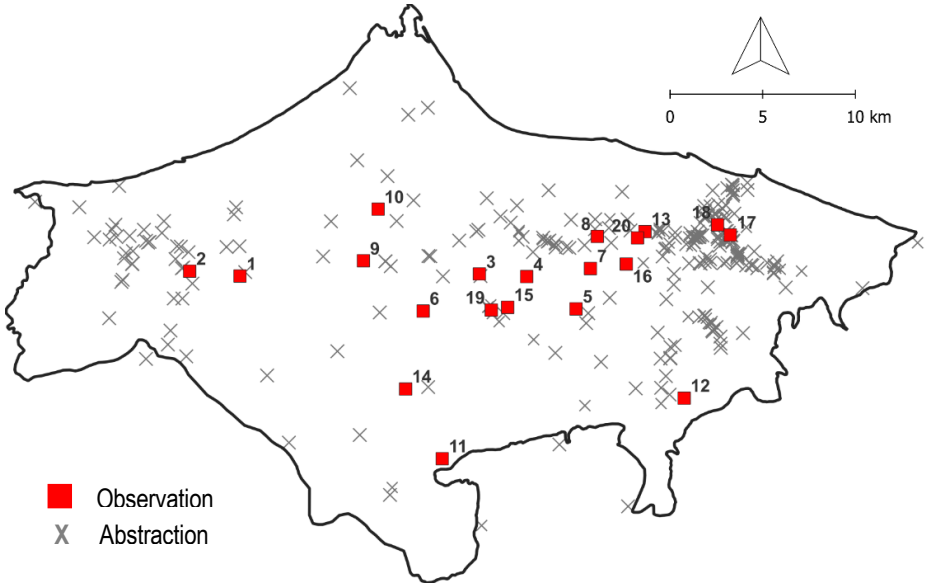

Figure 5.16 Distribution of observation and abstraction wells

5.6.1 Head observation wells

In the groundwater flow simulation model, water levels from observation wells (often called "observed head") are used for calibration. This is the process of adjusting the simulated groundwater levels (calculated head) to match the observed groundwater levels. During field data collection, groundwater level measurements were available from 20 locations for the year 2020, as presented in Table 5.4, with their spatial distribution shown in Figure 5.16.

Table 5.4 Observation well location and water level data in 2020

No	Name	X	Y	Observed Value (m.amsl)
1	SB Serang	327658.57	9236155.77	9.53
2	SB Pedurungan	324942.39	9236410.00	10.93
3	SB Sukorejo	340560.45	9236311.23	-9.03
4	SB Tengeng	343110.48	9236176.57	-9.23
5	SB Kadipaten	345772.80	9234441.61	-2.28
6	SB Pendowo	337536.29	9234300.65	4.30
7	SB Kampil	346544.38	9236618.95	-10.09
8	SB Kauman	346911.75	9238352.79	-11.63
9	SB Candimeka	334307.86	9237001.86	-5.15
10	SB Sidokare	335090.21	9239784.62	-1.55
11	SB Krandon	338588.02	9226349.14	13.90
12	SB Kedungwun	351617.51	9229649.46	13.17
13	SB Bener	349477.01	9238617.81	-23.93
14	SB Bulaksari	336603.60	9230097.80	15.64
15	SB Sragi	342088.97	9234516.91	2.80
16	SB Dadirejo	348477.84	9236868.82	-9.78
17	Hotel Sidji	354076.97	9238450.58	-12.55
18	PT Sampangan	353390.09	9238993.36	-11.66
19	PG Sragi	341209.35	9234365.68	-0.45
20	PT Loji	349076.47	9238277.79	-21.19

5.6.2 Results of transient model

The groundwater flow model under transient conditions shows time-dependent contour levels. Figures 5.17 illustrate the groundwater table in the study area for 1990, 2000, 2010, and 2020, respectively. Groundwater abstraction data indicates that the increase in the number of wells is mostly concentrated in the Pekalongan City area, which has led to a continuous decline in groundwater levels, forming cones of depression in this region.

In 1990, the groundwater pattern appeared normal, with groundwater levels 15 meters above sea level in the southern part of the study area, and the flow pattern running from the south toward the coastal areas in the north. By 2000, a decline in groundwater levels had begun to appear in the northeastern part of the study area, with the groundwater level reaching -1 meter above sea level. In 2020, a more drastic decline is evident, showing two cones of depression, with groundwater levels at -7 and -4 meters above sea level.

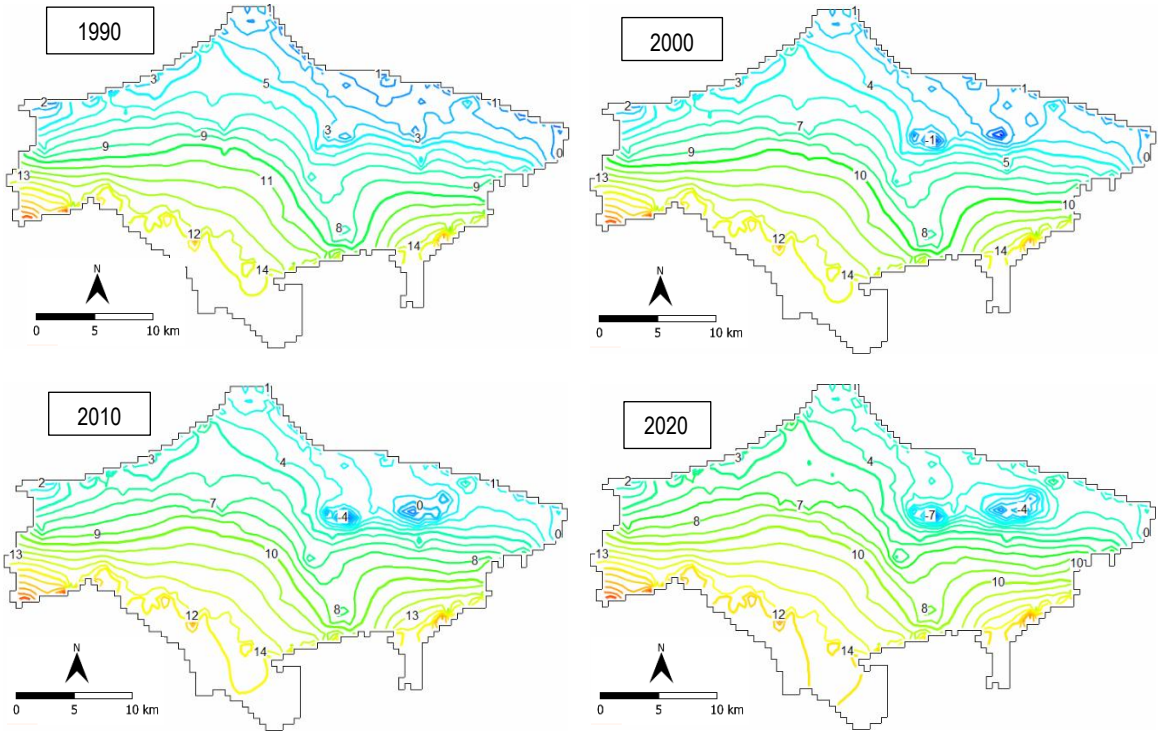

Figure 5.17 Simulated head of transient model output of 1990, 2000, 2010, and 2020

The residual values, or the differences between the simulated groundwater levels and the observed groundwater levels, vary significantly. At some points, the difference is minimal, less than 1 meter. However, at several reference points or observation wells, the residuals are quite large, with the highest values recorded at SB Bener and PT Loji, reaching 21.01 and 20.05 metres, respectively. The comparison graph of the water level (head) from the transient model simulation with observations in 2020 can be seen in Table 5.5. Figure 5.18 shows the residuals between observed and simulated head for each observation well. Based on these

results, the RMSE (Root Mean Square Error) between observed and simulated head values is 11.297, with the comparison graph shown in Figure 5.19.

Table 5.5 Observed and simulated head and the residual

Observation Name	Observed head (m.amsl)	Simulated head (m.amsl)	Residual (m.amsl)
PG Sragi	-0.45	4.83	-5.28
PT Loji	-21.19	-1.14	-20.05
PT Sampanga	-11.66	-0.88	-10.78
SB Bener	-23.93	-2.92	-21.01
SB Bulaksari	15.64	12.51	3.13
SB Candimeka	-5.15	9.37	-14.52
SB Dadirejo	-9.78	4.05	-13.83
SB Kadipaten	-2.28	7.56	-9.84
SB Kampil	-10.09	4.89	-14.98
SB Kauman	-11.63	0.52	-12.15
SB Kedungwuni	13.17	13.83	-0.66
SB Krandon	13.90	13.83	0.07
SB Pedurungan	10.93	9.16	1.77
SB Pendowo	4.30	10.48	-6.18
SB Serang	9.53	10.04	-0.51
SB Sidokare	-1.55	6.23	-7.78
SB Sragi	2.80	5.63	-2.83
SB Sukorejo	-9.03	5.75	-14.78
SB Tengeng	-9.23	4.36	-13.59
The Sidj Hotel	-12.55	0.53	-13.08

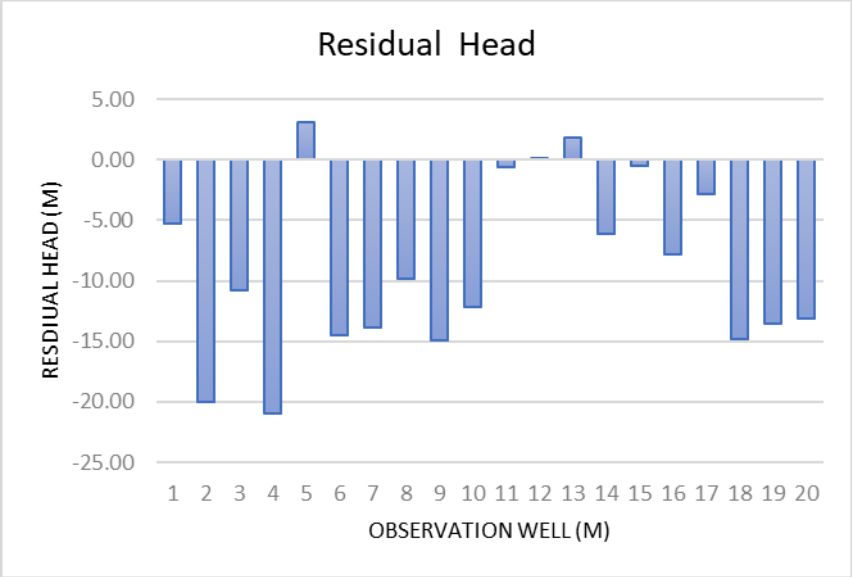

Figure 5.18 The residual head for transient model running

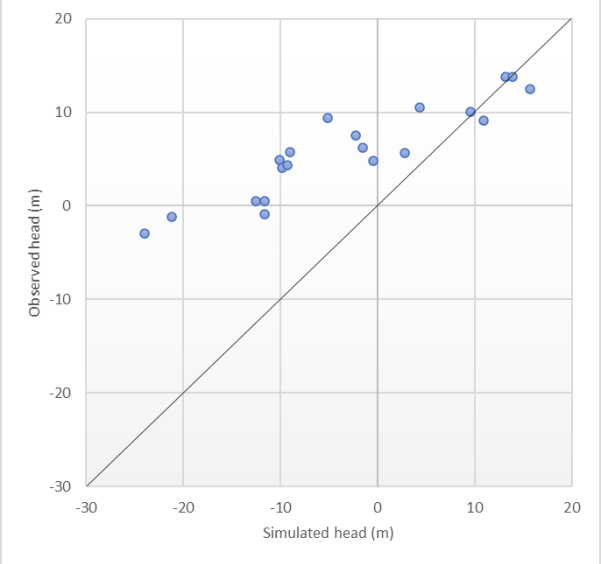

Figure 5.19 Graph showing observed head vs simulated head of observation wells before calibration

5.7 Model calibration and sensitivity analysis

As outlined in Chapter 4 on methodology, this model employs automatic parameter calibration rather than manual calibration. Automatic calibration, which utilizes a search algorithm to identify optimal parameter values, is significantly faster and generally produces more accurate results compared to manual approaches. PEST, a nonlinear parameter estimation and optimization package, provides model-independent optimization procedures (Doherty, 2015).

5.7.1 PEST calibration process

Given the limitation of observational data to groundwater level measurements from monitoring wells, PEST was utilized in an automated inverse modeling approach to iteratively adjust parameters and minimize discrepancies between observed and simulated groundwater heads. The calibration workflow involved:

1. Defining calibration targets

   Observed groundwater levels from monitoring wells were used as calibration reference points. As previously explained, 20 wells were utilized as calibration reference points, with their data and spatial distribution presented in Table 5.4 and Figure 5.18.

2. Selecting parameter for adjustment

   As previously discussed in Chapter 3 on model calibration, hydraulic conductivity is the primary parameter targeted for calibration in this study. The objective of this calibration process is to determine the optimal hydraulic conductivity values for each lithotype, ensuring that the simulated groundwater head closely aligns with the observed head at each monitoring well.

3. Initial model run and sensitivity analysis

   Before calibration, a sensitivity analysis was performed to identify the parameters that had the most significant impact on the model outputs, specifically the hydraulic conductivity values for each lithotype. This ensured that the calibration process focused on the most influential parameters. The explanation of the sensitivity analysis process and its results will be provided in the following section.

4. PEST iterative adjustment

   PEST optimized hydraulic conductivity (K) values using a nonlinear least-squares approach to minimize residuals—the differences between observed and simulated groundwater heads. Model accuracy was evaluated based on the residual magnitude at each observation point, with smaller residuals indicating a closer match between simulated and observed values. Effective calibration ultimately reduces the Root Mean Square Error (RMSE), improving the model's overall performance and predictive reliability.

5.7.2 Sensitivity analysis

Sensitivity analysis is a valuable tool for identifying key model parameters, testing model conceptualization, and enhancing the model structure. It offers insights into the model's implementation and the physical processes influencing the behaviour of critical inputs. Sensitivity analysis results can guide model calibration and serve as a basis for prioritizing future data collection efforts. Moreover, it is crucial for verifying the model's results using calibrated parameters, ensuring accuracy and reliability.

Table 5.6 Model error (RMSE) during changes in K of each lithotype

Lithotype	Kx Decreased by			Kx Decreased by		
	-25%	-50%	-75%	+25%	+50%	+75%
Clay	11.295	11.285	11.227	11.301	11.297	11.296
Clayey sand	11.092	10.796	10.242	11.448	11.563	11.654
Sandy clay	11.168	11.000	10.375	11.405	11.496	11.571
Sand	11.193	11.055	10.835	11.386	11.458	11.519
Breecia	11.274	11.243	11.202	11.320	11.333	11.345

The simulation was performed by altering the initial K value for each lithotype, with adjustments of -25%, -50%, and -75%, also +25%, +50%, and +75%, for each lithotype. While modifying the K of one lithotype, the K values of the other four lithotypes were held constant. This approach helps identify which lithotype's K is most sensitive to changes. The resulting root mean square error (RMSE) for each adjustment is presented in Table 5.6 and visualized in Figure 5.20.

The variation in RMSE with changes in hydraulic conductivity (K) reflects the model's sensitivity to permeability adjustments for each lithotype. A significant increase in RMSE when K is modified indicates that the model is highly dependent on that lithotype's hydraulic properties, highlighting the need for precise calibration. Conversely, if RMSE remains relatively stable across different K values, the model exhibits lower sensitivity, suggesting that minor inaccuracies in K have a minimal impact on model performance.

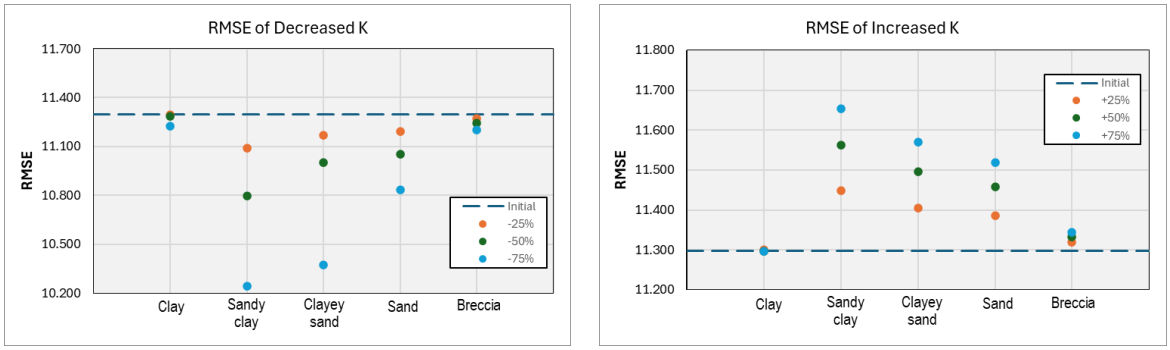

Figure 5.20 Sensitivity analysis for K adjustment by lithotype. (a) RMSE results for each decrease in K values for each lithotype (b) RMSE results for each increase in K values for each lithotype

The results indicate that clay and breccia show minimal RMSE variations, implying low sensitivity to changes in their hydraulic conductivity. In contrast, sandy clay demonstrates moderate sensitivity, with RMSE increasing notably at higher K adjustments, particularly at +50% and +75%. The highest sensitivity is observed in

clayey sand and sand, where RMSE rises sharply with increasing K, suggesting that overestimating their hydraulic conductivity leads to significant errors, whereas reducing K has a comparatively smaller effect. Overall, the findings underline the necessity of precise K calibration for more permeable lithotypes, such as sandy clay, clayey sand, and sand, to ensure model accuracy, while less permeable units like clay and breccia have a relatively lower influence on RMSE fluctuations.

5.7.3 Calibration outcomes

To perform PEST calibration in MODFLOW, it is essential to define PEST parameters to achieve the desired calibration output. This includes determining the observation group, calibration mode, the number of iterations, and especially the lower and upper bounds for each parameter. Setting appropriate bounds, as detailed in Table 5.7, ensures that the calibration results remain within acceptable limits and do not exceed reference values for each lithotype. These bounds are essential for maintaining realistic and physically meaningful results throughout the calibration process.

Table 5.7 Lower and upper bound for PEST Calibration

Lithotype	Initial Kx	Lower Bound	Upper Bound
	m/sec	m/sec	m/sec
Clay	2.10E-08	2.10E-10	2.10E-06
Sandy Clay	7.20E-08	7.20E-10	7.20E-06
Clayey Sand	4.83E-07	4.83E-09	4.83E-05
Sand	1.21E-06	1.21E-08	1.21E-04
Breccia	9.32E-07	9.32E-09	9.32E-05

From the results of the PEST calibration, the single value of hydraulic conductivity for each lithotype is shown in Table 5.8. The most significant changes in K were observed for sandy clay and clayey sand, which aligns with the sensitivity analysis findings indicating that these two lithotypes are the most sensitive. The post-calibration RMSE improved to 7.228, a significant reduction from the previous value of 11.298, as shown in Figure 5.21.

The RMSE improved because the PEST calibration process optimized the model's parameters, particularly each lithotype's hydraulic conductivity (K) values. Calibration adjusts these parameters to better fit the observed data, minimizing the discrepancies between the simulated and observed water levels.

Table 5.8 The value of calibrated K and the change from the initial value

Lithotype	Initial Kx	Calibrated Kx	The change
	m/sec	m/sec	%
Clay	2.10E-08	1.90E-08	-9.52
Sandy clay	7.20E-08	1.00E-08	-86.11
Clayey sand	4.83E-07	4.83E-08	-90.00
Sand	1.21E-06	7.86E-07	-35.04
Breccia	9.25E-07	8.45E-07	-8.65

Sandy clay and clayey sand were identified as the most sensitive lithotypes during the sensitivity analysis, meaning that small changes in their hydraulic conductivity values significantly impacted model performance. By fine-tuning these values during the calibration, the model could more accurately represent the groundwater behaviour, resulting in a lower RMSE. The improvement from 11.298 to 7.228 reflects a better match between the simulated and observed data, indicating an enhanced model fit and overall performance.

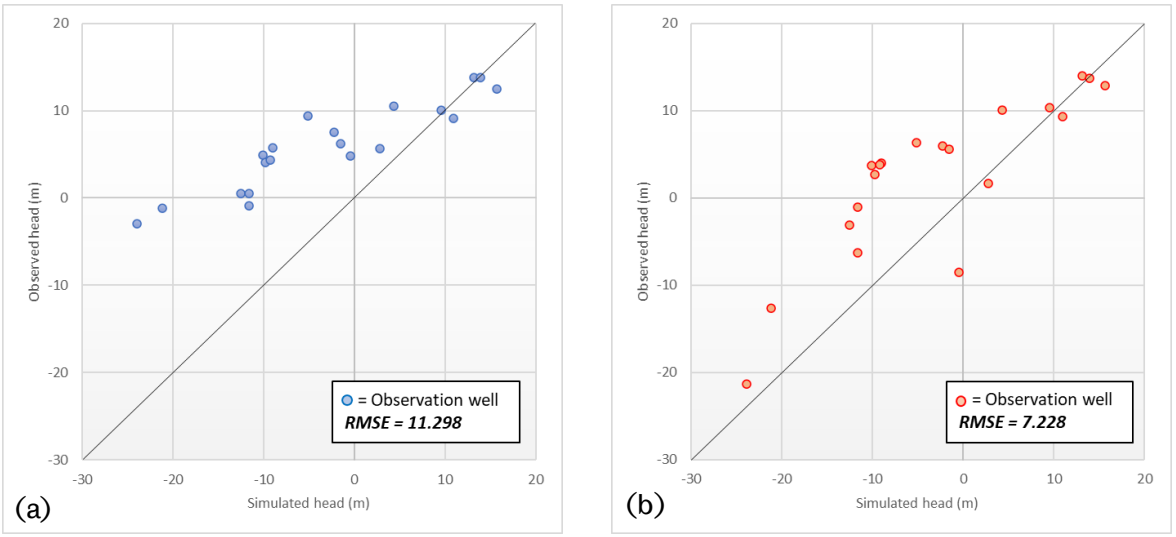

Figure 5.21 Graph showing (a) observed head vs simulated head before calibration, and (b) Observed head vs simulated head after calibration.

The final calibrated model demonstrated an improved match between observed and simulated groundwater levels, with residuals reduced significantly across most monitoring wells. The Root Mean Square Error (RMSE) were evaluated to assess the calibration quality. The results indicated that:

- The calibrated K values aligned with expected ranges based on each lithotype.
- Uncertainty remained in areas with sparse monitoring wells, emphasizing the need for additional field data to refine calibration further.

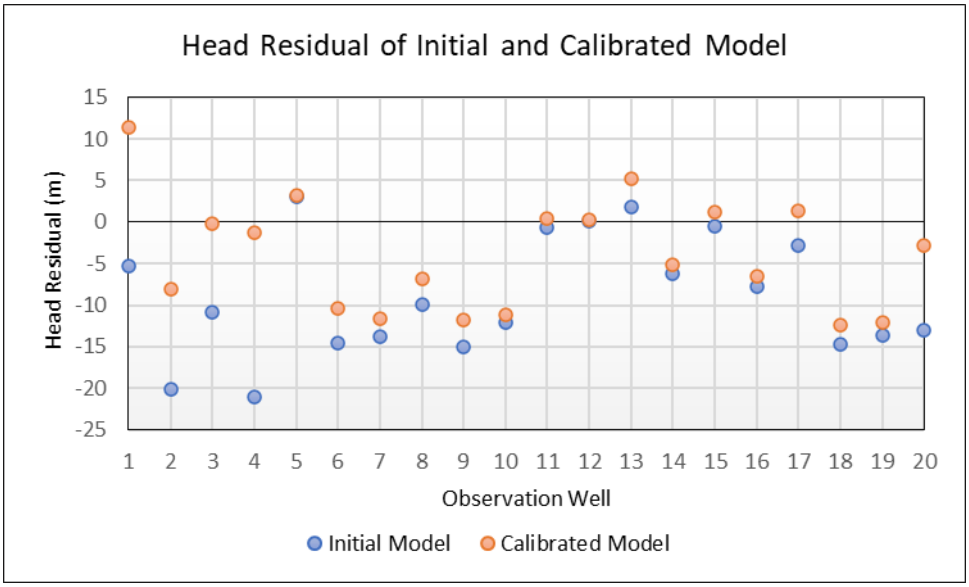

Figure 5.22 The comparison of the head residual of initial and calibrated K

5.7.4 Calibrated transient model

Figure 5.23 illustrates the water level patterns after calibration. Overall, the pattern does not show significant changes compared to the pre-calibration results. A groundwater cone of depression is observed in the northeastern part of the study area, particularly in central Pekalongan. Smaller cones of depression are also evident in other locations, indicating that groundwater abstraction in those areas has likely increased. In other areas, the groundwater table still follows the same pattern, with flow direction from the south to the north.

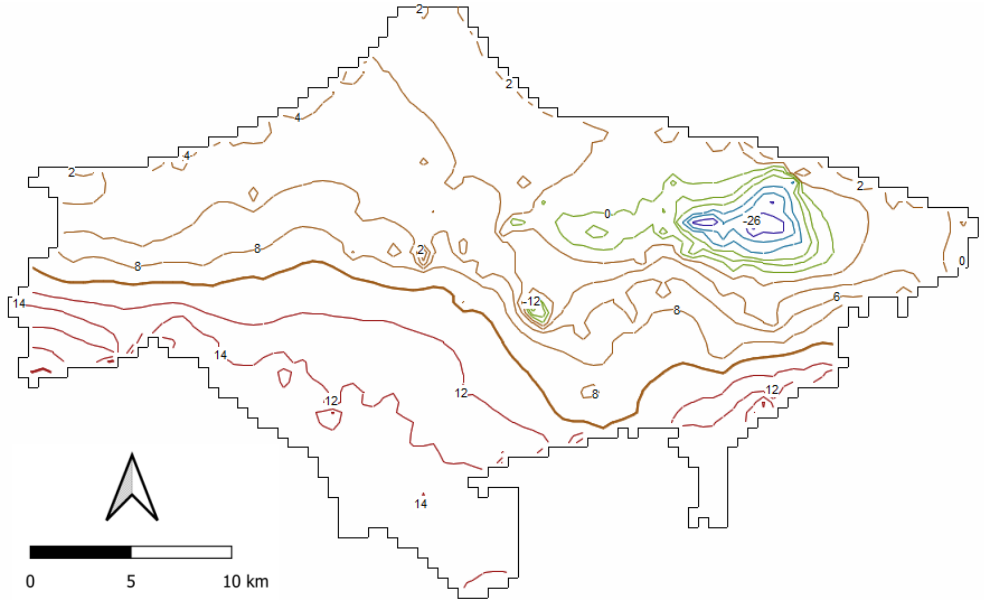

Figure 5.23 Simulated head of study area after K calibration

The progression of groundwater drawdown from 1990 to 2020, as illustrated in Figure 5.24, reveals a clear trend of steadily decreasing groundwater levels. In 1990, the drawdown was minimal, but by 2020, it had become severe. Such significant groundwater depletion can lead to serious consequences, including reduced groundwater availability in the study area, potentially causing wells to dry up. In regions with high compressibility, such as coastal areas composed of young sedimentary materials, extreme groundwater drawdown is often accompanied by subsidence. This is particularly concerning in the study area, which is dominated by clay and other fine-grained sediments, making it highly susceptible to land subsidence.

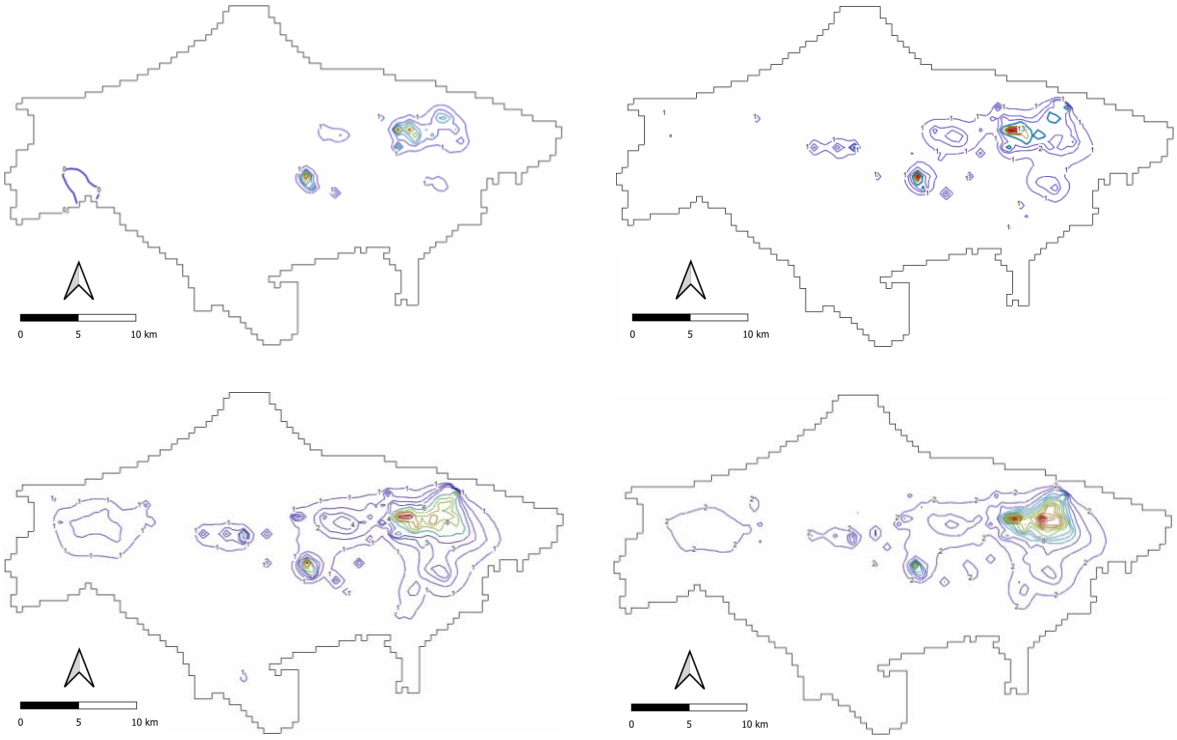

Figure 5.24 Drawdown of groundwater levels from 1990 to 2020

5.8 Conclusion

The application of a 3D groundwater flow model for Pekalongan coastal area in the northern part of Java Island using MODFLOW provides important information regarding groundwater dynamics in the area. The results of this study include groundwater flow patterns, the impact of land use and groundwater withdrawal, and how the calibration process is effective on the most important parameters of

the model. This conclusion is important to inform future groundwater management strategies in the area.

- Groundwater flow pattern

  This model successfully identified the overall groundwater flow pattern, which generally moves from the southern part of the study area to the northern coastal area. However, groundwater withdrawal increasingly disturbs the flow pattern, causing the formation of a depression cone, especially in areas experiencing rapid urbanization and industrial development.

- Impact of land use changes on groundwater recharge

  In addition to calculating the water balance in the study area, especially groundwater recharge, which is the primary input for the model, spatial groundwater recharge data from the SWAT model results also show significant changes from 1990 to 2020, caused mainly by changes in land use. Expanding impermeable surfaces, such as built-up areas and industrial zones, have reduced water infiltration into the soil, limiting groundwater recharge. This exacerbates the problem of groundwater subsidence, especially in areas where natural land cover has been replaced by urban infrastructure.

- Impact of groundwater abstraction

  The groundwater level in the study area has continuously declined over the past few decades, with significant cones of depression forming in highly urbanized areas such as Pekalongan City. Model results indicate that the groundwater level dropped to 26 meters below sea level in 2020. This ongoing decline threatens the long-term sustainability of groundwater resources in the area and highlights the need to manage groundwater abstraction activities carefully.

- Model sensitivity and calibration

  Sensitivity analysis and calibration using the PEST automatic parameter optimization technique determined that the sandy clay and clayey sand lithotypes were the most sensitive parameters affecting model accuracy and fine-tuning the hydraulic conductivity values for these lithotypes significantly improved model performance, reducing the RMSE from 11.297 to 7.228. The

improved calibration results provide a more accurate representation of groundwater levels and flow patterns.

- Potential groundwater depletion and land subsidence
  The model highlights the growing concerns about groundwater depletion and associated land subsidence risks in the region. Areas composed of fine-grained sediments, such as clay, are particularly vulnerable to subsidence as groundwater levels continue to decline. Without intervention, further groundwater withdrawal could lead to severe environmental and infrastructure challenges.

In summary, the 3D groundwater flow model provides a valuable tool for understanding and predicting the impacts of groundwater extraction and land-use change on the water table in the region. The next chapter will discuss land subsidence further. Chapter 6 will also discuss land subsidence projections for the next few years with several scenarios related to land and climate change and growth in groundwater withdrawals.

CHAPTER 6

Subsidence and Future Projections Based on Climate-Land Use Change and Groundwater Abstraction Scenarios

6.1 Introduction

This chapter focuses on land subsidence in the Pekalongan region, a pressing issue of national significance. The primary concern is the relationship between land subsidence and groundwater abstraction. In this chapter, we explore the current status of land subsidence and projections for future scenarios. These projections include assessments based on anticipated changes in climate, land use, and groundwater abstraction.

Various methods are employed to measure land subsidence, such as direct GPS measurements and InSAR remote sensing, enhancing our understanding of subsidence trends. These findings are then compared to the subsidence calculations in this study, which utilize Subsidence (SUB) module from MODFLOW-2005.

As a result, the subsidence data obtained was not calibrated due to the absence of accurate field observation data that could serve as a basis for calibration. Both the subsidence and GPS data have a limited analysis period, yet they exhibit relatively good accuracy and consistency. Moreover, subsidence measurements from InSAR and GPS represent total subsidence, capturing the combined effects of all contributing factors, including human engineering activities such as infrastructure loading and groundwater abstraction. In contrast, subsidence data derived from SUB modelling specifically reflects the impact of groundwater abstraction in the study area.

Further analysis investigates subsidence evolution over several decades, identifying significant increases in subsidence rates and the extent of the affected areas. This chapter also examines the relationship between groundwater level decline and land

subsidence, highlighting a clear correlation between increased subsidence and higher drawdown rates.

Finally, the chapter discusses future scenarios, incorporating climate change, land-use changes, and regulatory interventions. The projections consider the impact of government regulations on groundwater abstraction, potential changes due to economic growth, and the broader implications of climate change on recharge patterns and groundwater level decline, especially the subsidence rate in the area.

6.2 Subsidence measurement

There are various methods for calculating or measuring subsidence, as discussed in the literature review chapter. The primary methods commonly employed in different locations include direct measurement using GPS, *InSAR* modelling with remote sensing as the main data source, and modelling using soil or rock parameters, which are typically directly related to groundwater usage in the area, as is the case in this study.

6.2.1 Subsidence modelling (SUB) package

SUB is one of the modules in MODFLOW-2005 used to simulate land subsidence. This package is typically employed in studies to assess the impact of groundwater exploitation on land subsidence, which has been confirmed through direct measurements or other field evidence. The primary parameter required by the SUB module is Specific Storage (SS), in addition to other parameters such as pre-consolidation head and compressible layer thickness.

Based on the analysed input parameters, the stress period for the subsidence module is consistent with that of the flow package, covering a 10-year interval from 1990 to 2020. As a result, the subsidence results represent cumulative rates over each 10-year period. Figure 6.1 illustrates the evolution of subsidence from 1990, 2000, 2010, and 2020, showing a marked increase in the subsidence over time. In 1990, the maximum subsidence value was only 2.1 m, and the area affected by subsidence remained relatively small. By 2000 and 2010, the maximum value increased to 3.32 m and 3.465 m, respectively. However, by 2020, the maximum value had escalated to 5.7 m, with a significantly larger affected area.

Spatial analysis reveals that the areas experiencing subsidence in 2020 correspond closely with regions of groundwater level decline during the same year (Figure 6.2). Zones with significant groundwater drawdown align with areas of highest subsidence. This relationship between subsidence and groundwater drawdown is illustrated in Figure 6.3, which also demonstrates a positive correlation between these variables, exhibiting a linear trend: as groundwater drawdown increases, subsidence becomes more pronounced.

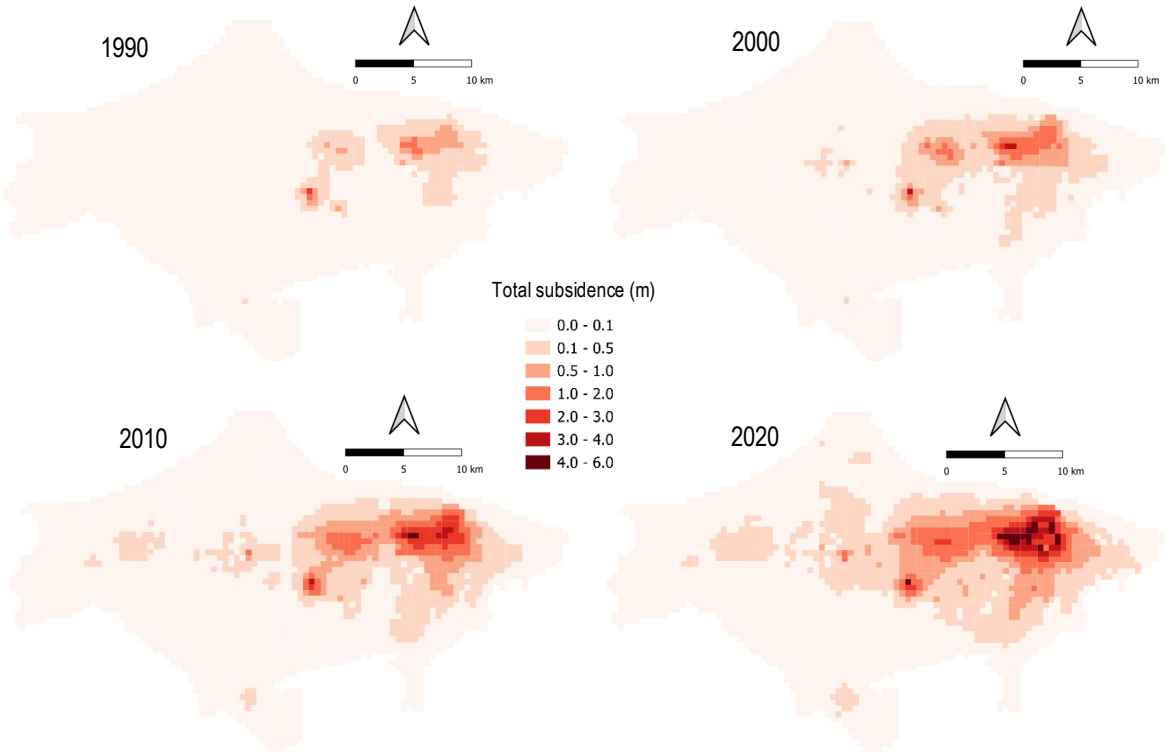

Figure 6.1 Total subsidence of SUB Model output in 1990, 2000, 2010 and 2020

The 2020 subsidence derived from the SUB module (Figure 6.2), reflects the cumulative subsidence over a 50-year period, beginning in 1970, the model's start year. By subtracting the total subsidence recorded in 2010 from that in 2020, the subsidence rate of 10 years period (2010–2020) was calculated, as shown in Figure 6.4. The maximum subsidence rate during this period was 2.98 m (or 280 cm), resulting in an average annual subsidence rate of 28 cm. This figure also highlights the spatial distribution of groundwater abstraction wells, which are predominantly located in areas with high subsidence rates. From Table 6.3, it can be observed that a 10% decrease in aquifer recharge results in only a 1 mm change in the subsidence rate.

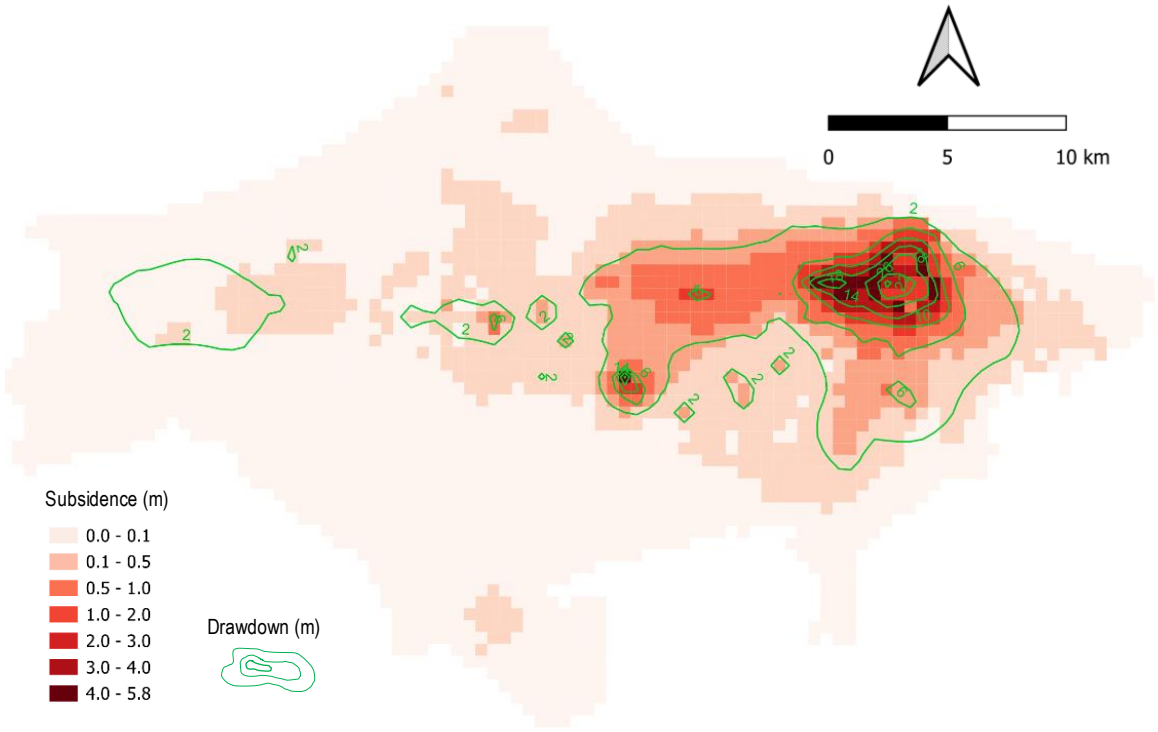

Figure 6.2 Total SUB subsidence overlaid with groundwater drawdown in 2020

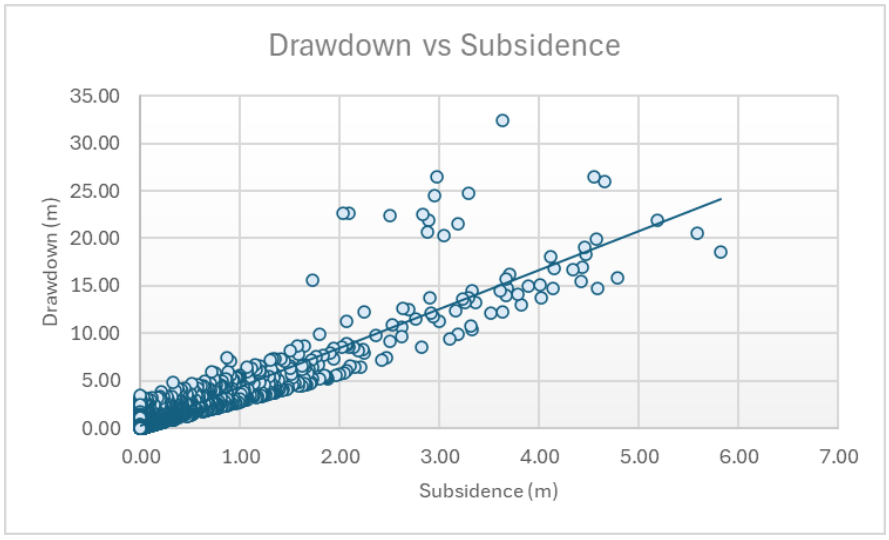

Figure 6.3 Drawdown and total subsidence correlation in the study area

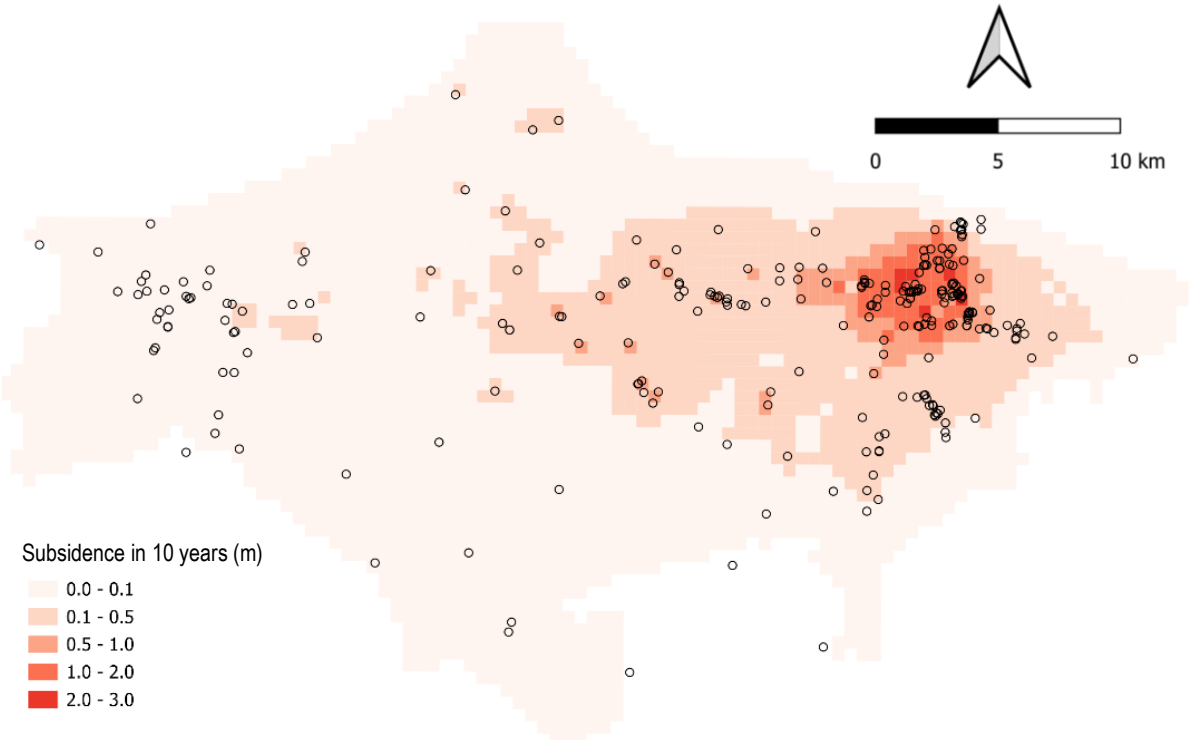

Figure 6.4 Subsidence rate over a 10-year Period (2010–2020).
Black circles represent groundwater abstraction wells located within the study area.

6.2.2 Subsidence of InSAR and GPS measurement

In general, the InSAR process involves extracting line-of-sight (LOS) displacement information from radar data. By using the Sentinel-1 satellite, which has a revisit time of 6 to 12 days, the resulting temporal resolution is sufficiently accurate. As explained in Chapter 3, the method used in this study is SBAS InSAR, which focuses on reducing errors and improving the accuracy of displacement measurements, particularly for long-term, slow-moving ground deformation.

The InSAR analysis was conducted over the study area for a one-year period, with the reference point located at Latitude 9236714.2445 and Longitude 351770.2664, UTM Zone 49S. The analysis spans from September 2019 to September 2020, aligning with the groundwater level data collection at observation wells in September 2020 to ensure consistency in subsidence and groundwater dynamics assessment. The results, as shown in Figure 6.5, illustrate the variations in land subsidence over the one-year period. Areas with significant subsidence are concentrated in the northeastern part of the study area, particularly in the city of Pekalongan, where the maximum subsidence rate reached 15.36 cm/year.

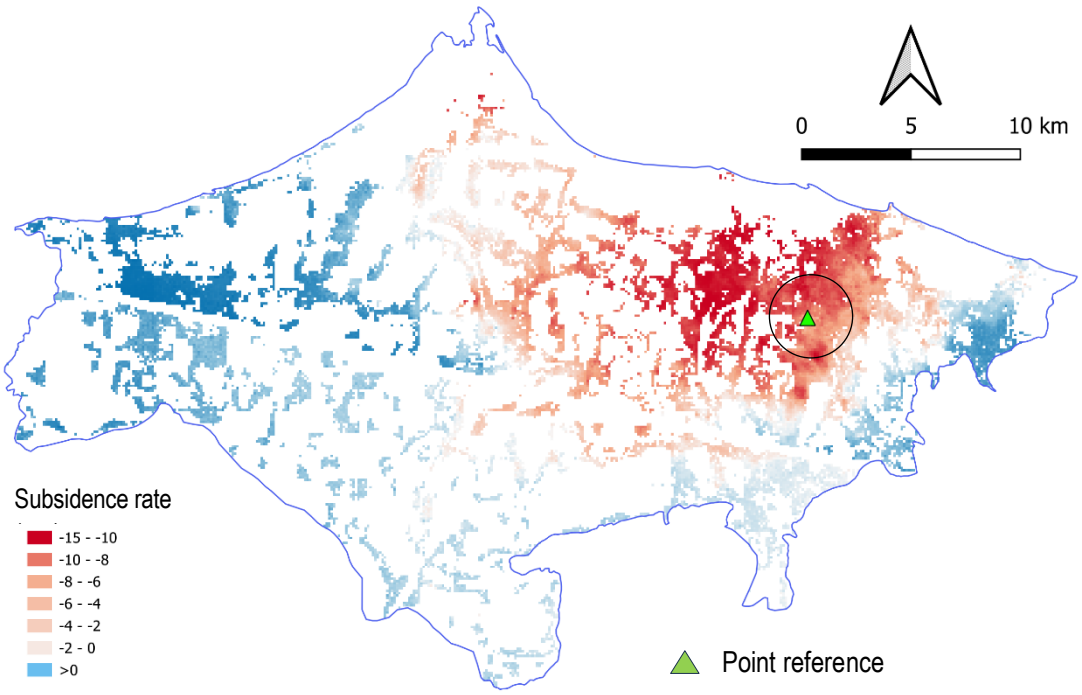

Figure 6.5 Subsidence rate of 2020 based on InSAR analysis

The map indicates that not all areas or pixels have subsidence values derived from the InSAR analysis. This is largely due to several factors, with temporal decorrelation being the primary cause. Temporal decorrelation occurs when the ground surface undergoes significant changes between satellite passes, such as through vegetation growth or reduction, agricultural activities, or construction alterations. Some areas are also unsuitable for analysis, including water bodies and surfaces that are too rough or heterogeneous, such as regions with steep hills and cliffs, where radar waves behave unpredictably, making it difficult for the radar signal to maintain coherence.

In addition to the InSAR analysis, subsidence measurements were also conducted in the study area using GPS by the Centre for Groundwater and Environmental Geology – Geological Agency, beginning in 2020. A total of 26 benchmarks were established in the study area, though they are only distributed in the eastern part, as shown in Figure 6.6. Measurements were conducted on a group of four benchmarks simultaneously before proceeding to the next group, and they were carried out three times a year from September 2020 to September 2021, yielding the results shown in Table 6.1. The GPS measurements were performed using the

static mode, which is a suitable method for measuring slow subsidence trends over months to years.

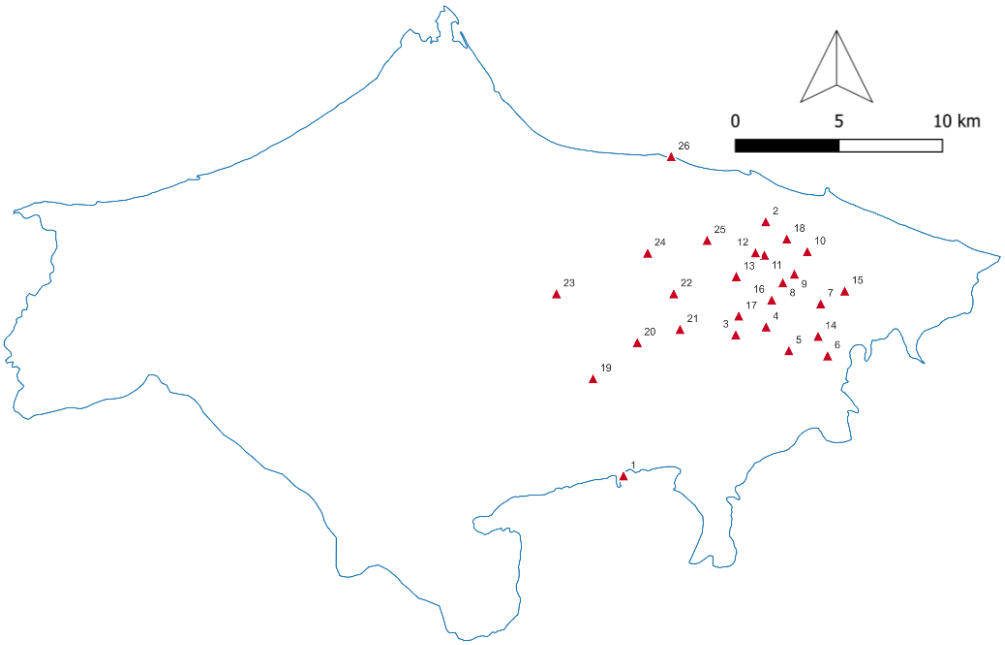

Figure 6.6 Distribution of 26 monitoring benchmarks for GPS measurement. The locations of GPS are concentrated in the eastern part of the study area, corresponding to the city of Pekalongan.

One of the main limitations of this study is the restricted temporal sampling of GPS measurements, which may affect the accuracy of subsidence estimates. Unlike InSAR, which provides continuous spatial subsidence data, GPS measurements are often constrained by infrequent temporal coverage, with data collection intervals heavily influenced by institutional programmes and budgets. This temporal limitation makes it challenging to capture the full variability of land subsidence dynamics, particularly short-term fluctuations caused by seasonal groundwater extraction. Consequently, subsidence trends derived from GPS data may not fully represent the continuous deformation processes.

The limited temporal sampling of GPS data also significantly impacts model calibration. Since model calibration relies on matching simulated subsidence with observed data, an inadequate number of GPS observations may lead to misrepresentation of subsidence rates and spatial patterns, ultimately reducing the predictive reliability of the model.

Table 6.1 Results of GPS measurement in 26 benchmarks

No	Name	X	Y	Displacement (m)
1	TRPK	345583.111	9227822.55	0.000
2	BM01	352550.652	9240339.85	-0.230
3	BM05	351090.569	9234780.52	-0.177
4	BM06	352582.330	9235171.37	-0.043
5	BM07	353706.924	9234003.71	-0.080
6	BM08	355614.703	9233757.92	-0.142
7	BM09	355269.147	9236317.73	-0.063
8	BM10	353401.454	9237343.88	-0.150
9	BM11	353969.671	9237771.14	-0.089
10	BM12	354601.873	9238878.85	-0.030
11	BM13	352490.202	9238701.90	-0.061
12	BM14	352050.073	9238813.93	-0.120
13	BM15	351109.178	9237646.82	-0.097
14	TP16	355146.954	9234716.44	0.019
15	TP17	356448.550	9236947.30	-0.091
16	TP18	352854.528	9236494.67	-0.160
17	TP19	351234.815	9235704.61	-0.272
18	TP20	353590.382	9239495.09	-0.094
19	TP21	344068.136	9232594.16	-0.018
20	TP22	346244.147	9234385.51	-0.050
21	TP23	348346.014	9235035.69	-0.128
22	TP24	348031.625	9236787.07	-0.226
23	TP25	342254.408	9236769.23	0.145
24	TP27	346740.917	9238786.48	-0.123
25	TP28	349666.579	9239420.54	-0.156
26	TP29	347886.882	9243535.71	0.005

The graph in Figure 6.7 comparlonges the subsidence rate from GPS and InSAR measurements using point-to-pixel comparison. Both sets of subsidence measurements show a positive trend, as indicated by the upward slope of the trend line. However, the low R^2 value suggests that the data points do not closely follow the trend line, indicating considerable variability in the alignment between the GPS and InSAR measurements.

The weak correlation between the GPS and InSAR subsidence measurements is likely due to a combination of factors. InSAR effectively captures large-scale subsidence patterns, while GPS provides precise point measurements. The differences in spatial resolution, accuracy, and sensitivity of these methods can lead to discrepancies in their results.

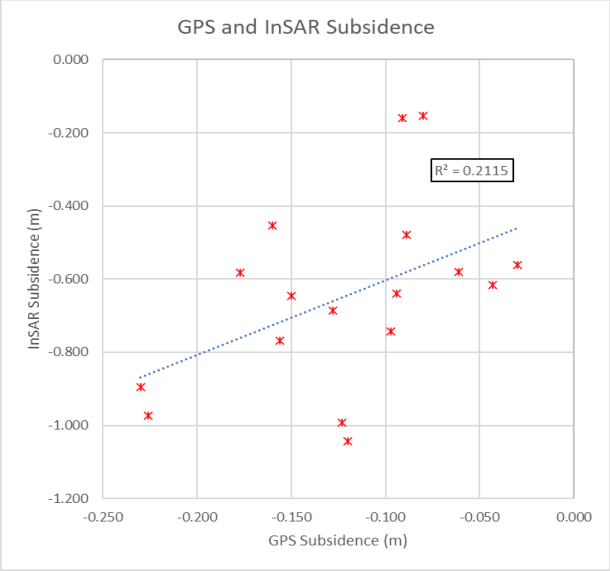

Figure 6.7 Point to pixel comparison between GPS and InSAR subsidence

6.3 InSAR and SUB subsidence comparison

The InSAR and SUB models provide spatial subsidence data, allowing for a spatial comparison of the subsidence results from the two methods. InSAR provides high spatial resolution coverage over large areas, enabling the detection of spatially continuous subsidence patterns across the study area. However, due to differences in data acquisition methods and representation, discrepancies may arise when comparing InSAR-derived subsidence with GPS measurements. GPS stations, being point-based, record displacement at specific fixed locations, which may not coincide with the most affected subsidence zones detected by InSAR. If GPS stations are sparsely distributed or situated outside the primary subsidence area, they may fail to capture the peak subsidence observed in InSAR results. Additionally, factors such as local ground conditions, differences in temporal observation periods, and atmospheric disturbances can cause shifts in the apparent subsidence center in InSAR measurements relative to GPS data.

Moreover, InSAR and GPS may report significantly different subsidence magnitudes due to variations in measurement accuracy and data processing techniques. InSAR measures displacement along the satellite's line of sight (LoS), which integrates both vertical and horizontal motion. Significant horizontal displacement can distort the true vertical subsidence magnitude, leading to discrepancies when compared to GPS, which directly measures three-dimensional displacement with high

precision. Furthermore, differences in data acquisition frequency and recording techniques—such as phase unwrapping errors in InSAR or potential instrumental drift in GPS—may contribute to variations in reported subsidence rates. (Bürgmann et al., 2000)

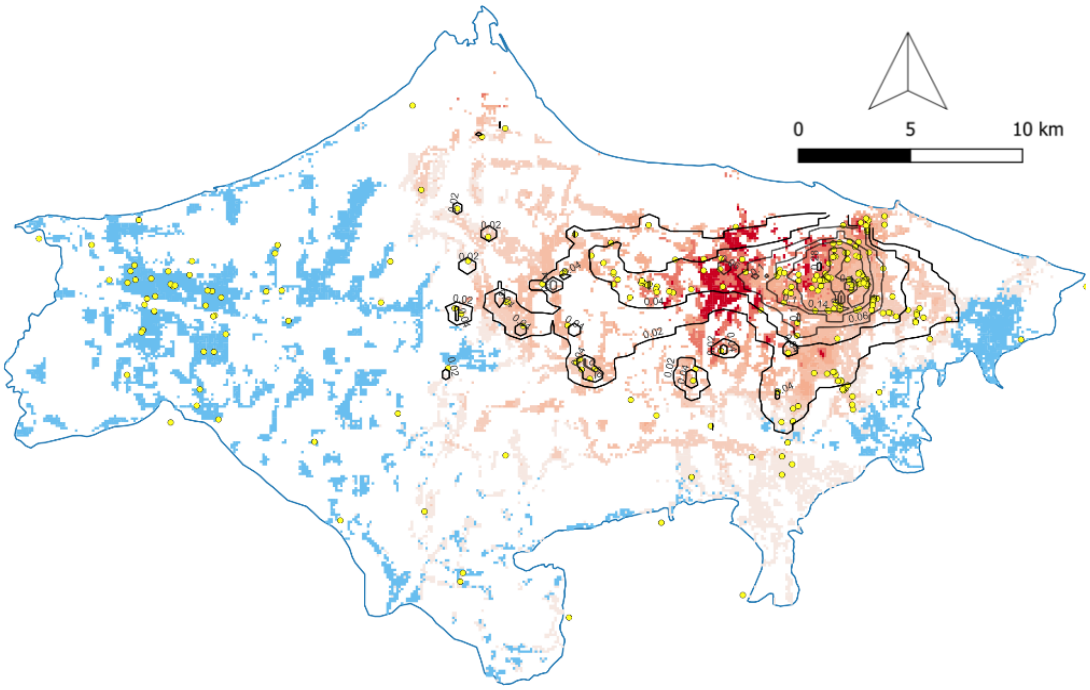

Figure 6.8 InSAR subsidence and SUB subsidence (in contour line), and abstraction well distribution

Figure 6.8 illustrates the comparison of the subsidence between these methods, with SUB subsidence displayed in contour form for improved visualisation. The subsidence areas are generally located in the same region, specifically in the northeastern part of the study area, which corresponds to the centre of Pekalongan City. However, it is evident that the subsidence peak, or the area with the highest subsidence values, does not occur in the exact location. The InSAR subsidence shows a peak that slightly shifts to the west compared to the SUB subsidence.

A pixel-to-pixel comparison of the two subsidence results is necessary to compare the subsidence rate values. The two subsidence results have different resolutions; InSAR subsidence has a pixel resolution of 100x100 m, whereas the SUB subsidence has a resolution of 500x500 m, in line with the resolution of the mudflow model. Therefore, it is necessary to standardise the resolution before making comparisons.

This can be achieved by applying downscaling to the SUB subsidence and adjusting it to a resolution of 100x100 m to match the resolution of InSAR.

From the graph, it can be observed that the subsidence values from the SUB analysis have a higher average compared to those from the InSAR subsidence. There is a positive relationship between SUB subsidence and InSAR subsidence, but it is not particularly strong. The data is mostly concentrated around lower subsidence values, indicating that low subsidence rates dominate the dataset. The low R^2 value suggests that the model outcomes do not match well the observations. It is possible that other factors not considered in this model may influence the InSAR subsidence.

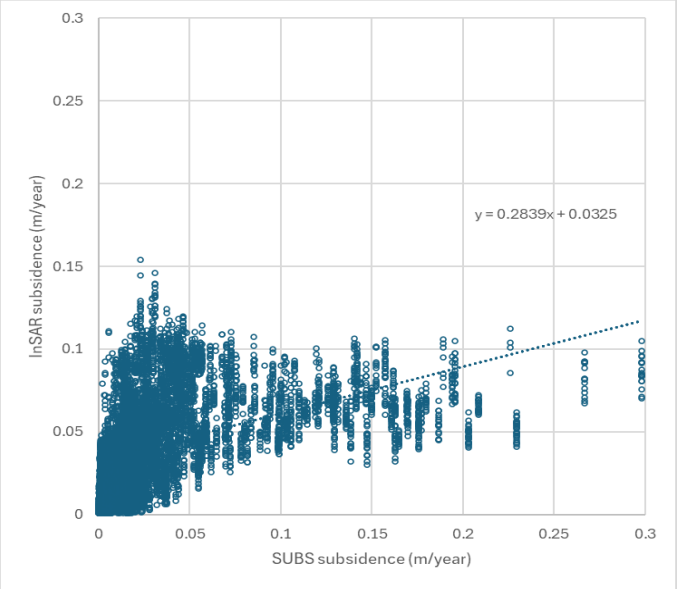

Figure 6.9 Graph showing pixel to pixel comparison InSAR and SUB subsidence

6.4 Subsidence projection with scenarios

The application of the numerical model involves predictions from the calibrated transient flow model, as well as the subsidence module. These predictions are based on future changes, both natural, such as climate change, and anthropogenic, including land use changes and groundwater abstraction due to projected water demand for various uses. The analysis will focus on the year 2030, maintaining a 10-year stress period as was used in the previous analysis. A summary of the scenarios considered in this study is presented in Table 6.2, where **LU** represents land use, **CC** denotes climate change, and **GA** stands for groundwater abstraction.

Table 6.2 A summary of projection scenarios

Type	Scenario	LU	CC	GA	Description
LU-CC	1	Unchanged	Changed	*not considered*	Land use remains unchanged, temperature increases
	2	Changed	Unchanged		Projected land use changes with no temperature increase.
	3	Changed	Changed		Both land use and temperature increase
GA	4	*not considered*		Unregulated	Increased groundwater abstraction with no regulatory intervention.
	5			Regulated	Increased abstraction with regulatory control

6.4.1 Land use and climate change scenarios

Climate change and land use dynamics have become vital factors influencing water resources, particularly groundwater. Globally, rising temperatures, shifting rainfall patterns, and the increasing frequency and intensity of extreme events such as droughts and floods directly affect the hydrological balance. These changes primarily impact groundwater recharge and result in a reduction in the aquifer's water storage capacity.

Furthermore, unsustainable land use practices, such as converting agricultural land into urban areas and rapid industrialisation, accelerate the degradation of groundwater resources. These activities often lead to excessive groundwater abstraction for irrigation, domestic, and industrial purposes, which can cause a significant decline in groundwater levels. In urban areas, the impermeability of land due to concrete development reduces the land's ability to absorb water, impeding the aquifer recharge process and exacerbating groundwater conditions. The combination of excessive groundwater abstraction and reduced recharge can trigger land subsidence.

6.4.1.1 Land use change and temperature change prediction

The prediction of land use changes for 2030 was analysed using Google Earth Engine (GEE), with Landsat imagery as the primary data source and past land use data as model inputs. Choudhary et al. (2022) in their paper state that machine learning algorithms on the Google Earth Engine can be employed to classify and predict land

use and land cover for various purposes, such as crop mapping, yield prediction, and forest mapping. As a result, the projected land use 2030 was obtained, as shown in Figure 6.10.

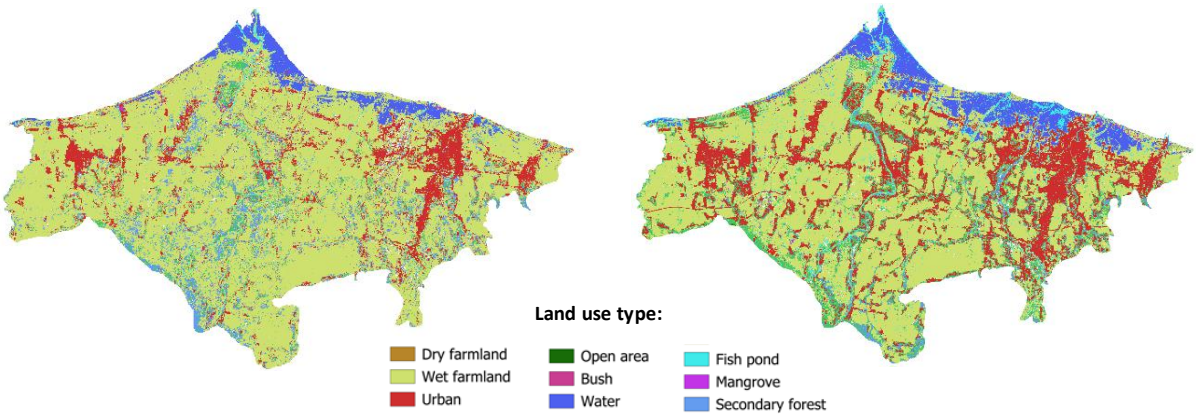

Figure 6.10 Land use of 2020 and projected land use of 2030

The predicted land use changes will be the basis for estimating groundwater recharge, a key input in MODFLOW, including the SUB model. In addition to land use, the projected temperature increase by 2030 due to climate change will also be considered in the scenarios for calculating groundwater recharge. Therefore, the scenarios created based on changes in land use and temperature are as follows:

1. Land use remains unchanged, and temperature increases.
   In this scenario, land use is assumed to remain unchanged by 2030, while temperature rises by 0.86°C, in line with IPCC estimates.
2. Land use changes, and the temperature remains constant.
   This scenario uses the projected land use for 2030, as estimated by GEE, assuming no temperature increase.
3. Land use changes, and temperature increases
   This scenario combines scenarios 1 and 2, where land use changes, and the temperature rises.

With the additional assumption that rainfall remains unchanged and other climatic parameters are also considered constant, no scenario assumes increased groundwater abstraction. This aims to assess the sensitivity of changes resulting solely from land use and temperature (climate parameters). Subsequently, the

SWAT model will be re-run to obtain groundwater recharge values for each scenario.

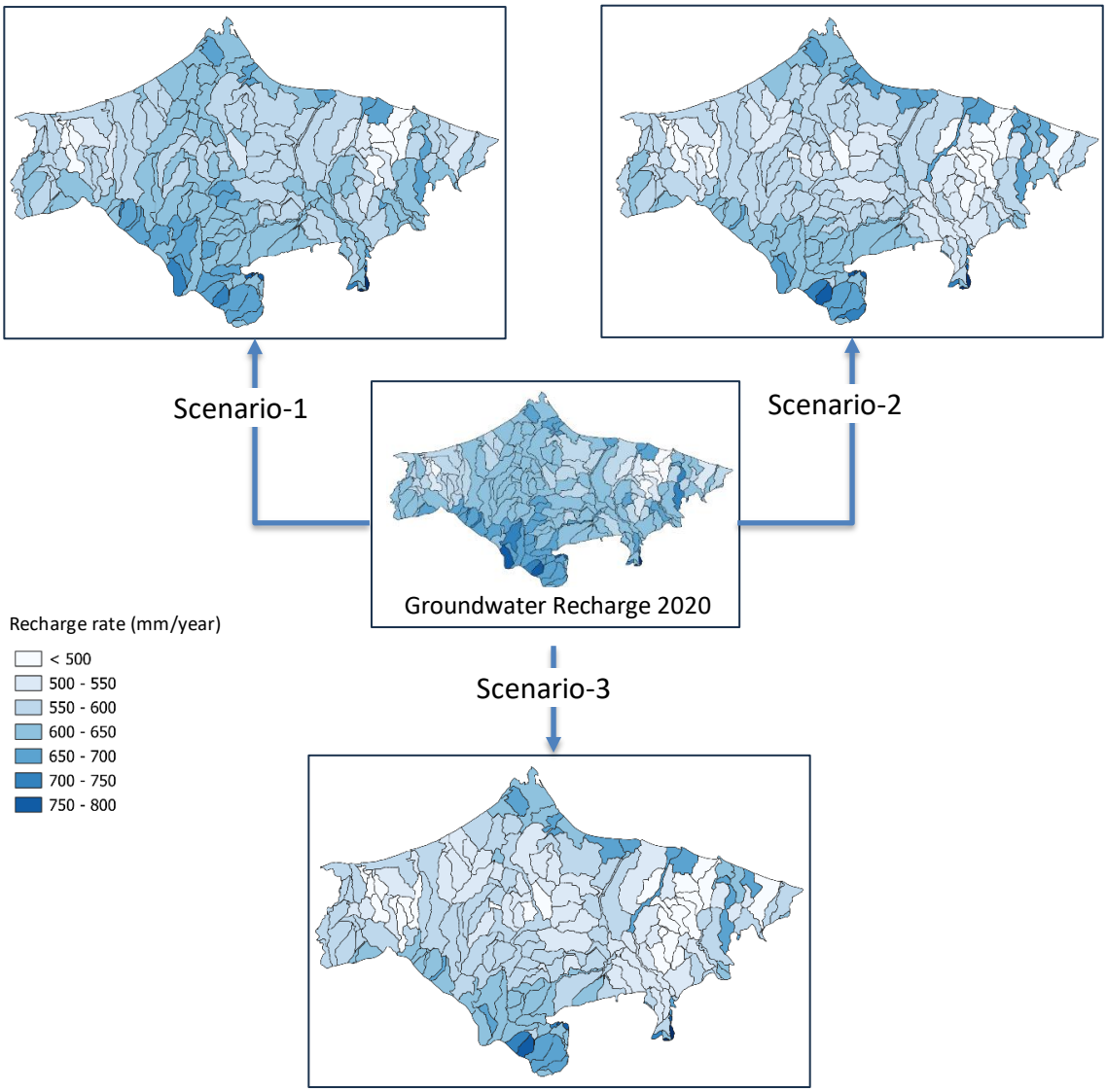

Figure 6.11 Spatial distribution of groundwater recharge due to land use and temperature change scenario

Figure 6.11 shows the values and spatial distribution of groundwater recharge for each scenario. Groundwater recharge values vary across each scenario, with differing changes observed for each sub-basin unit. The total annual values and the extent of changes are presented in Table 6.3.

The table shows that both changes in land use and temperature increases are causing a decrease in groundwater recharge rate. Land use changes have a more significant impact than temperature increases. When both factors are combined, the reduction in groundwater recharge becomes even more noticeable, reaching

9.13% by 2030. Figure 6.12 and 6.13 displays the residual values, representing the reduction in groundwater recharge for each sub-basin unit, compared to the 2020 groundwater recharge levels.

Table 6.3 Annual value and the change of groundwater recharge of each scenario

Scenario of Change	Groundwater recharge (mm/year)	The change (%)
Initial Land use and initial T (°C)	66,720.48	-
Unchanged Land use and T +0.86°C	65,404.33	-2.01%
Changed land use and Unchanged T (°C)	62,399.84	-6.92%
Changed land use and T +0.86°C	61,140.23	-9.13%

Figure 6.12 illustrates the changes in groundwater recharge due to temperature increase (Scenario 1) and land use change (Scenario 2). In Scenario 1, groundwater recharge consistently decreases across all sub-basins as temperature rises, with reductions ranging from 8.86 to 12.06 mm/year. The decrease is relatively uniform, primarily driven by increased evapotranspiration, which reduces the amount of water infiltrating into the subsurface. In contrast, Scenario 2 exhibits a much larger average reduction in groundwater recharge of 36.64 mm/year, but with significant spatial variability. Unlike Scenario 1, where changes are more uniform, Scenario 2 shows both extreme increases and decreases in groundwater recharge across different sub-basins. The most notable increase occurs in coastal areas affected by subsidence and tidal flooding, where wet farmland has been converted into fishponds, leading to the expansion of waterlogged areas and modifying local recharge patterns.

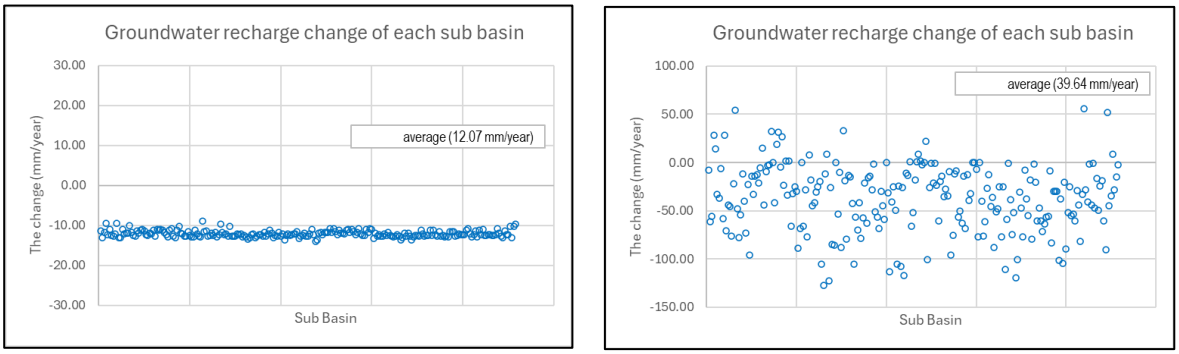

Figure 6.12 Groundwater recharge change of scenario 1 and 2

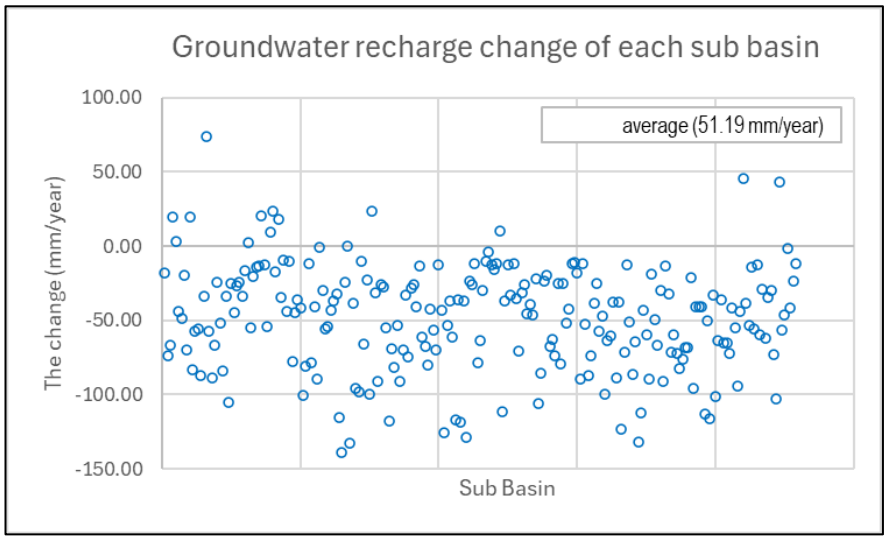

Figure 6.13 Groundwater recharge change of scenario 3; changed land use (land use 2030) and increased temperature (T = +0.86^{0}C)

Meanwhile, in Scenario 3 (Figure 6.13), which represents a combination of Scenarios 1 and 2, groundwater recharge exhibits substantial variations, ranging from approximately -150 mm/year to +100 mm/year. This indicates that the combined effects of temperature increase and land use change lead to significant spatial fluctuations in recharge patterns across different sub-basins. Some areas experience a notable increase in groundwater recharge, while others undergo a severe reduction, reflecting the complex interplay between climate-induced evapotranspiration and land cover modifications. The higher variability in recharge values suggests that integrating both climate and land use projections introduces greater uncertainty and diverse hydrological impacts, making groundwater recharge trends less predictable across the study area.

6.4.1.2 Effect of land use and climate change on subsidence in 2030

Groundwater recharge is an essential input parameter in groundwater and subsidence modelling, meaning that any change in recharge will affect the model's output. With various scenarios leading to changes in groundwater recharge, MODFLOW and the SUB package need to be re-run with updated recharge values to assess the impact of land use and temperature changes on the resulting model outputs.

The results of the model simulations for various scenarios of groundwater recharge changes due to land use and temperature alterations show the projected

subsidence in the study area by 2030, as seen in Figure 6.14. The increase in the subsidence across different scenarios is not substantially different, as illustrated in the graph in Figure 6.15.

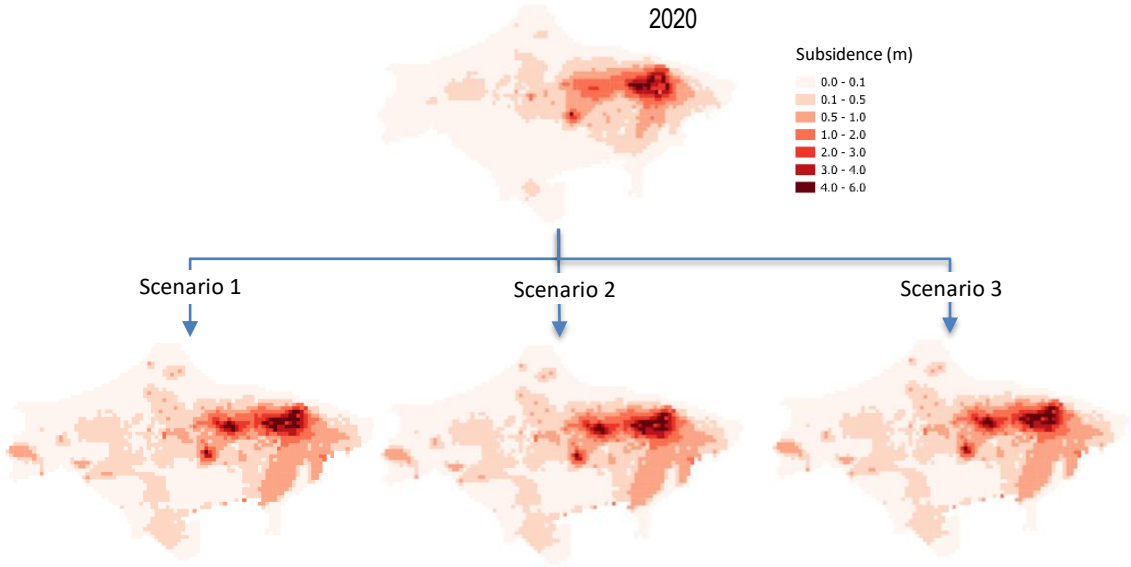

Figure 6.14 Predicted subsidence of scenario 1,2 and 3 compared to subsidence of 2020

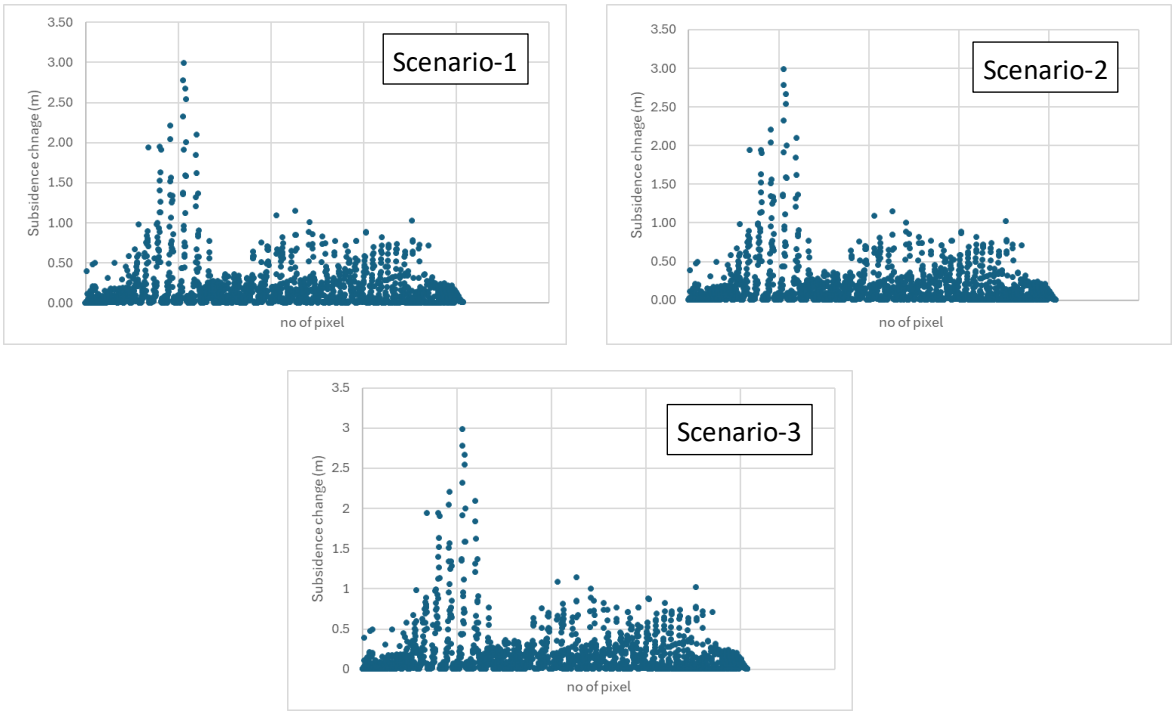

Figure 6.15 Change in subsidence for scenarios 1, 2, and 3 based on the 2020 rate. It is observed that all scenarios show nearly identical increases in subsidence.

Table 6.4 Statistic of subsidence change of each scenario

	Subsidence rate change from 2020 (m)		
	Scenario-1	Scenario-2	Scenario-3
average	0.1077	0.1053	0.1054
max	2.9901	2.9859	2.9861
min	-2.8482	-2.8482	-2.8482

While, Table 6.4 shows that the decrease in groundwater recharge, driven by changes in land use and rising temperatures results in only about 1 mm of subsidence. This suggests that while recharge reduction plays a role in subsidence, its overall impact is relatively small compared to other factors, especially excessive groundwater abstraction, which remains the dominant driver of land subsidence in the study area.

6.4.2 Groundwater abstraction scenarios

6.4.2.1 Abstraction scenarios based on growth of groundwater withdrawal

The primary water demands in the study area, similar to other regions, stem from industrial, agricultural, and domestic use. The number of wells and the associated abstraction volumes are based on registered wells, as provided by the local government, as outlined in the well data sub-section of Chapter 3. However, there is no available data regarding the growth of industrial and agricultural areas, which could be used to project future water needs for these sectors. In addition to groundwater wells, industrial water demand is partially met by the Water Supply Company (PDAM) through piped water, although the proportion supplied by this source remains relatively small.

Table 6.5 Increasing abstraction rate from 1990 to 2020

Year	Abstraction rate (m^3/year)	Increase (%)
1990	1,734,480	-
2000	3,342,816	93%
2010	5,708,016	71%
2020	8,451,648	48%

For domestic use, water demand is generally met through two primary sources: individual household wells, typically less than 10 m deep with a maximum discharge of 5 m^3/day, and services provided by PDAM. According to research by Asri Cahaya

et al. (2021), PDAM meets 40% of household clean water demand in Pekalongan City. In contrast, the percentages are much lower in the Pekalongan Regency and Pemalang Regency regions. On average, piped water services provided by water supply companies nationally covered 20.69% of the population in 2020 (BPS, 2020). PDAM in these regions also relies on groundwater as their primary water source.

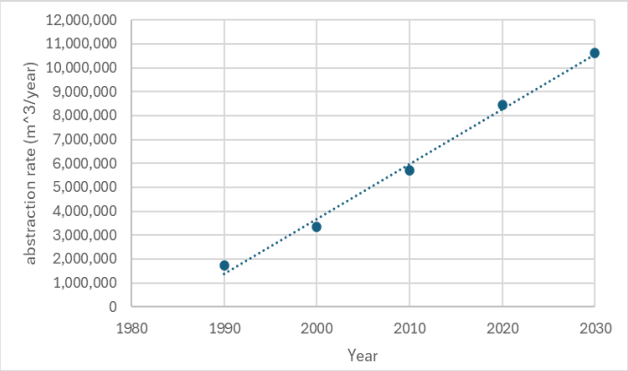

Figure 6.16 Previous data of abstraction rate and projected growth in 2030

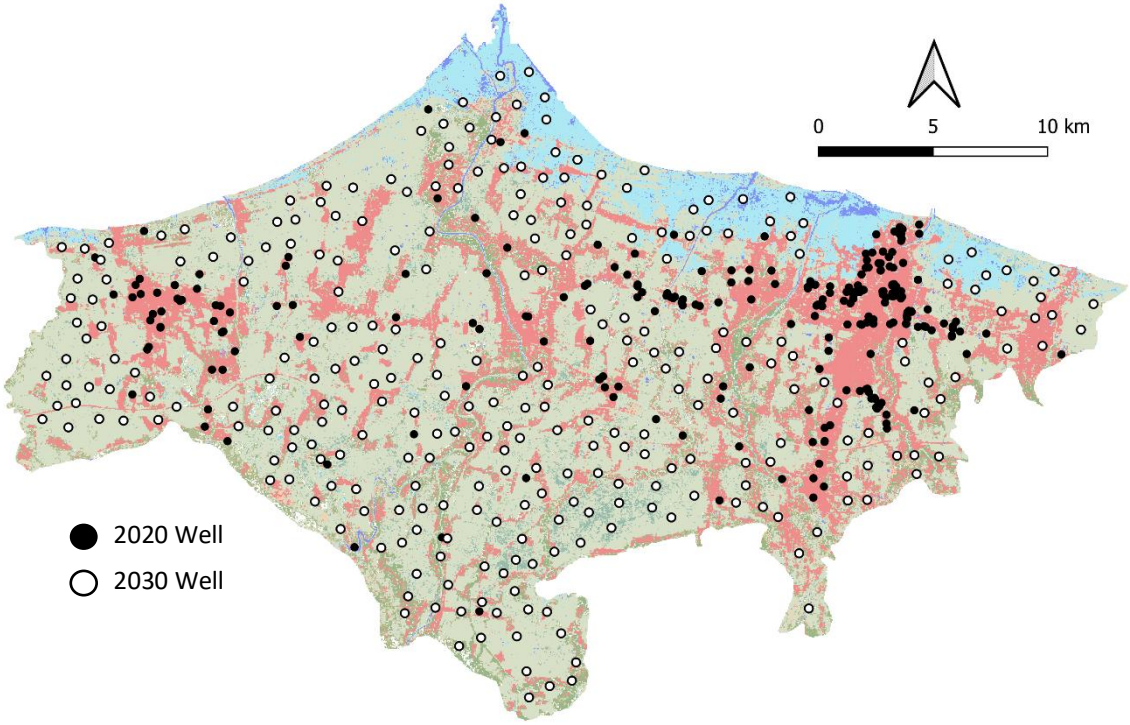

Figure 6.17 Abstraction well of 2020 and projected well in 2030

The lack of precise data on water demand growth across all sectors in this region has led to the decision that this scenario will be based on an increase in groundwater use, using historical data on abstraction volumes per well. Based on groundwater abstraction in previous years, the total abstraction for 2030 is projected to reach

10,637,244 m³/year (Table 6.5), a 26% increase from 2020. With an estimated discharge per well of approximately 100 m³/day, the number of abstraction wells in 2030 is expected to be 291 wells. The locations of new wells were randomly placed using vector creation module in Q-GIS with a 750-m buffer between wells to ensure adequate spacing between them (Figure 6.17).

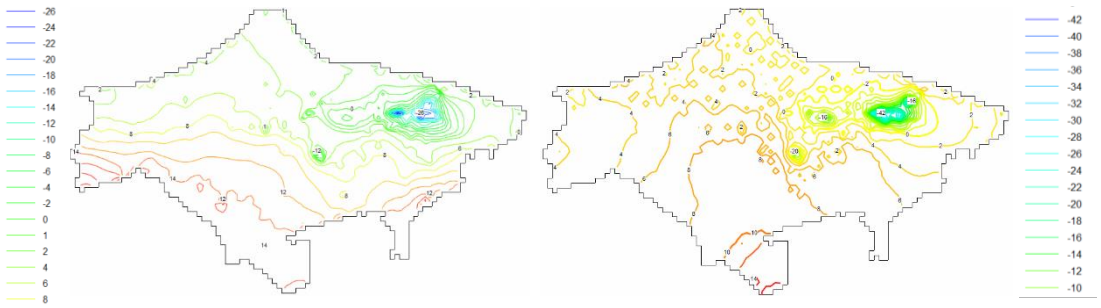

Figure 6.18 Groundwater level of 2020 dan projected 2030 for abstraction scenario without regulatory intervention

By 2030, without regulatory intervention, groundwater decline is expected to worsen, with the deepest cone of depression, which reached -26 m in 2020, deepening further to -42 m by 2030. Several small to medium cones of depression have also appeared in other locations, suggesting a significant decline in the groundwater table over time. The maps indicate that the most severe depletion areas have grown, signalling a critical decline in groundwater availability over the next decade if no measures are taken.

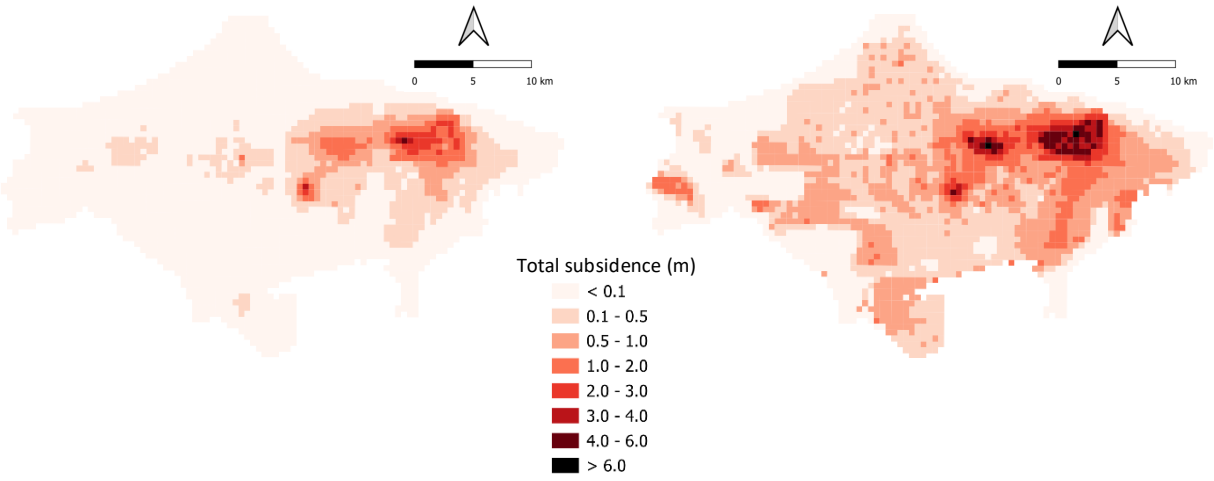

Figure 6.19 Total subsidence in 2020 and projected subsidence of 2030 under abstraction scenario without intervention

In Figure 6.19, the results of subsidence under the groundwater abstraction growth scenario are displayed. There has been a significant overall increase in subsidence, with new subsidence areas appearing where it was not previously observed. The expansion of new abstraction wells is the primary factor driving this extreme increase in land subsidence and the continued abstraction from older wells. In 2030, the subsidence under this extreme scenario reaches 6.81 meters, which is 4.34 meters higher than the 2020 subsidence. The pixel-by-pixel increases can be observed in Figure 6.20.

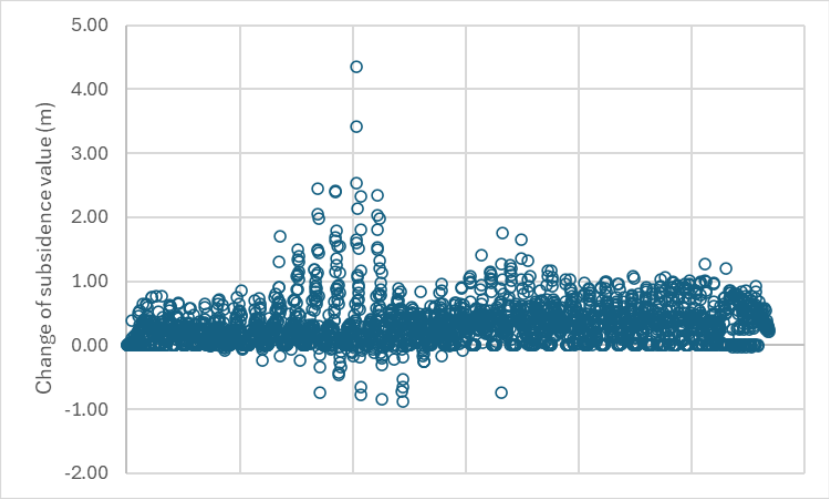

Figure 6.20 The changes of subsidence rate of each pixel

6.4.2.2 Abstraction scenarios with regulatory intervention

The Indonesian government has implemented policies concerning groundwater utilisation through several established regulations, one of which is controlling groundwater abstraction using a groundwater conservation zone map. The permitted volume of groundwater abstraction must align with the zoning on this map, with the aim of preventing groundwater degradation and subsequent hazards such as land subsidence and seawater intrusion. This regulation is part of the Minister of Energy and Mineral Resources Decree No. 259.K/GL.01/MEM.G/2022 on Standards for Groundwater Abstraction Licensing. The procedure for calculating the division of conservation zones can be seen in Figure 6.21, with the criteria provided in Table 6.6 (Effendi and Pasaribu, 2016).

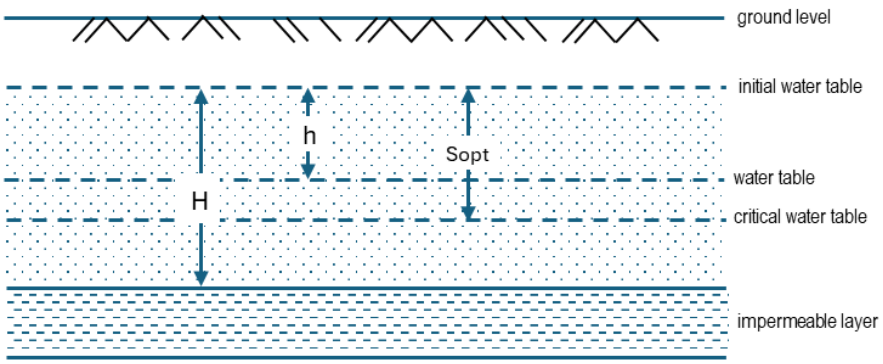

Sopt = declined water level due to groundwater abstraction with optimum pumping volume
= 60/100 x H
H = thickness of unconfined aquifer system
= thickness of initial groundwater column
h = declined groundwater column after groundwater abstraction

Changes in groundwater column (s) = h/Sopt x 100%
Safe : s < 40%
Vulnerabale : s between 40% - 60%
Critical : s between 60% - 80%
Broken : s > 80%

Figure 6.21 Criteria for groundwater damage for unconfined aquifer system

The most recent Groundwater Conservation Zone Map for this basin remains the reference for this scenario. This map was published and established by the Regional Government of Central Java (PT. Giri Awas, 2012) in 2012 (Figure 6.22). The areas classified as vulnerable, critical, and damaged zones are only located within Pekalongan City, while most of the other areas in the basin remain in the safe zone. The number and classification of wells based on this conservation zone map is shown in Table 6.7.

Table 6.6 Classification of groundwater damage

Decline of groundwater level / Groundwater quality	<40%	40% - 60%	60% - 80%	>80%
TDS < 1000 mg/l EC < 1000 µs/cm	Safe			
TDS < 1000 mg/l EC 1000 - 1500 µs/cm	Vulnerable			
TDS 10,000 - 100,000 mg/l EC 1500 - 5000 µs/cm	Critical			
TDS >100,000 mg/l EC > 5000 µs/cm	Broken			

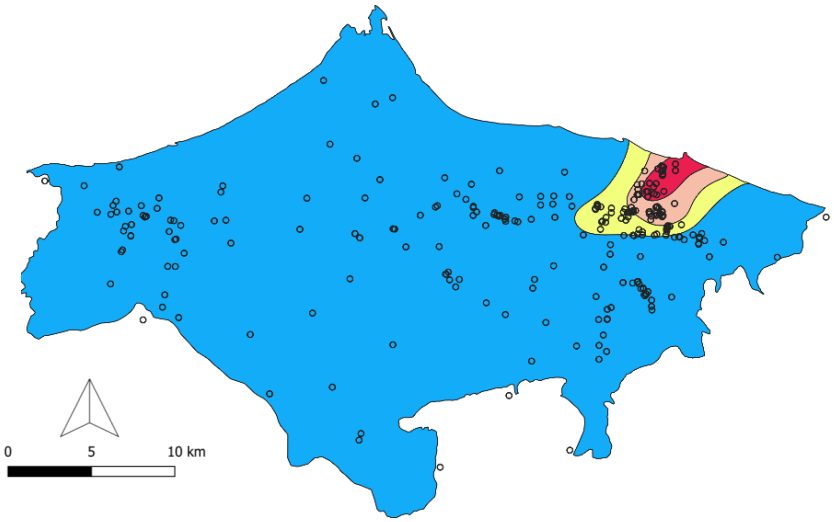

Figure 6.22 Map of groundwater conservation zone and well distribution

Table 6.7 Number of well based on conservation zone classification

Category	Number of Well
Safe	150
Vulnerable	59
Critical	34
Broken	23

Based on the explanation above, the assumptions used for the 2030 projection with regulatory interventions are as follows:

1. Groundwater recharge used in this scenario is derived from the land use change scenario combined with a temperature increase of 0.86°C.
2. No additional groundwater abstraction wells will be established by 2030.
3. The abstraction volume of existing wells will be adjusted according to the conservation zone of each well, with the following conditions:
    - *Safe zone*: abstraction volume remains unchanged
    - *Vulnerable zone*: well discharge reduced by 10%
    - *Critical zone*: well discharge reduced by 25%
    - *Broken zone*: well discharge reduced by 50%

Based on the above scenarios and assumptions, the model was re-run to obtain the predicted groundwater conditions and, more importantly, land subsidence for the year 2030.

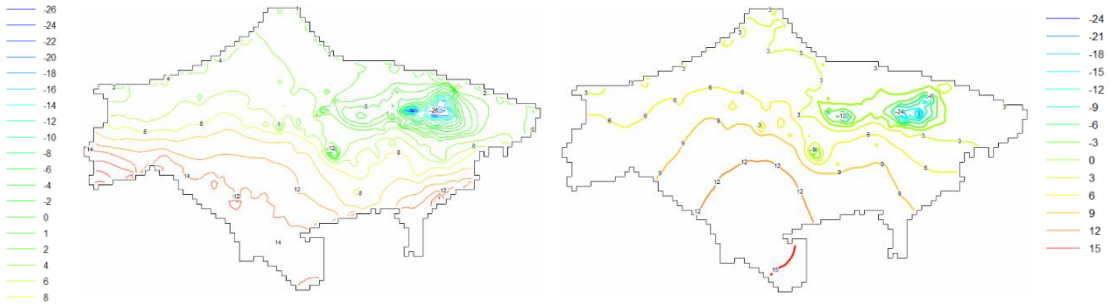

Figure 6.23 Simulated head of 2020 dan projected 2030 for abstraction scenario with regulatory intervention

In this groundwater abstraction scenario, the groundwater levels in the study area generally improve. The water level in the cone of depression, which was at -26 m in 2020, is projected to rise to -24 m by 2030 (Figure 6.23). This improvement is due to reduced abstraction rates from wells in critical and damaged zones. However, groundwater levels continue to decline in other locations as abstraction rates remain the same in areas classified as safe zones.

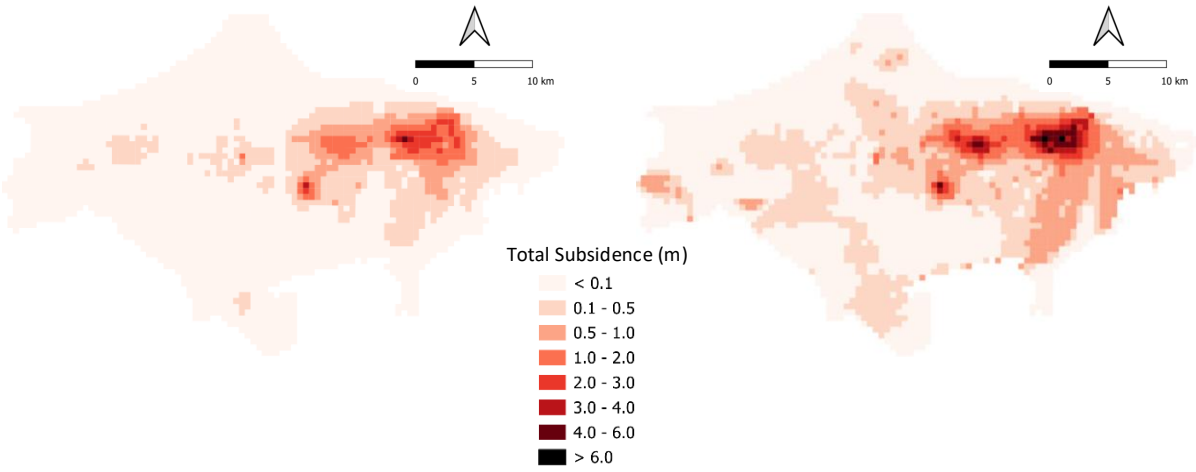

Figure 6.24 Total subsidence rate 2020 and projected subsidence of 2030 under abstraction scenario

In Figure 6.24, it is obvious that even with the current regulations, controlling groundwater abstraction still causes an increase in subsidence and the expansion of affected areas in the study region. However, there are some areas that show improvement or a decrease in subsidence. The graph in Figure 6.25 depicts the changes in subsidence for each pixel from 2020, showing an average increase of 0.058 m with a maximum increase of 2.63 m. In contrast, uplift or a reduction in total subsidence is observed over the 10-year period (2020–2030), with a maximum value

reaching 2.49 metres. This is a significant change, and although it is a predicted model outcome, it is physically challenging to occur in reality.

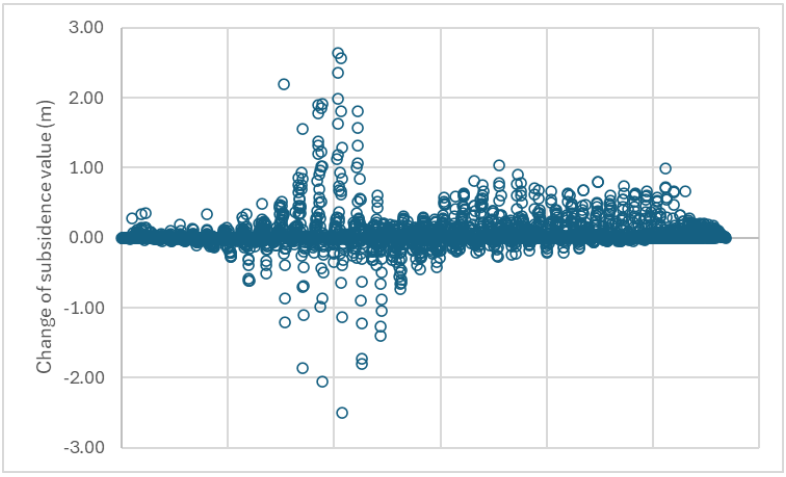

Figure 6.25 The changes of subsidence value of each pixel

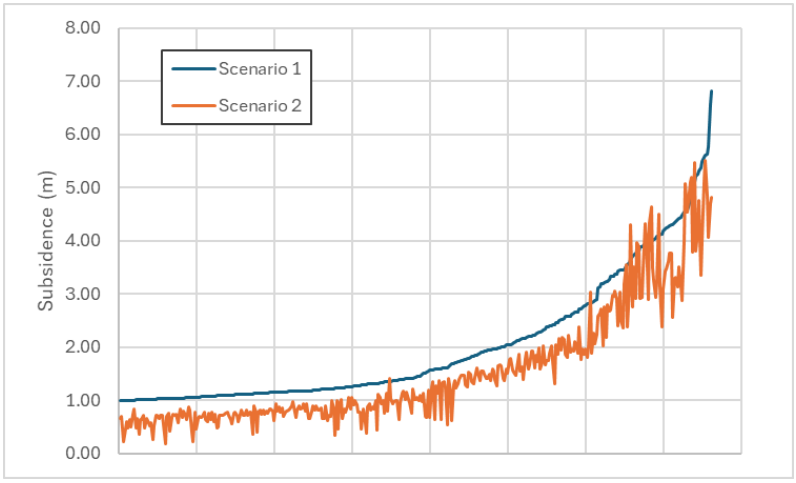

Figure 6.26 Pixel to pixel subsidence rate comparison of abstraction scenario 1 (without intervention) and scenario 2 (with regulatory intervention)

In comparison to the previous scenario, where groundwater extraction increased significantly without being regulated, the scenario where extraction is regulated shows a more positive impact, especially in slowing the rate of subsidence. Subsidence rates above 1 m experienced a 24% reduction, with a pixel-to-pixel comparison of the two subsidence scenarios shown in Figure 6.26. Although some improvement is observed, land subsidence continues because groundwater abstraction persists, albeit with reduced volumes.

6.5 Mitigation strategy to control subsidence through groundwater management

The scenarios analysed indicate that, despite current regulatory measures, land subsidence persists in the region. Therefore, stricter mitigation actions are needed to prevent further subsidence-related impacts in Pekalongan and surrounding areas. The most direct approach would involve the cessation of all groundwater extraction within the study area, with an alternative water supply sourced from surface water, potentially by constructing dams for raw water reservoirs. However, this is not feasible in the short term, as groundwater remains the primary water source in this region and in nearly all major cities in Indonesia.

Considering the conditions explained above, several mitigation scenarios have been proposed for the study area to address land subsidence issues effectively:

1. Incorporating subsidence criteria into groundwater conservation regulations, with the following classifications:
   - Zones with a subsidence rate exceeding 10 cm/year are classified as *Broken Zone*
   - Zones with a subsidence rate of 3–10 cm/year are classified as *Critical Zone*
   - Zones with a subsidence rate of 1-3 cm/year are classified as *Vulnerable Zone*

   Consequently, *Map of Groundwater Conservation Zone* for the Pekalongan Groundwater Basin should be updated to serve as a basis for issuing groundwater abstraction permits.
2. Cessation of groundwater extraction in critical and damaged zones.
3. Groundwater abstraction from existing wells in safe zones will be permitted to continue, while in vulnerable zones, abstraction rates will be reduced by 75%.
4. No new groundwater abstraction permits will be issued. It is assumed that by 2030, additional water demand will be met by raw water supplied from surface water reservoirs planned for construction in the southern region.

Based on the assumptions outlined in the proposed scenarios, an analysis and delineation of conservation zones were conducted, as illustrated in Figure 6.27. From this figure, it is evident that the damaged and critical zones, defined by subsidence rate levels, cover a larger area compared to those classified based on groundwater level decline criteria.

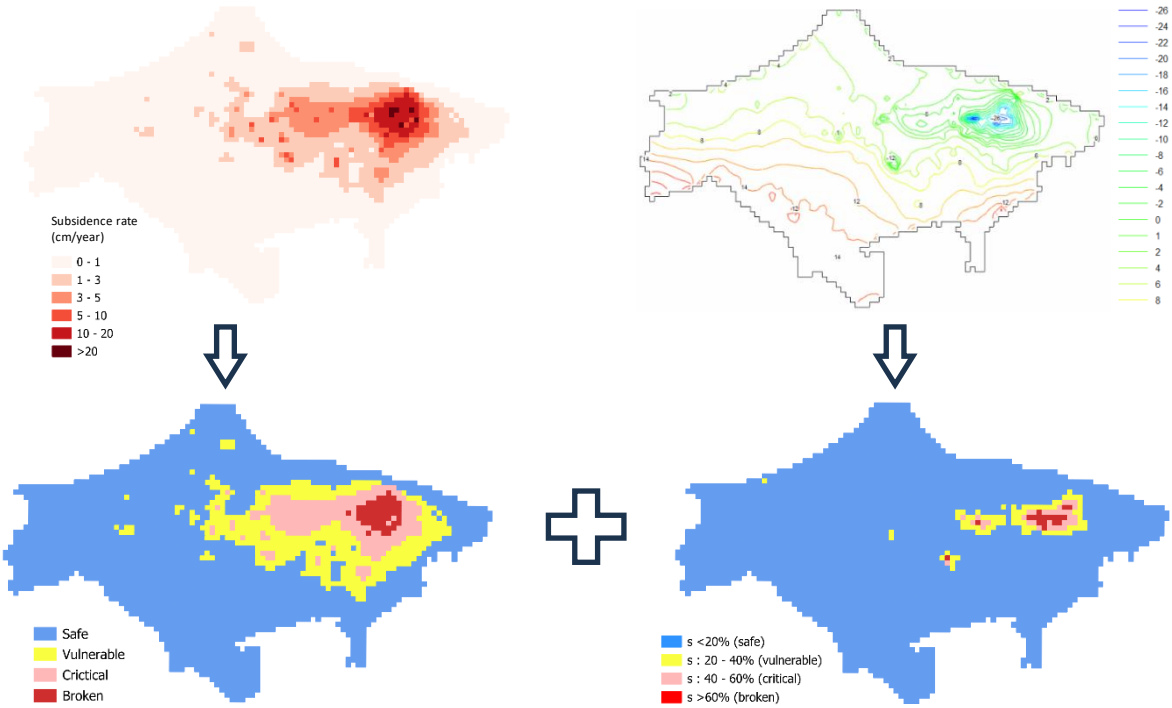

Figure 6.27 Classification of groundwater conservation zones based on subsidence rate and groundwater level

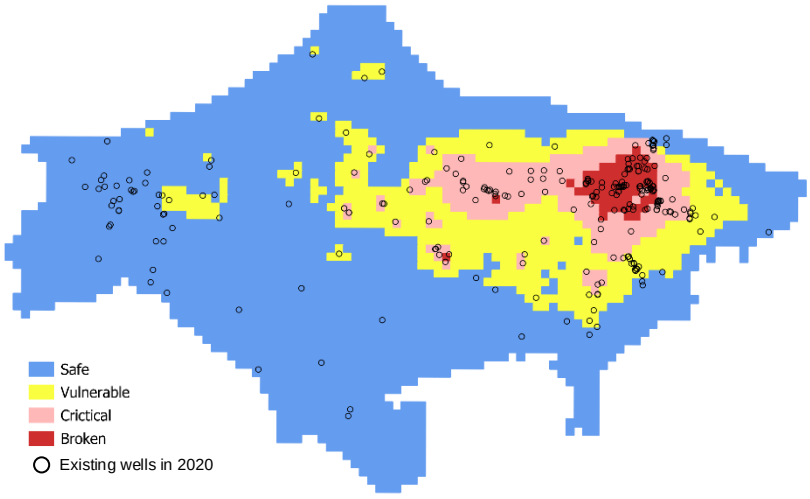

Figure 6.28 Combination of groundwater conservation zone from subsidence rate and groundwater level classification and distribution of existing wells in 2020

Table 6.8 Number of well based on new classification of conservation zone

Category	Number of well
Safe	60
Vulnerable	36
Critical	91
Broken	75

Using the groundwater conservation zone map, which integrates multiple criteria as shown in Figure 6.28, the number and classification of groundwater abstraction

wells, as presented in Table 6.8. This new classification, developed according to the proposed mitigation scenarios, reveals that the number of wells in the damaged and critical zones is significantly higher compared to the previous classification (see Subsection 6.4.2.2). Subsequently, the proposed scenario will be applied to a predictive model to evaluate whether the mitigation objectives—restoring groundwater levels and slowing or even halting the subsidence rate—can be effectively achieved.

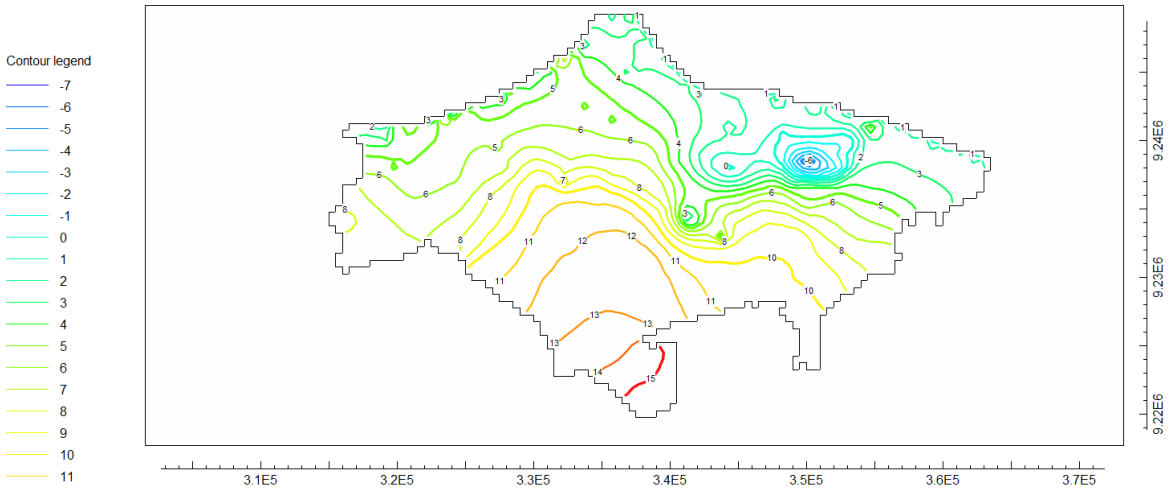

Figure 6.29 Simulated head of 2030 after mitigation scenario implementation

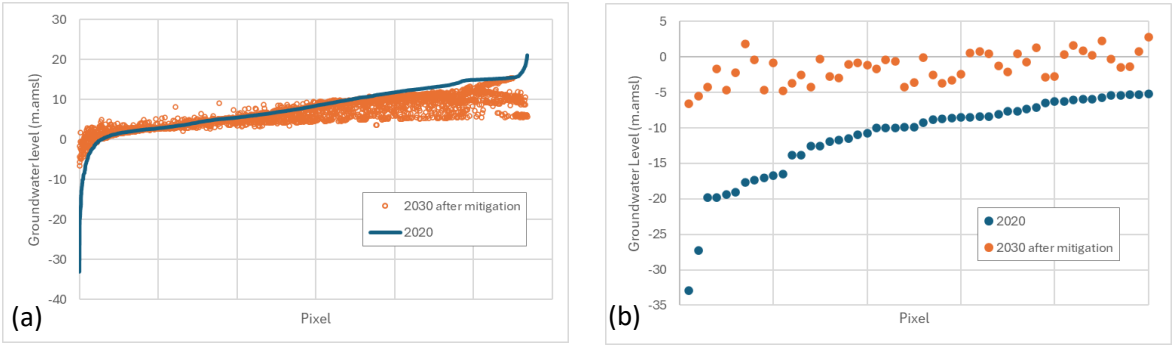

Figure 6.30 Groundwater level changes from 2020 to 2030: (a) across all pixels and (b) for groundwater levels deeper than -5 m above mean sea level (amsl)

From Figures 6.29 and 6.30, it can be concluded that with the planned mitigation scenario, the groundwater level in the study area recovers quite significantly. This is especially confirmed for groundwater levels deeper than -5 m amsl, which show a dramatic rise, as seen in Figure 6.30(b). For instance, a location with a groundwater depth of -32.9 m amsl in 2020 has recovered to -6.6 m amsl by 2030.

To assess the impact of the mitigation scenario on subsidence in the study area, a comparison is made between subsidence in 2020 and 2030 following the implementation of the mitigation measures. Figure 6.31 illustrates the total subsidence in 2010, 2020, and 2030 after mitigation efforts. It is shows that in areas with high subsidence, significant changes or increases in subsidence are observed from 2010 to 2030. However, from 2020 to 2030, minimal changes are seen, even though subsidence continues to occur in other areas.

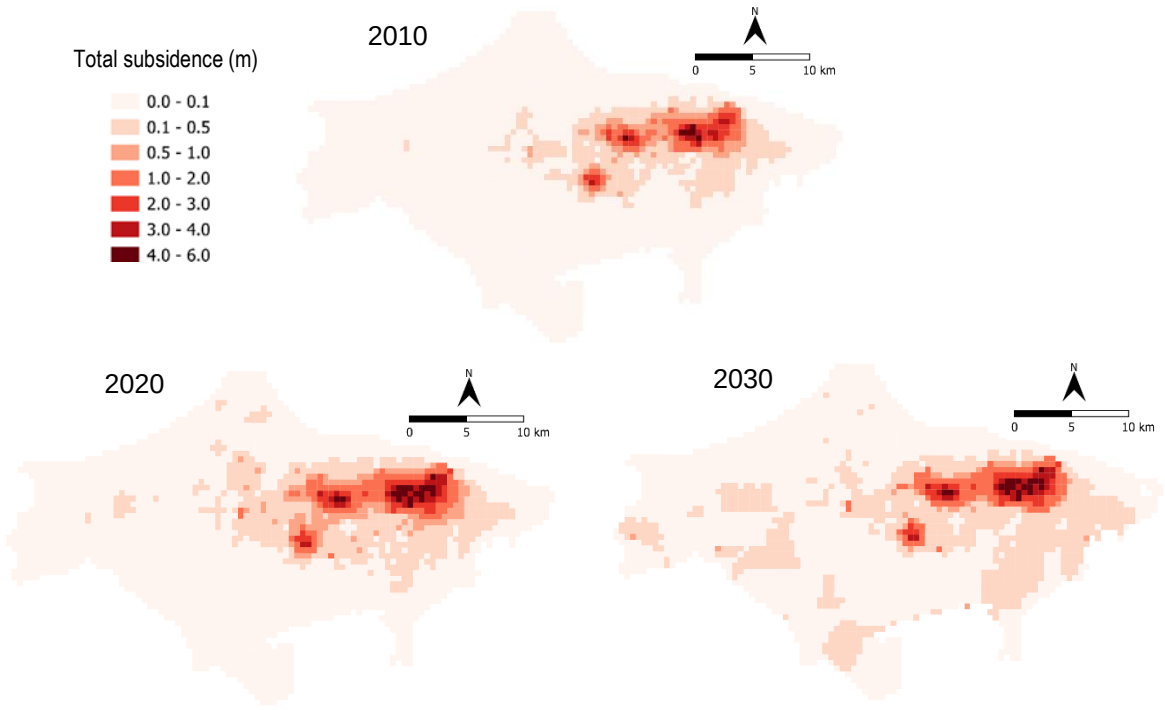

Figure 6.31 Total subsidence of 2010, 2020 dan 2030

The annual subsidence rate in *centimetres* unit can be seen in Figure 6.32, which also shows the distribution of groundwater abstraction wells. In the 2010-2020 period, areas with a high subsidence rate of over 5 cm/year spanned a relatively large area, with the maximum subsidence rate reaching 24.9 cm/year. This was due to the continued intensive abstraction of groundwater in the region. In contrast, during the 2020-2030 period, after mitigation efforts were implemented—such as halting groundwater abstraction in *critical and broken zones* (areas with high groundwater drawdown and subsidence)—the subsidence rate in these areas significantly slowed, even nearly halting altogether. Although subsidence with a rate less than 3 cm/year was still observed in other areas, this was because groundwater

abstraction continued in those regions, which are symbolized by the blue and red circles in the figure.

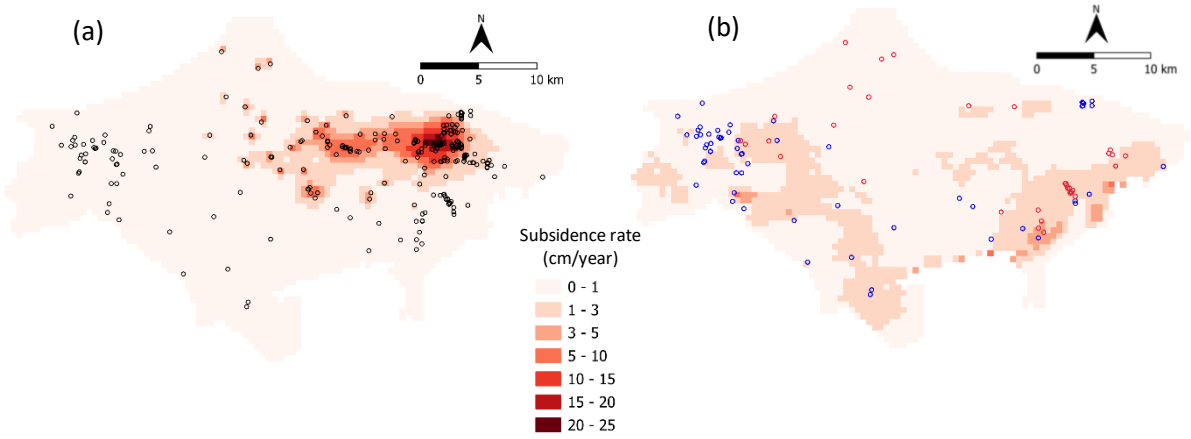

Figure 6.32 (a) Annual rate of subsidence and abstraction well in 2010-2020 and (b) annual rate of subsidence and abstraction well in 2020-2030; in cm/year

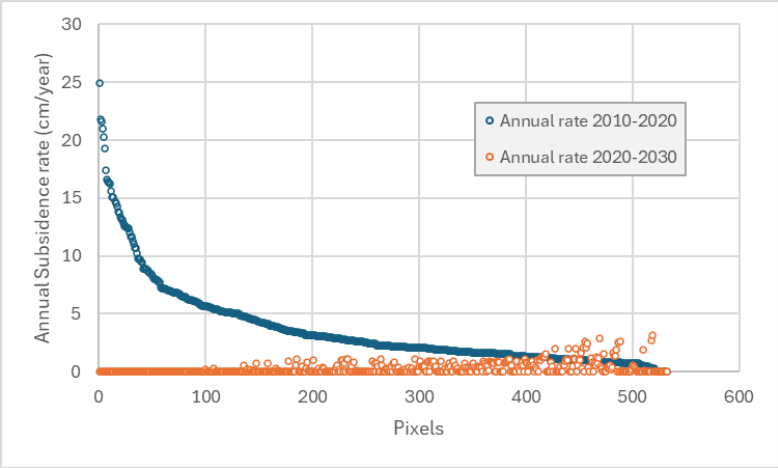

Figure 6.33 Comparison of annual rates for the periods 2010–2020 and 2020–2030

6.6 Conclusion

This chapter provides an in-depth explanation of the land subsidence issue in the Pekalongan region, highlighting its causes, current status, and future projections based on various influencing factors, including groundwater abstraction, land use changes, and climate change. The analysis confirms that land subsidence has become a severe issue in the study area, with a significant increase in subsidence rates observed over recent decades.

Generally, the subsidence results from both InSAR and SUB MODFLOW show the same trend. However, due to the entirely different analysis and calculation methods,

the results from the two are slightly different, with the SUB model producing slightly higher subsidence values. The GPS results, which were expected to serve as the most reliable reference data, also show a weak correlation with the InSAR results, making the plan to validate the subsidence results from the SUB model with InSAR less relevant. A more in-depth study is needed on subsidence analysis methods using remote sensing that can produce reliable results and be used as a basis for the validation and calibration of SUB modelling.

The future projections presented in this chapter consider several scenarios based on anticipated changes in climate policy, land use, and groundwater management. Although land use and climate change do not directly cause subsidence, their impact on groundwater recharge and water availability will likely exacerbate the issue. As temperatures rise and rainfall patterns become less predictable, the region will face more pressure on its already overexploited groundwater resources. Adaptation strategies focusing on enhancing natural groundwater recharge and reducing dependence on groundwater abstraction will be crucial to mitigating the long-term effects of land subsidence.

CHAPTER 7
Conclusion

This study employs a comprehensive approach to understanding land subsidence associated with groundwater abstraction in the study area, a coastal region with aquifers composed of young alluvial materials. This approach integrates a conceptual understanding of the study area, employs diverse methodological approaches, and utilizes varied data sources.

7.1 Summary of aims

The research aims to investigate the impact of groundwater abstraction on land subsidence in the Pekalongan region, a coastal area in Java, Indonesia. This study seeks to estimate subsidence using remote sensing and GPS measurements as comparative data. By developing a comprehensive lithological model and estimating key aquifer parameters, particularly hydraulic conductivity, a hydrogeological conceptual model of the area is designed for implementation in MODFLOW-2005. This model evaluates how subsurface dynamics contribute to subsidence and predicts future subsidence. The ultimate goal is to inform groundwater management strategies that can mitigate subsidence under various climate change scenarios, land use changes, and groundwater abstraction practices.

7.2 The explanation of each chapter to the research questions

These are the comprehensive overview of the justification of each chapter to the research questions posed earlier:

1. *How does groundwater abstraction affect land subsidence rate and spatial distribution in coastal regions, particularly in the study area?*

   Chapters 5 and 6 explicitly address this inquiry. Chapter 5 reveals that intensive groundwater abstraction in the study area has led to a significant drop in groundwater levels, creating several cones of depression. This decline in water

levels directly correlates with observable land subsidence, mainly manifesting in areas where groundwater depression is most acute.

2. *What roles do remote sensing and numerical modelling play in accurately estimating future land subsidence due to groundwater withdrawal in the study area?*

   Chapter 5 discusses groundwater modelling using calibrated input parameters, which enables the application of the SUB Package to estimate subsidence rates.

   Chapter 6 explains how remote sensing and numerical modelling provide essential spatial data on regional subsidence rates. Interestingly, while these approaches are valuable individually, they exhibit poor correlation when compared directly. GPS data intended as a validation reference for InSAR measurements also showed a weak correlation with the subsidence patterns detected by InSAR. This difference indicates there might be issues with the current models or data collection. It highlights the need to improve remote sensing and numerical modelling to predict future land subsidence better.

3. *How does land-use change affect land subsidence in coastal tropical areas compared to climate change?*

   Chapter 6 concludes that although changes in land use and anticipated temperature increase affect groundwater recharge, their impact on projected subsidence rates by 2030 is relatively minimal. Instead, continued and increased groundwater abstraction remains the dominant factor exacerbating land subsidence within the study area.

4. *Which groundwater management and adaptation strategies could effectively mitigate land subsidence while supporting sustainable water resources in the study area?*

   Chapter 6 further investigates potential management strategies, indicating that existing regulations that limit groundwater abstraction, particularly in regions identified as high-risk for subsidence, have not succeeded in stabilizing or reversing subsidence rates. To address this, stricter groundwater abstraction

regulations are necessary, particularly in areas experiencing high subsidence. Additionally, prioritizing the construction of a raw water reservoir dam south of Pekalongan would reduce the community's dependence on groundwater, helping to mitigate subsidence rates.

7.3 Overview of the research contribution

Some of the original contributions of this study include:

1. *Data Input and Calibration Process*

   This study provides a detailed lithological model using field data from geotechnical and groundwater drilling, as well as geoelectrical surveys. The lithotypes obtained from this model are then integrated with hydraulic conductivity data derived from pumping tests, allowing for determining hydraulic conductivity values for each lithotype. Hydraulic conductivity values are calibrated to each lithotype, ensuring that hydraulic conductivity remains within the typical range for each lithotype. Accurate calibration of hydraulic conductivity is an essential stage in improving the model's ability to replicate observed groundwater levels and flow patterns, leading to more reliable predictions.

2. *Conceptual and Methodological Advancements*

   The research presents conceptual and methodological advancements by integrating MODFLOW-2005 with a tailored approach designed for specific hydrogeological and geological conditions in a tropical coastal environment. The project also incorporates InSAR and GPS measurements, enhancing subsidence model accuracy and offering new data on subsidence rates in the study area.

3. *Scenario-Based Projections*

   The research offers projections on subsidence trends based on future land use, climate change, and groundwater abstraction scenarios, particularly applying existing regulations currently used to limit groundwater usage. This approach provides insights into the long-term implications of extensive groundwater use in the study area and aids in developing adaptation and mitigation strategies to address future subsidence-related hazards.

7.4 Implications of the research

The findings of this study have significant practical implications for groundwater and land use management in both the study area and similar regions:

1. *Informed Policy Development*

   This study establishes the link between land subsidence and groundwater abstraction, providing a foundation for developing regulations to limit groundwater pumping, particularly in regions at high risk of subsidence. By identifying areas most susceptible to subsidence due to excessive groundwater abstraction, policymakers can implement targeted mitigation strategies. Furthermore, the findings can contribute to the development of groundwater conservation policies, including restrictions on pumping rates. Integrating subsidence data into regional planning efforts could also help prioritize monitoring and early-warning systems in vulnerable areas, ensuring that mitigation measures are implemented.

   Beyond the study area, the insights from this research have broader implications for groundwater management in regions facing similar challenges. Given the increasing global concern over land subsidence linked to groundwater extraction, these findings provide valuable guidance for other areas, particularly urban coastal regions and other areas where groundwater serves as a primary water source. The application of modelling approaches, such as the one used in this study, combined with localized data, can be adapted for other regions to predict and mitigate subsidence. Moreover, the integration of subsidence data into groundwater management strategies could serve as a critical tool for policymakers to ensure sustainable water use and preserve land stability in vulnerable regions worldwide.

2. *Enhanced Subsidence Mitigation and Adaptation*

   The study demonstrates a strong correlation between subsidence and groundwater abstraction, underscoring the necessity of alternative water sources and strict regulatory controls on groundwater usage. Additional interventions, such as artificial groundwater recharge, should be considered to

mitigate subsidence in coastal urban areas. Furthermore, the study's subsidence projections offer valuable insights for adaptation programs and regional development planning, assisting in designing more resilient infrastructure and sustainable land use practices.

7.5 Limitation of the study

This study acknowledges several limitations that introduce uncertainties to the findings and may influence the reliability of the results. The three primary limitations are discussed below:

1. *Long-term stress period*

   The study employs a long-term stress period of 10 years for modelling and analysis. While this approach is effective for capturing decadal trends, it does not account for year-to-year fluctuations or specific annual events, such as the effects of exceptionally high rainfall or severe droughts in particular seasons.

   Shorter stress periods, such as one year, would require high-resolution temporal data, including detailed records of groundwater abstraction rates, recharge rates, and other time-sensitive parameters. Unfortunately, such data are scarce, and existing records are often aggregated over extended periods. This issue is compounded by inconsistent data management practices among relevant agencies, making the acquisition of high-resolution data particularly challenging.

   To address these limitations, the study relies on general assumptions and averages for parameters like recharge and abstraction rates over the 10-year period. Additionally, short-term variations in land use and climate were excluded. While this simplification reduces sensitivity to annual fluctuations and streamlines modelling and calibration, it aligns with the study's primary focus on long-term trends, such as groundwater dynamics and land subsidence over a decade.

2. *Accuracy of subsidence data*

   The accuracy and spatial distribution of subsidence data present significant uncertainties, affecting the reliability of the model. Field data for verification and

calibration are limited, with available GPS measurements offering sparse spatial coverage, inconsistent trends, and weak correlation with InSAR-derived subsidence results. Consequently, the subsidence data obtained from SUB-MODFLOW modelling in this research was not calibrated. This lack of calibration represents a notable limitation, as it prevents the model from being adjusted to match observed subsidence patterns. Without calibration, the model's accuracy in predicting subsidence at specific locations or over time is diminished, and its results should be interpreted with caution.

Despite these challenges, the subsidence model remains valuable for identifying general trends and highlighting areas vulnerable to groundwater-induced subsidence. The results provide insights into zones experiencing significant subsidence due to high groundwater abstraction, which can inform targeted conservation and management efforts.

While the limited precision of the subsidence data poses constraints, the findings contribute to a broader understanding of the long-term impacts of groundwater abstraction on land subsidence. These insights form a foundation for developing resource management policies, designing conservation strategies, and implementing effective mitigation measures.

3. *The partial knowledge of the basin hydrogeological setting.*

The limited understanding of the basin's hydrogeological setting introduces uncertainties in groundwater-subsidence modeling, affecting its accuracy. Insufficient borehole and hydrogeological data create gaps in developing the hydrogeological model and characterizing aquifer properties. Consequently, extrapolations across large areas and certain assumptions are necessary, which may not fully capture the system's complexity. These uncertainties impact the reliability of model outcomes and the effectiveness of subsidence mitigation strategies. To address this limitation, the study incorporates available geological and hydrogeological data to refine the conceptual model. However, further borehole investigations, pumping tests, and geophysical surveys are recommended to enhance hydrogeological understanding. Expanding data

collection in the future will help reduce uncertainties and improve the accuracy of groundwater-subsidence predictions.

4. *Temporal verification issue*

   The study does not continuously analyse the temporal variability of groundwater levels, primarily due to the lack of continuous monitoring data from observation wells in the study area. Existing groundwater monitoring wells often have incomplete data, as monitoring equipment frequently malfunctions, leading to gaps in records. This limitation significantly affects the study since groundwater levels naturally fluctuate over time due to seasonal variations, climatic conditions, groundwater extraction rates, and recharge events. Without continuous data, the model cannot undergo temporal verification, limiting its ability to reflect the dynamic behaviour of groundwater systems over time.

   Nonetheless, the model remains valuable for long-term trend analysis and scenario testing, which align with the study's primary objective: to assess the impacts of groundwater extraction scenarios on groundwater levels and land subsidence. While it cannot fully capture the temporal dynamics of the system, the model provides useful insights into the potential responses of groundwater levels to specific management or policy interventions.

REFERENCES

Abidin, H. Z., Andreas, H., Gumilar, I., Fukuda, Y., Pohan, Y. E., & Deguchi, T. (2011). Land subsidence of Jakarta (Indonesia) and its relation with urban development. *Natural Hazards*, *59*(3), 1753–1771. https://doi.org/10.1007/s11069-011-9866-9

Ahmed, A. A. (2009). Using lithologic modeling techniques for aquifer characterization and groundwater flow modeling of the Sohag area, Egypt. *Hydrogeology Journal*, *17*(5), 1189–1201. https://doi.org/10.1007/s10040-009-0461-z

Ahmed, S., Hiraga, Y., & Kazama, S. (2024). Land subsidence in Bangkok vicinity: Causes and long-term trend analysis using InSAR and machine learning. *Science of The Total Environment*, *946*, 174285. https://doi.org/10.1016/j.scitotenv.2024.174285

Anderson, M., Woessner, W., & Hunt, R. (2015). *Applied Ground Water Modeling: Simulation of Flow and Advective Transport*.

Andreas, H., Usriyah, Zainal Abidin, H., & Anggreni Sarsito, D. (2017). Tidal inundation ('Rob') investigation using time series of high resolution satellite image data and from institu measurements along northern coast of Java (Pantura). *IOP Conference Series: Earth and Environmental Science*, *71*(1). https://doi.org/10.1088/1755-1315/71/1/012005

Andreas, H., Zainal Abidin, H., Gumilar, I., Purnama Sidiq, T., Anggreni Sarsito, D., & Pradipta, D. (2019). On the acceleration of land subsidence rate in Semarang City as detected from GPS surveys. *E3S Web of Conferences*, *94*. https://doi.org/10.1051/e3sconf/20199404002

Andreas, H., Zainal Abidin, H., Pradipta, D., Anggreni Sarsito, Di., & Gumilar, I. (2018). Insight look the subsidence impact to infrastructures in Jakarta and Semarang area; Key for adaptation and mitigation. *MATEC Web of Conferences*, *147*(June 2006), 1–8. https://doi.org/10.1051/matecconf/201814708001

Arnold, J. G., & Fohrer, N. (2005). SWAT2000: Current capabilities and research opportunities in applied watershed modelling. *Hydrological Processes*, *19*(3), 563–572. https://doi.org/10.1002/hyp.5611

Bagheri-Gavkosh, M., Hosseini, S. M., Ataie-Ashtiani, B., Sohani, Y., Ebrahimian, H., Morovat, F., & Ashrafi, S. (2021). Land subsidence: A global challenge. *Science of The Total Environment*, *778*, 146193. https://doi.org/10.1016/j.scitotenv.2021.146193

Balica, S. F., Wright, N. G., & van der Meulen, F. (2012). A flood vulnerability index for coastal cities and its use in assessing climate change impacts. In *Natural Hazards* (Vol. 64, Issue 1). https://doi.org/10.1007/s11069-012-0234-1

Baud, B., Lachassagne, P., Dumont, M., Toulier, A., Hendrayana, H., Fadillah, A., & Dorfliger, N. (2024). Review: Andesitic aquifers—hydrogeological conceptual models and insights relevant to applied hydrogeology. *Hydrogeology Journal*, *32*(5), 1259–1286. https://doi.org/10.1007/s10040-024-02784-0

Beek, W., Letitre, B., Hadiyanto, H., & Sudarno, S. (2019). Alternatives to groundwater abstraction as a measure to stop land subsidence: A case study of Semarang, Indonesia. *E3S Web of Conferences*, *125*(201 9). https://doi.org/10.1051/e3sconf/201912501003

Brandenburg, J. P. (2020). *Geologic Frameworks for Groundwater Flow Models*. The Groundwater Project. https://doi.org/10.21083/978-1-7770541-9-9

Brutsaert, W. (2023). *Hydrology: An Introduction* (2nd ed.). Cambridge University Press; Cambridge Core. https://doi.org/10.1017/9781316471562

Bürgmann, R., Rosen, P. A., & Fielding, E. J. (2000). Synthetic Aperture Radar Interferometry to Measure Earth's Surface Topography and Its Deformation. *Annual Review of Earth and Planetary Sciences*, *28*(1), 169–209. https://doi.org/10.1146/annurev.earth.28.1.169

Catur Karsa, P. S. (2011). *Eksplorasi Dan Pelayanan Air Bersih Melalui Pemboran Air Tanah Dalam, Desa Bodeh, Kecamatan Bodeh, Kabupaten Pemalang, Provinsi Jawa Tengah*. Badan Geologi.

Catur Karsa, P. S. (2016a). *Eksplorasi Dan Pelayanan Air Bersih Melalui Pemboran Air Tanah Dalam Desa Pesanggrahan, Kecamatan Wonokerto, Kabupaten Pekalongan, Provinsi Jawa Tengah*. Badan Geologi.

Catur Karsa, P. S. (2016b). *Eksplorasi Dan Pelayanan Air Bersih Melalui Pemboran Air Tanah Dalam Desa Pesanggrahan, Kecamatan Wonokerto, Kabupaten Pekalongan, Provinsi Jawa Tengah*. Badan Geologi.

Catur Karsa, P. S. (2016c). *Eksplorasi Dan Pelayanan Air Bersih Melalui Pemboran Air Tanah Dalam Desa Pododadi, Kecamatan Karanganyar, Kabupaten Pekalongan, Provinsi Jawa Tengah*. Badan Geologi.

Catur Karsa, P. S. (2017). *Eksplorasi Dan Pelayanan Air Bersih Melalui Pemboran Air Tanah Dalam, Desa Wanarata, Kecamatan Bantarbolang, Kabupaten Pemalang, Provinsi Jawa Tengah*. Badan Geologi.

Chaussard, E., Amelung, F., Abidin, H., & Hong, S. H. (2013). Sinking cities in Indonesia: ALOS PALSAR detects rapid subsidence due to groundwater and gas extraction. *Remote Sensing of Environment*, *128*, 150–161. https://doi.org/10.1016/j.rse.2012.10.015

Cherubini, C., Sathish, S., & Pastore, N. (2023). Dynamics of Coastal Aquifers: Conceptualization and Steady-State Calibration of Multilayer Aquifer System—Southern Coast of Emilia Romagna. *Water*, *15*(13), 2384. https://doi.org/10.3390/w15132384

Cui, Y., Su, C., Shao, J., Wang, Y., & Cao, X. (2014). Development and application of a regional land subsidence model for the plain of Tianjin. *Journal of Earth Science*, *25*(3), 550–562. https://doi.org/10.1007/s12583-014-0447-1

DEMNAS. (2020). Http://Tides.Big.Go.Id/DEMNAS.

Deng, X., Li, F., Zhao, Y., & Li, S. (2018). Regulation of deep groundwater based on MODFLOW in the water intake area of the South-to-North Water Transfer Project in Tianjin,

China. *Journal of Hydroinformatics*, *20*(4), 989–1007. https://doi.org/10.2166/hydro.2018.126

Dey, S., Bhatt, D., Haq, S., & Mall, R. K. (2020). Potential impact of rainfall variability on groundwater resources: A case study in Uttar Pradesh, India. *Arabian Journal of Geosciences*, *13*(3). https://doi.org/10.1007/s12517-020-5083-8

Du, Z., Ge, L., Ng, A. H. M., Zhu, Q., Yang, X., & Li, L. (2018). Correlating the subsidence pattern and land use in Bandung, Indonesia with both Sentinel-1/2 and ALOS-2 satellite images. *International Journal of Applied Earth Observation and Geoinformation*, *67*(January), 54–68. https://doi.org/10.1016/j.jag.2018.01.001

Erban, L. E., Gorelick, S. M., & Zebker, H. A. (2014). Groundwater extraction, land subsidence, and sea-level rise in the Mekong Delta, Vietnam. *Environmental Research Letters*, *9*(8). https://doi.org/10.1088/1748-9326/9/8/084010

Erkens, G., & Stouthamer, E. (2020). The 6M approach to land subsidence. *Proceedings of the International Association of Hydrological Sciences*, *382*, 733–740. https://doi.org/10.5194/piahs-382-733-2020

Ferguson, G., & Gleeson, T. (2012). Vulnerability of coastal aquifers to groundwater use and climate change. *Nature Climate Change*, *2*(5), 342–345. https://doi.org/10.1038/nclimate1413

Fetter, C. W. (2014). *Applied Hydrogeology*.

Freeze, R.A.; Cherry, J. A. (1979). *Groundwater*.

Galloway, D. L., & Burbey, T. J. (2011). Review: Regional land subsidence accompanying groundwater extraction. *Hydrogeology Journal*, *19*(8), 1459–1486. https://doi.org/10.1007/s10040-011-0775-5

Gambolati, G., Gatto, P., & Freeze, R. A. (1974). Mathematical simulation of the subsidence of Venice: 2. Results. *Water Resources Research*, *10*(3), 563–577. https://doi.org/10.1029/WR010i003p00563

Gambolati, G., & Teatini, P. (2013). Venice Shall Rise Again: Engineered Uplift of Venice Through Seawater Injection. *Venice Shall Rise Again: Engineered Uplift of Venice Through Seawater Injection*, 1–83.

Gambolati, G., & Teatini, P. (2021). *Land Subsidence and its Mitigation*. The Groundwater Project. https://doi.org/10.21083/978-1-77470-001-3

Geokarsa, P. (2018a). *Eksplorasi Dan Pelayanan Air Bersih Melalui Pemboran Air Tanah Dalam, Desa Sragi, Kecamatan Sragi, Kabupaten Pekalongan, Provinsi Jawa Tengah*. Badan Geologi.

Geokarsa, P. (2018b). *Eksplorasi Dan Pelayanan Air Bersih Melalui Pemboran Air Tanah Dalam, Desa Sukowangi, Kecamatan Taman, Kabupaten Pemalang, Provinsi Jawa Tengah*. Badan Geologi.

Geokarsa, P. (2018c). *Eksplorasi Dan Pelayanan Air Bersih Melalui Pemboran Air Tanah Dalam, Desa Tanah Baya, Kecamatan Randu Dongkal, Kabupaten Pemalang, Provinsi Jawa Tengah*. Badan Geologi.

Geokarsa, P. (2018d). *Eksplorasi Dan Pelayanan Air Bersih Melalui Pemboran Air Tanah Dalam, Desa Tumbal, Kecamatan Comal, Kabupaten Pemalang, Provinsi Jawa Tengah*. Badan Geologi.

Griffioen, J., Klein, J., & Van Gaans, P. F. M. (2012). Reaction capacity characterization of shallow sedimentary deposits in geologically different regions of the Netherlands. *Journal of Contaminant Hydrology*, *127*(1–4), 30–46. https://doi.org/10.1016/j.jconhyd.2011.04.001

Guzy, A., & Malinowska, A. A. (2020). State of the art and recent advancements in the modelling of land subsidence induced by groundwater withdrawal. *Water (Switzerland)*, *12*(7). https://doi.org/10.3390/w12072051

Gyamfi, C., Ndambuki, J. M., Anornu, G. K., & Kifanyi, G. E. (2017). Groundwater recharge modelling in a large scale basin: An example using the SWAT hydrologic model. *Modeling Earth Systems and Environment*, *3*(4), 1361–1369. https://doi.org/10.1007/s40808-017-0383-z

Harbaugh, A. W. (2005). *MODFLOW-2005, the U.S. Geological Survey modular ground-water model [electronic resource]: The ground-water flow process*. Reston, Va. : U.S. Dept. of the Interior, U.S. Geological Survey, 2005.

Hoffmann, J., Leake, S. A., Galloway, D. L., & Wilson, A. M. (2003). MODFLOW-2000 ground-water model—User guide to the Subsidence and Aquifer-System Compaction (SUB) Package. *US Geological Survey Open-File Report 03-233*, 46.

Iooss, B., & Saltelli, A. (2016). Introduction to Sensitivity Analysis. In R. Ghanem, D. Higdon, & H. Owhadi (Eds.), *Handbook of Uncertainty Quantification* (pp. 1–20). Springer International Publishing. https://doi.org/10.1007/978-3-319-11259-6_31-1

Jafari, F., Javadi, S., Golmohammadi, G., Karimi, N., & Mohammadi, K. (2016). Numerical simulation of groundwater flow and aquifer-system compaction using simulation and InSAR technique: Saveh basin, Iran. *Environmental Earth Sciences*, *75*(9), 1–10. https://doi.org/10.1007/s12665-016-5654-x

Leterme, B., & Mallants, D. (2012). Climate and land-use change impacts on groundwater recharge. *IAHS-AISH Publication*, *355*(September), 313–319.

Lillesand, T., Kiefer, R., & Chipman, J. (2004). Remote Sensing and Image Interpretation (Fifth Edition). In *The Geographical Journal* (Vol. 146). https://doi.org/10.2307/634969

Lubis, R. F., & Delinom, R. (2010). Perubahan iklim dan pemanasan global di Indonesia: Dampaknya terhadap kondisi bawah permukaan studi kasus: DKI Jakarta. *Widyariset*, *13*(3), 65–70.

Lunati, I., Bernard, D., Giudici, M., Parravicini, G., & Ponzini, G. (2001). *A numerical comparison between two upscaling techniques: Non-local inverse based scaling and simpli®ed renormalization*.

Luo, Z. J., Zhao, S. J., Jin, W., Ma, Q. S., & Wu, X. H. (2016). Evaluation model coupling exploitable groundwater resources and land subsidence control in regional loose

sediments. *IOP Conference Series: Earth and Environmental Science*, *39*(1). https://doi.org/10.1088/1755-1315/39/1/012009

Lutfitiana, P., Ramadhani, R. P., & Eka, Y. (2022). *KAJIAN BANJIR KOTA PEKALONGAN*.

Marfai, M. A., & King, L. (2007). Monitoring land subsidence in Semarang, Indonesia. *Environmental Geology*, *53*(3), 651–659. https://doi.org/10.1007/s00254-007-0680-3

Marker, B. R. (2013). Land Subsidence. In P. T. Bobrowsky (Ed.), *Encyclopedia of Natural Hazards* (pp. 583–590). Springer Netherlands. https://doi.org/10.1007/978-1-4020-4399-4_208

McDonald, M. G., & Harbaugh, A. W. (1988). *A modular three-dimensional finite-difference ground-water flow model* (Report Nos. 06-A1; Techniques of Water-Resources Investigations). USGS Publications Warehouse. https://doi.org/10.3133/twri06A1

Mohammed, M. A. A., Szabó, N. P., & Szűcs, P. (2023). Exploring hydrogeological parameters by integration of geophysical and hydrogeological methods in northern Khartoum state, Sudan. *Groundwater for Sustainable Development*, *20*, 100891. https://doi.org/10.1016/j.gsd.2022.100891

Phien-wej, N., Giao, P. H., & Nutalaya, P. (2006). Land subsidence in Bangkok, Thailand. *Engineering Geology*, *82*(4), 187–201. https://doi.org/10.1016/j.enggeo.2005.10.004

Psomiadis, E., Soulis, K. X., & Efthimiou, N. (2020). Using SCS-CN and Earth Observation for the Comparative Assessment of the Hydrological Effect of Gradual and Abrupt Spatiotemporal Land Cover Changes. *Water*, *12*(5), 1386. https://doi.org/10.3390/w12051386

PT. Giri Awas. (2012). *Penyusunan Zona Pemanfaatan dan Zona Konservasi Air Tanah Pada CAT Pekalongan–Pemalang, Jawa Tengah*. DINAS ENERGI DAN SUMBER DAYA MINERAL, JAWA TENGAH.

Raflyndo Pratama, P. (2021, October). *Laporan Akhir Pembangunan Stasiun Pengamatan Penurunan Permukaan Tanah, Desa Depok, Kota Pekalongan*.

Ramapratama, P. G. (2013). *Eksplorasi Dan Pelayanan Air Bersih Melalui Pemboran Air Tanah Dalam, Desa Widodaren, Kecamatan Petarukan, Kabupaten Pemalang, Provinsi Jawa Tengah*. Badan Geologi.

Ramapratama, P. G. (2014). *Eksplorasi Dan Pelayanan Air Bersih Melalui Pemboran Air Tanah Dalam – Desa Legokclile, Kecamatan Bojong, Kabupaten Pekalongan, Provinsi Jawa Tengah*. Badan Geologi.

Reay, D., Sabine, C., Smith, P., & Hymus, G. (2007). Intergovernmental Panel on Climate Change. Fourth Assessment Report. Geneva, Switzerland: Inter-gov- ernmental Panel on Climate Change. Cambridge; UK: Cambridge University Press; 2007. Available from: Www. Ipcc.ch. In *Intergovernmental Panel on Climate Change.* https://doi.org/10.1038/446727a

Rongrong, L., Weifang, Y., & Deyan, L. (2020). Land Deformation Monitoring in Lanzhou City Based on SBAS-InSAR Technology. *IOP Conference Series: Earth and Environmental Science*, *608*(1), 299–304. https://doi.org/10.1088/1755-1315/608/1/012013

Sarah, D., Syahbana, A. J., Lubis, R. F., & Mulyono, A. (2011). Modelling of Land Subsidence Along Tanah Mas -Pelabuhan Section Semarang City Using Finite Element Method. *Jurnal RISET Geologi Dan Pertambangan*, *21*(1), 105. https://doi.org/10.14203/risetgeotam2011.v21.50

Sato, C., Haga, M., & Nishino, J. (2006). *Land Subsidence and Groundwater Management in Tokyo*. *6*(2).

Shen, S. L., & Xu, Y. S. (2011). Numerical evaluation of land subsidence induced by groundwater pumping in Shanghai. *Canadian Geotechnical Journal*, *48*(9), 1378–1392. https://doi.org/10.1139/t11-049

Silva, R. (2015). Effect of Climate Change on Potential Groundwater Recharge in the Dry Zone of Sri Lanka. *British Journal of Environment and Climate Change*, *5*(1), 23–36. https://doi.org/10.9734/bjecc/2015/16018

Sneed, B. M., Ikehara, M. E., Stork, S. V., Amelung, F., & Devin, L. (2003). Detection and Measurement of Land Subsidence Using Interferometric Synthetic Aperture Radar and Global Positioning System , San Bernardino County , Mojave Desert , California Detection and Measurement of Land Subsidence Using Interferometric Synthetic Ape. *US Geological Survey Water Resources Investigations*, *Report 03-4015*, 1–66.

Sudadi, P. (2004). *Kajian Zonasi Konfigurasi dan Tata Guna Air Bawah Tanah di daerah Pekalongan – Pemalang,*. ESDM Provinsi Jawa Tengah.

Teatini, P., Castelletto, N., Ferronato, M., Gambolati, G., & Tosi, L. (2011). A new hydrogeologic model to predict anthropogenic uplift of Venice. *Water Resources Research*, *47*(12), 2011WR010900. https://doi.org/10.1029/2011WR010900

Teatini, P., Martelli, G., Comerlati, A., Paiero, G., & Zoccarato, C. (2020). Managed Versus Natural Recharge of Pre-Alpine Phreatic Aquifers. *Water Resources Research*, *56*(9), e2020WR027848. https://doi.org/10.1029/2020WR027848

Teatini, P., Tosi, L., Strozzi, T., Carbognin, L., Wegmuller, U., & Rizzetto, F. (2005). Mapping regional land displacements in the Venice coastland by an integrated monitoring system. *Remote Sensing of Environment*, *98*(4), 403–413. https://doi.org/10.1016/j.rse.2005.08.002

Tirta Jaya, P. B. (2013). *Eksplorasi Dan Pelayanan Air Bersih Melalui Pemboran Air Tanah Dalam Desa Wonokerto Wetan, Kecamatan Wonokerto, Kabupaten Pekalongan, Provinsi Jawa Tengah*. Badan Geologi.

Tirta Jaya, P. B. (2014). *Eksplorasi Dan Pelayanan Air Bersih Melalui Pemboran Air Tanah Dalam, Desa Nyalembeng, Kecamatan Pulosari, Kabupaten Pemalang, Provinsi Jawa Tengah*. Badan Geologi.

Tirta Jaya, P. B. (2015a). *Eksplorasi Dan Pelayanan Air Bersih Melalui Pemboran Air Tanah Dalam, Desa Kalirandu, Kecamatan Petarukan, Kabupaten Pemalang, Provinsi Jawa Tengah*. Badan Geologi.

Tirta Jaya, P. B. (2015b). *Eksplorasi Dan Pelayanan Air Bersih Melalui Pemboran Air Tanah Dalam Desa Mrican, Kecamatan Sragi, Kabupaten Pekalongan, Provinsi Jawa Tengah*. Badan Geologi.

Tirta Jaya, P. B. (2018a). *Eksplorasi Dan Pelayanan Air Bersih Melalui Pemboran Air Tanah Dalam, Desa Dadirejo, Kecamatan Tirto, Kabupaten Pekalongan, Provinsi Jawa Tengah*. Badan Geologi.

Tirta Jaya, P. B. (2018b). *Eksplorasi Dan Pelayanan Air Bersih Melalui Pemboran Air Tanah Dalam, Desa Warungpring, Kecamatan Warungpring, Kabupaten Pemalang, Provinsi Jawa Tengah*. Badan Geologi.

Tirta Jaya, P. B. (2018c). *Eksplorasi Dan Pelayanan Air Bersih Melalui Pemboran Air Tanah Dalam, Desa Wiradesa, Kecamatan Wiradesa, Kabupaten Pekalongan, Provinsi Jawa Tengah*. Badan Geologi.

Tirta Mandiri, P. K. (2019a). *Eksplorasi Dan Pelayanan Air Bersih Melalui Pemboran Air Tanah Dalam, Desa Bener, Kecamatan Wiradesa, Kabupaten Pekalongan, Provinsi Jawa Tengah*. Badan Geologi.

Tirta Mandiri, P. K. (2019b). *Eksplorasi Dan Pelayanan Air Bersih Melalui Pemboran Air Tanah Dalam, Desa Cibuyur, Kecamatan Warungpring, Kabupaten Pemalang, Provinsi Jawa Tengah*. Badan Geologi.

Tirta Mandiri, P. K. (2019c). *Eksplorasi Dan Pelayanan Air Bersih Melalui Pemboran Air Tanah Dalam, Desa Jantirejo, Kecamatan Ampelgading, Kabupaten Pemalang, Provinsi Jawa Tengah*. Badan Geologi.

Tirta Mandiri, P. K. (2019d). *Eksplorasi Dan Pelayanan Air Bersih Melalui Pemboran Air Tanah Dalam, Desa Kauman, Kecamatan Wiradesa, Kabupaten Pekalongan, Provinsi Jawa Tengah*. Badan Geologi.

Tirta Mandiri, P. K. (2019e). *Eksplorasi Dan Pelayanan Air Bersih Melalui Pemboran Air Tanah Dalam, Desa Kedungwuni Timur, Kecamatan Kedungwuni, Kabupaten Pekalongan, Provinsi Jawa Tengah*. Badan Geologi.

Tirta Mandiri, P. K. (2019f). *Eksplorasi Dan Pelayanan Air Bersih Melalui Pemboran Air Tanah Dalam, Desa Petanjungan, Kecamatan Petarukan, Kabupaten Pemalang, Provinsi Jawa Tengah*. Badan Geologi.

Tirta Mandiri, P. K. (2019g). *Eksplorasi Dan Pelayanan Air Bersih Melalui Pemboran Air Tanah Dalam, Desa Serang, Kecamatan Petarukan, Kabupaten Pemalang, Provinsi Jawa Tengah*. Badan Geologi.

Tirta Mandiri, P. K. (2019h). *Eksplorasi Dan Pelayanan Air Bersih Melalui Pemboran Air Tanah Dalam, Desa Tegalsari Barat, Kecamatan Ampel Gading, Kabupaten Pemalang, Provinsi Jawa Tengah*. Badan Geologi.

Tulus Pramudyo, & Wafid, M. (2015). Penyelidikan Geologi Teknik Potensi Penurunan Tanah Kota Pekalongan Provinsi Jawa Tengah. *Pusat Air Tanah dan Geologi Tata Lingkungan, Badan Geologi*.

van Eekelen, M. W., Bastiaanssen, W. G. M., Jarmain, C., Jackson, B., Ferreira, F., van der Zaag, P., Saraiva Okello, A., Bosch, J., Dye, P., Bastidas-Obando, E., Dost, R. J. J., & Luxemburg, W. M. J. (2015). A novel approach to estimate direct and indirect water withdrawals from satellite measurements: A case study from the Incomati basin. *Agriculture, Ecosystems and Environment*, *200*, 126–142. https://doi.org/10.1016/j.agee.2014.10.023

Van Huijgevoort, M. H. J., Voortman, B. R., Rijpkema, S., Nijhuis, K. H. S., & Witte, J. P. M. (2020). Influence of climate and land use change on the groundwater system of the veluwe, the netherlands: A historical and future perspective. *Water (Switzerland)*, *12*(10), 1–16. https://doi.org/10.3390/w12102866

Vilá, O., Smith, G., Cutts, B., Gyawali, S., & Bhattarai, S. (2022). Equity in FEMA hazard mitigation assistance programs: The role of state hazard mitigation officers. *Environmental Science & Policy*, *136*, 632–641. https://doi.org/10.1016/j.envsci.2022.07.027

Wang, J., Gao, W., Xu, S., & Yu, L. (2012). Evaluation of the combined risk of sea level rise, land subsidence, and storm surges on the coastal areas of Shanghai, China. *Climatic Change*, *115*. https://doi.org/10.1007/s10584-012-0468-7

Winston, R. (2009). ModelMuse-A graphical user interface for MODFLOW-2005 and PHAST. In *U.S. Geological Survey Techniques and Methods 6-A29*.

Woessner, W. W., & Poeter, E. P. (2023). *Hydrogeologic properties of earth materials and principles of groundwater flow*. The Groundwater Project. https://doi.org/10.21083/978-1-7770541-2-0

Yang, X., Jia, C., Sun, H., Yang, T., & Yao, Y. (2024). Integrating multi-source data to assess land subsidence sensitivity and management policies. *Environmental Impact Assessment Review*, *104*, 107315. https://doi.org/10.1016/j.eiar.2023.107315

Ye, S., Xue, Y., Wu, J., Yan, X., & Yu, J. (2016). Progression and mitigation of land subsidence in China. *Hydrogeology Journal*, *24*(3), 685–693. https://doi.org/10.1007/s10040-015-1356-9

Zainal Abidin, H. (1999). *Penentuan Posisi dengan GPS dan Aplikasinya*. PT. Pradnya Paramita.

Zangeneh, M., Tabrizi, M. S., Khosrojerdi, A., & Saremi, A. (2023). Developing a decision-making model for improving the groundwater balance to control land subsidence. *Soil and Water Research*, *18*(1), 55–65. https://doi.org/10.17221/57/2022-SWR

Zhang, J., Gao, J., & Gao, F. (2024). Time series land subsidence monitoring and prediction based on SBAS-InSAR and GeoTemporal transformer model. *Earth Science Informatics*, *17*(6), 5899–5911. https://doi.org/10.1007/s12145-024-01487-0

APPENDICES

1. 3D Isoresistivity Map
2. Data And Analysis of Pumping Test
3. Consolidation Test (ASTM D 2435) Result

Appendix 1

This appendix consists of 3D Isoresistivity Maps at various analysis depths, which are the results of geoelectric measurements using the Vertical Electrical Sounding (VES) technique, also known as 2D geoelectric.

Elevation z = 30 m

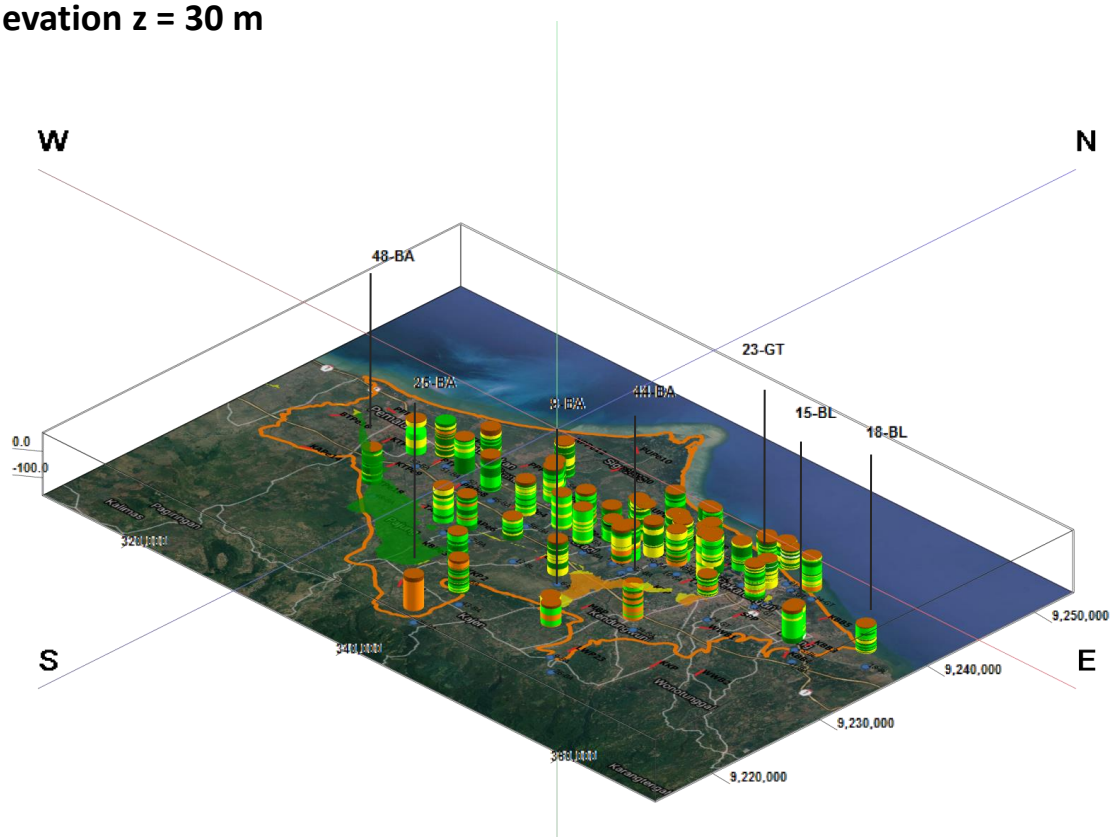

Description:

- < 3 Ohm-meter
- 3 – 11 Ohm-meter
- 11 – 60 Ohm-meter
- > 60 Ohm-meter

Lithology

- breccia
- breccia tufa
- clay
- clayed sand
- clayed tufa
- claystone
- lignit
- sand
- sandstone
- sandy breccia
- sandy clay
- sandy silt
- sandy tufa
- silt
- silty sand
- soil
- tufa
- tuffaceous clay
- tuffaceous sand
- Tuffaceous silt

Elevation z = 20 m

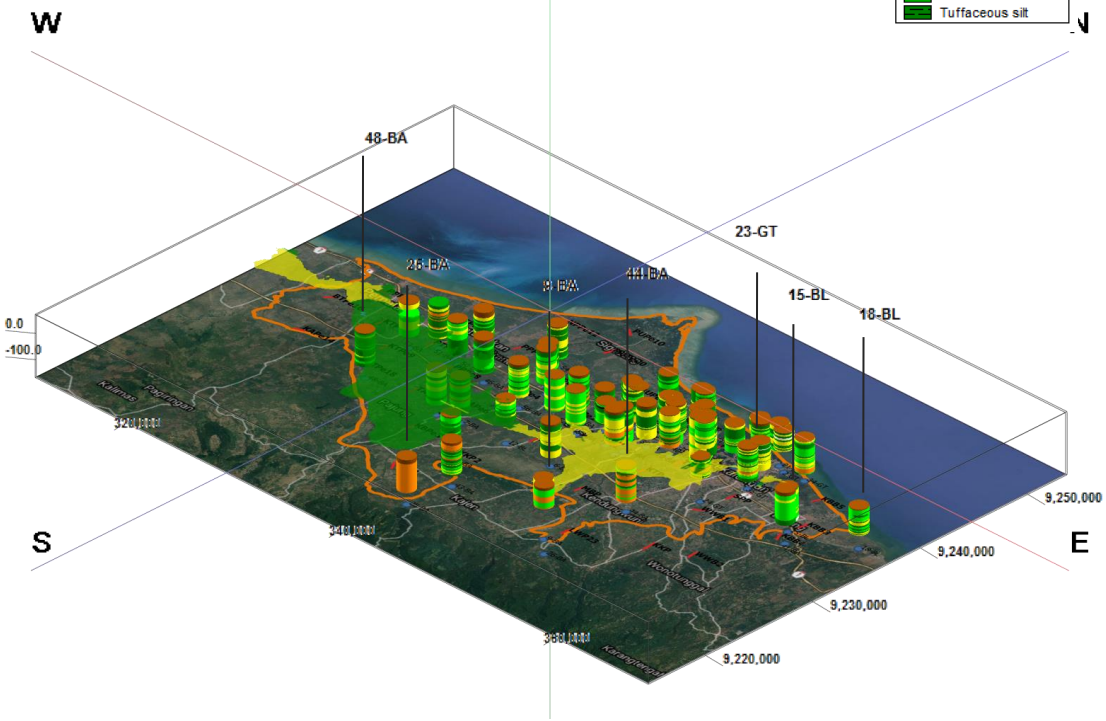

Elevation z = 10 m

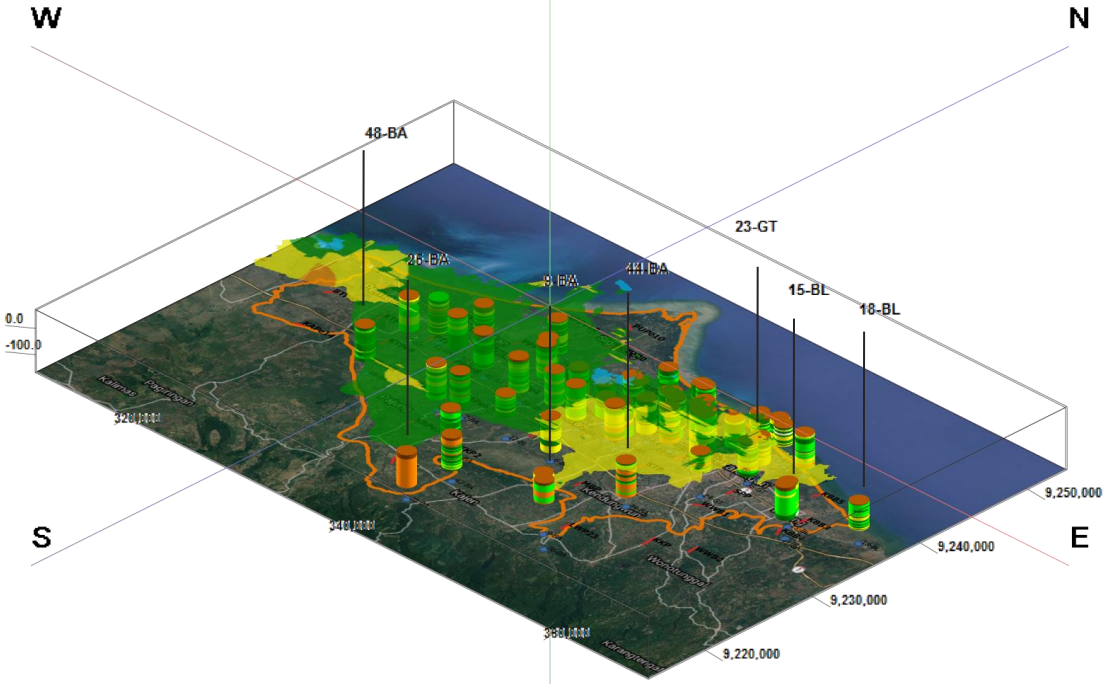

Description:

- < 3 Ohm-meter
- 3 – 11 Ohm-meter
- 11 – 60 Ohm-meter
- > 60 Ohm-meter

Lithology

- breccia
- breccia tufa
- clay
- clayed sand
- clayed tufa
- claystone
- lignit
- sand
- sandstone
- sandy breccia
- sandy clay
- sandy silt
- sandy tufa
- silt
- silty sand
- soil
- tufa
- tuffaceous clay
- tuffaceous sand
- Tuffaceous silt

Elevation z = 0 m

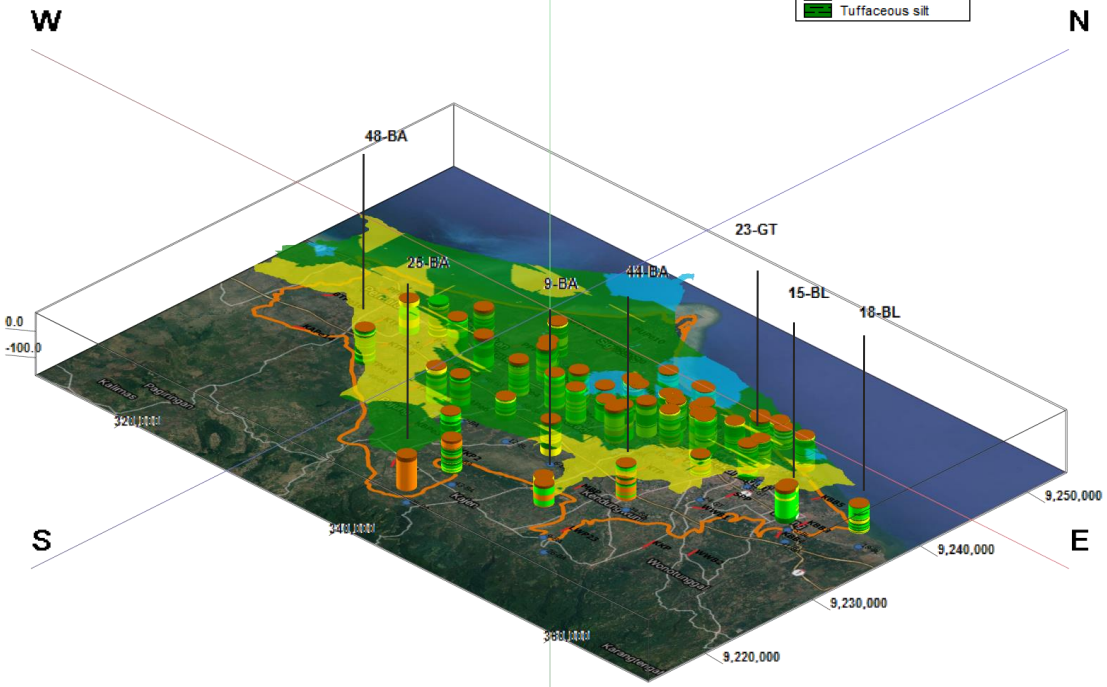

Elevation z = -10 m

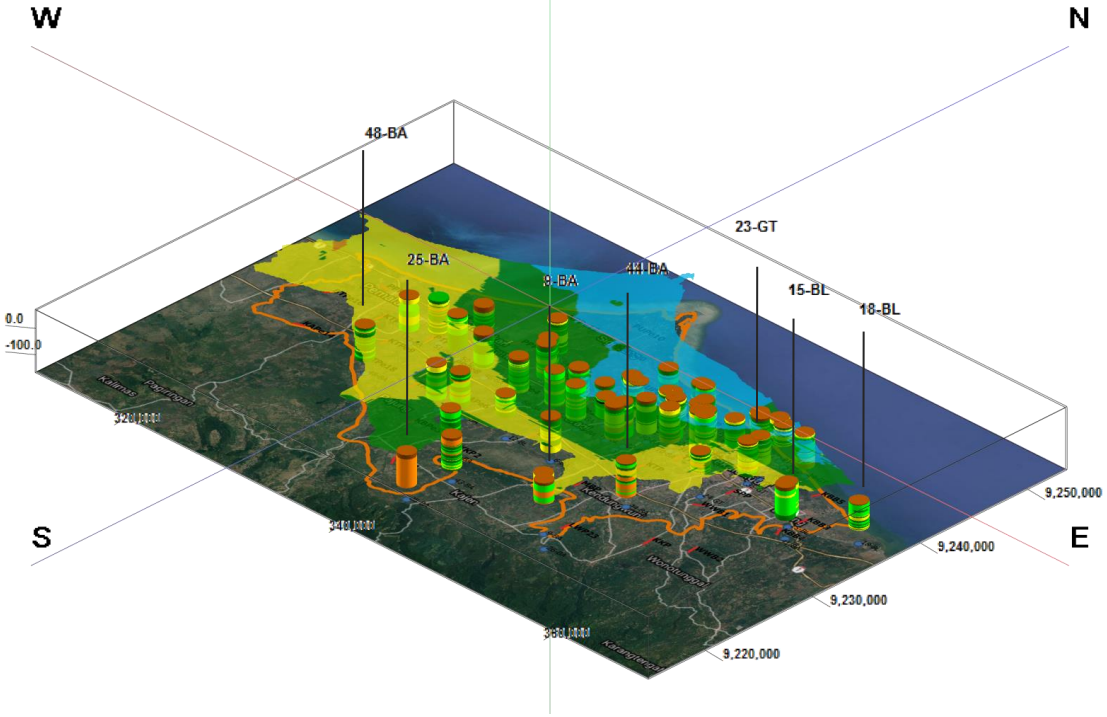

Description:

- < 3 Ohm-meter
- 3 – 11 Ohm-meter
- 11 – 60 Ohm-meter
- > 60 Ohm-meter

Lithology

- breccia
- breccia tufa
- clay
- clayed sand
- clayed tufa
- claystone
- lignit
- sand
- sandstone
- sandy breccia
- sandy clay
- sandy silt
- sandy tufa
- silt
- silty sand
- soil
- tufa
- tuffaceous clay
- tuffaceous sand
- Tuffaceous silt

Elevation z = -20 m

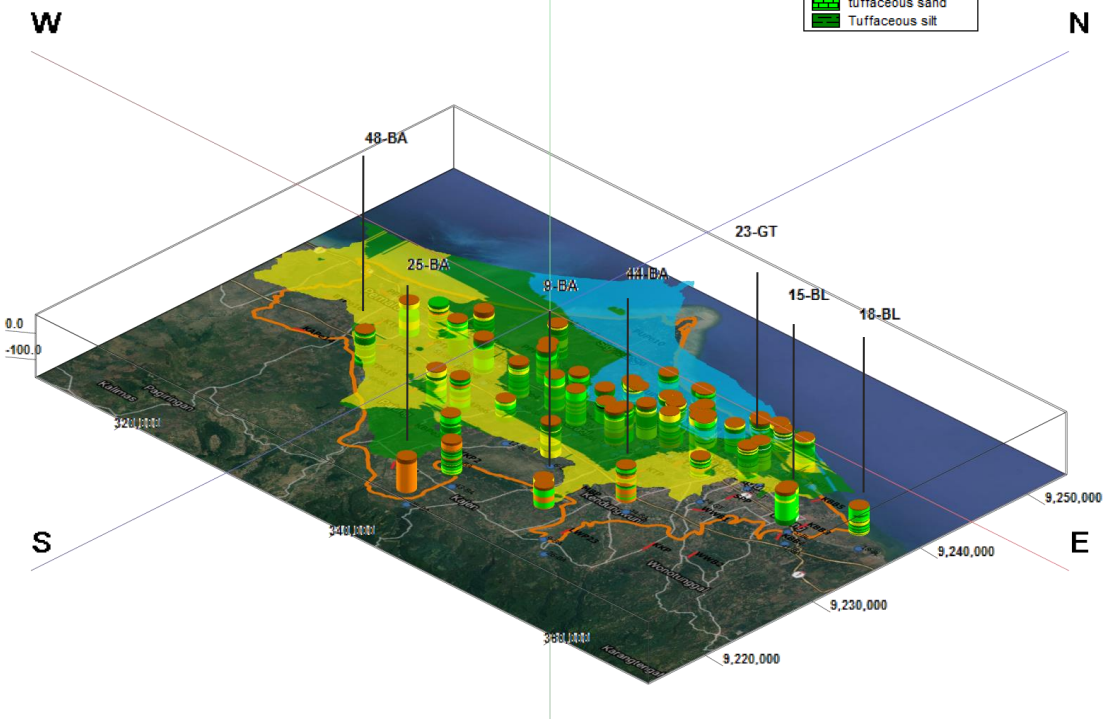

Elevation z = -30 m

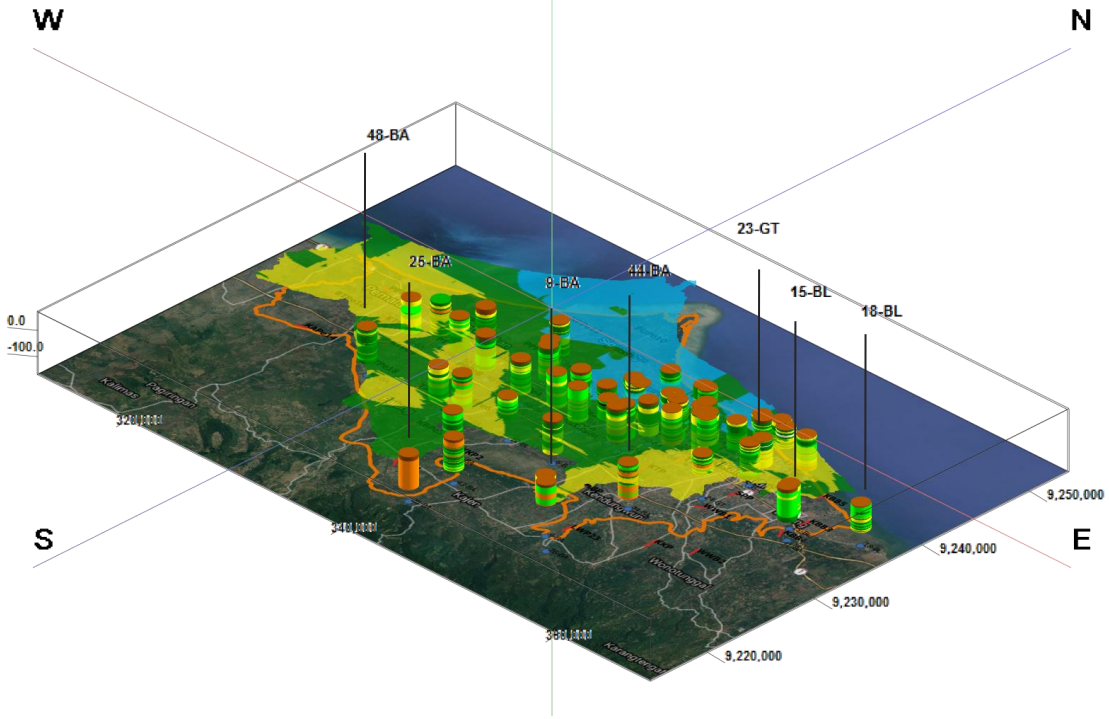

Description:

- < 3 Ohm-meter
- 3 – 11 Ohm-meter
- 11 – 60 Ohm-meter
- > 60 Ohm-meter

Lithology

- breccia
- breccia tufa
- clay
- clayed sand
- clayed tufa
- claystone
- lignit
- sand
- sandstone
- sandy breccia
- sandy clay
- sandy silt
- sandy tufa
- silt
- silty sand
- soil
- tufa
- tuffaceous clay
- tuffaceous sand
- Tuffaceous silt

Elevation z = -40 m

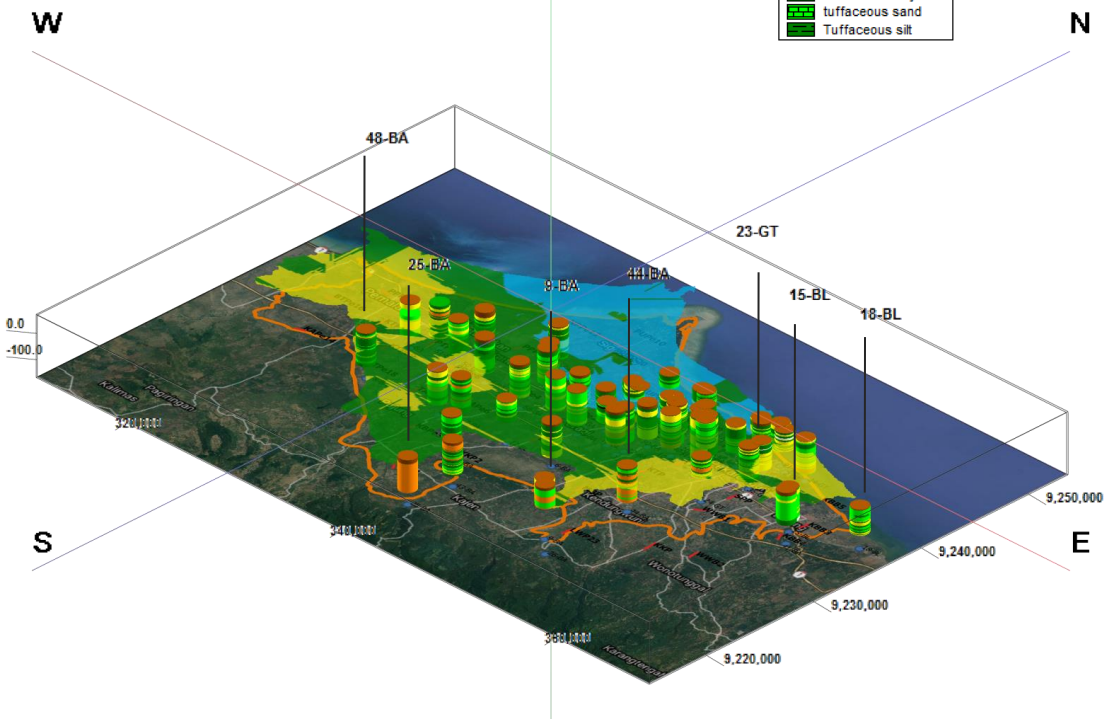

Elevation z = -50 m

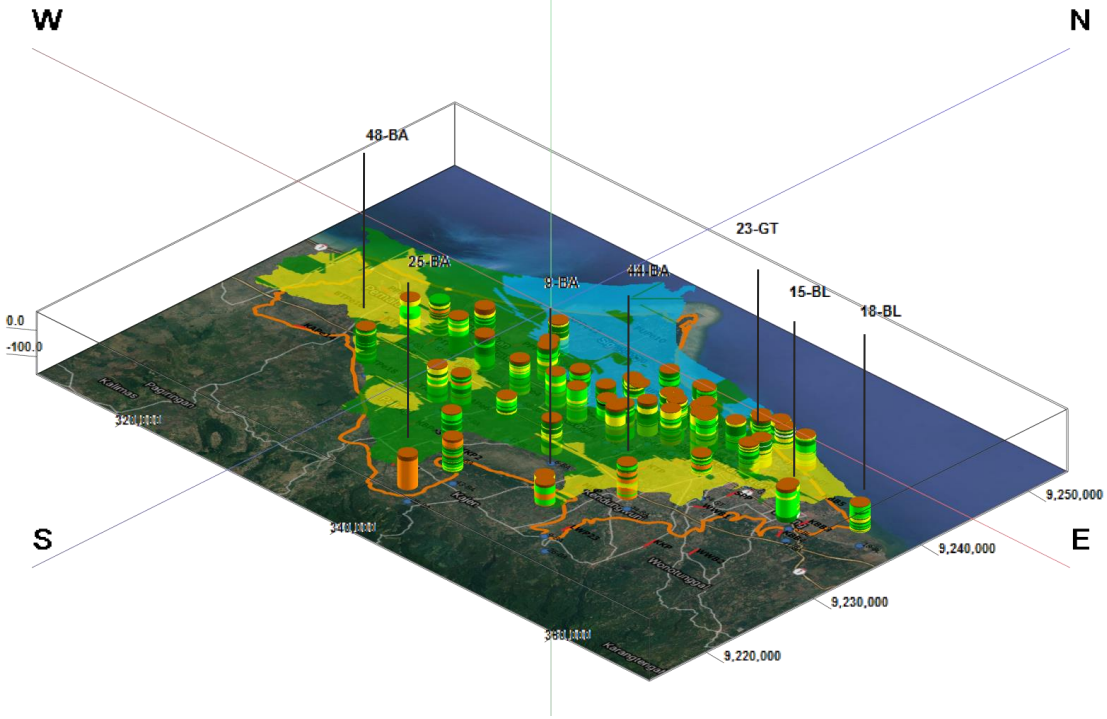

Description:

- < 3 Ohm-meter
- 3 – 11 Ohm-meter
- 11 – 60 Ohm-meter
- > 60 Ohm-meter

Lithology

- breccia
- breccia tufa
- clay
- clayed sand
- clayed tufa
- claystone
- lignit
- sand
- sandstone
- sandy breccia
- sandy clay
- sandy silt
- sandy tufa
- silt
- silty sand
- soil
- tufa
- tuffaceous clay
- tuffaceous sand
- Tuffaceous silt

Elevation z = -60 m

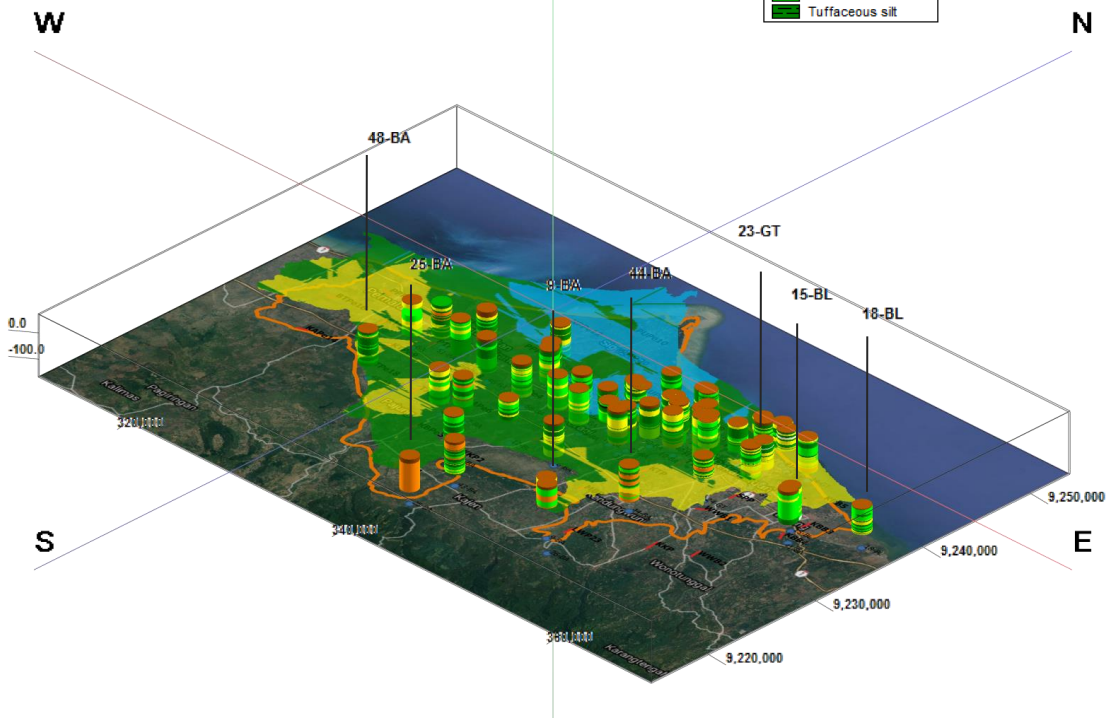

Elevation z = -70 m

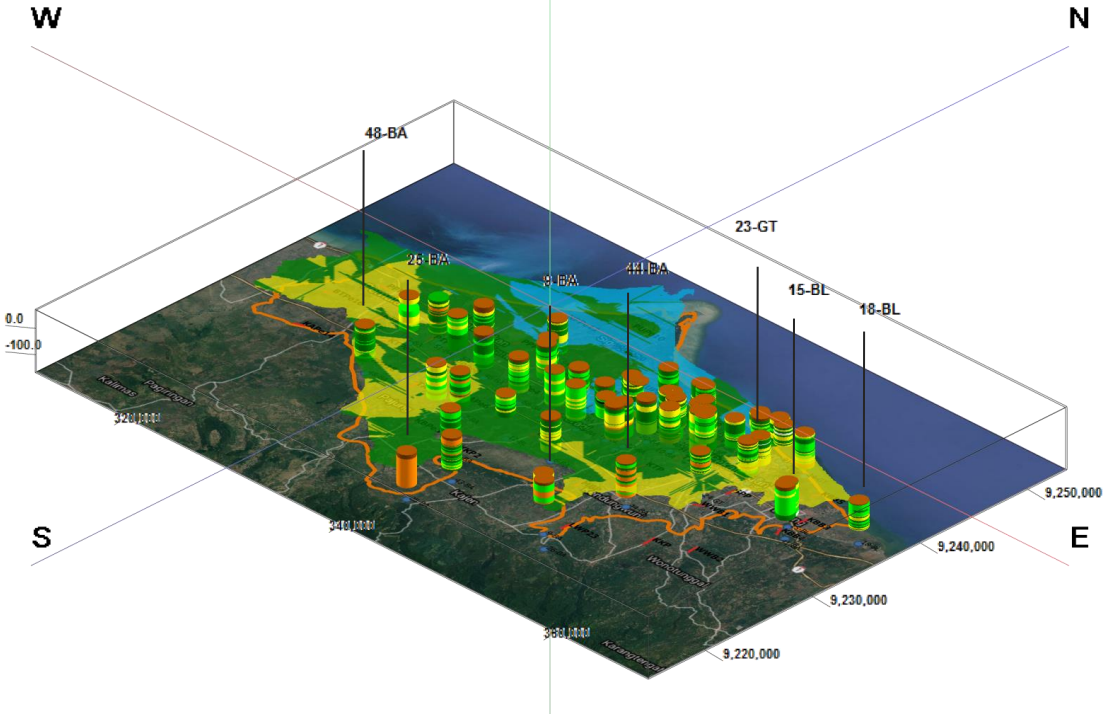

Description:

- < 3 Ohm-meter
- 3 – 11 Ohm-meter
- 11 – 60 Ohm-meter
- > 60 Ohm-meter

Lithology

- breccia
- breccia tufa
- clay
- clayed sand
- clayed tufa
- claystone
- lignit
- sand
- sandstone
- sandy breccia
- sandy clay
- sandy silt
- sandy tufa
- silt
- silty sand
- soil
- tufa
- tuffaceous clay
- tuffaceous sand
- Tuffaceous silt

Elevation z = -80 m

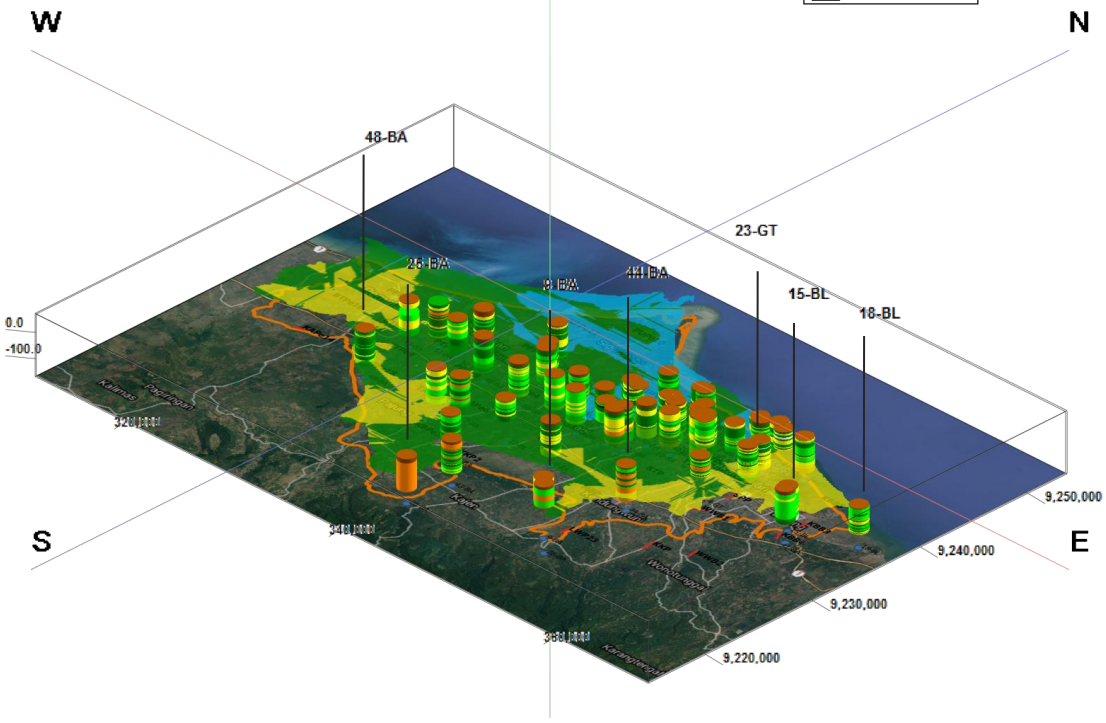

Elevation z = -90 m

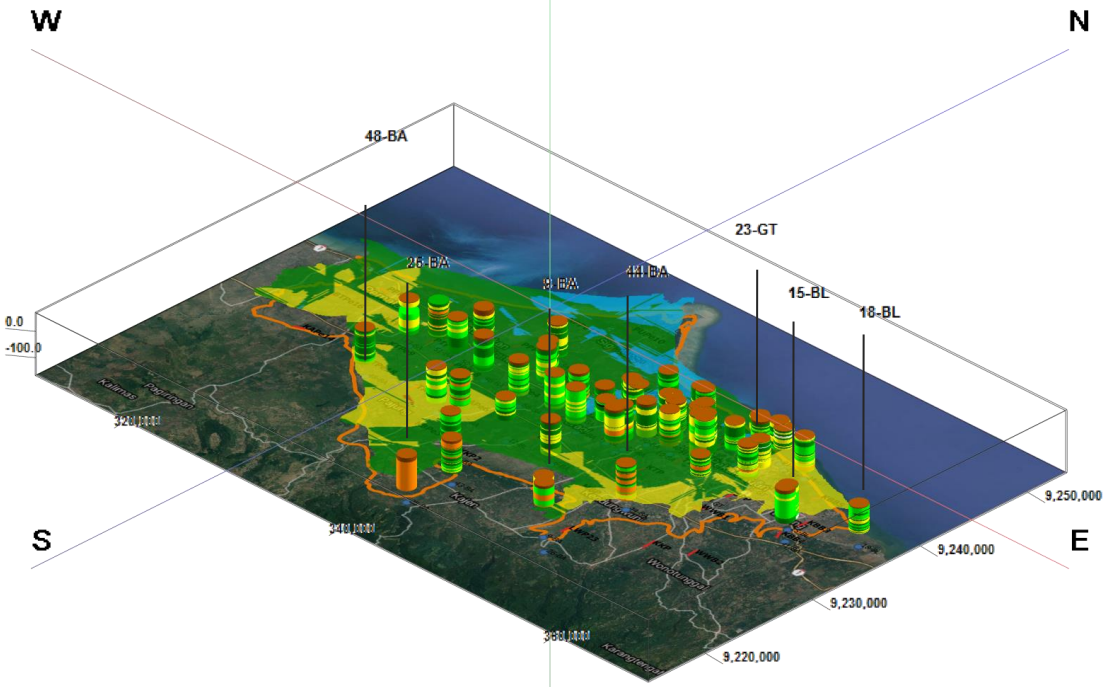

Description:

- < 3 Ohm-meter
- 3 – 11 Ohm-meter
- 11 – 60 Ohm-meter
- > 60 Ohm-meter

Lithology

- breccia
- breccia tufa
- clay
- clayed sand
- clayed tufa
- claystone
- lignit
- sand
- sandstone
- sandy breccia
- sandy clay
- sandy silt
- sandy tufa
- silt
- silty sand
- soil
- tufa
- tuffaceous clay
- tuffaceous sand
- Tuffaceous silt

Elevation z = -100 m

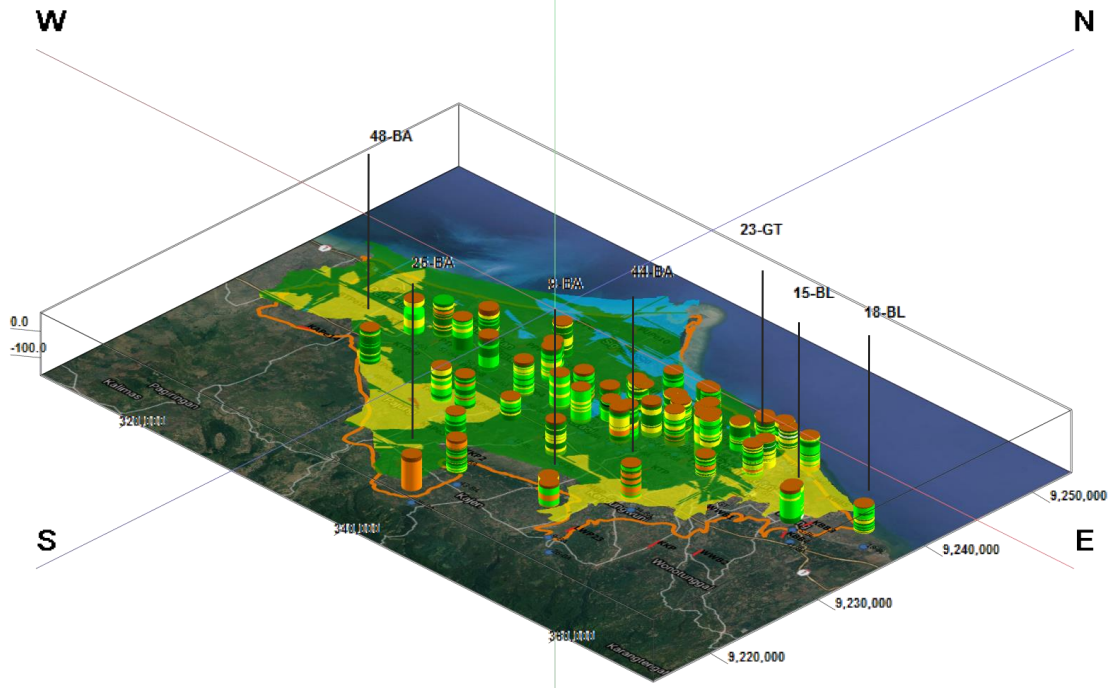

Elevation z = -110 m

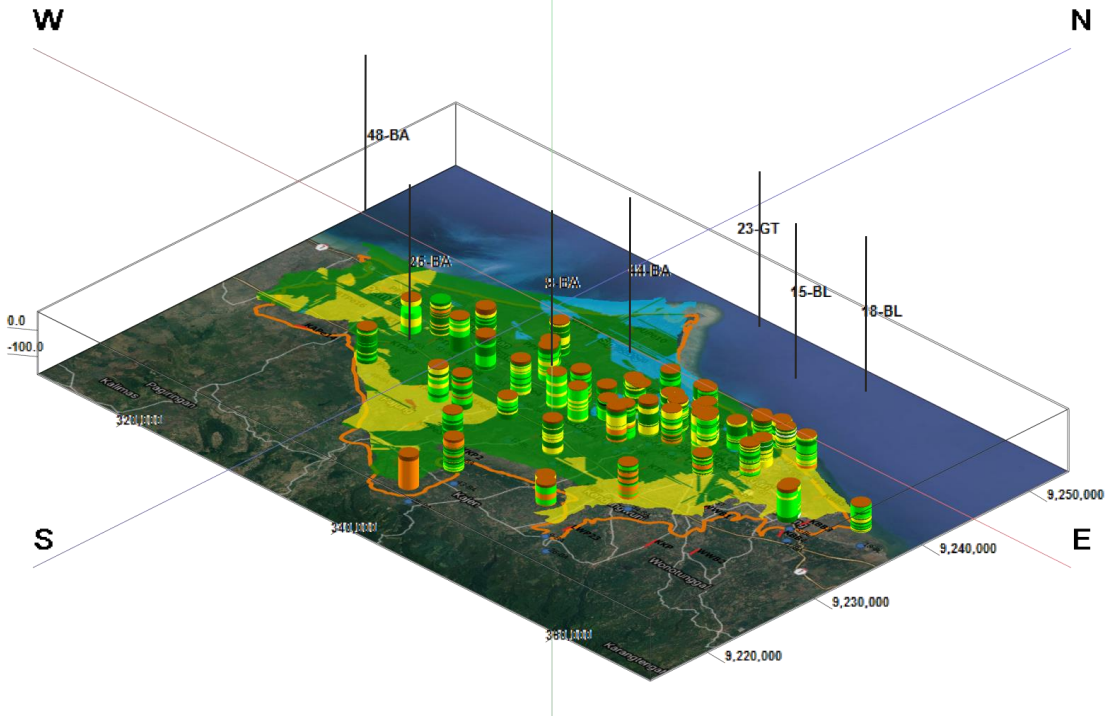

Description:

- < 3 Ohm-meter
- 3 – 11 Ohm-meter
- 11 – 60 Ohm-meter
- > 60 Ohm-meter

Lithology

- breccia
- breccia tufa
- clay
- clayed sand
- clayed tufa
- claystone
- lignit
- sand
- sandstone
- sandy breccia
- sandy clay
- sandy silt
- sandy tufa
- silt
- silty sand
- soil
- tufa
- tuffaceous clay
- tuffaceous sand
- Tuffaceous silt

Elevation z = -120 m

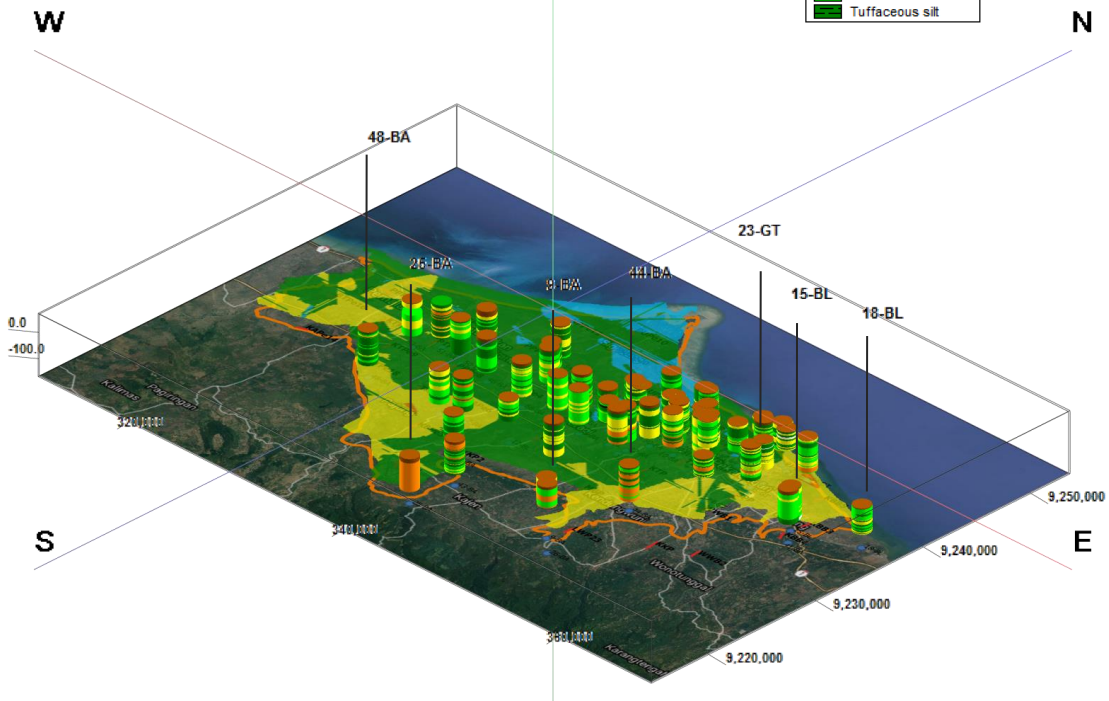

Elevation z = -130 m

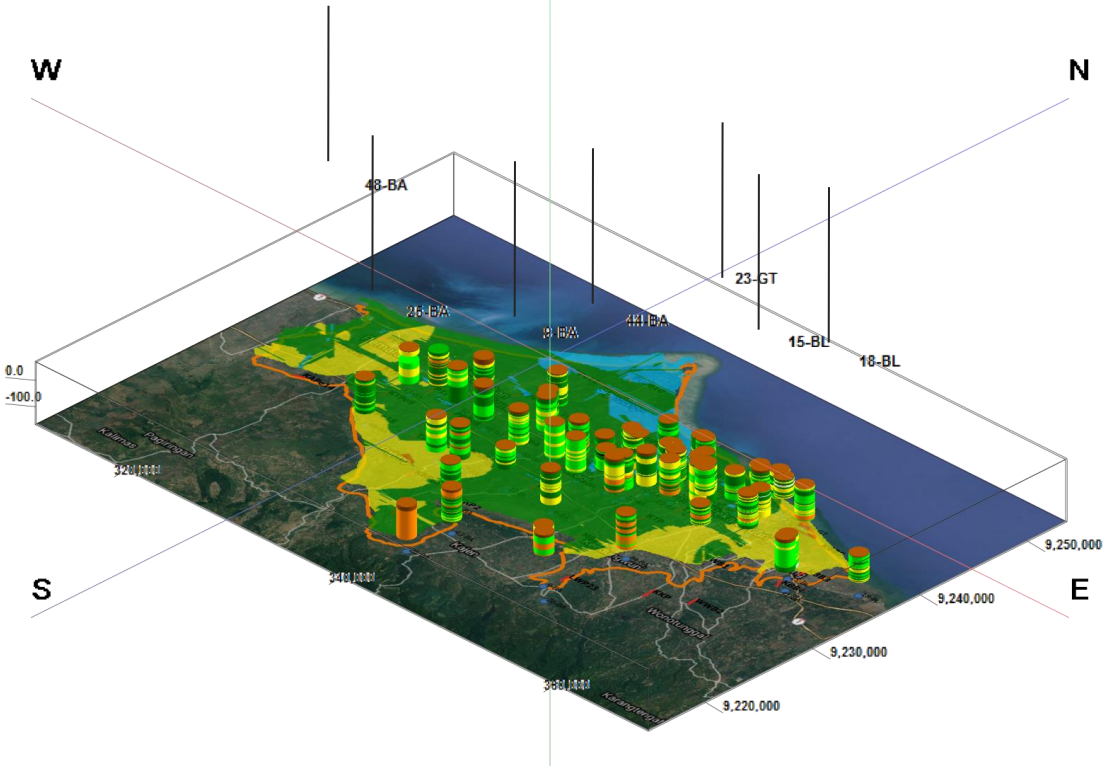

Description:

- < 3 Ohm-meter
- 3 – 11 Ohm-meter
- 11 – 60 Ohm-meter
- > 60 Ohm-meter

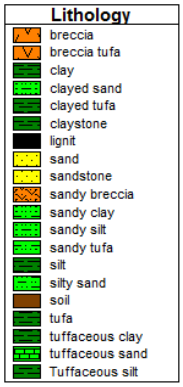

Elevation z = -140 m

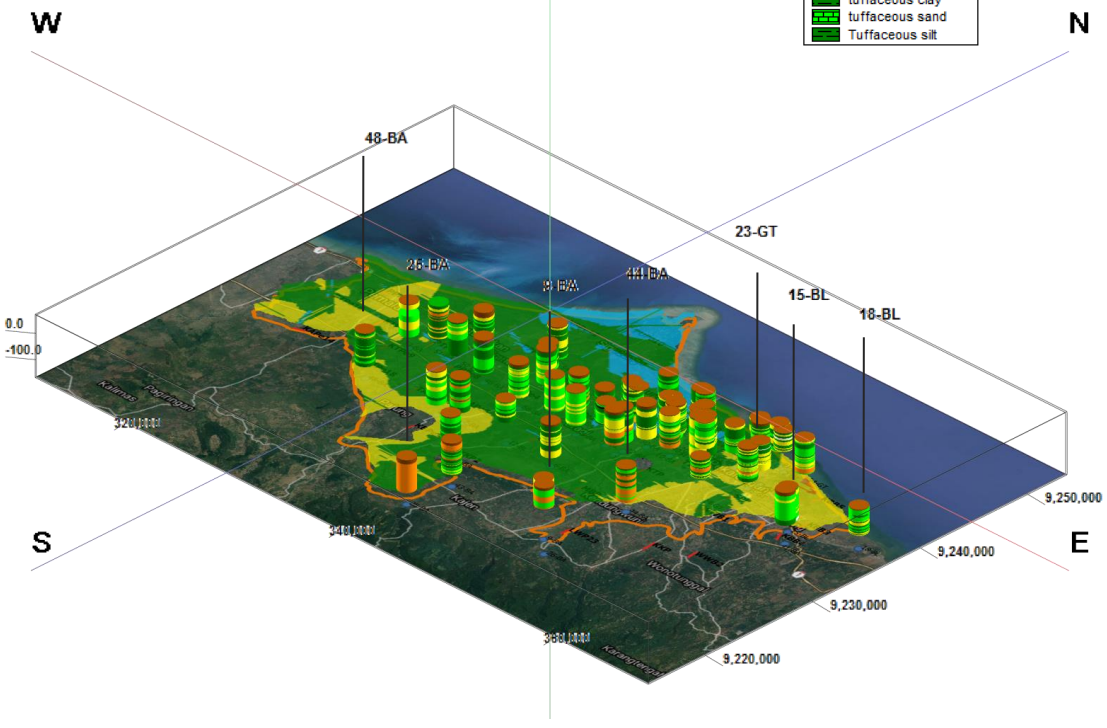

Elevation z = -150 m

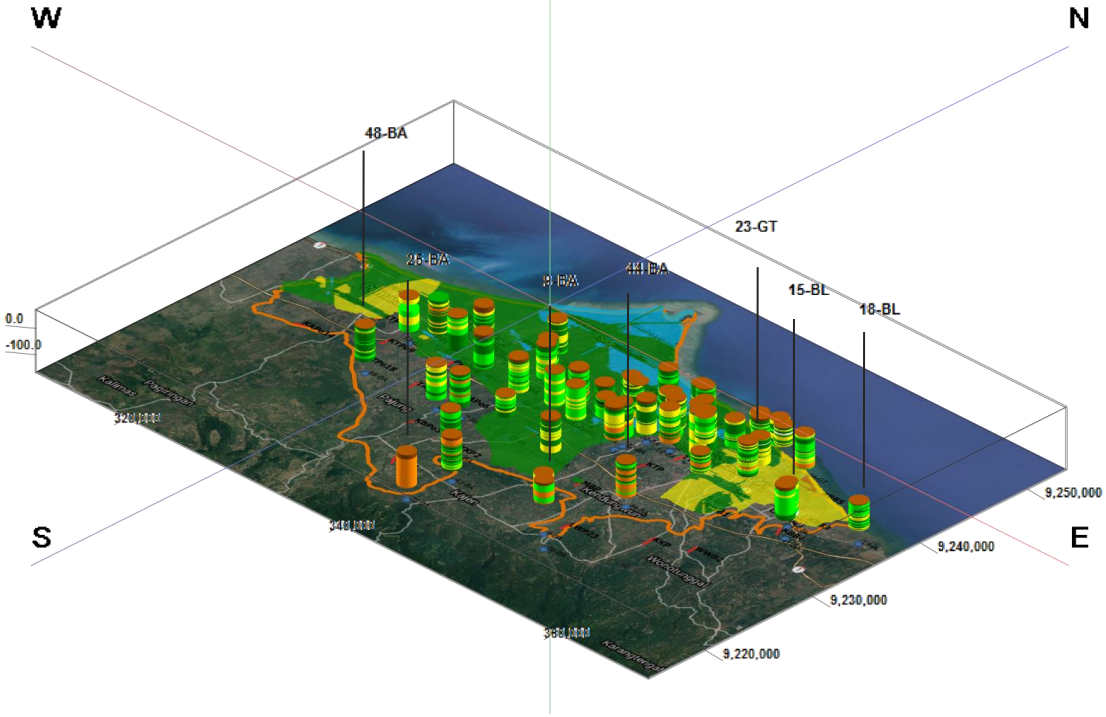

Description:

- < 3 Ohm-meter
- 3 – 11 Ohm-meter
- 11 – 60 Ohm-meter
- > 60 Ohm-meter

Lithology

- breccia
- breccia tufa
- clay
- clayed sand
- clayed tufa
- claystone
- lignit
- sand
- sandstone
- sandy breccia
- sandy clay
- sandy silt
- sandy tufa
- silt
- silty sand
- soil
- tufa
- tuffaceous clay
- tuffaceous sand
- Tuffaceous silt

Elevation z = -160 m

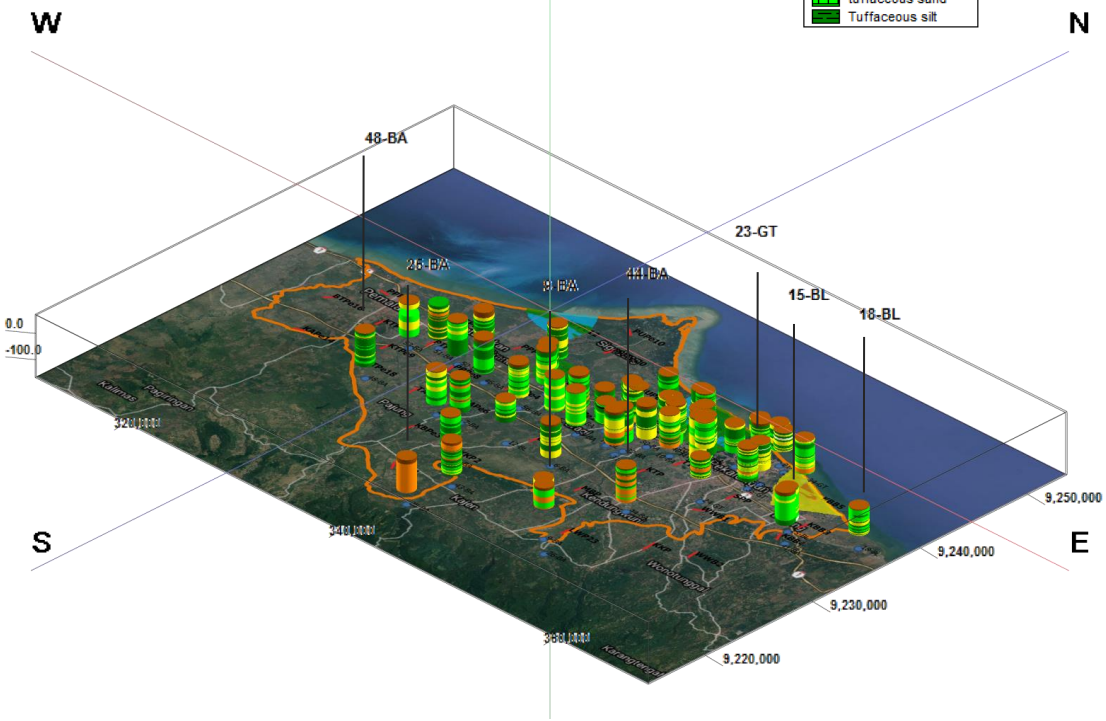

3D ISORESISTIVITY MAP OF PEKALONGAN GROUNDWATER BASIN

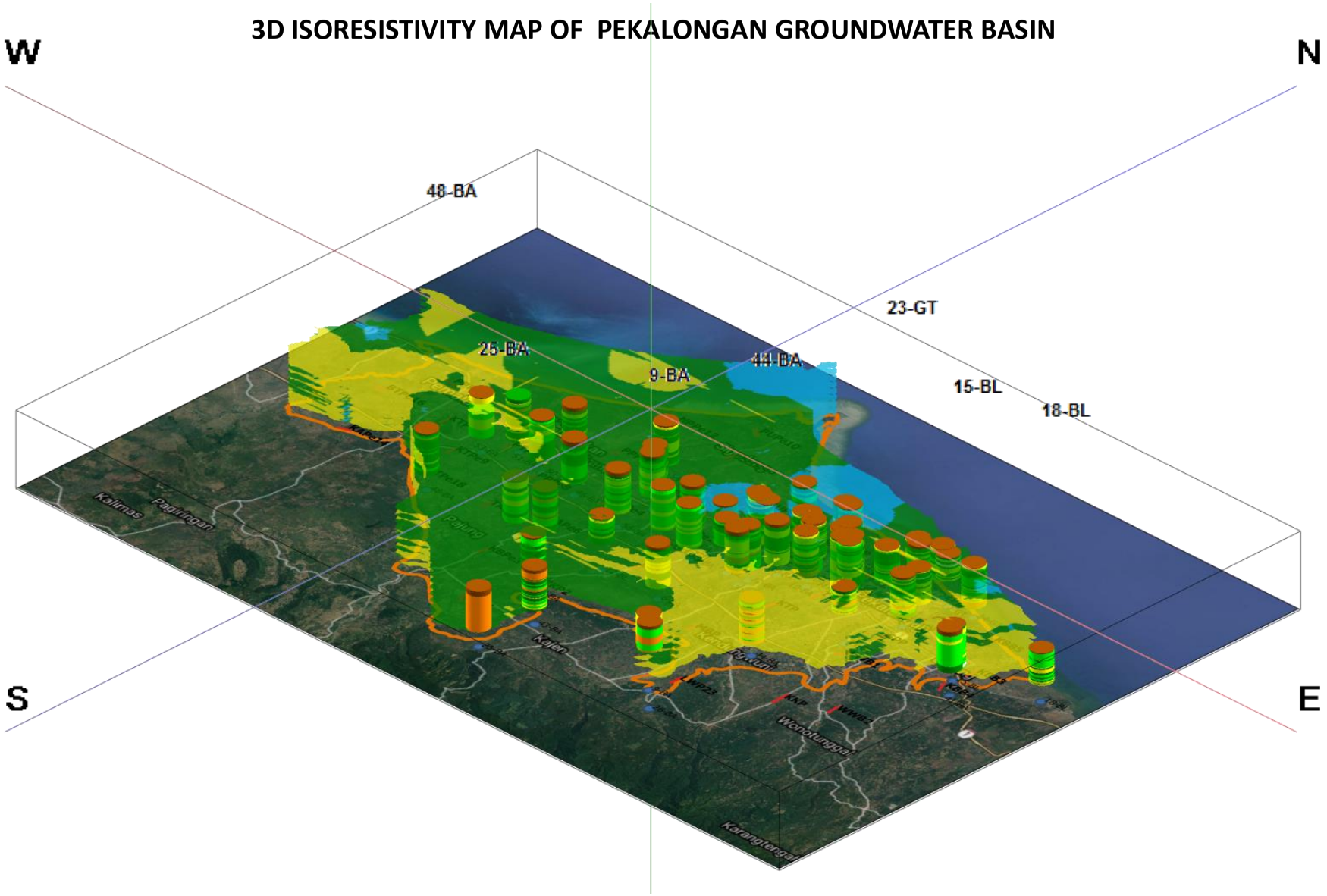

Appendix 2

It contains data from the pumping tests conducted at the observation wells in the study area, as well as the results of plotting and analysis using the Cooper-Jacob method for the single-well aquifer test.

WELL ID: SB 21-Desa Bener

Local ID: Sumur Bor Desa Bener
Date:
Time: 00:00

INPUT

Construction:		
Casing dia. (d_c)	6	Inch
Annulus dia. (d_w)	8	Inch
Screen Length (L)	21	Meter
Depths to:		
water level (DTW)	43.93	Meter
Top of Aquifer	84	Meter
Base of Aquifer	123	Meter
Annular Fill:		
across screen --	Gravel	
above screen --	Cement	
Aquifer Material --	Fine Sand	
FLOW RATE	1.7	liters/s

COMPUTED

Aquifer thickness = 130 Feet

Slope = 0.62398 Feet/log10

Input is consistent.

K = 3.6 Feet/Day
T = 460 Feet²/Day

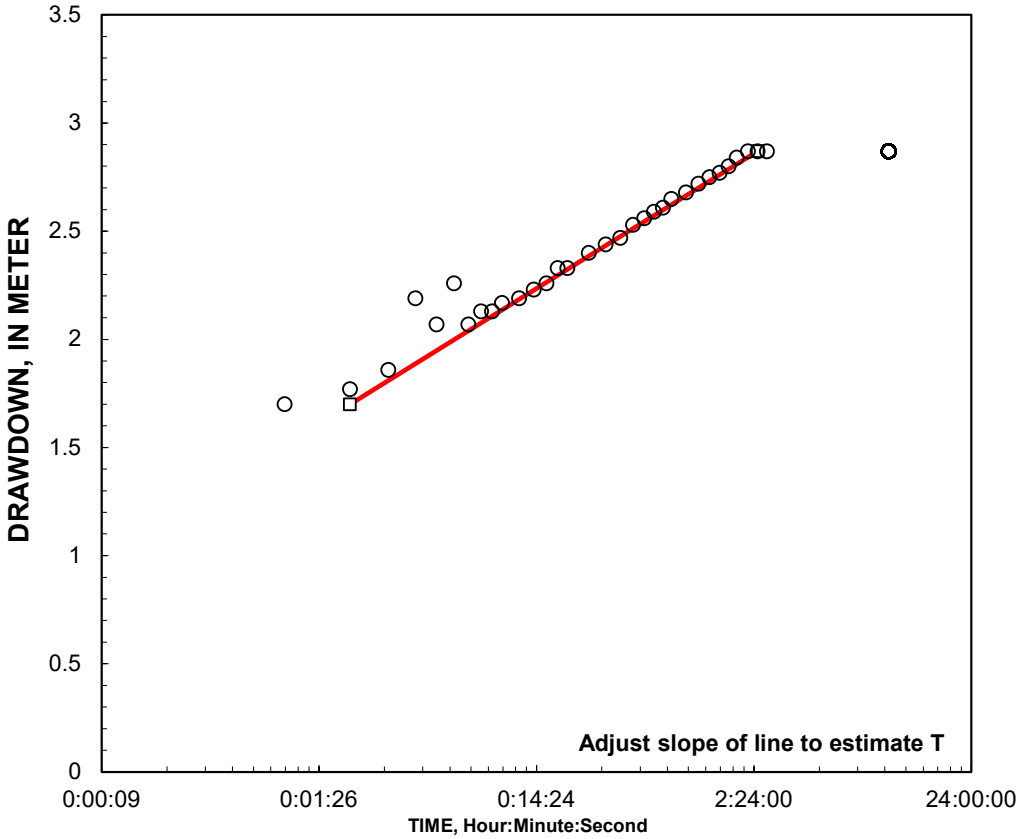

REMARKS: Cooper-Jacob analysis of single-well aquifer test

K = 12.80 m/day
T = 576 m^2/day

Reduced Data

Entry	Time, Date Hr:Min:Sec	Water Level Meter
1	1/0/00 0:00:00	43.93
2	1/0/00 0:01:00	45.63
3	1/0/00 0:02:00	45.70
4	1/0/00 0:03:00	45.79
5	1/0/00 0:04:00	46.12
6	1/0/00 0:05:00	46.00
7	1/0/00 0:06:00	46.19
8	1/0/00 0:07:00	46.00
9	1/0/00 0:08:00	46.06
10	1/0/00 0:09:00	46.06
11	1/0/00 0:10:00	46.10
12	1/0/00 0:12:00	46.12
13	1/0/00 0:14:00	46.16
14	1/0/00 0:16:00	46.19
15	1/0/00 0:18:00	46.26
16	1/0/00 0:20:00	46.26
17	1/0/00 0:25:00	46.33
18	1/0/00 0:30:00	46.37
19	1/0/00 0:35:00	46.40
20	1/0/00 0:40:00	46.46
21	1/0/00 0:45:00	46.49
22	1/0/00 0:50:00	46.52
23	1/0/00 0:55:00	46.54
24	1/0/00 1:00:00	46.58
25	1/0/00 1:10:00	46.61
26	1/0/00 1:20:00	46.65
27	1/0/00 1:30:00	46.68
28	1/0/00 1:40:00	46.70
29	1/0/00 1:50:00	46.73
30	1/0/00 2:00:00	46.77
31	1/0/00 2:15:00	46.80
32	1/0/00 2:30:00	46.80
33	1/0/00 2:45:00	46.80
34	1/0/00 3:00:00	0.00
35	1/0/00 3:15:00	0.00
36	1/0/00 3:30:00	0.00
37	1/0/00 4:00:00	0.00
38	1/0/00 4:30:00	0.00
39	1/0/00 5:00:00	0.00
40	1/0/00 5:30:00	0.00
41	1/0/00 6:00:00	0.00
42	1/0/00 6:30:00	0.00
43	1/0/00 7:00:00	0.00
44	1/0/00 7:30:00	0.00
45	1/0/00 8:00:00	0.00
46	1/0/00 8:30:00	0.00
47	1/0/00 9:00:00	0.00
48	1/0/00 9:30:00	0.00

WELL ID: SB 23-Desa Bulaksari

Local ID: Sumur Bor Desa Bulaksari
Date:
Time: 00:00

INPUT

Construction:		
Casing dia. (d_c)	6	Inch
Annulus dia. (d_w)	8	Inch
Screen Length (L)	21	Meter
Depths to:		
water level (DTW)	2.36	Meter
Top of Aquifer	70	Meter
Base of Aquifer	118	Meter
Annular Fill:		
across screen --	Gravel	
above screen --	Cement	
Aquifer Material --	Medium Sand	
FLOW RATE	2.5	liters/s

COMPUTED

Aquifer thickness = 160 Feet

Slope = 1.240194 Feet/log10

Input is consistent.

K =	2.2	Feet/Day
T =	340	Feet²/Day

K= 2.2 is less than likely minimum of 20 for Medium Sand

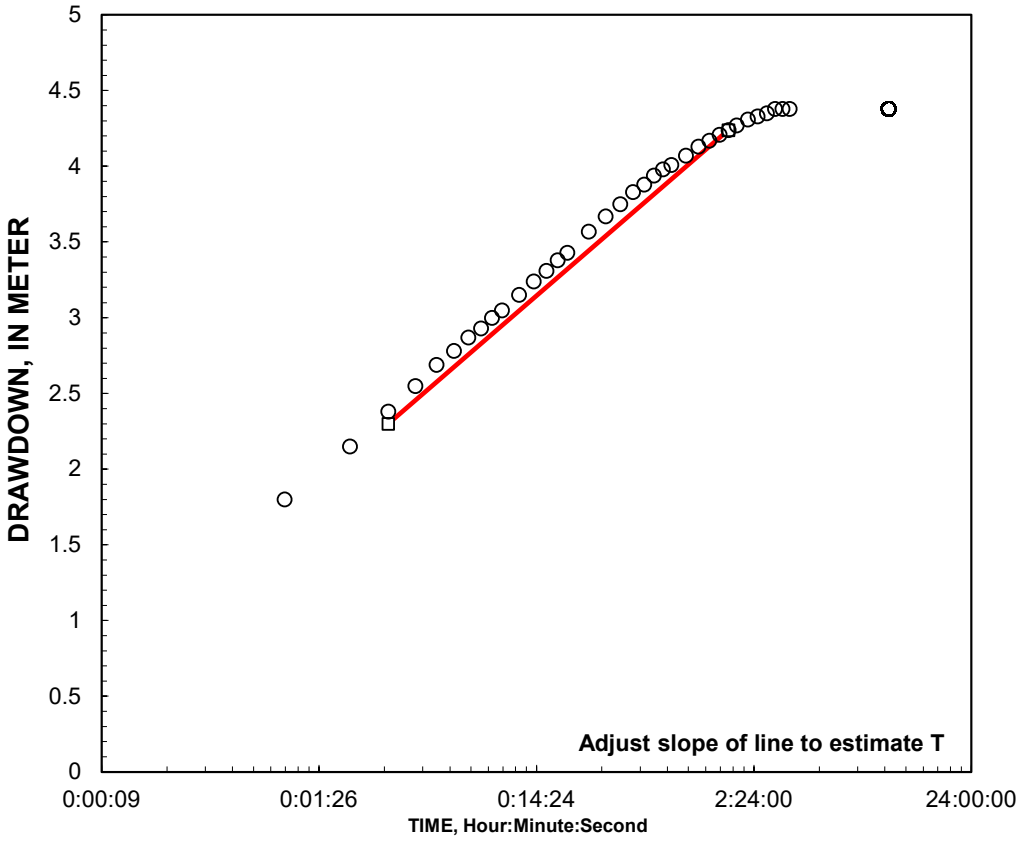

REMARKS: Cooper-Jacob analysis of single-well aquifer test

K = 12.80 m/day
T = 576 m^2/day

Reduced Data

Entry	Time, Date Hr:Min:Sec	Water Level Meter
1	1/0/00 0:00:00	2.36
2	1/0/00 0:01:00	4.16
3	1/0/00 0:02:00	4.51
4	1/0/00 0:03:00	4.74
5	1/0/00 0:04:00	4.91
6	1/0/00 0:05:00	5.05
7	1/0/00 0:06:00	5.14
8	1/0/00 0:07:00	5.23
9	1/0/00 0:08:00	5.29
10	1/0/00 0:09:00	5.36
11	1/0/00 0:10:00	5.41
12	1/0/00 0:12:00	5.51
13	1/0/00 0:14:00	5.60
14	1/0/00 0:16:00	5.67
15	1/0/00 0:18:00	5.74
16	1/0/00 0:20:00	5.79
17	1/0/00 0:25:00	5.93
18	1/0/00 0:30:00	6.03
19	1/0/00 0:35:00	6.11
20	1/0/00 0:40:00	6.19
21	1/0/00 0:45:00	6.24
22	1/0/00 0:50:00	6.30
23	1/0/00 0:55:00	6.34
24	1/0/00 1:00:00	6.37
25	1/0/00 1:10:00	6.43
26	1/0/00 1:20:00	6.49
27	1/0/00 1:30:00	6.53
28	1/0/00 1:40:00	6.57
29	1/0/00 1:50:00	6.60
30	1/0/00 2:00:00	6.63
31	1/0/00 2:15:00	6.67
32	1/0/00 2:30:00	6.69
33	1/0/00 2:45:00	6.71
34	1/0/00 3:00:00	6.74
35	1/0/00 3:15:00	6.74
36	1/0/00 3:30:00	6.74
37	1/0/00 4:00:00	0.00
38	1/0/00 4:30:00	0.00
39	1/0/00 5:00:00	0.00
40	1/0/00 5:30:00	0.00
41	1/0/00 6:00:00	0.00
42	1/0/00 6:30:00	0.00
43	1/0/00 7:00:00	0.00
44	1/0/00 7:30:00	0.00
45	1/0/00 8:00:00	0.00
46	1/0/00 8:30:00	0.00
47	1/0/00 9:00:00	0.00
48	1/0/00 9:30:00	0.00

WELL ID: SB-14 PT. CANDIMEKAR

Local ID: SB-14 CANDIMEKAR
Date: ########
Time: 00:00

INPUT

Construction:		
Casing dia. (d_c)	6	Inch
Annulus dia. (d_w)	12	Inch
Screen Length (L)	18	Meter
Depths to:		
water level (DTW)	13.98	Meter
Top of Aquifer	60	Meter
Base of Aquifer	135	Meter
Annular Fill:		
across screen --	Gravel	
above screen --	Cement	
Aquifer Material --	Sand and Gravel Mixe	
FLOW RATE	2.93	liters/s

COMPUTED

Aquifer thickness = 250 Feet

Slope = 0.081296 Feet/log10

Input is consistent.

K = 25 Feet/Day
T = 6100 Feet²/Day

K= 25 is less than likely minimum of 30 for Sand and Gravel Mixes

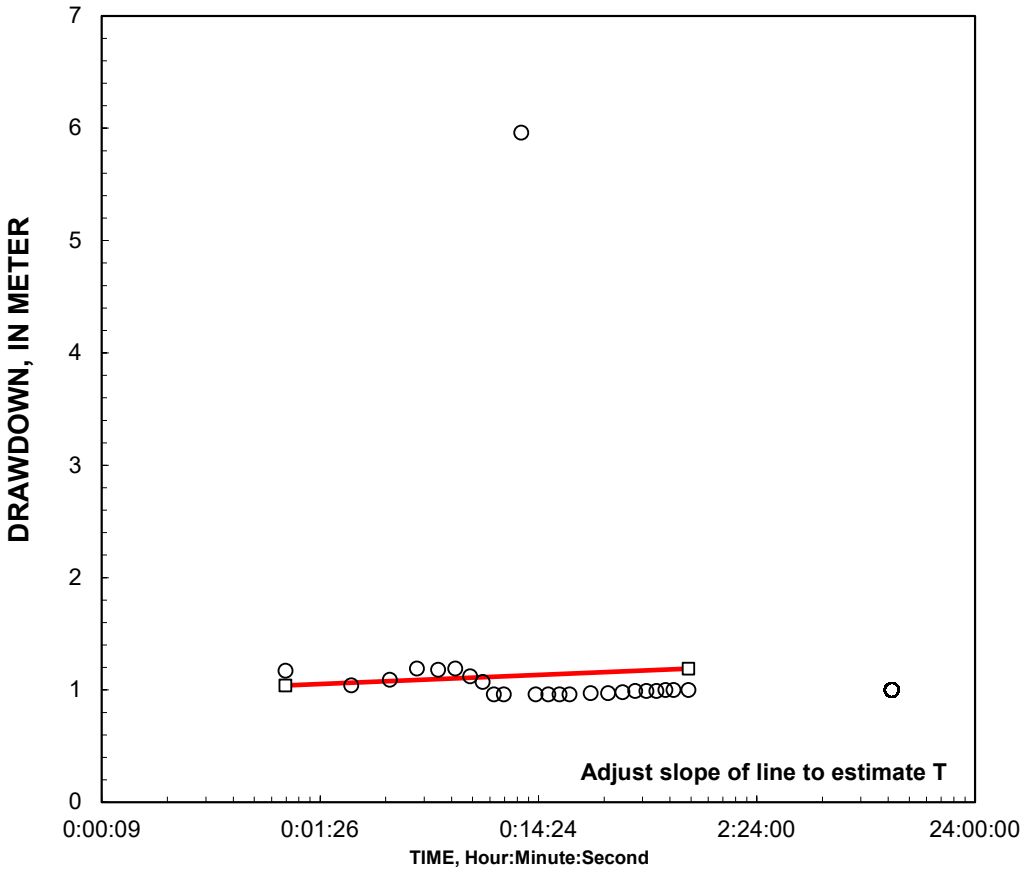

REMARKS: Cooper-Jacob analysis of single-well aquifer test

K = 12.80 m/day
T = 576 m²/day

Reduced Data

Entry	Time, Date Hr:Min:Sec	Water Level Meter
1	1/0/00 0:00:00	13.98
2	1/0/00 0:01:00	15.15
3	1/0/00 0:02:00	15.02
4	1/0/00 0:03:00	15.07
5	1/0/00 0:04:00	15.17
6	1/0/00 0:05:00	15.16
7	1/0/00 0:06:00	15.17
8	1/0/00 0:07:00	15.10
9	1/0/00 0:08:00	15.05
10	1/0/00 0:09:00	14.94
11	1/0/00 0:10:00	14.94
12	1/0/00 0:12:00	19.94
13	1/0/00 0:14:00	14.94
14	1/0/00 0:16:00	14.94
15	1/0/00 0:18:00	14.94
16	1/0/00 0:20:00	14.94
17	1/0/00 0:25:00	14.95
18	1/0/00 0:30:00	14.95
19	1/0/00 0:35:00	14.96
20	1/0/00 0:40:00	14.97
21	1/0/00 0:45:00	14.97
22	1/0/00 0:50:00	14.97
23	1/0/00 0:55:00	14.98
24	1/0/00 1:00:00	14.98
25	1/0/00 1:10:00	14.98
26	1/0/00 1:20:00	0.00
27	1/0/00 1:30:00	0.00
28	1/0/00 1:40:00	0.00
29	1/0/00 1:50:00	0.00
30	1/0/00 2:00:00	0.00
31	1/0/00 2:15:00	0.00
32	1/0/00 2:30:00	0.00
33	1/0/00 2:45:00	0.00
34	1/0/00 3:00:00	0.00
35	1/0/00 3:15:00	0.00
36	1/0/00 3:30:00	0.00
37	1/0/00 4:00:00	0.00
38	1/0/00 4:30:00	0.00
39	1/0/00 5:00:00	0.00
40	1/0/00 5:30:00	0.00
41	1/0/00 6:00:00	0.00
42	1/0/00 6:30:00	0.00
43	1/0/00 7:00:00	0.00
44	1/0/00 7:30:00	0.00
45	1/0/00 8:00:00	0.00
46	1/0/00 8:30:00	0.00
47	1/0/00 9:00:00	0.00
48	1/0/00 9:30:00	0.00

WELL ID: SB-25 DADIREJO

Local ID: SB-25 DADIREJO
Date: ########
Time: 00:00

INPUT

Construction:		
Casing dia. (d_c)	6	Inch
Annulus dia. (d_w)	12	Inch
Screen Length (L)	21	Meter
Depths to:		
water level (DTW)	33.1	Meter
Top of Aquifer	60	Meter
Base of Aquifer	135	Meter
Annular Fill:		
across screen --	Gravel	
above screen --	Cement	
Aquifer Material --	Fine Sand	
FLOW RATE	1.9	liters/s

COMPUTED

Aquifer thickness = 250 Feet

Slope = 0.724268 Feet/log10

Input is consistent.

K =	1.8	Feet/Day
T =	450	Feet²/Day

K= 1.8 is less than likely minimum of 3 for Fine Sand

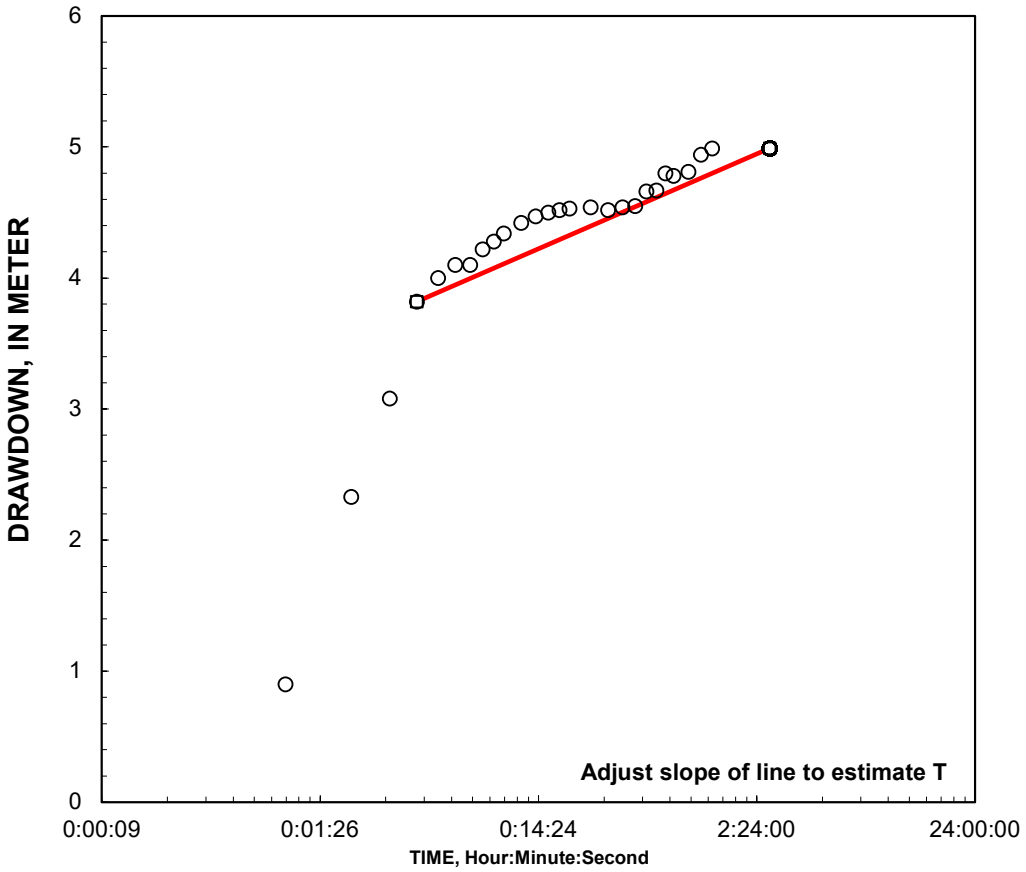

REMARKS: Cooper-Jacob analysis of single-well aquifer test

K = 12.80 m/day
T = 576 m²/day

Reduced Data

Entry	Time, Date Hr:Min:Sec	Water Level Meter
1	1/0/00 0:00:00	33.10
2	1/0/00 0:01:00	34.00
3	1/0/00 0:02:00	35.43
4	1/0/00 0:03:00	36.18
5	1/0/00 0:04:00	36.92
6	1/0/00 0:05:00	37.10
7	1/0/00 0:06:00	37.20
8	1/0/00 0:07:00	37.20
9	1/0/00 0:08:00	37.32
10	1/0/00 0:09:00	37.38
11	1/0/00 0:10:00	37.44
12	1/0/00 0:12:00	37.52
13	1/0/00 0:14:00	37.57
14	1/0/00 0:16:00	37.60
15	1/0/00 0:18:00	37.62
16	1/0/00 0:20:00	37.63
17	1/0/00 0:25:00	37.64
18	1/0/00 0:30:00	37.62
19	1/0/00 0:35:00	37.64
20	1/0/00 0:40:00	37.65
21	1/0/00 0:45:00	37.76
22	1/0/00 0:50:00	37.77
23	1/0/00 0:55:00	37.90
24	1/0/00 1:00:00	37.88
25	1/0/00 1:10:00	37.91
26	1/0/00 1:20:00	38.04
27	1/0/00 1:30:00	38.09
28	1/0/00 1:40:00	0.00
29	1/0/00 1:50:00	0.00
30	1/0/00 2:00:00	0.00
31	1/0/00 2:15:00	0.00
32	1/0/00 2:30:00	0.00

WELL ID: SB-20 HARJOSARI

Local ID: SB-20 HARJOSARI
Date: ########
Time: 00:00

INPUT

Construction:		
Casing dia. (d_c)	6	Inch
Annulus dia. (d_w)	12	Inch
Screen Length (L)	21	Meter
Depths to:		
water level (DTW)	0.05	Meter
Top of Aquifer	60	Meter
Base of Aquifer	135	Meter
Annular Fill:		
across screen --	Gravel	
above screen --	Cement	
Aquifer Material --	Fine Sand	
FLOW RATE	2.05	liters/s

COMPUTED

Aquifer thickness = 250 Feet

Slope = 4.478018 Feet/log10

Input is consistent.

K =	0.32	Feet/Day
T =	78	Feet²/Day

K= 0.32 is less than likely minimum of 3 for Fine Sand

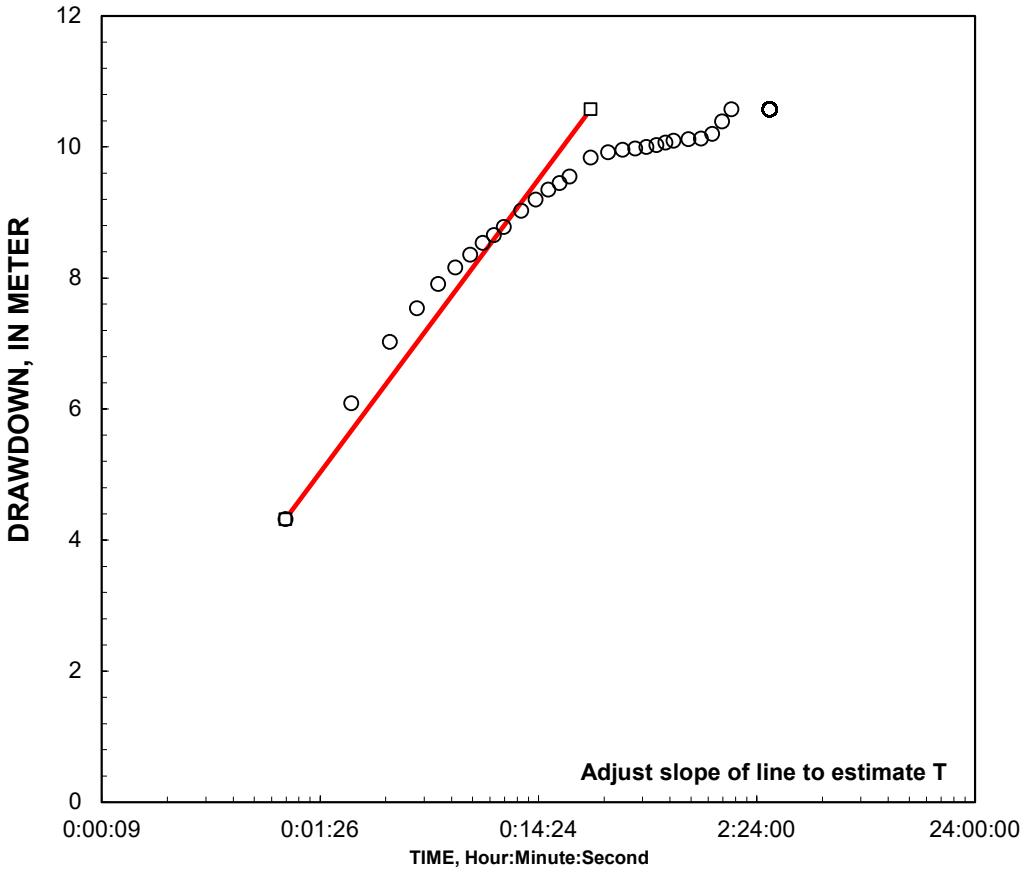

REMARKS: Cooper-Jacob analysis of single-well aquifer test

K = 12.80 m/day
T = 576 m²/day

Reduced Data

Entry	Time, Date Hr:Min:Sec	Water Level Meter
1	1/0/00 0:00:00	0.05
2	1/0/00 0:01:00	4.37
3	1/0/00 0:02:00	6.14
4	1/0/00 0:03:00	7.08
5	1/0/00 0:04:00	7.59
6	1/0/00 0:05:00	7.96
7	1/0/00 0:06:00	8.21
8	1/0/00 0:07:00	8.41
9	1/0/00 0:08:00	8.59
10	1/0/00 0:09:00	8.71
11	1/0/00 0:10:00	8.83
12	1/0/00 0:12:00	9.08
13	1/0/00 0:14:00	9.25
14	1/0/00 0:16:00	9.40
15	1/0/00 0:18:00	9.50
16	1/0/00 0:20:00	9.60
17	1/0/00 0:25:00	9.89
18	1/0/00 0:30:00	9.97
19	1/0/00 0:35:00	10.01
20	1/0/00 0:40:00	10.03
21	1/0/00 0:45:00	10.05
22	1/0/00 0:50:00	10.08
23	1/0/00 0:55:00	10.12
24	1/0/00 1:00:00	10.15
25	1/0/00 1:10:00	10.17
26	1/0/00 1:20:00	10.18
27	1/0/00 1:30:00	10.25
28	1/0/00 1:40:00	10.44
29	1/0/00 1:50:00	10.63
30	1/0/00 2:00:00	0.00
31	1/0/00 2:15:00	0.00
32	1/0/00 2:30:00	0.00

WELL ID: SB 10-Desa Kadipaten

Local ID: Sumur Bor Desa Kadipaten
Date:
Time: 00:00

INPUT

Construction:		
Casing dia. (d_c)	6	Inch
Annulus dia. (d_w)	8	Inch
Screen Length (L)	21	Meter
Depths to:		
water level (DTW)	19.28	Meter
Top of Aquifer	80	Meter
Base of Aquifer	125	Meter
Annular Fill:		
across screen --	Gravel	
above screen --	Cement	
Aquifer Material --	Fine Sand	
FLOW RATE	2.17	liters/s

COMPUTED

Aquifer thickness = 150 Feet

Slope = 0.430623 Feet/log10

Input is consistent.

K = 5.8 Feet/Day
T = 860 Feet²/Day

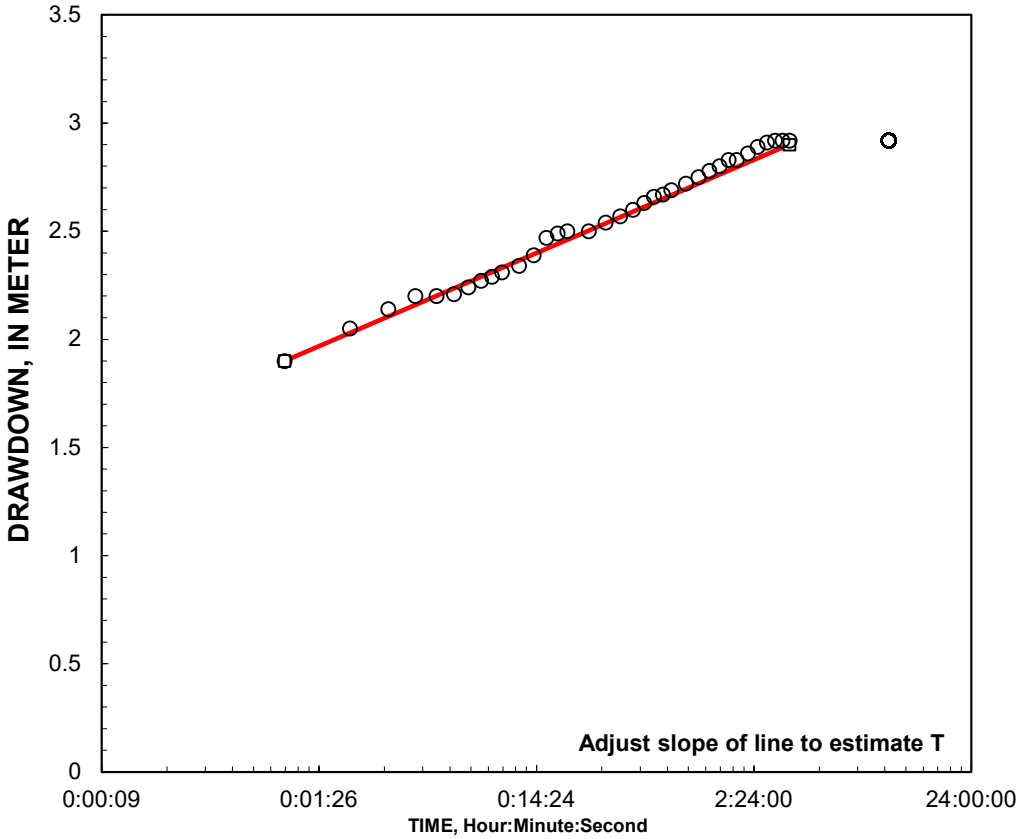

REMARKS: Cooper-Jacob analysis of single-well aquifer test

K = 12.80 m/day
T = 576 m²/day

Reduced Data

Entry	Time, Date Hr:Min:Sec	Water Level Meter
1	1/0/00 0:00:00	19.28
2	1/0/00 0:01:00	21.18
3	1/0/00 0:02:00	21.33
4	1/0/00 0:03:00	21.42
5	1/0/00 0:04:00	21.48
6	1/0/00 0:05:00	21.48
7	1/0/00 0:06:00	21.49
8	1/0/00 0:07:00	21.52
9	1/0/00 0:08:00	21.55
10	1/0/00 0:09:00	21.57
11	1/0/00 0:10:00	21.59
12	1/0/00 0:12:00	21.62
13	1/0/00 0:14:00	21.67
14	1/0/00 0:16:00	21.75
15	1/0/00 0:18:00	21.77
16	1/0/00 0:20:00	21.78
17	1/0/00 0:25:00	21.78
18	1/0/00 0:30:00	21.82
19	1/0/00 0:35:00	21.85
20	1/0/00 0:40:00	21.88
21	1/0/00 0:45:00	21.91
22	1/0/00 0:50:00	21.94
23	1/0/00 0:55:00	21.95
24	1/0/00 1:00:00	21.97
25	1/0/00 1:10:00	22.00
26	1/0/00 1:20:00	22.03
27	1/0/00 1:30:00	22.06
28	1/0/00 1:40:00	22.08
29	1/0/00 1:50:00	22.11
30	1/0/00 2:00:00	22.11
31	1/0/00 2:15:00	22.14
32	1/0/00 2:30:00	22.17
33	1/0/00 2:45:00	22.19
34	1/0/00 3:00:00	22.20
35	1/0/00 3:15:00	22.20
36	1/0/00 3:30:00	22.20
37	1/0/00 4:00:00	0.00
38	1/0/00 4:30:00	0.00
39	1/0/00 5:00:00	0.00
40	1/0/00 5:30:00	0.00
41	1/0/00 6:00:00	0.00
42	1/0/00 6:30:00	0.00
43	1/0/00 7:00:00	0.00
44	1/0/00 7:30:00	0.00
45	1/0/00 8:00:00	0.00
46	1/0/00 8:30:00	0.00
47	1/0/00 9:00:00	0.00
48	1/0/00 9:30:00	0.00

WELL ID: SB-12 KAMPIL

Local ID: SB-12 KAMPIL
Date: ########
Time: 00:00

INPUT

Construction:		
Casing dia. (d_c)	6	Inch
Annulus dia. (d_w)	12	Inch
Screen Length (L)	21	Meter
Depths to:		
water level (DTW)	27.09	Meter
Top of Aquifer	60	Meter
Base of Aquifer	135	Meter
Annular Fill:		
across screen --	Gravel	
above screen --	Cement	
Aquifer Material --	Fine Sand	
FLOW RATE	2.12	liters/s

COMPUTED

Aquifer thickness = 250 Feet

Slope = 0.392337 Feet/log10

Input is consistent.

K = 3.7 Feet/Day
T = 920 Feet²/Day

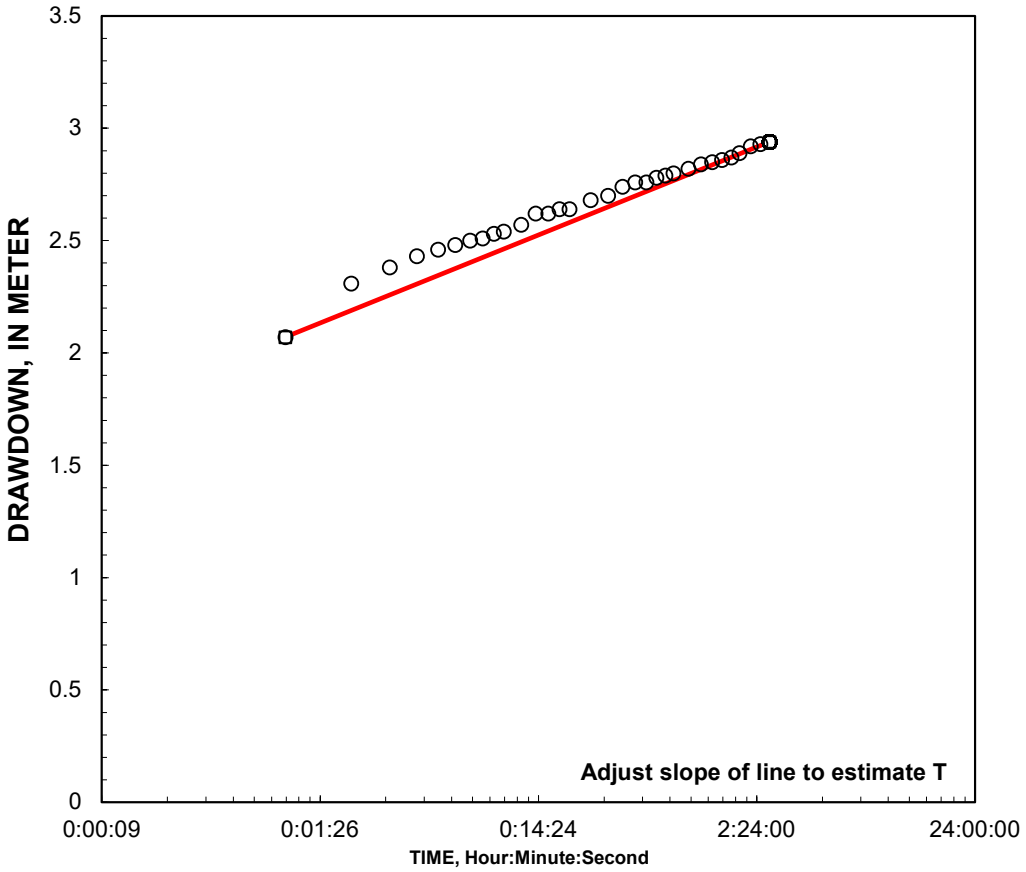

REMARKS: Cooper-Jacob analysis of single-well aquifer test

K = 12.80 m/day
T = 576 m²/day

Reduced Data

Entry	Time, Date Hr:Min:Sec	Water Level Meter
1	1/0/00 0:00:00	27.09
2	1/0/00 0:01:00	29.16
3	1/0/00 0:02:00	29.40
4	1/0/00 0:03:00	29.47
5	1/0/00 0:04:00	29.52
6	1/0/00 0:05:00	29.55
7	1/0/00 0:06:00	29.57
8	1/0/00 0:07:00	29.59
9	1/0/00 0:08:00	29.60
10	1/0/00 0:09:00	29.62
11	1/0/00 0:10:00	29.63
12	1/0/00 0:12:00	29.66
13	1/0/00 0:14:00	29.71
14	1/0/00 0:16:00	29.71
15	1/0/00 0:18:00	29.73
16	1/0/00 0:20:00	29.73
17	1/0/00 0:25:00	29.77
18	1/0/00 0:30:00	29.79
19	1/0/00 0:35:00	29.83
20	1/0/00 0:40:00	29.85
21	1/0/00 0:45:00	29.85
22	1/0/00 0:50:00	29.87
23	1/0/00 0:55:00	29.88
24	1/0/00 1:00:00	29.89
25	1/0/00 1:10:00	29.91
26	1/0/00 1:20:00	29.93
27	1/0/00 1:30:00	29.94
28	1/0/00 1:40:00	29.95
29	1/0/00 1:50:00	29.96
30	1/0/00 2:00:00	29.98
31	1/0/00 2:15:00	30.01
32	1/0/00 2:30:00	30.02

WELL ID: SB-13 KAUMAN

Local ID: SB-13 KAUMAN
Date: ########
Time: 00:00

INPUT

Construction:		
Casing dia. (d_c)	6	Inch
Annulus dia. (d_w)	12	Inch
Screen Length (L)	21	Meter
Depths to:		
water level (DTW)	27.09	Meter
Top of Aquifer	60	Meter
Base of Aquifer	135	Meter
Annular Fill:		
across screen --	Gravel	
above screen --	Cement	
Aquifer Material --	Fine Sand	
FLOW RATE	2	liters/s

COMPUTED

Aquifer thickness = 250 Feet

Slope = 1.08352 Feet/log10

Input is consistent.

K = 1.3 Feet/Day
T = 310 Feet²/Day

K= 1.3 is less than likely minimum of 3 for Fine Sand

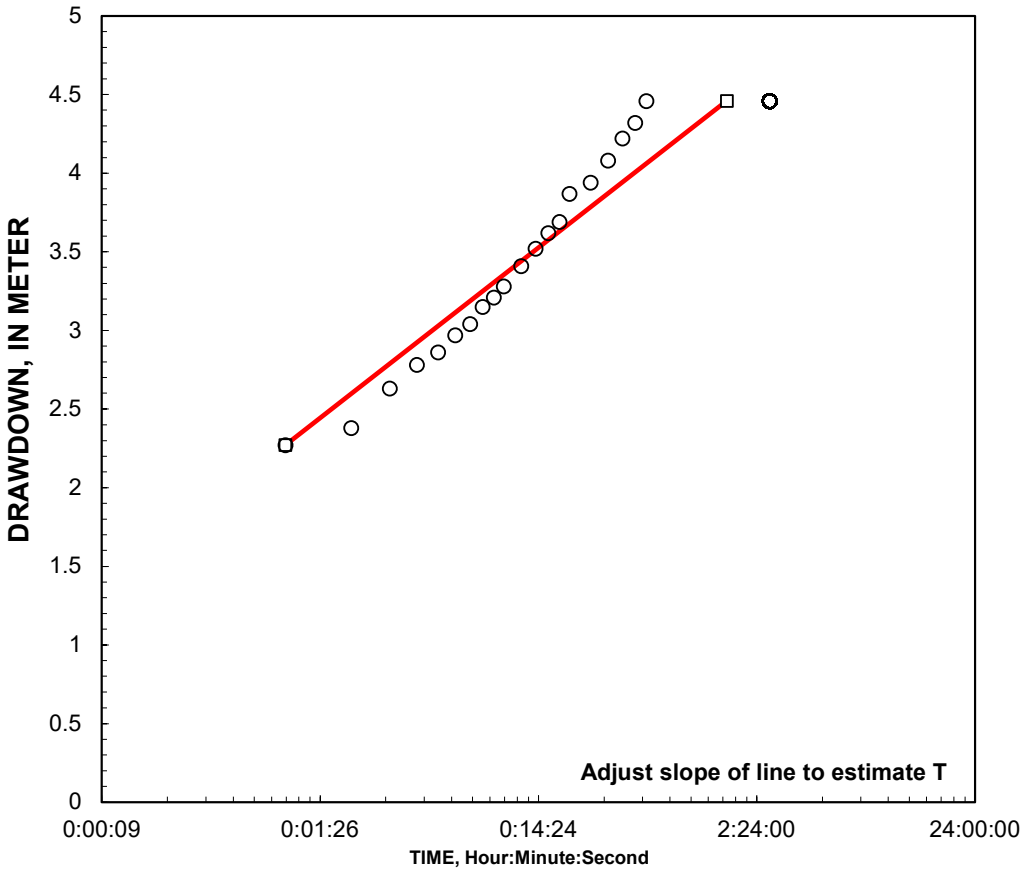

REMARKS: Cooper-Jacob analysis of single-well aquifer test

K = 12.80 m/day
T = 576 m²/day

Reduced Data

Entry	Time, Date Hr:Min:Sec	Water Level Meter
1	1/0/00 0:00:00	30.63
2	1/0/00 0:01:00	32.90
3	1/0/00 0:02:00	33.01
4	1/0/00 0:03:00	33.26
5	1/0/00 0:04:00	33.41
6	1/0/00 0:05:00	33.49
7	1/0/00 0:06:00	33.60
8	1/0/00 0:07:00	33.67
9	1/0/00 0:08:00	33.78
10	1/0/00 0:09:00	33.84
11	1/0/00 0:10:00	33.91
12	1/0/00 0:12:00	34.04
13	1/0/00 0:14:00	34.15
14	1/0/00 0:16:00	34.25
15	1/0/00 0:18:00	34.32
16	1/0/00 0:20:00	34.50
17	1/0/00 0:25:00	34.57
18	1/0/00 0:30:00	34.71
19	1/0/00 0:35:00	34.85
20	1/0/00 0:40:00	34.95
21	1/0/00 0:45:00	35.09
22	1/0/00 0:50:00	0.00
23	1/0/00 0:55:00	0.00
24	1/0/00 1:00:00	0.00
25	1/0/00 1:10:00	0.00
26	1/0/00 1:20:00	0.00
27	1/0/00 1:30:00	0.00
28	1/0/00 1:40:00	0.00
29	1/0/00 1:50:00	0.00
30	1/0/00 2:00:00	0.00
31	1/0/00 2:15:00	0.00
32	1/0/00 2:30:00	0.00

WELL ID: SB 19-Desa Kedungwuni Timur

Local ID: Sumur Bor Desa Kedungwuni
Date:
Time: 00:00

INPUT

Construction:		
Casing dia. (d_c)	6	Inch
Annulus dia. (d_w)	8	Inch
Screen Length (L)	21	Meter
Depths to:		
water level (DTW)	1.83	Meter
Top of Aquifer	72	Meter
Base of Aquifer	112	Meter
Annular Fill:		
across screen --	Gravel	
above screen --	Cement	
Aquifer Material --	Fine Sand	
FLOW RATE	2.07	liters/s

COMPUTED

Aquifer thickness = 130 Feet

Slope = 0.87465 Feet/log10

Input is consistent.

K = 3.1 Feet/Day
T = 400 Feet²/Day

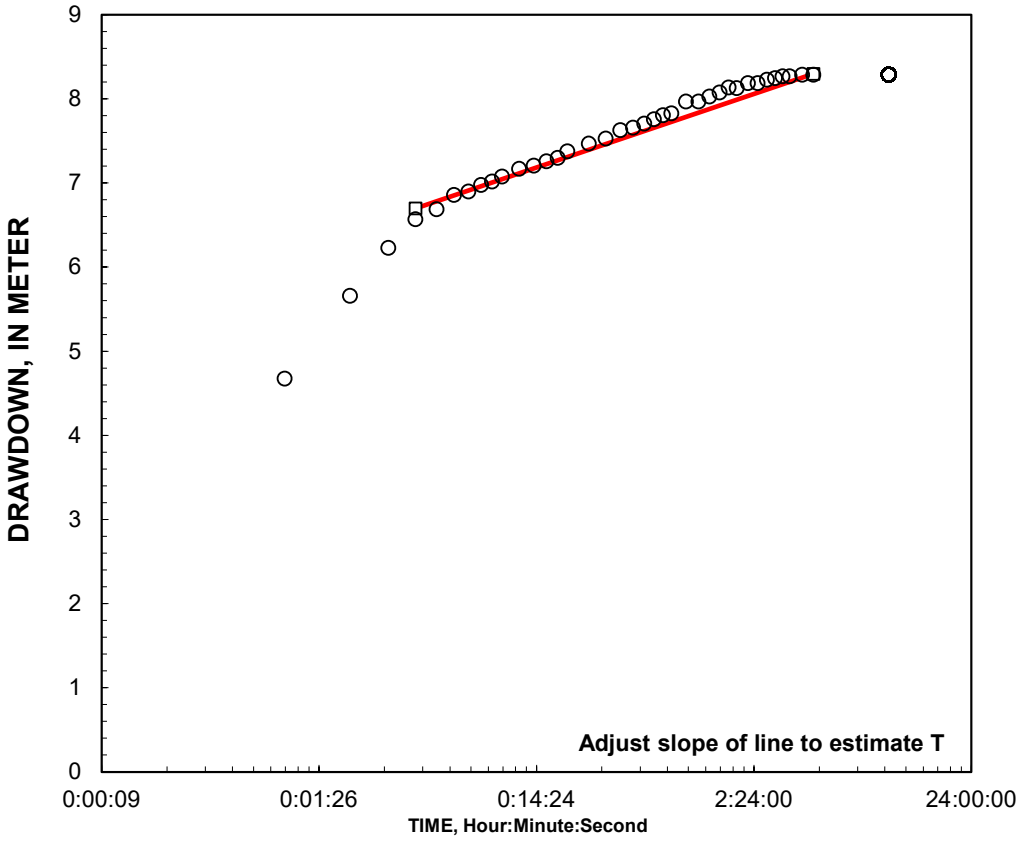

REMARKS: Cooper-Jacob analysis of single-well aquifer test

K = 12.80 m/day
T = 576 m²/day

Reduced Data

Timur Entry	Time, Date Hr:Min:Sec	Water Level Meter
1	1/0/00 0:00:00	1.83
2	1/0/00 0:01:00	6.51
3	1/0/00 0:02:00	7.49
4	1/0/00 0:03:00	8.06
5	1/0/00 0:04:00	8.40
6	1/0/00 0:05:00	8.52
7	1/0/00 0:06:00	8.69
8	1/0/00 0:07:00	8.73
9	1/0/00 0:08:00	8.81
10	1/0/00 0:09:00	8.85
11	1/0/00 0:10:00	8.91
12	1/0/00 0:12:00	9.00
13	1/0/00 0:14:00	9.04
14	1/0/00 0:16:00	9.09
15	1/0/00 0:18:00	9.13
16	1/0/00 0:20:00	9.21
17	1/0/00 0:25:00	9.30
18	1/0/00 0:30:00	9.36
19	1/0/00 0:35:00	9.46
20	1/0/00 0:40:00	9.49
21	1/0/00 0:45:00	9.54
22	1/0/00 0:50:00	9.59
23	1/0/00 0:55:00	9.64
24	1/0/00 1:00:00	9.66
25	1/0/00 1:10:00	9.80
26	1/0/00 1:20:00	9.80
27	1/0/00 1:30:00	9.86
28	1/0/00 1:40:00	9.91
29	1/0/00 1:50:00	9.97
30	1/0/00 2:00:00	9.96
31	1/0/00 2:15:00	10.02
32	1/0/00 2:30:00	10.02
33	1/0/00 2:45:00	10.06
34	1/0/00 3:00:00	10.08
35	1/0/00 3:15:00	10.10
36	1/0/00 3:30:00	10.10
37	1/0/00 4:00:00	10.12
38	1/0/00 4:30:00	10.12
39	1/0/00 5:00:00	0.00
40	1/0/00 5:30:00	0.00
41	1/0/00 6:00:00	0.00
42	1/0/00 6:30:00	0.00
43	1/0/00 7:00:00	0.00
44	1/0/00 7:30:00	0.00
45	1/0/00 8:00:00	0.00
46	1/0/00 8:30:00	0.00
47	1/0/00 9:00:00	0.00
48	1/0/00 9:30:00	0.00

WELL ID: SB 17-Desa Kradon

Local ID: Sumur Bor Desa Kradon
Date:
Time: 00:00

INPUT

Construction:		
Casing dia. (d_c)	6	Inch
Annulus dia. (d_w)	8	Inch
Screen Length (L)	21	Meter
Depths to:		
water level (DTW)	19.28	Meter
Top of Aquifer	35	Meter
Base of Aquifer	119	Meter
Annular Fill:		
across screen --	Gravel	
above screen --	Cement	
Aquifer Material --	Fine Sand	
FLOW RATE	2.17	liters/s

COMPUTED

Aquifer thickness = 280 Feet

Slope = 0.173835 Feet/log10

Input is consistent.

K = 7.7 Feet/Day
T = 2100 Feet²/Day

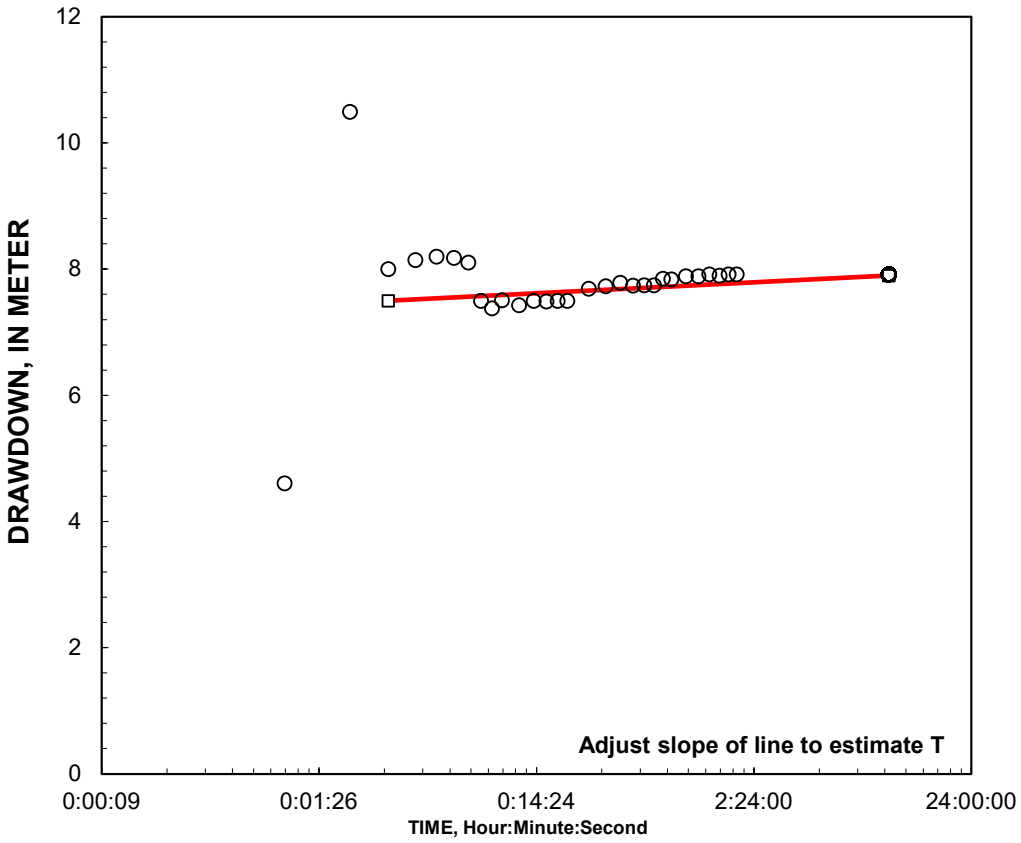

REMARKS: Cooper-Jacob analysis of single-well aquifer test

K = 12.80 m/day
T = 576 m²/day

Reduced Data

Entry	Time, Date Hr:Min:Sec	Water Level Meter
1	1/0/00 0:00:00	3.70
2	1/0/00 0:01:00	8.31
3	1/0/00 0:02:00	14.20
4	1/0/00 0:03:00	11.70
5	1/0/00 0:04:00	11.85
6	1/0/00 0:05:00	11.90
7	1/0/00 0:06:00	11.88
8	1/0/00 0:07:00	11.81
9	1/0/00 0:08:00	11.20
10	1/0/00 0:09:00	11.08
11	1/0/00 0:10:00	11.21
12	1/0/00 0:12:00	11.13
13	1/0/00 0:14:00	11.20
14	1/0/00 0:16:00	11.19
15	1/0/00 0:18:00	11.20
16	1/0/00 0:20:00	11.20
17	1/0/00 0:25:00	11.39
18	1/0/00 0:30:00	11.43
19	1/0/00 0:35:00	11.49
20	1/0/00 0:40:00	11.44
21	1/0/00 0:45:00	11.45
22	1/0/00 0:50:00	11.45
23	1/0/00 0:55:00	11.55
24	1/0/00 1:00:00	11.54
25	1/0/00 1:10:00	11.59
26	1/0/00 1:20:00	11.59
27	1/0/00 1:30:00	11.62
28	1/0/00 1:40:00	11.60
29	1/0/00 1:50:00	11.62
30	1/0/00 2:00:00	11.62
31	1/0/00 2:15:00	0.00
32	1/0/00 2:30:00	0.00
33	1/0/00 2:45:00	0.00
34	1/0/00 3:00:00	0.00
35	1/0/00 3:15:00	0.00
36	1/0/00 3:30:00	0.00
37	1/0/00 4:00:00	0.00
38	1/0/00 4:30:00	0.00
39	1/0/00 5:00:00	0.00
40	1/0/00 5:30:00	0.00
41	1/0/00 6:00:00	0.00
42	1/0/00 6:30:00	0.00
43	1/0/00 7:00:00	0.00
44	1/0/00 7:30:00	0.00
45	1/0/00 8:00:00	0.00
46	1/0/00 8:30:00	0.00
47	1/0/00 9:00:00	0.00
48	1/0/00 9:30:00	0.00

WELL ID: SB-05 Pedurungan

Local ID: SB-05 PEDURUNGAN
Date: ########
Time: 00:00

INPUT

Construction:		
Casing dia. (d_c)	6	Inch
Annulus dia. (d_w)	12	Inch
Screen Length (L)	21	Meter
Depths to:		
water level (DTW)	3.07	Meter
Top of Aquifer	42	Meter
Base of Aquifer	102	Meter
Annular Fill:		
across screen --	Gravel	
above screen --	Cement	
Aquifer Material --	Medium Sand	
FLOW RATE	2.01	liters/s

COMPUTED

Aquifer thickness = 200 Feet

Slope = 0.20087 Feet/log10

Input is consistent.

K = 8.7 Feet/Day
T = 1700 Feet²/Day

K= 8.7 is less than likely minimum of 20 for Medium Sand

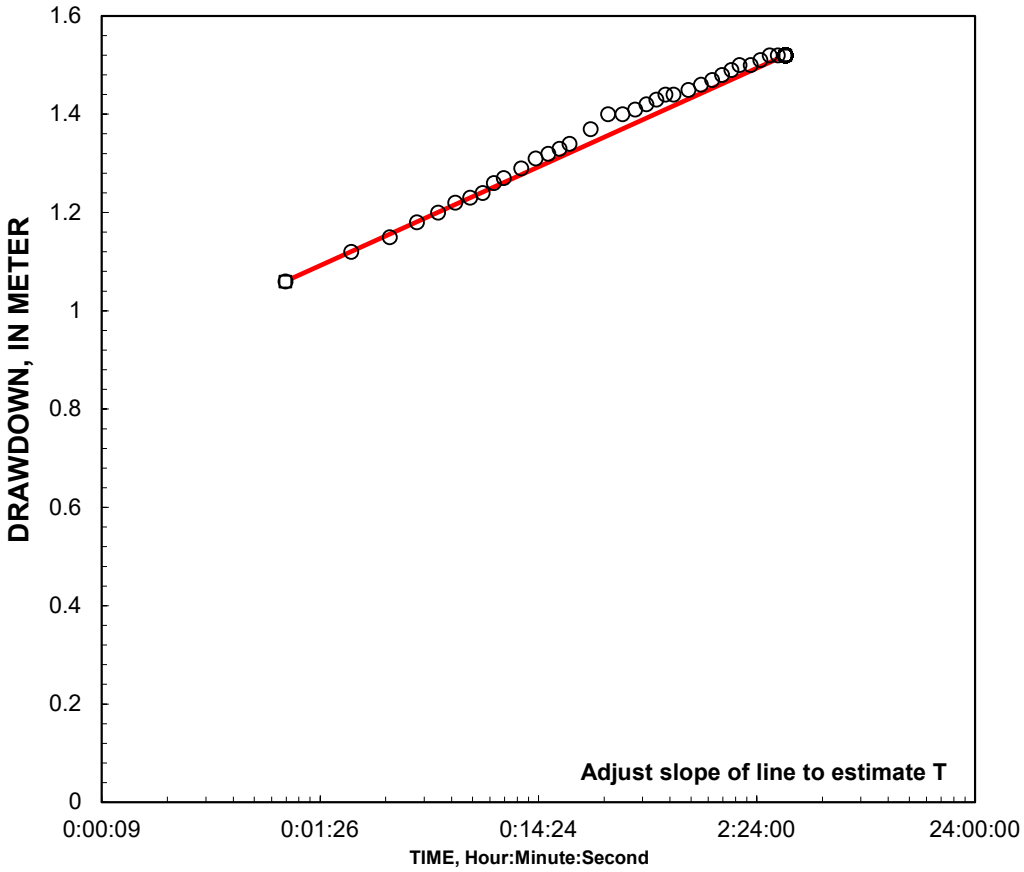

REMARKS: Cooper-Jacob analysis of single-well aquifer test

K = 12.80 m/day
T = 576 m²/day

Reduced Data

Entry	Time, Date Hr:Min:Sec	Water Level Meter
1	1/0/00 0:00:00	3.07
2	1/0/00 0:01:00	4.13
3	1/0/00 0:02:00	4.19
4	1/0/00 0:03:00	4.22
5	1/0/00 0:04:00	4.25
6	1/0/00 0:05:00	4.27
7	1/0/00 0:06:00	4.29
8	1/0/00 0:07:00	4.30
9	1/0/00 0:08:00	4.31
10	1/0/00 0:09:00	4.33
11	1/0/00 0:10:00	4.34
12	1/0/00 0:12:00	4.36
13	1/0/00 0:14:00	4.38
14	1/0/00 0:16:00	4.39
15	1/0/00 0:18:00	4.40
16	1/0/00 0:20:00	4.41
17	1/0/00 0:25:00	4.44
18	1/0/00 0:30:00	4.47
19	1/0/00 0:35:00	4.47
20	1/0/00 0:40:00	4.48
21	1/0/00 0:45:00	4.49
22	1/0/00 0:50:00	4.50
23	1/0/00 0:55:00	4.51
24	1/0/00 1:00:00	4.51
25	1/0/00 1:10:00	4.52
26	1/0/00 1:20:00	4.53
27	1/0/00 1:30:00	4.54
28	1/0/00 1:40:00	4.55
29	1/0/00 1:50:00	4.56
30	1/0/00 2:00:00	4.57
31	1/0/00 2:15:00	4.57
32	1/0/00 2:30:00	4.58
33	1/0/00 2:45:00	4.59
34	1/0/00 3:00:00	4.59

WELL ID: SB11-Pendowo

Local ID: SB-11 Pendowo
Date: ########
Time: 00:00

INPUT

Construction:		
Casing dia. (d_c)	6	Inch
Annulus dia. (d_w)	12	Inch
Screen Length (L)	21	Meter
Depths to:		
water level (DTW)	12.7	Meter
Top of Aquifer	40	Meter
Base of Aquifer	110	Meter
Annular Fill:		
across screen --	Gravel	
above screen --	Cement	
Aquifer Material --	Fine Sand	
FLOW RATE	2	liters/s

COMPUTED

Aquifer thickness = 230 Feet

Slope = 7.909559 Feet/log10

Input is consistent.

K =	0.19	Feet/Day
T =	43	Feet²/Day

K= 0.19 is less than likely minimum of 3 for Fine Sand

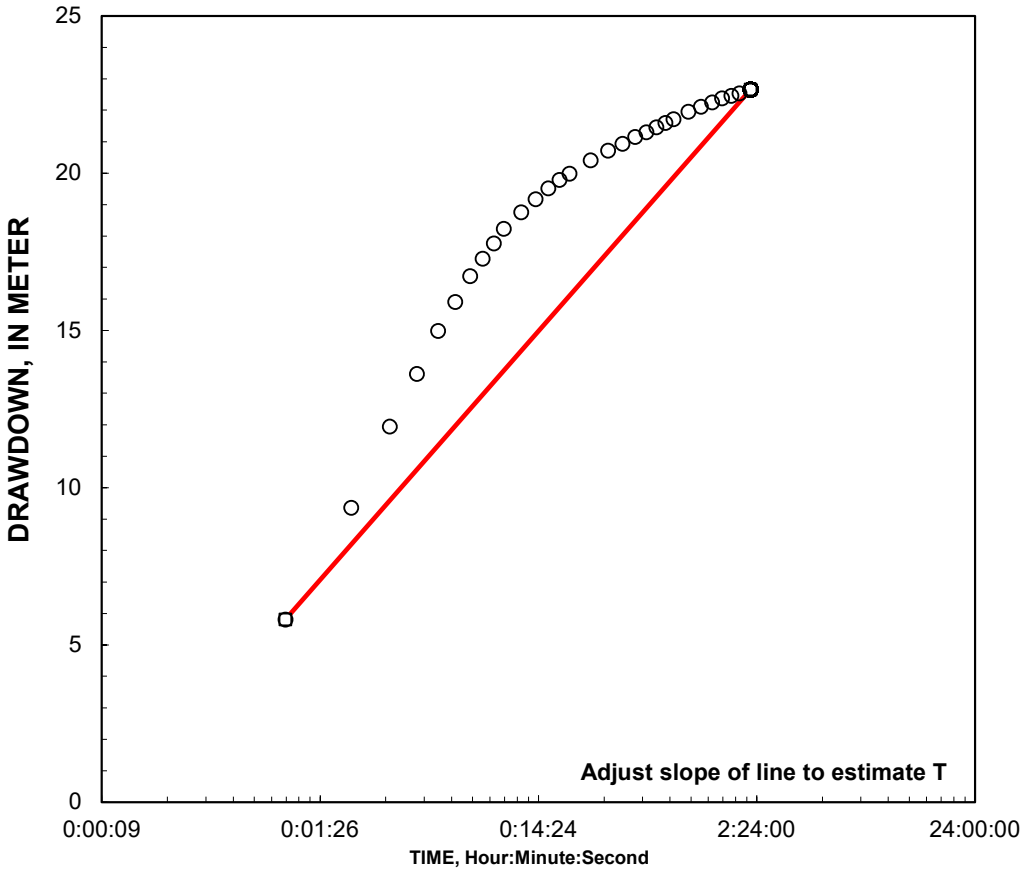

REMARKS: Cooper-Jacob analysis of single-well aquifer test

K = 12.80 m/day
T = 576 m^2/day

Reduced Data

Entry	Time, Date Hr:Min:Sec	Water Level Meter
1	1/0/00 0:00:00	12.70
2	1/0/00 0:01:00	18.51
3	1/0/00 0:02:00	22.07
4	1/0/00 0:03:00	24.64
5	1/0/00 0:04:00	26.32
6	1/0/00 0:05:00	27.69
7	1/0/00 0:06:00	28.61
8	1/0/00 0:07:00	29.43
9	1/0/00 0:08:00	29.98
10	1/0/00 0:09:00	30.47
11	1/0/00 0:10:00	30.93
12	1/0/00 0:12:00	31.46
13	1/0/00 0:14:00	31.88
14	1/0/00 0:16:00	32.22
15	1/0/00 0:18:00	32.49
16	1/0/00 0:20:00	32.69
17	1/0/00 0:25:00	33.11
18	1/0/00 0:30:00	33.42
19	1/0/00 0:35:00	33.63
20	1/0/00 0:40:00	33.86
21	1/0/00 0:45:00	34.01
22	1/0/00 0:50:00	34.16
23	1/0/00 0:55:00	34.30
24	1/0/00 1:00:00	34.42
25	1/0/00 1:10:00	34.66
26	1/0/00 1:20:00	34.82
27	1/0/00 1:30:00	34.95
28	1/0/00 1:40:00	35.09
29	1/0/00 1:50:00	35.17
30	1/0/00 2:00:00	35.24

WELL ID: SB 19-Desa Sangkanjoyo

Local ID: Sumur Bor Desa Sangkanjoyo
Date:
Time: 00:00

INPUT

Construction:		
Casing dia. (d_c)	6	Inch
Annulus dia. (d_w)	8	Inch
Screen Length (L)	21	Meter
Depths to:		
water level (DTW)	0	Meter
Top of Aquifer	78	Meter
Base of Aquifer	114	Meter
Annular Fill:		
across screen --	Gravel	
above screen --	Cement	
Aquifer Material --	Fine Sand	
FLOW RATE	2.3	liters/s

COMPUTED

Aquifer thickness = 120 Feet

Slope = 0.521797 Feet/log10

Input is consistent.

K = 6.4 Feet/Day
T = 750 Feet²/Day

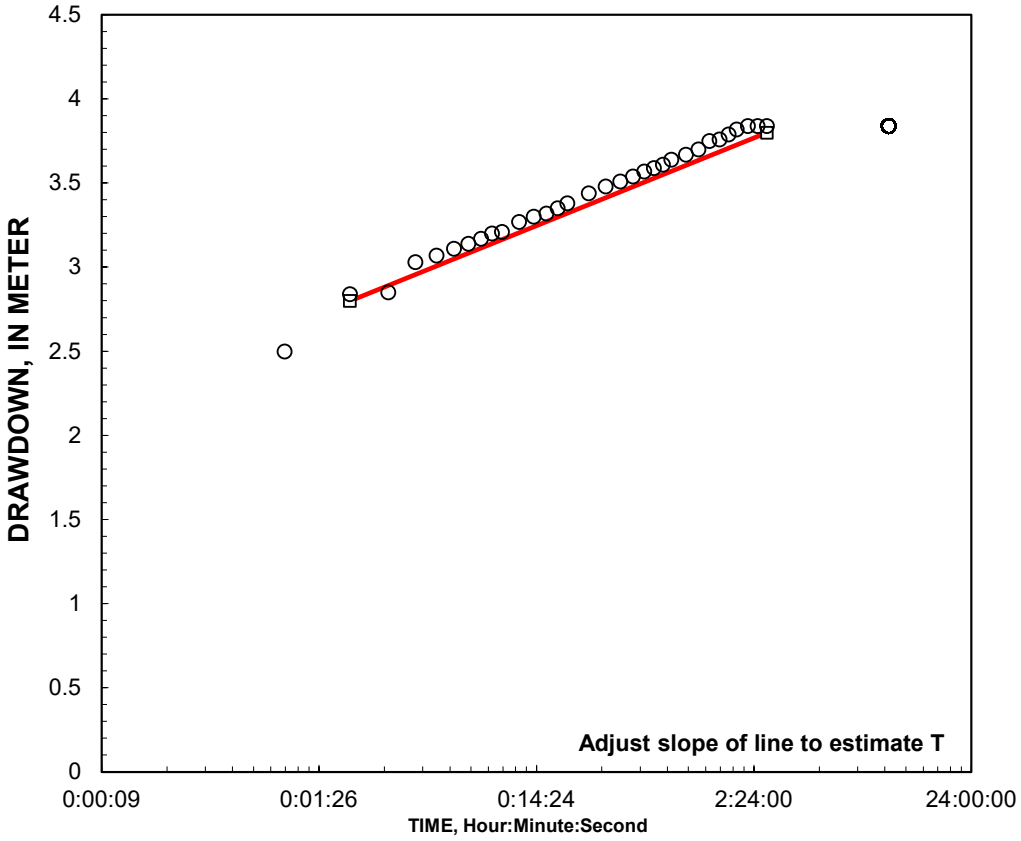

REMARKS: Cooper-Jacob analysis of single-well aquifer test

K = 12.80 m/day
T = 576 m²/day

Reduced Data

Entry	Time, Date Hr:Min:Sec	Water Level Meter
1	1/0/00 0:00:00	0.00
2	1/0/00 0:01:00	2.50
3	1/0/00 0:02:00	2.84
4	1/0/00 0:03:00	2.85
5	1/0/00 0:04:00	3.03
6	1/0/00 0:05:00	3.07
7	1/0/00 0:06:00	3.11
8	1/0/00 0:07:00	3.14
9	1/0/00 0:08:00	3.17
10	1/0/00 0:09:00	3.20
11	1/0/00 0:10:00	3.21
12	1/0/00 0:12:00	3.27
13	1/0/00 0:14:00	3.30
14	1/0/00 0:16:00	3.32
15	1/0/00 0:18:00	3.35
16	1/0/00 0:20:00	3.38
17	1/0/00 0:25:00	3.44
18	1/0/00 0:30:00	3.48
19	1/0/00 0:35:00	3.51
20	1/0/00 0:40:00	3.54
21	1/0/00 0:45:00	3.57
22	1/0/00 0:50:00	3.59
23	1/0/00 0:55:00	3.61
24	1/0/00 1:00:00	3.64
25	1/0/00 1:10:00	3.67
26	1/0/00 1:20:00	3.70
27	1/0/00 1:30:00	3.75
28	1/0/00 1:40:00	3.76
29	1/0/00 1:50:00	3.79
30	1/0/00 2:00:00	3.82
31	1/0/00 2:15:00	3.84
32	1/0/00 2:30:00	3.84
33	1/0/00 2:45:00	3.84
34	1/0/00 3:00:00	0.00
35	1/0/00 3:15:00	0.00
36	1/0/00 3:30:00	0.00
37	1/0/00 4:00:00	0.00
38	1/0/00 4:30:00	0.00
39	1/0/00 5:00:00	0.00
40	1/0/00 5:30:00	0.00
41	1/0/00 6:00:00	0.00
42	1/0/00 6:30:00	0.00
43	1/0/00 7:00:00	0.00
44	1/0/00 7:30:00	0.00
45	1/0/00 8:00:00	0.00
46	1/0/00 8:30:00	0.00
47	1/0/00 9:00:00	0.00
48	1/0/00 9:30:00	0.00

WELL ID: SB 03-Desa Serang

Local ID: Sumur Bor Desa Serang
Date:
Time: 00:00

INPUT

Construction:		
Casing dia. (d_c)	6	Inch
Annulus dia. (d_w)	8	Inch
Screen Length (L)	18	Meter
Depths to:		
water level (DTW)	2.47	Meter
Top of Aquifer	42	Meter
Base of Aquifer	123	Meter
Annular Fill:		
across screen --	Gravel	
above screen --	Cement	
Aquifer Material --	Sand and Gravel Mixe	
FLOW RATE	2.2	liters/s

COMPUTED

Aquifer thickness = 270 Feet

Slope = 0.561135 Feet/log10

Input is consistent.

K = 2.5 Feet/Day
T = 670 Feet²/Day

K= 2.5 is less than likely minimum of 30 for Sand and Gravel Mixes

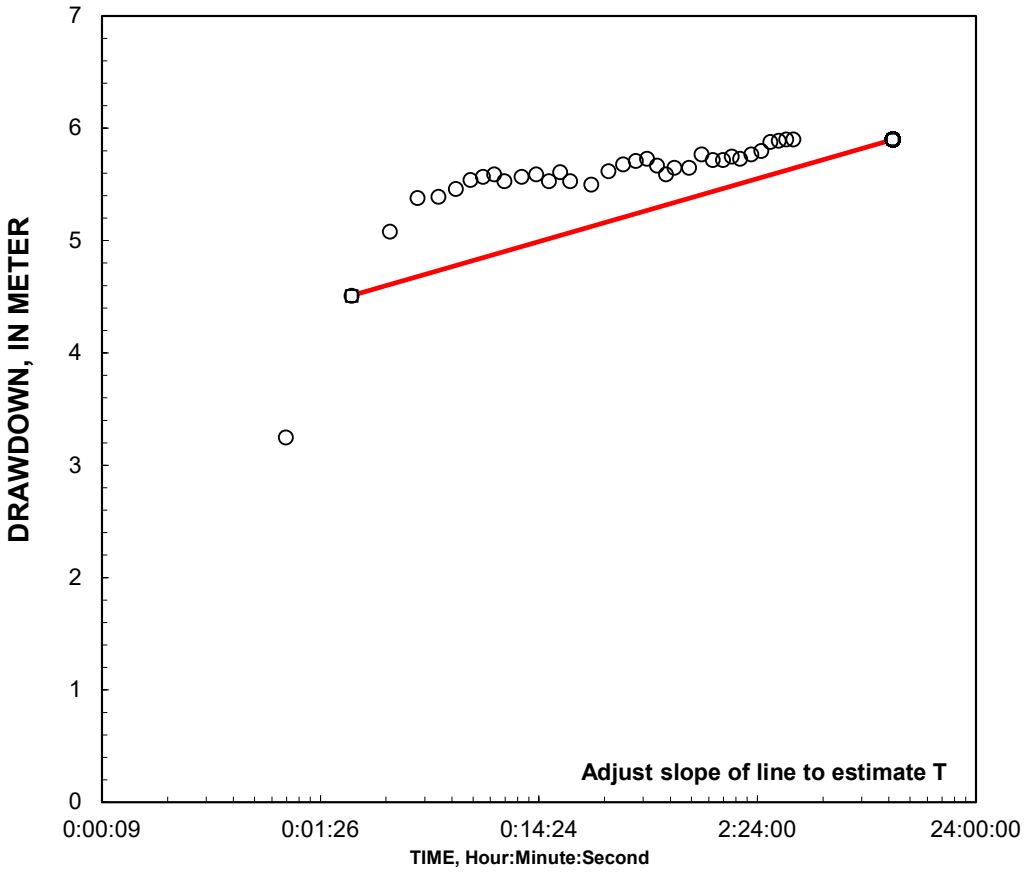

REMARKS: Cooper-Jacob analysis of single-well aquifer test

K = 12.80 m/day
T = 576 m²/day

Reduced Data

Entry	Time, Date Hr:Min:Sec	Water Level Meter
1	1/0/00 0:00:00	2.47
2	1/0/00 0:01:00	5.72
3	1/0/00 0:02:00	6.98
4	1/0/00 0:03:00	7.55
5	1/0/00 0:04:00	7.85
6	1/0/00 0:05:00	7.86
7	1/0/00 0:06:00	7.93
8	1/0/00 0:07:00	8.01
9	1/0/00 0:08:00	8.04
10	1/0/00 0:09:00	8.06
11	1/0/00 0:10:00	8.00
12	1/0/00 0:12:00	8.04
13	1/0/00 0:14:00	8.06
14	1/0/00 0:16:00	8.00
15	1/0/00 0:18:00	8.08
16	1/0/00 0:20:00	8.00
17	1/0/00 0:25:00	7.97
18	1/0/00 0:30:00	8.09
19	1/0/00 0:35:00	8.15
20	1/0/00 0:40:00	8.18
21	1/0/00 0:45:00	8.20
22	1/0/00 0:50:00	8.14
23	1/0/00 0:55:00	8.06
24	1/0/00 1:00:00	8.12
25	1/0/00 1:10:00	8.12
26	1/0/00 1:20:00	8.24
27	1/0/00 1:30:00	8.19
28	1/0/00 1:40:00	8.19
29	1/0/00 1:50:00	8.22
30	1/0/00 2:00:00	8.20
31	1/0/00 2:15:00	8.24
32	1/0/00 2:30:00	8.27
33	1/0/00 2:45:00	8.35
34	1/0/00 3:00:00	8.36
35	1/0/00 3:15:00	8.37
36	1/0/00 3:30:00	8.37
37	1/0/00 4:00:00	0.00
38	1/0/00 4:30:00	0.00
39	1/0/00 5:00:00	0.00
40	1/0/00 5:30:00	0.00
41	1/0/00 6:00:00	0.00
42	1/0/00 6:30:00	0.00
43	1/0/00 7:00:00	0.00
44	1/0/00 7:30:00	0.00
45	1/0/00 8:00:00	0.00
46	1/0/00 8:30:00	0.00
47	1/0/00 9:00:00	0.00
48	1/0/00 9:30:00	0.00

WELL ID: SB-16 SIDOKARE

Local ID: SB-16 SIDOKARE
Date: ########
Time: 00:00

INPUT

Construction:		
Casing dia. (d_c)	6	Inch
Annulus dia. (d_w)	12	Inch
Screen Length (L)	21	Meter
Depths to:		
water level (DTW)	13.98	Meter
Top of Aquifer	60	Meter
Base of Aquifer	135	Meter
Annular Fill:		
across screen --	Gravel	
above screen --	Cement	
Aquifer Material --	Fine Sand	
FLOW RATE	1.8	liters/s

COMPUTED

Aquifer thickness = 250 Feet

Slope = 11.52911 Feet/log10

Input is consistent.

K =	0.11	Feet/Day
T =	27	Feet²/Day

K= 0.11 is less than likely minimum of 3 for Fine Sand

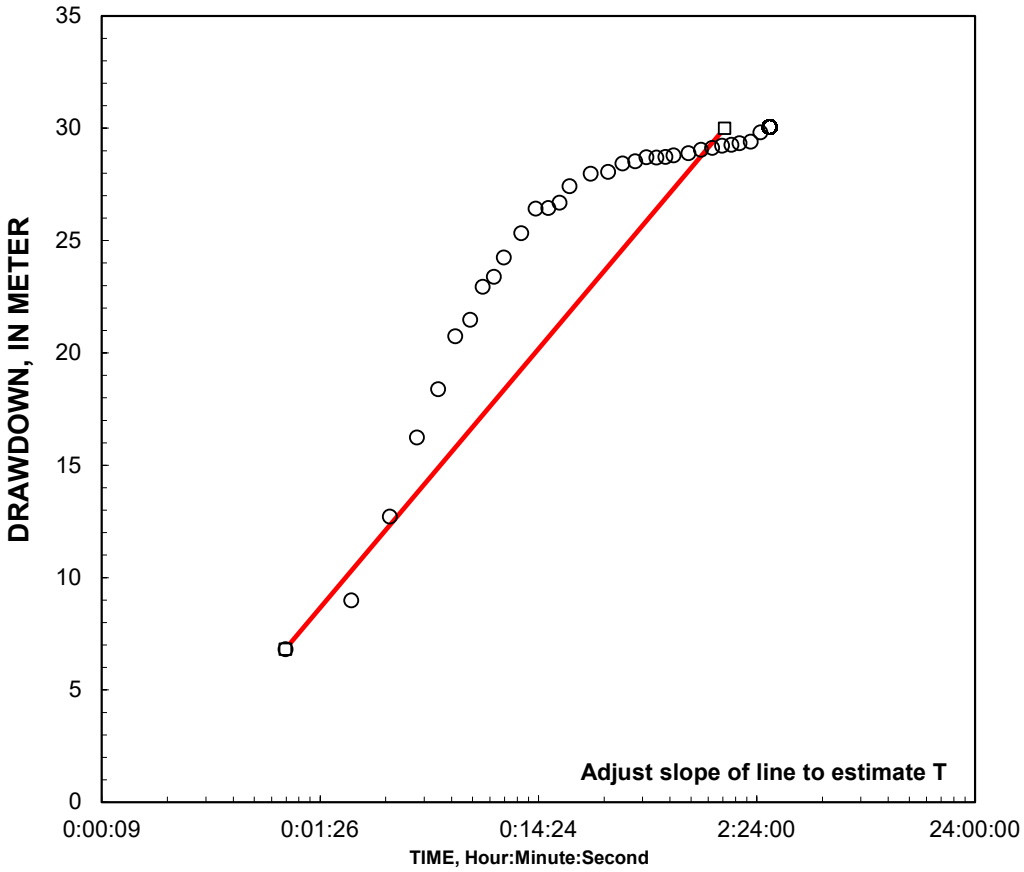

REMARKS: Cooper-Jacob analysis of single-well aquifer test

K = 12.80 m/day
T = 576 m²/day

Reduced Data

Entry	Time, Date Hr:Min:Sec	Water Level Meter
1	1/0/00 0:00:00	12.55
2	1/0/00 0:01:00	19.36
3	1/0/00 0:02:00	21.53
4	1/0/00 0:03:00	25.26
5	1/0/00 0:04:00	28.80
6	1/0/00 0:05:00	30.94
7	1/0/00 0:06:00	33.30
8	1/0/00 0:07:00	34.04
9	1/0/00 0:08:00	35.50
10	1/0/00 0:09:00	35.94
11	1/0/00 0:10:00	36.80
12	1/0/00 0:12:00	37.89
13	1/0/00 0:14:00	38.97
14	1/0/00 0:16:00	39.00
15	1/0/00 0:18:00	39.24
16	1/0/00 0:20:00	39.97
17	1/0/00 0:25:00	40.54
18	1/0/00 0:30:00	40.61
19	1/0/00 0:35:00	40.98
20	1/0/00 0:40:00	41.08
21	1/0/00 0:45:00	41.27
22	1/0/00 0:50:00	41.24
23	1/0/00 0:55:00	41.28
24	1/0/00 1:00:00	41.34
25	1/0/00 1:10:00	41.44
26	1/0/00 1:20:00	41.60
27	1/0/00 1:30:00	41.68
28	1/0/00 1:40:00	41.78
29	1/0/00 1:50:00	41.82
30	1/0/00 2:00:00	41.89
31	1/0/00 2:15:00	41.96
32	1/0/00 2:30:00	42.37

WELL ID: SB-24 SRAGI

Local ID: SB-24 SRAGI
Date: ########
Time: 00:00

INPUT

Construction:		
Casing dia. (d_c)	6	Inch
Annulus dia. (d_w)	12	Inch
Screen Length (L)	21	Meter
Depths to:		
water level (DTW)	8.2	Meter
Top of Aquifer	60	Meter
Base of Aquifer	135	Meter
Annular Fill:		
across screen --	Gravel	
above screen --	Cement	
Aquifer Material --	Fine Sand	
FLOW RATE	2.14	liters/s

COMPUTED

Aquifer thickness = 250 Feet

Slope = 0.248029 Feet/log10

Input is consistent.

K =	6	Feet/Day
T =	1500	Feet²/Day

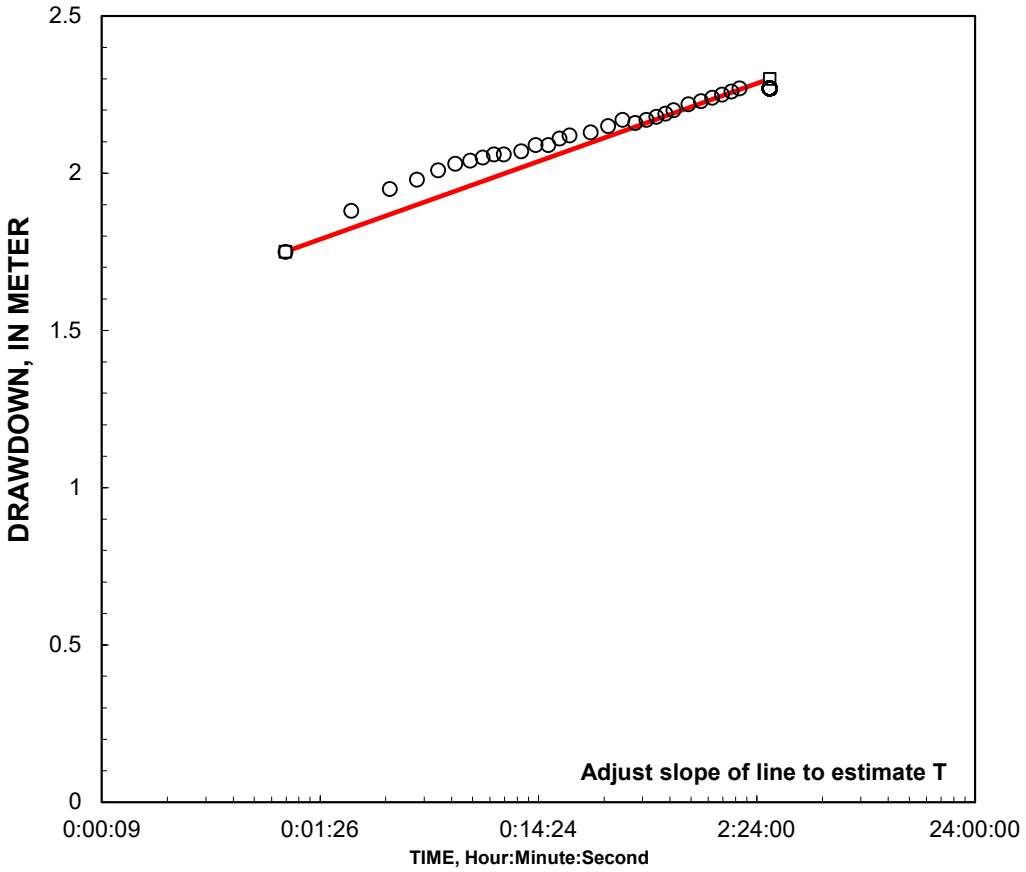

REMARKS: Cooper-Jacob analysis of single-well aquifer test

K = 12.80 m/day
T = 576 m²/day

Reduced Data

Entry	Time, Date Hr:Min:Sec	Water Level Meter
1	1/0/00 0:00:00	11.50
2	1/0/00 0:01:00	13.25
3	1/0/00 0:02:00	13.38
4	1/0/00 0:03:00	13.45
5	1/0/00 0:04:00	13.48
6	1/0/00 0:05:00	13.51
7	1/0/00 0:06:00	13.53
8	1/0/00 0:07:00	13.54
9	1/0/00 0:08:00	13.55
10	1/0/00 0:09:00	13.56
11	1/0/00 0:10:00	13.56
12	1/0/00 0:12:00	13.57
13	1/0/00 0:14:00	13.59
14	1/0/00 0:16:00	13.59
15	1/0/00 0:18:00	13.61
16	1/0/00 0:20:00	13.62
17	1/0/00 0:25:00	13.63
18	1/0/00 0:30:00	13.65
19	1/0/00 0:35:00	13.67
20	1/0/00 0:40:00	13.66
21	1/0/00 0:45:00	13.67
22	1/0/00 0:50:00	13.68
23	1/0/00 0:55:00	13.69
24	1/0/00 1:00:00	13.70
25	1/0/00 1:10:00	13.72
26	1/0/00 1:20:00	13.73
27	1/0/00 1:30:00	13.74
28	1/0/00 1:40:00	13.75
29	1/0/00 1:50:00	13.76
30	1/0/00 2:00:00	13.77
31	1/0/00 2:15:00	0.00
32	1/0/00 2:30:00	0.00

WELL ID: SB 06-Desa Sukorejo

Local ID: Sumur Bor Desa Sukorejo
Date:
Time: 00:00

INPUT

Construction:		
Casing dia. (d_c)	6	Inch
Annulus dia. (d_w)	8	Inch
Screen Length (L)	21	Meter
Depths to:		
water level (DTW)	18.03	Meter
Top of Aquifer	80	Meter
Base of Aquifer	120	Meter
Annular Fill:		
across screen --	Gravel	
above screen --	Cement	
Aquifer Material --	Fine Sand	
FLOW RATE	2.08	liters/s

COMPUTED

Aquifer thickness = 130 Feet

Slope = 1.004056 Feet/log10

Input is consistent.

K =	2.7	Feet/Day
T =	350	Feet²/Day

K= 2.7 is less than likely minimum of 3 for Fine Sand

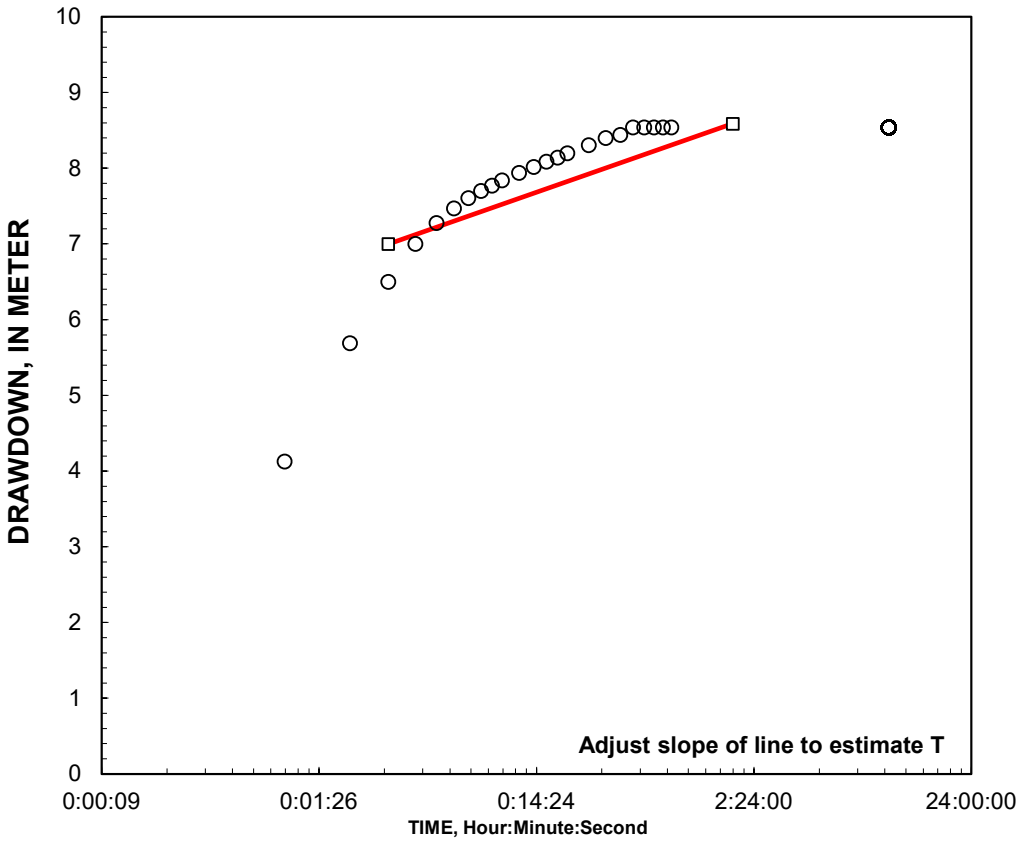

REMARKS: Cooper-Jacob analysis of single-well aquifer test

K = 12.80 m/day
T = 576 m^2/day

Reduced Data

Entry	Time, Date Hr:Min:Sec	Water Level Meter
1	1/0/00 0:00:00	18.03
2	1/0/00 0:01:00	22.16
3	1/0/00 0:02:00	23.72
4	1/0/00 0:03:00	24.53
5	1/0/00 0:04:00	25.03
6	1/0/00 0:05:00	25.31
7	1/0/00 0:06:00	25.50
8	1/0/00 0:07:00	25.64
9	1/0/00 0:08:00	25.73
10	1/0/00 0:09:00	25.80
11	1/0/00 0:10:00	25.87
12	1/0/00 0:12:00	25.97
13	1/0/00 0:14:00	26.05
14	1/0/00 0:16:00	26.12
15	1/0/00 0:18:00	26.17
16	1/0/00 0:20:00	26.23
17	1/0/00 0:25:00	26.34
18	1/0/00 0:30:00	26.43
19	1/0/00 0:35:00	26.47
20	1/0/00 0:40:00	26.57
21	1/0/00 0:45:00	26.57
22	1/0/00 0:50:00	26.57
23	1/0/00 0:55:00	26.57
24	1/0/00 1:00:00	26.57
25	1/0/00 1:10:00	0.00
26	1/0/00 1:20:00	0.00
27	1/0/00 1:30:00	0.00
28	1/0/00 1:40:00	0.00
29	1/0/00 1:50:00	0.00
30	1/0/00 2:00:00	0.00
31	1/0/00 2:15:00	0.00
32	1/0/00 2:30:00	0.00
33	1/0/00 2:45:00	0.00
34	1/0/00 3:00:00	0.00
35	1/0/00 3:15:00	0.00
36	1/0/00 3:30:00	0.00
37	1/0/00 4:00:00	0.00
38	1/0/00 4:30:00	0.00
39	1/0/00 5:00:00	0.00
40	1/0/00 5:30:00	0.00
41	1/0/00 6:00:00	0.00
42	1/0/00 6:30:00	0.00
43	1/0/00 7:00:00	0.00
44	1/0/00 7:30:00	0.00
45	1/0/00 8:00:00	0.00
46	1/0/00 8:30:00	0.00
47	1/0/00 9:00:00	0.00
48	1/0/00 9:30:00	0.00

WELL ID: SB 06-Desa Tegalsari Barat

Local ID: Sumur Bor Desa Tegalsari Bar
Date:
Time: 00:00

INPUT

Construction:		
Casing dia. (d_c)	6	Inch
Annulus dia. (d_w)	8	Inch
Screen Length (L)	21	Meter
Depths to:		
water level (DTW)	12.51	Meter
Top of Aquifer	48	Meter
Base of Aquifer	114	Meter
Annular Fill:		
across screen --	Gravel	
above screen --	Cement	
Aquifer Material --	Fine Sand	
FLOW RATE	0.45	liters/s

COMPUTED

Aquifer thickness = 220 Feet

Slope = 1.427475 Feet/log10

Input is consistent.

K =	0.25	Feet/Day
T =	54	Feet²/Day

K= 0.25 is less than likely minimum of 3 for Fine Sand

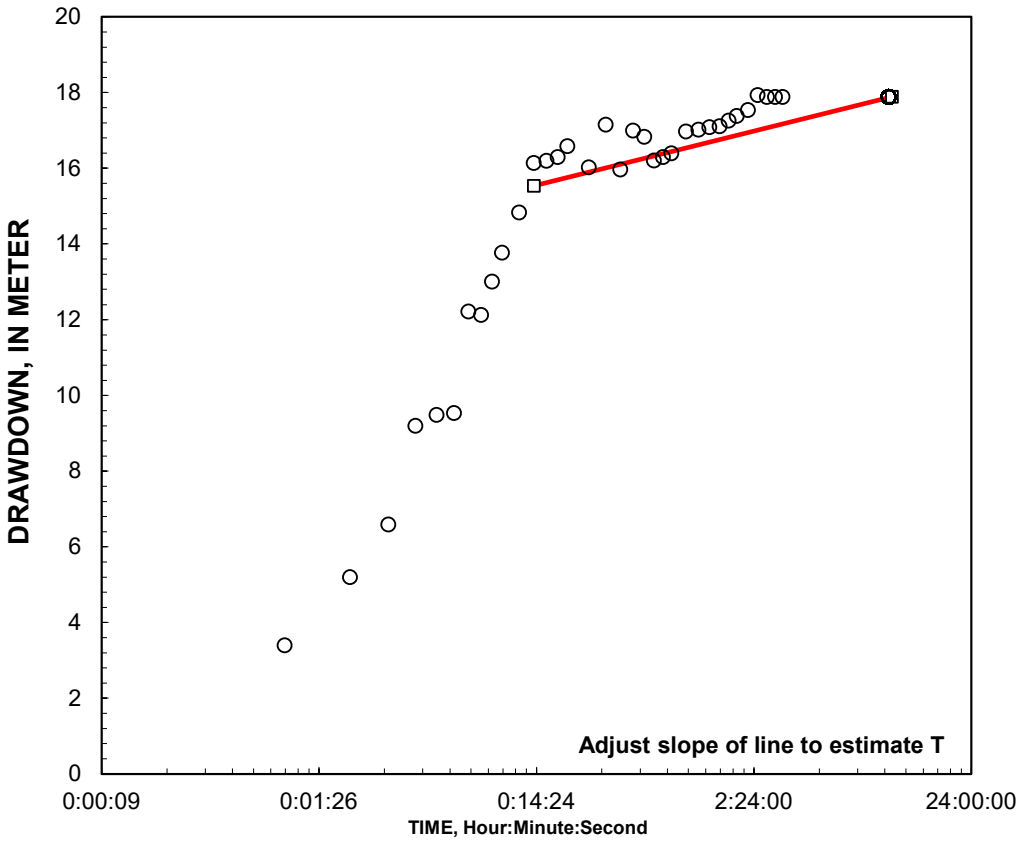

REMARKS: Cooper-Jacob analysis of single-well aquifer test

K = 12.80 m/day
T = 576 m^2/day

at Entry	Reduced Data Time, Date Hr:Min:Sec	Water Level Meter
1	1/0/00 0:00:00	12.51
2	1/0/00 0:01:00	15.91
3	1/0/00 0:02:00	17.71
4	1/0/00 0:03:00	19.10
5	1/0/00 0:04:00	21.71
6	1/0/00 0:05:00	22.00
7	1/0/00 0:06:00	22.05
8	1/0/00 0:07:00	24.73
9	1/0/00 0:08:00	24.64
10	1/0/00 0:09:00	25.52
11	1/0/00 0:10:00	26.28
12	1/0/00 0:12:00	27.35
13	1/0/00 0:14:00	28.65
14	1/0/00 0:16:00	28.71
15	1/0/00 0:18:00	28.81
16	1/0/00 0:20:00	29.10
17	1/0/00 0:25:00	28.54
18	1/0/00 0:30:00	29.67
19	1/0/00 0:35:00	28.48
20	1/0/00 0:40:00	29.51
21	1/0/00 0:45:00	29.35
22	1/0/00 0:50:00	28.72
23	1/0/00 0:55:00	28.81
24	1/0/00 1:00:00	28.91
25	1/0/00 1:10:00	29.49
26	1/0/00 1:20:00	29.53
27	1/0/00 1:30:00	29.60
28	1/0/00 1:40:00	29.62
29	1/0/00 1:50:00	29.77
30	1/0/00 2:00:00	29.90
31	1/0/00 2:15:00	30.05
32	1/0/00 2:30:00	30.45
33	1/0/00 2:45:00	30.40
34	1/0/00 3:00:00	30.40
35	1/0/00 3:15:00	30.40
36	1/0/00 3:30:00	0.00
37	1/0/00 4:00:00	0.00
38	1/0/00 4:30:00	0.00
39	1/0/00 5:00:00	0.00
40	1/0/00 5:30:00	0.00
41	1/0/00 6:00:00	0.00
42	1/0/00 6:30:00	0.00
43	1/0/00 7:00:00	0.00
44	1/0/00 7:30:00	0.00
45	1/0/00 8:00:00	0.00
46	1/0/00 8:30:00	0.00
47	1/0/00 9:00:00	0.00
48	1/0/00 9:30:00	0.00

WELL ID: SB09-TengengWetan

Local ID: SB-09 TengengWetan
Date: ########
Time: 00:00

INPUT

Construction:		
Casing dia. (d_c)	4	Inch
Annulus dia. (d_w)	6	Inch
Screen Length (L)	18	Meter
Depths to:		
water level (DTW)	16.23	Meter
Top of Aquifer	40	Meter
Base of Aquifer	110	Meter
Annular Fill:		
across screen --	Gravel	
above screen --	Cement	
Aquifer Material --	Medium Sand	
FLOW RATE	1.56	liters/s

COMPUTED

Aquifer thickness = 230 Feet

Slope = 1.139689 Feet/log10

Input is consistent.

K = 1 Feet/Day
T = 230 Feet²/Day

K= 1 is less than likely minimum of 20 for Medium Sand

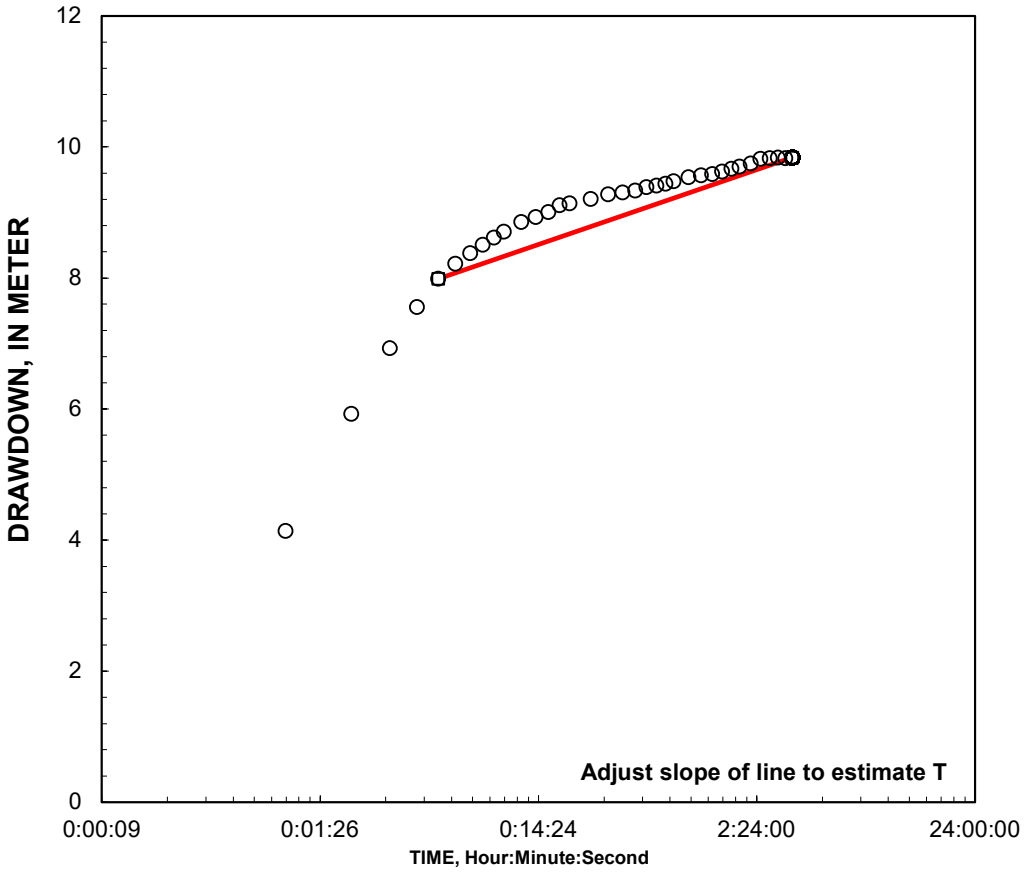

REMARKS: Cooper-Jacob analysis of single-well aquifer test

K = 12.80 m/day
T = 576 m²/day

Reduced Data

Entry	Time, Date Hr:Min:Sec	Water Level Meter
1	1/0/00 0:00:00	16.23
2	1/0/00 0:01:00	20.37
3	1/0/00 0:02:00	22.16
4	1/0/00 0:03:00	23.16
5	1/0/00 0:04:00	23.79
6	1/0/00 0:05:00	24.22
7	1/0/00 0:06:00	24.45
8	1/0/00 0:07:00	24.61
9	1/0/00 0:08:00	24.74
10	1/0/00 0:09:00	24.85
11	1/0/00 0:10:00	24.94
12	1/0/00 0:12:00	25.09
13	1/0/00 0:14:00	25.16
14	1/0/00 0:16:00	25.24
15	1/0/00 0:18:00	25.34
16	1/0/00 0:20:00	25.37
17	1/0/00 0:25:00	25.44
18	1/0/00 0:30:00	25.51
19	1/0/00 0:35:00	25.54
20	1/0/00 0:40:00	25.57
21	1/0/00 0:45:00	25.62
22	1/0/00 0:50:00	25.64
23	1/0/00 0:55:00	25.67
24	1/0/00 1:00:00	25.71
25	1/0/00 1:10:00	25.77
26	1/0/00 1:20:00	25.80
27	1/0/00 1:30:00	25.82
28	1/0/00 1:40:00	25.86
29	1/0/00 1:50:00	25.90
30	1/0/00 2:00:00	25.93
31	1/0/00 2:15:00	25.98
32	1/0/00 2:30:00	26.05
33	1/0/00 2:45:00	26.06
34	1/0/00 3:00:00	26.07
35	1/0/00 3:15:00	26.06

WELL ID: SB 02-Desa UJUNG GEDE

Local ID: Sumur Bor Desa Ujung Gede
Date:
Time: 00:00

INPUT

Construction:		
Casing dia. (d_c)	6	Inch
Annulus dia. (d_w)	8	Inch
Screen Length (L)	20	Meter
Depths to:		
water level (DTW)	2.47	Meter
Top of Aquifer	50	Meter
Base of Aquifer	120	Meter
Annular Fill:		
across screen --	Gravel	
above screen --	Cement	
Aquifer Material --	Medium Sand	
FLOW RATE	2.12	liters/s

COMPUTED

Aquifer thickness = 230 Feet

Slope = 0.508691 Feet/log10

Input is consistent.

K = 3.1 Feet/Day
T = 710 Feet²/Day

K= 3.1 is less than likely minimum of 20 for Medium Sand

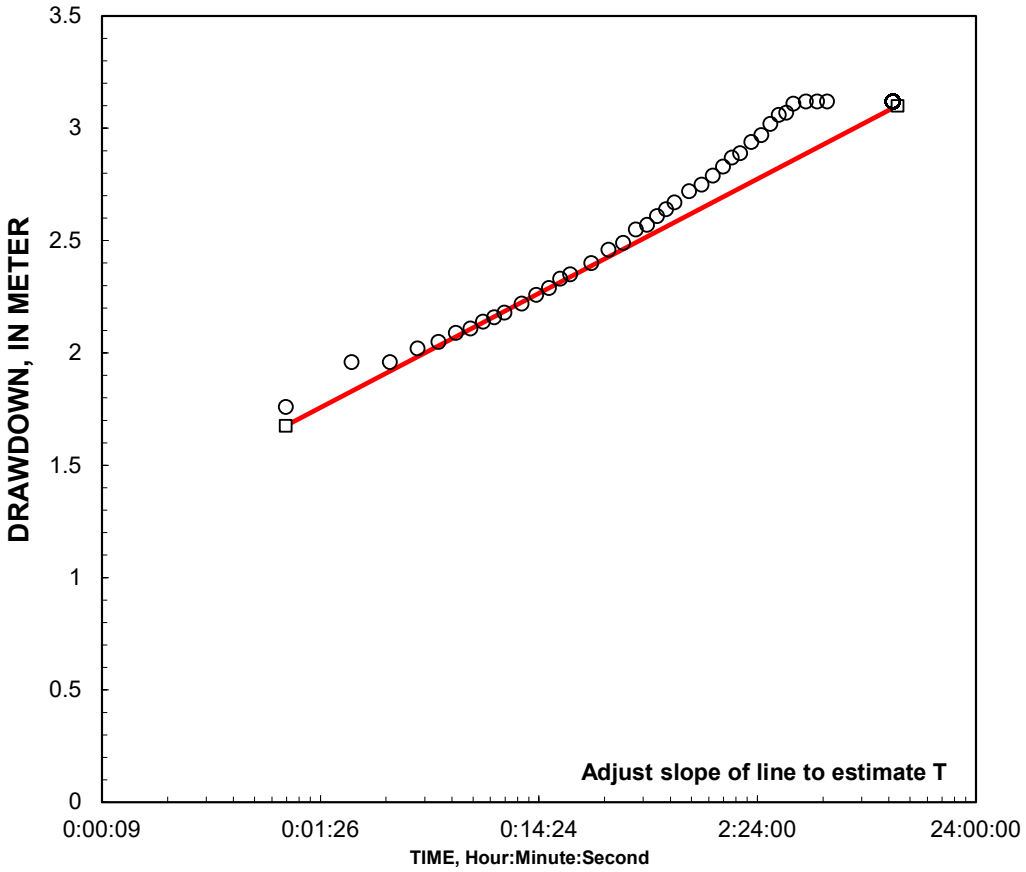

REMARKS: Cooper-Jacob analysis of single-well aquifer test

K = 12.80 m/day
T = 576 m²/day

Reduced Data

Entry	Time, Date Hr:Min:Sec	Water Level Meter
1	1/0/00 0:00:00	14.38
2	1/0/00 0:01:00	16.14
3	1/0/00 0:02:00	16.34
4	1/0/00 0:03:00	16.34
5	1/0/00 0:04:00	16.40
6	1/0/00 0:05:00	16.43
7	1/0/00 0:06:00	16.47
8	1/0/00 0:07:00	16.49
9	1/0/00 0:08:00	16.52
10	1/0/00 0:09:00	16.54
11	1/0/00 0:10:00	16.56
12	1/0/00 0:12:00	16.60
13	1/0/00 0:14:00	16.64
14	1/0/00 0:16:00	16.67
15	1/0/00 0:18:00	16.71
16	1/0/00 0:20:00	16.73
17	1/0/00 0:25:00	16.78
18	1/0/00 0:30:00	16.84
19	1/0/00 0:35:00	16.87
20	1/0/00 0:40:00	16.93
21	1/0/00 0:45:00	16.95
22	1/0/00 0:50:00	16.99
23	1/0/00 0:55:00	17.02
24	1/0/00 1:00:00	17.05
25	1/0/00 1:10:00	17.10
26	1/0/00 1:20:00	17.13
27	1/0/00 1:30:00	17.17
28	1/0/00 1:40:00	17.21
29	1/0/00 1:50:00	17.25
30	1/0/00 2:00:00	17.27
31	1/0/00 2:15:00	17.32
32	1/0/00 2:30:00	17.35
33	1/0/00 2:45:00	17.40
34	1/0/00 3:00:00	17.44
35	1/0/00 3:15:00	17.45
36	1/0/00 3:30:00	17.49
37	1/0/00 4:00:00	17.50
38	1/0/00 4:30:00	17.50
39	1/0/00 5:00:00	17.50
40	1/0/00 5:30:00	0.00
41	1/0/00 6:00:00	0.00
42	1/0/00 6:30:00	0.00
43	1/0/00 7:00:00	0.00
44	1/0/00 7:30:00	0.00
45	1/0/00 8:00:00	0.00
46	1/0/00 8:30:00	0.00
47	1/0/00 9:00:00	0.00
48	1/0/00 9:30:00	0.00

WELL ID: SB 22-Desa Wonosari

Local ID: Sumur Bor Desa Wonosari
Date:
Time: 00:00

INPUT

Construction:		
Casing dia. (d_c)	6	Inch
Annulus dia. (d_w)	8	Inch
Screen Length (L)	21	Meter
Depths to:		
water level (DTW)	7.62	Meter
Top of Aquifer	70	Meter
Base of Aquifer	118	Meter
Annular Fill:		
across screen --	Gravel	
above screen --	Cement	
Aquifer Material --	Medium Sand	
FLOW RATE	2.07	liters/s

COMPUTED

Aquifer thickness = 160 Feet

Slope = 1.289016 Feet/log10

Input is consistent.

K = 1.7 Feet/Day
T = 270 Feet²/Day

K= 1.7 is less than likely minimum of 20 for Medium Sand

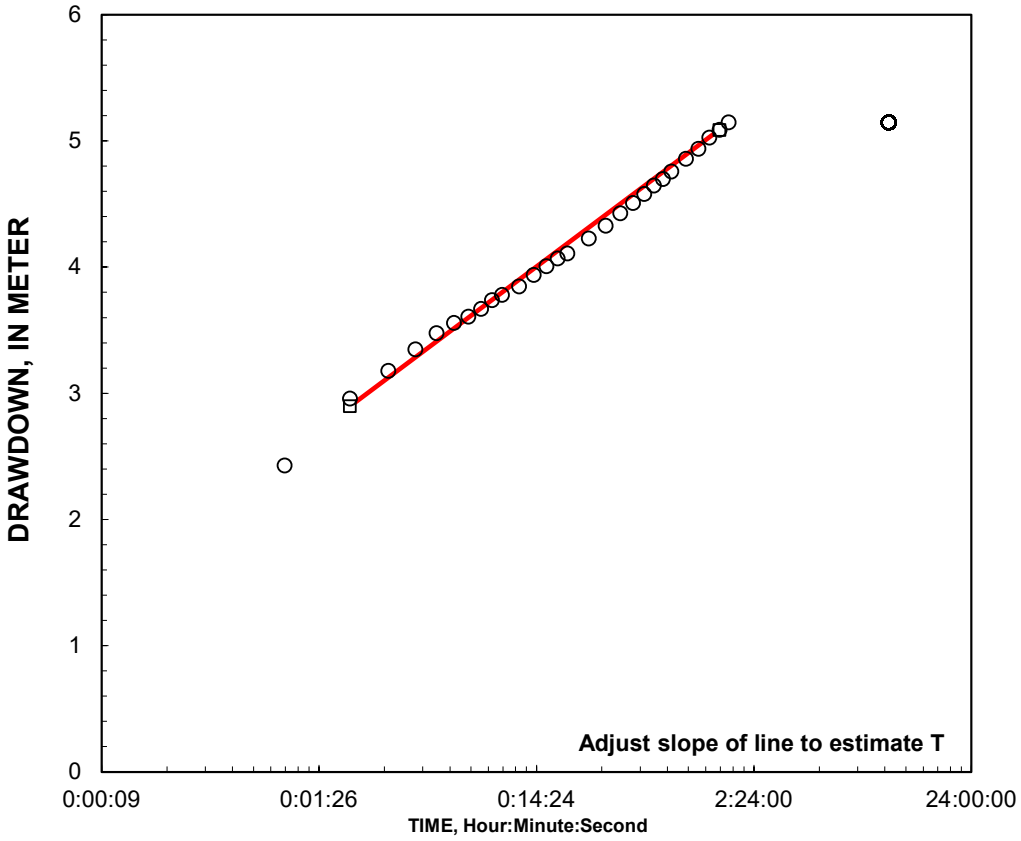

REMARKS: Cooper-Jacob analysis of single-well aquifer test

K = 12.80 m/day
T = 576 m²/day

Reduced Data

Entry	Time, Date Hr:Min:Sec	Water Level Meter
1	1/0/00 0:00:00	7.62
2	1/0/00 0:01:00	10.05
3	1/0/00 0:02:00	10.58
4	1/0/00 0:03:00	10.80
5	1/0/00 0:04:00	10.97
6	1/0/00 0:05:00	11.10
7	1/0/00 0:06:00	11.18
8	1/0/00 0:07:00	11.23
9	1/0/00 0:08:00	11.29
10	1/0/00 0:09:00	11.36
11	1/0/00 0:10:00	11.40
12	1/0/00 0:12:00	11.47
13	1/0/00 0:14:00	11.56
14	1/0/00 0:16:00	11.63
15	1/0/00 0:18:00	11.69
16	1/0/00 0:20:00	11.73
17	1/0/00 0:25:00	11.85
18	1/0/00 0:30:00	11.95
19	1/0/00 0:35:00	12.05
20	1/0/00 0:40:00	12.13
21	1/0/00 0:45:00	12.20
22	1/0/00 0:50:00	12.27
23	1/0/00 0:55:00	12.32
24	1/0/00 1:00:00	12.38
25	1/0/00 1:10:00	12.48
26	1/0/00 1:20:00	12.56
27	1/0/00 1:30:00	12.65
28	1/0/00 1:40:00	12.71
29	1/0/00 1:50:00	12.77
30	1/0/00 2:00:00	0.00
31	1/0/00 2:15:00	0.00
32	1/0/00 2:30:00	0.00
33	1/0/00 2:45:00	0.00
34	1/0/00 3:00:00	0.00
35	1/0/00 3:15:00	0.00
36	1/0/00 3:30:00	0.00
37	1/0/00 4:00:00	0.00
38	1/0/00 4:30:00	0.00
39	1/0/00 5:00:00	0.00
40	1/0/00 5:30:00	0.00
41	1/0/00 6:00:00	0.00
42	1/0/00 6:30:00	0.00
43	1/0/00 7:00:00	0.00
44	1/0/00 7:30:00	0.00
45	1/0/00 8:00:00	0.00
46	1/0/00 8:30:00	0.00
47	1/0/00 9:00:00	0.00
48	1/0/00 9:30:00	0.00

Appendix 3

It includes the consolidation test results using ASTM D 2435 standard from geotechnical drilling samples collected in the study area.

LABORATORIUM MEKANIKA TANAH
PT. SUWANDA KARYA MANDIRI
Komp. Bumi Asri Mekar Rahayu Blok II No. B-7, Kopo Bandung (40218)
Telp. (022 - 5417700) Fax. (022 - 5412700)
email : pt_suwanda_karya_mandiri@yahoo.com

LSSM-045-IDN

CONSOLIDATION

ASTM D 2435

PROJECT : **Pembangunan Stasiun Pengamatan Permukaan Tanah**
BORING NO. : **SPPT-02**
DEPTH : **7.00 - 7.50 m**

TESTED BY : Faizal
DATE : 17/09/2021

LOCATION : **Kel. Degayu, Kec. Pekalongan Utara, Kota Pekalongan**
DESCRIPT. : **-**

APPARATUS MEASUREMENTS
CONTAINER HEIGHT : 2.000 cm
CONTAINER DIAMETER : 5.000 cm
CONTAINER AREA (A) : 19.635 cm2

SPECIFIC GRAVITY (Gs) : 2.6664
SOLIDS HEIGHT (Hs) IN cm : 0.974
Hs = Ws/(Gs.γ_w. A)

DEGREE OF SATURATION IN %
TEST START : 114.61
TEST END :

WATER CONTENT

	BEGINNING OF TEST			
CONTAINER NO.	3B			
WT. CONTAINER + WET SOIL IN g	137.950			
WT. CONTAINER IN g	63.870			
WT. WET SOIL IN g	74.080			
WT. DRY SOIL (Ws) IN g	50.990			
WT. WATER (Ww) IN g	23.09			
WATER CONTENT (w) IN %	45.28			

APPLIED PRESSURE kg/cm^2	FINAL DIAL cm	DIAL CHANGE (ΔH) cm	Δe = ΔH/Hs	e = eo - ΣΔe	AVERAGE HEIGHT FOR LOAD cm	H cm	FITTING TIME (t 90) sec	Cv $\frac{0.848\ H^2}{t\ 90}$ cm^2/sec
0.00	0.9000			1.054	2.000			
		0.0340	0.0349			0.992	179.57	0.00464
0.25	0.8660			1.019	1.966			
		0.0200	0.0205			0.978	285.14	0.00284
0.50	0.8460			0.998	1.946			
		0.0260	0.0267			0.967	357.22	0.00222
1.00	0.8200			0.971	1.920			
		0.0380	0.0390			0.951	415.01	0.00185
2.00	0.7820			0.932	1.882			
		0.0470	0.0483			0.929	450.46	0.00163
4.00	0.7350			0.884	1.835			
		0.0710	0.0729			0.900	443.90	0.00155
8.00	0.6640			0.811	1.764			
		0.0140	0.0144			0.886		
2.00	0.6780			0.826	1.778			
		0.0120	0.0123			0.892		
0.50	0.6900			0.838	1.790			

LABORATORIUM MEKANIKA TANAH
PT. SUWANDA KARYA MANDIRI
Komp. Bumi Asri Mekar Rahayu Blok II No. B-7, Kopo Bandung (40218)
Telp. (022 - 5417700) Fax. (022 - 5412700)
email : pt_suwanda_karya_mandiri@yahoo.com

LSSM-045-IDN

CONSOLIDATION

ASTM D 2435

PROJECT	: Pembangunan Stasiun Pengamatan Permukaan Tanah			
LOCATION	: Kel. Degayu, Kec. Pekalongan Utara, Kota Pekalongan			
BORING NO.	: SPPT-02	Coefficient of Consolidation (Cv)	: 0.00181	cm^2/sec
DEPTH	: 7.00 - 7.50 m	Compression Index (Cc)	: 0.242	
TESTED BY	: Faizal	Swell Index (Cs)	: 0.018	
DATE	: 17/09/2021	Coeff. of Volume Comp. (mv)	: 0.030	cm^2/kg
DESCRIPTION	: -			

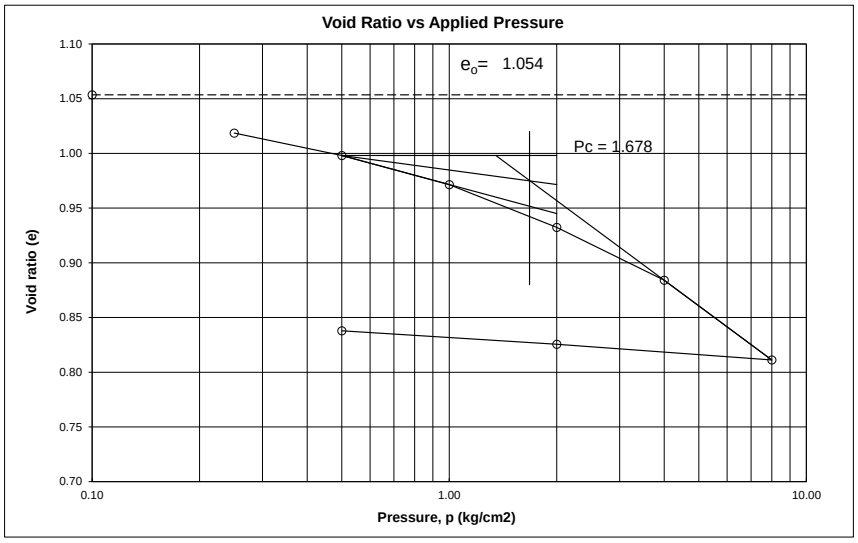

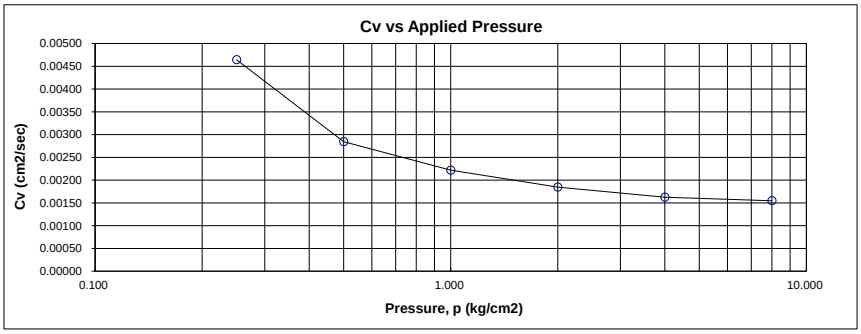

LABORATORIUM MEKANIKA TANAH
PT. SUWANDA KARYA MANDIRI
Komp. Bumi Asri Makar Rahayu Blok II No. B-7, Kopo Bandung (40218)
Telp. (022 - 5417700) Fax. (022 - 5412700)
email : pt_suwanda_karya_mandiri@yahoo.com

LSSM-045-IDN

CONSOLIDATION

ASTM D 2435

PROJECT : **Pembangunan Stasiun Pengamatan Permukaan Tanah**
BORING NO. : **SPPT-02**
DEPTH : **13.00 - 13.50 m**

TESTED BY : Faizal
DATE : 17/09/2021

LOCATION : **Kel. Degayu, Kec. Pekalongan Utara, Kota Pekalongan**
DESCRIPT. : **-**

APPARATUS MEASUREMENTS
CONTAINER HEIGHT : 2.000 cm
CONTAINER DIAMETER : 5.000 cm
CONTAINER AREA (A) : 19.635 cm2

SPECIFIC GRAVITY (Gs) : 2.6049

SOLIDS HEIGHT (Hs) IN cm : 0.944
Hs = Ws/(Gs.γ_w. A)

DEGREE OF SATURATION IN %
TEST START : 107.83
TEST END :

WATER CONTENT

	BEGINNING OF TEST		END OF TEST	
CONTAINER NO.	4B			
WT. CONTAINER + WET SOIL IN g	128.320			
WT. CONTAINER IN g	57.670			
WT. WET SOIL IN g	70.650			
WT. DRY SOIL (Ws) IN g	48.300			
WT. WATER (Ww) IN g	22.35			
WATER CONTENT (w) IN %	46.27			

APPLIED PRESSURE kg/cm^2	FINAL DIAL cm	DIAL CHANGE (ΔH) cm	Δe = ΔH/Hs	e = eo - ΣΔe	AVERAGE HEIGHT FOR LOAD cm	H cm	FITTING TIME (t 90) sec	Cv $\frac{0.848\ H^2}{t\ 90}$ cm^2/sec
0.00	0.9000			1.118	2.000			
		0.0940	0.0995			0.977	179.57	0.00450
0.25	0.8060			1.018	1.906			
		0.0450	0.0477			0.942	264.60	0.00284
0.50	0.7610			0.971	1.861			
		0.0530	0.0561			0.917	328.54	0.00217
1.00	0.7080			0.915	1.808			
		0.0650	0.0688			0.888	363.10	0.00184
2.00	0.6430			0.846	1.743			
		0.0680	0.0720			0.855	390.15	0.00159
4.00	0.5750			0.774	1.675			
		0.0850	0.0900			0.816	381.02	0.00148
8.00	0.4900			0.684	1.590			
		0.0180	0.0191			0.800		
2.00	0.5080			0.703	1.608			
		0.0270	0.0286			0.811		
0.50	0.5350			0.731	1.635			

LABORATORIUM MEKANIKA TANAH
PT. SUWANDA KARYA MANDIRI
Komp. Bumi Asri Mekar Rahayu Blok II No. B-7, Kopo Bandung (40218)
Telp. (022 - 5417706) Fax. (022 - 5412706)
email : pt_suwanda_karya_mandiri@yahoo.com

KAN Komite Akreditasi Nasional LSSM-045-IDN

CONSOLIDATION

ASTM D 2435

PROJECT	: Pembangunan Stasiun Pengamatan Permukaan Tanah			
LOCATION	: Kel. Degayu, Kec. Pekalongan Utara, Kota Pekalongan			
BORING NO.	: SPPT-02	Coefficient of Consolidation (Cv)	: 0.00177	cm^2/sec
DEPTH	: 13.00 - 13.50 m	Compression Index (Cc)	: 0.299	
TESTED BY	: Faizal	Swell Index (Cs)	: 0.032	
DATE	: 17/09/2021	Coeff. of Volume Comp. (mv)	: 0.068	cm^2/kg
DESCRIPTION	: -			

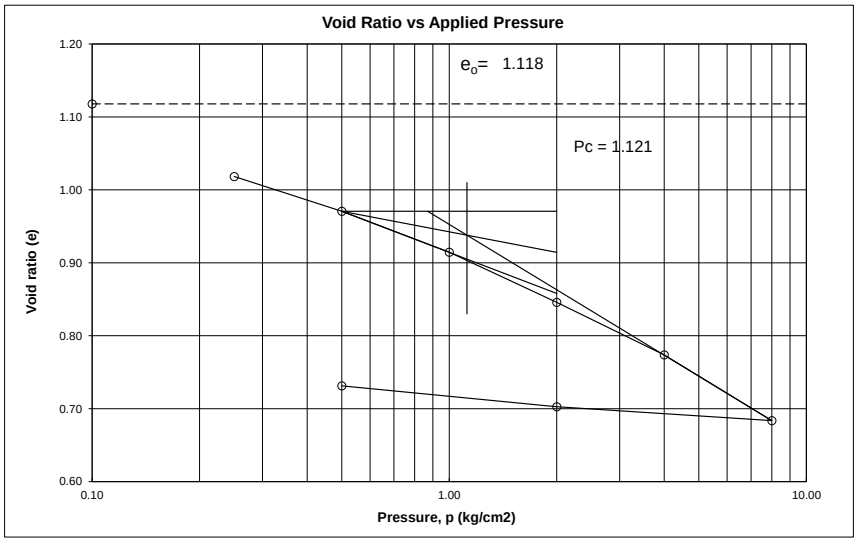

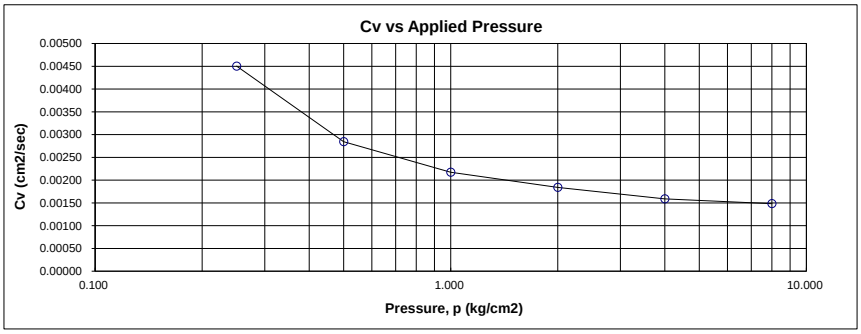

LABORATORIUM MEKANIKA TANAH
PT. SUWANDA KARYA MANDIRI
Komp. Bumi Asri Makar Rahayu Blok II No. B-7, Kopo Bandung (40218)
Telp. (022 - 5417700) Fax. (022 - 5412700)
email : pt_suwanda_karya_mandiri@yahoo.com

LSSM-045-IDN

CONSOLIDATION

ASTM D 2435

PROJECT : **Pembangunan Stasiun Pengamatan Permukaan Tanah**
BORING NO. : **SPPT-02**
DEPTH : **23.00 - 23.50 m**

TESTED BY : Faizal
DATE : 17/09/2021

LOCATION : **Kel. Degayu, Kec. Pekalongan Utara, Kota Pekalongan**
DESCRIPT. : **-**

APPARATUS MEASUREMENTS
CONTAINER HEIGHT : 2.000 cm
CONTAINER DIAMETER : 5.000 cm
CONTAINER AREA (A) : 19.635 cm2

SPECIFIC GRAVITY (Gs) : 2.5661

SOLIDS HEIGHT (Hs) IN cm : 0.718
Hs = Ws/(Gs.γ_w. A)

DEGREE OF SATURATION IN %
TEST START : 107.89
TEST END :

WATER CONTENT

	BEGINNING OF TEST			
CONTAINER NO.	1D			
WT. CONTAINER + WET SOIL IN g	129.130			
WT. CONTAINER IN g	65.800			
WT. WET SOIL IN g	63.330			
WT. DRY SOIL (Ws) IN g	36.170			
WT. WATER (Ww) IN g	27.16			
WATER CONTENT (w) IN %	75.09			

APPLIED PRESSURE kg/cm^2	FINAL DIAL cm	DIAL CHANGE (ΔH) cm	Δe = ΔH/Hs	e = eo - ΣΔe	AVERAGE HEIGHT FOR LOAD cm	H cm	FITTING TIME (t 90) sec	Cv $\frac{0.848\ H^2}{t\ 90}$ cm^2/sec
0.00	0.9000			1.786	2.000			
		0.1000	0.1393			0.975	483.94	0.00167
0.25	0.8000			1.647	1.900			
		0.0750	0.1045			0.931	697.69	0.00105
0.50	0.7250			1.542	1.825			
		0.1010	0.1407			0.887	821.40	0.00081
1.00	0.6240			1.402	1.724			
		0.1270	0.1769			0.830	907.93	0.00064
2.00	0.4970			1.225	1.597			
		0.1270	0.1769			0.767	950.42	0.00052
4.00	0.3700			1.048	1.470			
		0.1400	0.1950			0.700	912.60	0.00046
8.00	0.2300			0.853	1.330			
		0.0460	0.0641			0.677		
2.00	0.2760			0.917	1.376			
		0.0640	0.0892			0.704		
0.50	0.3400			1.006	1.440			

LABORATORIUM MEKANIKA TANAH
PT. SUWANDA KARYA MANDIRI
Komp. Bumi Asri Mekar Rahayu Blok II No. B-7, Kopo Bandung (40218)
Telp. (022 - 5417700) Fax. (022 - 5412700)
email : pt_suwanda_karya_mandiri@yahoo.com

CONSOLIDATION

ASTM D 2435

PROJECT	: Pembangunan Stasiun Pengamatan Permukaan Tanah			
LOCATION	: Kel. Degayu, Kec. Pekalongan Utara, Kota Pekalongan			
BORING NO.	: SPPT-02	Coefficient of Consolidation (Cv)	: 0.00061	cm^2/sec
DEPTH	: 23.00 - 23.50 m	Compression Index (Cc)	: 0.648	
TESTED BY	: Faizal	Swell Index (Cs)	: 0.102	
DATE	: 17/09/2021	Coeff. of Volume Comp. (mv)	: 0.101	cm^2/kg
DESCRIPTION	: -			

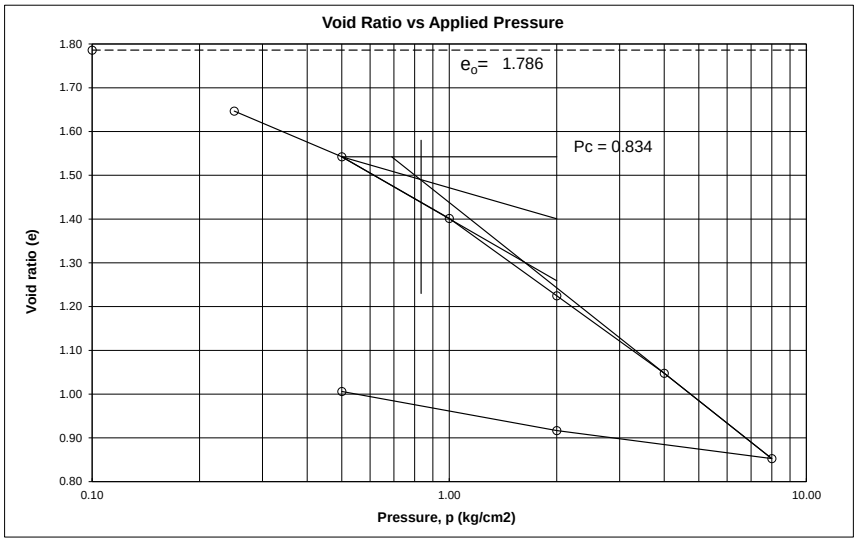

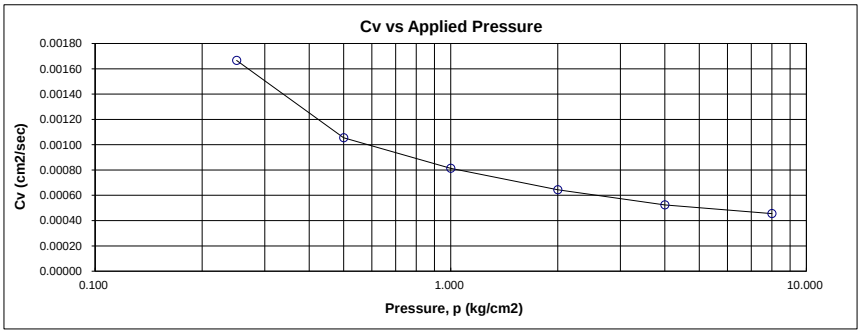

LABORATORIUM MEKANIKA TANAH
PT. SUWANDA KARYA MANDIRI
Komp. Bumi Asri Makar Rahayu Blok II No. B-7, Kopo Bandung (40218)
Telp. (022 - 5417700) Fax. (022 - 5412700)
email : pt_suwanda_karya_mandiri@yahoo.com

KAN Komite Akreditasi Nasional LSSM-045-IDN

CONSOLIDATION

ASTM D 2435

PROJECT : **Pembangunan Stasiun Pengamatan Permukaan Tanah**
BORING NO. : **SPPT-02**
DEPTH : **31.00 - 31.50 m**

TESTED BY : Faizal
DATE : 17/09/2021

LOCATION : **Kel. Degayu, Kec. Pekalongan Utara, Kota Pekalongan**
DESCRIPT. : **-**

APPARATUS MEASUREMENTS
CONTAINER HEIGHT : 2.000 cm
CONTAINER DIAMETER : 5.000 cm
CONTAINER AREA (A) : 19.635 cm2

SPECIFIC GRAVITY (Gs) : 2.6148

SOLIDS HEIGHT (Hs) IN cm : 0.942
Hs = Ws/(Gs.γ_w. A)

DEGREE OF SATURATION IN %
TEST START : 138.30
TEST END :

WATER CONTENT

	BEGINNING OF TEST			
CONTAINER NO.	2D			
WT. CONTAINER + WET SOIL IN g	134.140			
WT. CONTAINER IN g	57.040			
WT. WET SOIL IN g	77.100			
WT. DRY SOIL (Ws) IN g	48.378			
WT. WATER (Ww) IN g	28.72			
WATER CONTENT (w) IN %	59.37			

APPLIED PRESSURE kg/cm^2	FINAL DIAL cm	DIAL CHANGE (ΔH) cm	Δe = ΔH/Hs	e = eo - ΣΔe	AVERAGE HEIGHT FOR LOAD cm	H cm	FITTING TIME (t 90) sec	Cv $\frac{0.848\ H^2}{t\ 90}$ cm^2/sec
0.00	0.9000			1.123	2.000			
		0.1590	0.1687			0.960	328.54	0.00238
0.25	0.7410			0.954	1.841			
		0.0600	0.0637			0.906	470.40	0.00148
0.50	0.6810			0.890	1.781			
		0.0790	0.0838			0.871	554.50	0.00116
1.00	0.6020			0.806	1.702			
		0.0930	0.0987			0.828	610.57	0.00095
2.00	0.5090			0.708	1.609			
		0.0890	0.0945			0.782	637.66	0.00081
4.00	0.4200			0.613	1.520			
		0.1210	0.1284			0.730	606.74	0.00074
8.00	0.2990			0.485	1.399			
		0.0220	0.0233			0.705		
2.00	0.3210			0.508	1.421			
		0.0360	0.0382			0.720		
0.50	0.3570			0.546	1.457			

LABORATORIUM MEKANIKA TANAH
PT. SUWANDA KARYA MANDIRI
Komp. Bumi Asri Mekar Rahayu Blok II No. B-7, Kopo Bandung (40218)
Telp. (022 - 5417706) Fax. (022 - 5412706)
email : pt_suwanda_karya_mandiri@yahoo.com

CONSOLIDATION

ASTM D 2435

PROJECT	: Pembangunan Stasiun Pengamatan Permukaan Tanah			
LOCATION	: Kel. Degayu, Kec. Pekalongan Utara, Kota Pekalongan			
BORING NO.	: SPPT-02	Coefficient of Consolidation (Cv)	: 0.00092	cm^2/sec
DEPTH	: 31.00 - 31.50 m	Compression Index (Cc)	: 0.427	
TESTED BY	: Faizal	Swell Index (Cs)	: 0.041	
DATE	: 17/09/2021	Coeff. of Volume Comp. (mv)	: 0.107	cm^2/kg
DESCRIPTION	: -			

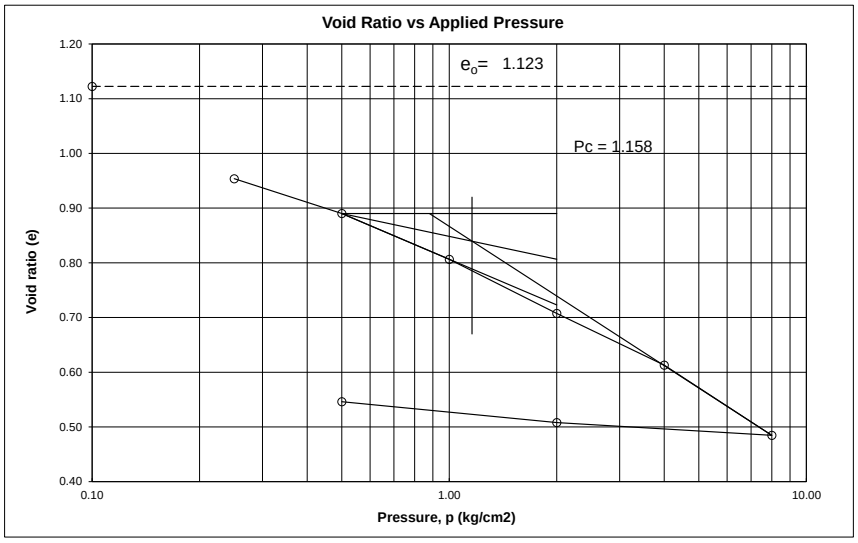

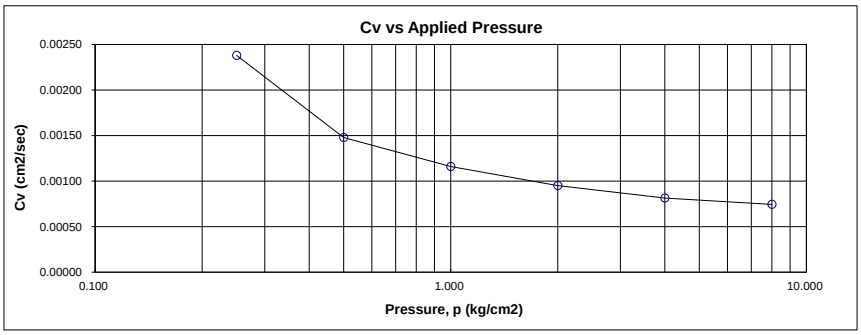

LABORATORIUM MEKANIKA TANAH
PT. SUWANDA KARYA MANDIRI
Komp. Bumi Asri Mekar Rahayu Blok II No. B-7, Kopo Bandung (40218)
Telp. (022 - 5417700) Fax. (022 - 5412700)
email : pt_suwanda_karya_mandiri@yahoo.com

KAN Komite Akreditasi Nasional LSSM-045-IDN

CONSOLIDATION

ASTM D 2435

PROJECT : **Pembangunan Stasiun Pengamatan Permukaan Tanah**
BORING NO. : **SPPT-05**
DEPTH : **3.00 - 3.55 m**

TESTED BY : Faizal
DATE : 27/08/2021

LOCATION : **Desa Depok, Kec. Siwalan, Kab. Pekalongan**
DESCRIPT. : **-**

APPARATUS MEASUREMENTS
CONTAINER HEIGHT : 2.000 cm
CONTAINER DIAMETER : 5.000 cm
CONTAINER AREA (A) : 19.635 cm2

SPECIFIC GRAVITY (Gs) : 2.6241
SOLIDS HEIGHT (Hs) IN cm : 0.696
Hs = Ws/(Gs.γ_w. A)

DEGREE OF SATURATION IN %
TEST START : 76.10
TEST END :

WATER CONTENT

	BEGINNING OF TEST		END OF TEST	
CONTAINER NO.	1B			
WT. CONTAINER + WET SOIL IN g	118.620			
WT. CONTAINER IN g	63.290			
WT. WET SOIL IN g	55.330			
WT. DRY SOIL (Ws) IN g	35.838			
WT. WATER (Ww) IN g	19.49			
WATER CONTENT (w) IN %	54.39			

APPLIED PRESSURE kg/cm^2	FINAL DIAL cm	DIAL CHANGE (ΔH) cm	Δe = ΔH/Hs	e = eo - ΣΔe	AVERAGE HEIGHT FOR LOAD cm	H cm	FITTING TIME (t 90) sec	Cv $\frac{0.848\ H^2}{t\ 90}$ cm^2/sec
0.00	0.9000			1.875	2.000			
		0.1122	0.1613			0.972	247.25	0.00324
0.25	0.7878			1.714	1.888			
		0.0598	0.0860			0.929	369.02	0.00198
0.50	0.7280			1.628	1.828			
		0.0890	0.1280			0.892	443.90	0.00152
1.00	0.6390			1.500	1.739			
		0.0950	0.1366			0.846	501.13	0.00121
2.00	0.5440			1.364	1.644			
		0.1070	0.1538			0.795	543.61	0.00099
4.00	0.4370			1.210	1.537			
		0.1160	0.1668			0.740	518.62	0.00089
8.00	0.3210			1.043	1.421			
		0.0430	0.0618			0.721		
2.00	0.3640			1.105	1.464			
		0.0450	0.0647			0.743		
0.50	0.4090			1.170	1.509			

LABORATORIUM MEKANIKA TANAH
PT. SUWANDA KARYA MANDIRI
Komp. Bumi Asri Mekar Rahayu Blok II No. B-7, Kopo Bandung (40218)
Telp. (022 - 5417706) Fax. (022 - 5412706)
email : pt_suwanda_karya_mandiri@yahoo.com

KAN Komite Akreditasi Nasional LSSM-045-IDN

CONSOLIDATION

ASTM D 2435

PROJECT	: Pembangunan Stasiun Pengamatan Permukaan Tanah			
LOCATION	: Desa Depok, Kec. Siwalan, Kab. Pekalongan			
BORING NO.	: SPPT-05	Coefficient of Consolidation (Cv)	: 0.00115	cm^2/sec
DEPTH	: 3.00 - 3.55 m	Compression Index (Cc)	: 0.554	
TESTED BY	: Faizal	Swell Index (Cs)	: 0.084	
DATE	: 27/08/2021	Coeff. of Volume Comp. (mv)	: 0.092	cm^2/kg
DESCRIPTION	: -			

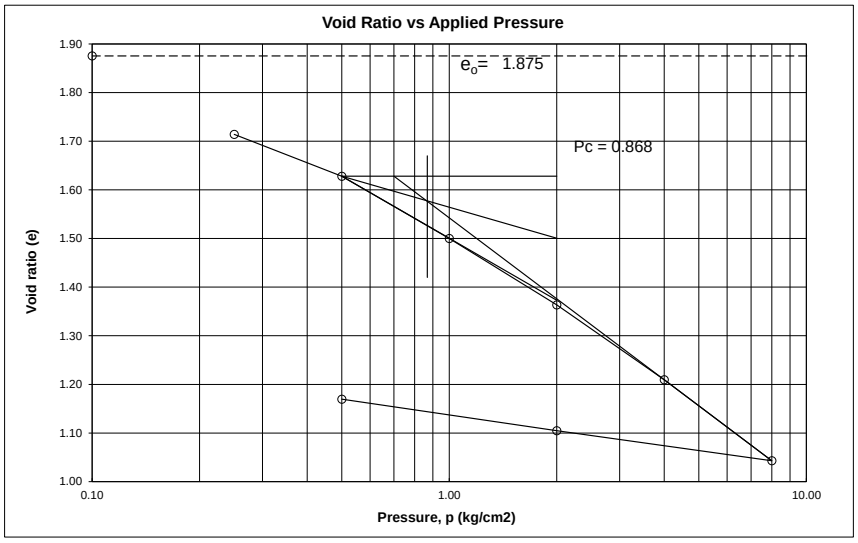

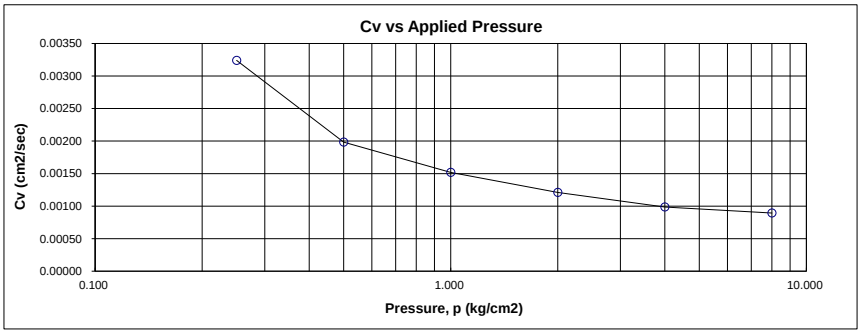

LABORATORIUM MEKANIKA TANAH
PT. SUWANDA KARYA MANDIRI
Komp. Bumi Asri Mekar Rahayu Blok II No. B-7, Kopo Bandung (40218)
Telp. (022 - 5417700) Fax. (022 - 5412700)
email : pt_suwanda_karya_mandiri@yahoo.com

KAN Komite Akreditasi Nasional LSSM-045-IDN

CONSOLIDATION

ASTM D 2435

PROJECT : **Pembangunan Stasiun Pengamatan Permukaan Tanah**
BORING NO. : **SPPT-05**
DEPTH : **13.00 - 13.55 m**

TESTED BY : Faizal
DATE : 27/08/2021

LOCATION : **Desa Depok, Kec. Siwalan, Kab. Pekalongan**
DESCRIPT. : **-**

APPARATUS MEASUREMENTS
CONTAINER HEIGHT : 2.000 cm
CONTAINER DIAMETER : 5.000 cm
CONTAINER AREA (A) : 19.635 cm2

SPECIFIC GRAVITY (Gs) : 2.6147

SOLIDS HEIGHT (Hs) IN cm : 0.720
Hs = Ws/(Gs.γ_w. A)

DEGREE OF SATURATION IN %
TEST START : 107.05
TEST END :

WATER CONTENT

	BEGINNING OF TEST		END OF TEST	
CONTAINER NO.	2B			
WT. CONTAINER + WET SOIL IN g	129.280			
WT. CONTAINER IN g	65.400			
WT. WET SOIL IN g	63.880			
WT. DRY SOIL (Ws) IN g	36.982			
WT. WATER (Ww) IN g	26.90			
WATER CONTENT (w) IN %	72.73			

APPLIED PRESSURE kg/cm^2	FINAL DIAL cm	DIAL CHANGE (ΔH) cm	Δe = ΔH/Hs	e = eo - ΣΔe	AVERAGE HEIGHT FOR LOAD cm	H cm	FITTING TIME (t 90) sec	Cv $\frac{0.848\ H^2}{t\ 90}$ cm^2/sec
0.00	0.9000			1.776	2.000			
		0.1720	0.2388			0.957	334.18	0.00232
0.25	0.7280			1.538	1.828			
		0.0700	0.0972			0.897	463.70	0.00147
0.50	0.6580			1.440	1.758			
		0.0920	0.1277			0.856	543.61	0.00114
1.00	0.5660			1.313	1.666			
		0.1060	0.1472			0.807	595.35	0.00093
2.00	0.4600			1.166	1.560			
		0.1040	0.1444			0.754	622.10	0.00077
4.00	0.3560			1.021	1.456			
		0.1080	0.1499			0.701	599.14	0.00070
8.00	0.2480			0.871	1.348			
		0.0420	0.0583			0.685		
2.00	0.2900			0.930	1.390			
		0.0480	0.0666			0.707		
0.50	0.3380			0.996	1.438			

LABORATORIUM MEKANIKA TANAH
PT. SUWANDA KARYA MANDIRI
Komp. Bumi Asri Mekar Sukoyo Blok II No. B-7, Kopo Bandung (40218)
Telp. (022 - 5417706) Fax. (022 - 5412706)
email : pt_suwanda_karya_mandiri@yahoo.com

Komite Akreditasi Nasional
LSSM-045-IDN

CONSOLIDATION

ASTM D 2435

PROJECT	: Pembangunan Stasiun Pengamatan Permukaan Tanah			
LOCATION	: Desa Depok, Kec. Siwalan, Kab. Pekalongan			
BORING NO.	: SPPT-05	Coefficient of Consolidation (Cv)	: 0.00088	cm^2/sec
DEPTH	: 13.00 - 13.55 m	Compression Index (Cc)	: 0.498	
TESTED BY	: Faizal	Swell Index (Cs)	: 0.083	
DATE	: 27/08/2021	Coeff. of Volume Comp. (mv)	: 0.120	cm^2/kg
DESCRIPTION	: -			

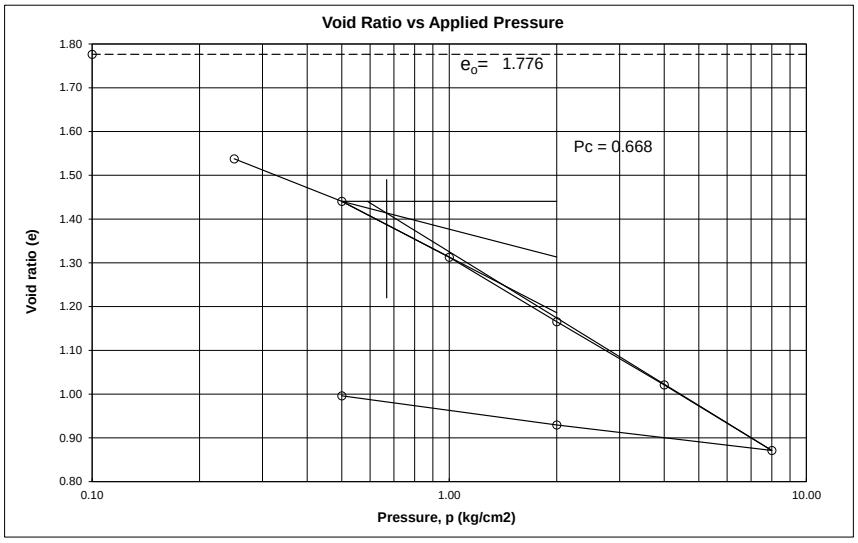

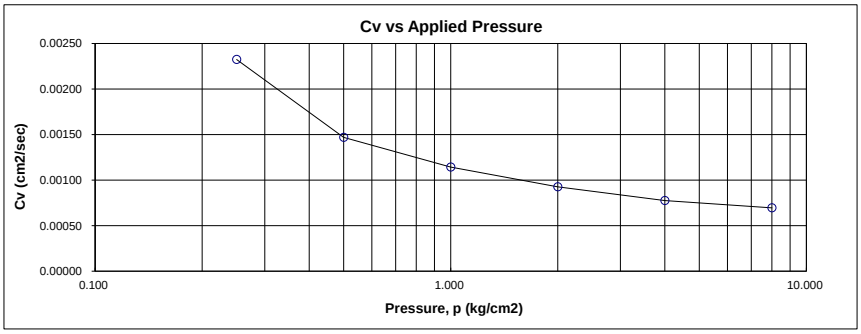

LABORATORIUM MEKANIKA TANAH
PT. SUWANDA KARYA MANDIRI
Komp. Bumi Asri Mekar Rahayu Blok II No. B-7, Kopo Bandung (40218)
Telp. (022 - 5417700) Fax. (022 - 5412700)
email : pt_suwanda_karya_mandiri@yahoo.com

LSSM-045-IDN

CONSOLIDATION

ASTM D 2435

PROJECT : **Pembangunan Stasiun Pengamatan Permukaan Tanah**
BORING NO. : **SPPT-05**
DEPTH : **21.00 - 21.55 m**

TESTED BY : Faizal
DATE : 27/08/2021

LOCATION : **Desa Depok, Kec. Siwalan, Kab. Pekalongan**
DESCRIPT. : **-**

APPARATUS MEASUREMENTS
CONTAINER HEIGHT : 2.000 cm
CONTAINER DIAMETER : 5.000 cm
CONTAINER AREA (A) : 19.635 cm2

SPECIFIC GRAVITY (Gs) : 2.6257

SOLIDS HEIGHT (Hs) IN cm : 0.773
Hs = Ws/(Gs.γ_w. A)

DEGREE OF SATURATION IN %
TEST START : 102.80
TEST END :

WATER CONTENT

	BEGINNING OF TEST		END OF TEST	
CONTAINER NO.	3B			
WT. CONTAINER + WET SOIL IN g	128.490			
WT. CONTAINER IN g	63.870			
WT. WET SOIL IN g	64.620			
WT. DRY SOIL (Ws) IN g	39.855			
WT. WATER (Ww) IN g	24.77			
WATER CONTENT (w) IN %	62.14			

APPLIED PRESSURE kg/cm^2	FINAL DIAL cm	DIAL CHANGE (ΔH) cm	Δe = ΔH/Hs	e = eo - ΣΔe	AVERAGE HEIGHT FOR LOAD cm	H cm	FITTING TIME (t 90) sec	Cv $\frac{0.848\ H^2}{t\ 90}$ cm^2/sec
0.00	0.9000			1.587	2.000			
		0.1320	0.1708			0.967	314.65	0.00252
0.25	0.7680			1.416	1.868			
		0.0830	0.1074			0.913	470.40	0.00150
0.50	0.6850			1.309	1.785			
		0.1210	0.1565			0.862	606.74	0.00104
1.00	0.5640			1.153	1.664			
		0.1230	0.1591			0.801	653.40	0.00083
2.00	0.4410			0.993	1.541			
		0.1360	0.1759			0.737	681.41	0.00068
4.00	0.3050			0.817	1.405			
		0.1470	0.1902			0.666	661.34	0.00057
8.00	0.1580			0.627	1.258			
		0.0620	0.0802			0.645		
2.00	0.2200			0.708	1.320			
		0.0620	0.0802			0.676		
0.50	0.2820			0.788	1.382			

LABORATORIUM MEKANIKA TANAH
PT. SUWANDA KARYA MANDIRI
Komp. Bumi Asri Mekar Rahayu Blok II No. B-7, Kopo Bandung (40218)
Telp. (022 - 5417706) Fax. (022 - 5412706)
email : pt_suwanda_karya_mandiri@yahoo.com

CONSOLIDATION

ASTM D 2435

PROJECT	: Pembangunan Stasiun Pengamatan Permukaan Tanah			
LOCATION	: Desa Depok, Kec. Siwalan, Kab. Pekalongan			
BORING NO.	: SPPT-05	Coefficient of Consolidation (Cv)	: 0.00078	cm^2/sec
DEPTH	: 21.00 - 21.55 m	Compression Index (Cc)	: 0.632	
TESTED BY	: Faizal	Swell Index (Cs)	: 0.107	
DATE	: 27/08/2021	Coeff. of Volume Comp. (mv)	: 0.120	cm^2/kg
DESCRIPTION	: -			

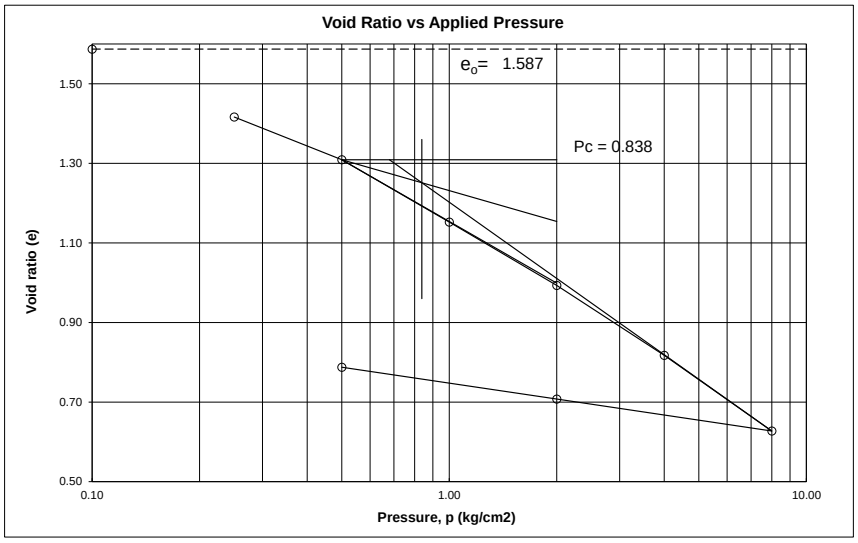

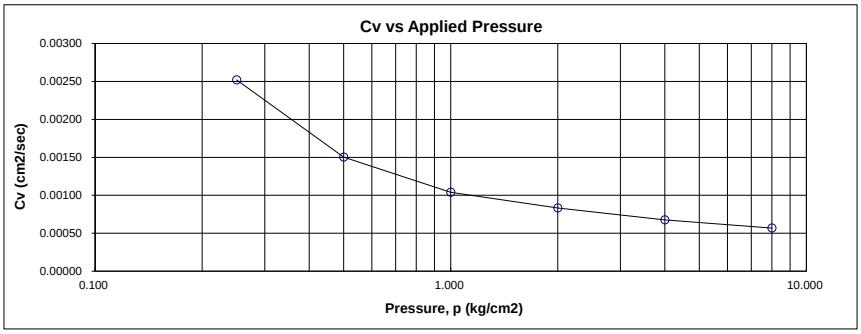

LABORATORIUM MEKANIKA TANAH
PT. SUWANDA KARYA MANDIRI
Komp. Bumi Asri Mekar Rahayu Blok II No. B-7, Kopo Bandung (40218)
Telp. (022 - 5417700) Fax. (022 - 5412700)
email : pt_suwanda_karya_mandiri@yahoo.com

KAN Komite Akreditasi Nasional LSSM-045-IDN

CONSOLIDATION

ASTM D 2435

PROJECT : **Pembangunan Stasiun Pengamatan Permukaan Tanah**
BORING NO. : **SPPT-05**
DEPTH : **33.00 - 33.55 m**

TESTED BY : Faizal
DATE : 27/08/2021

LOCATION : **Desa Depok, Kec. Siwalan, Kab. Pekalongan**
DESCRIPT. : **-**

APPARATUS MEASUREMENTS
CONTAINER HEIGHT : 2.000 cm
CONTAINER DIAMETER : 5.000 cm
CONTAINER AREA (A) : 19.635 cm2

SPECIFIC GRAVITY (Gs) : 2.6299

SOLIDS HEIGHT (Hs) IN cm : 0.965
Hs = Ws/(Gs.γ_w. A)

DEGREE OF SATURATION IN %
TEST START : 105.20
TEST END :

WATER CONTENT	BEGINNING OF TEST		END OF TEST	
CONTAINER NO.	4B			
WT. CONTAINER + WET SOIL IN g	128.870			
WT. CONTAINER IN g	57.670			
WT. WET SOIL IN g	71.200			
WT. DRY SOIL (Ws) IN g	49.813			
WT. WATER (Ww) IN g	21.39			
WATER CONTENT (w) IN %	42.93			

APPLIED PRESSURE kg/cm^2	FINAL DIAL cm	DIAL CHANGE (ΔH) cm	Δe = ΔH/Hs	e = eo - ΣΔe	AVERAGE HEIGHT FOR LOAD cm	H cm	FITTING TIME (t 90) sec	Cv $\frac{0.848\ H^2}{t\ 90}$ cm^2/sec
0.00	0.9000			1.073	2.000			
		0.0170	0.0176			0.996	171.37	0.00491
0.25	0.8830			1.056	1.983			
		0.0130	0.0135			0.988	290.40	0.00285
0.50	0.8700			1.042	1.970			
		0.0450	0.0466			0.974	378.01	0.00213
1.00	0.8250			0.996	1.925			
		0.0630	0.0653			0.947	427.73	0.00178
2.00	0.7620			0.930	1.862			
		0.0870	0.0902			0.909	453.75	0.00155
4.00	0.6750			0.840	1.775			
		0.0910	0.0943			0.865	434.17	0.00146
8.00	0.5840			0.746	1.684			
		0.0410	0.0425			0.852		
2.00	0.6250			0.788	1.725			
		0.0400	0.0415			0.873		
0.50	0.6650			0.830	1.765			

LABORATORIUM MEKANIKA TANAH
PT. SUWANDA KARYA MANDIRI
Komp. Bumi Asri Mekar Sukoyo Blok II No. B-7, Kopo Bandung (40218)
Telp. (022 - 5417706) Fax. (022 - 5412706)
email : pt_suwanda_karya_mandiri@yahoo.com

KAN Komite Akreditasi Nasional LSSM-045-IDN

CONSOLIDATION

ASTM D 2435

PROJECT	: Pembangunan Stasiun Pengamatan Permukaan Tanah			
LOCATION	: Desa Depok, Kec. Siwalan, Kab. Pekalongan			
BORING NO.	: SPPT-05	Coefficient of Consolidation (Cv)	: 0.00173	cm^2/sec
DEPTH	: 33.00 - 33.55 m	Compression Index (Cc)	: 0.313	
TESTED BY	: Faizal	Swell Index (Cs)	: 0.056	
DATE	: 27/08/2021	Coeff. of Volume Comp. (mv)	: 0.029	cm^2/kg
DESCRIPTION	: -			

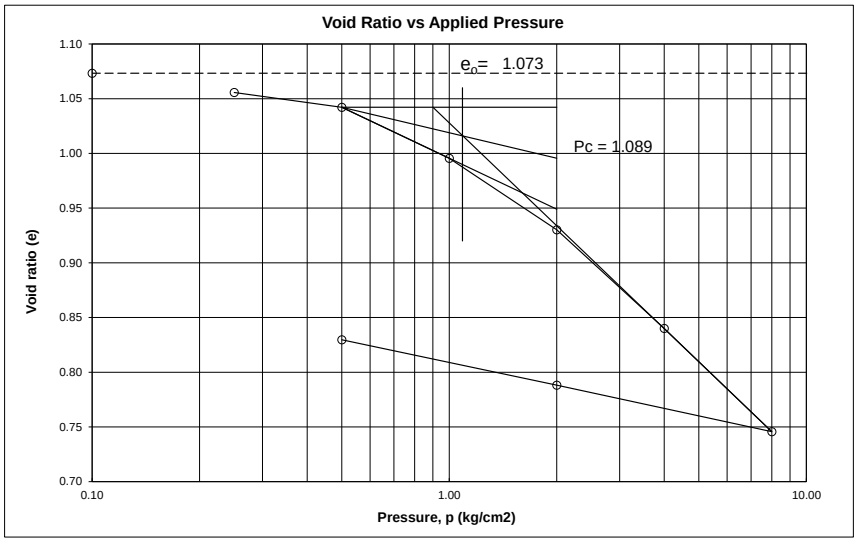

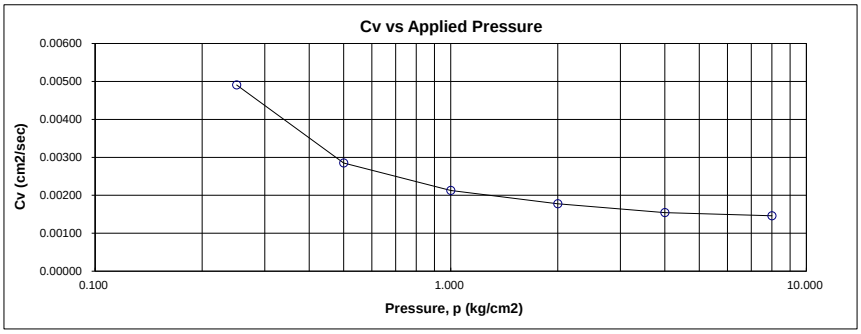

LABORATORIUM MEKANIKA TANAH
PT. SUWANDA KARYA MANDIRI
Komp. Bumi Asri Mekar Rahayu Blok II No. B-7, Kopo Bandung (40218)
Telp. (022 - 5417700) Fax. (022 - 5412700)
email : pt_suwanda_karya_mandiri@yahoo.com

LSSM-045-IDN

CONSOLIDATION

ASTM D 2435

PROJECT : **Pembangunan Stasiun Pengamatan Permukaan Tanah**
BORING NO. : **SPPT-05**
DEPTH : **41.00 - 41.55 m**

TESTED BY : Faizal
DATE : 27/08/2021

LOCATION : **Desa Depok, Kec. Siwalan, Kab. Pekalongan**
DESCRIPT. : **-**

APPARATUS MEASUREMENTS
CONTAINER HEIGHT : 2.000 cm
CONTAINER DIAMETER : 5.000 cm
CONTAINER AREA (A) : 19.635 cm2

SPECIFIC GRAVITY (Gs) : 2.6100

SOLIDS HEIGHT (Hs) IN cm : 0.929
Hs = Ws/(Gs.γ_w. A)

DEGREE OF SATURATION IN %
TEST START : 82.68
TEST END :

WATER CONTENT

	BEGINNING OF TEST		END OF TEST	
CONTAINER NO.	1D			
WT. CONTAINER + WET SOIL IN g	130.810			
WT. CONTAINER IN g	65.800			
WT. WET SOIL IN g	65.010			
WT. DRY SOIL (Ws) IN g	47.630			
WT. WATER (Ww) IN g	17.38			
WATER CONTENT (w) IN %	36.49			

APPLIED PRESSURE kg/cm^2	FINAL DIAL cm	DIAL CHANGE (ΔH) cm	Δe = ΔH/Hs	e = eo - ΣΔe	AVERAGE HEIGHT FOR LOAD cm	H cm	FITTING TIME (t 90) sec	Cv $\frac{0.848\ H^2}{t\ 90}$ cm^2/sec
0.00	0.9000			1.152	2.000			
		0.1270	0.1366			0.968	159.41	0.00499
0.25	0.7730			1.015	1.873			
		0.0480	0.0516			0.925	277.35	0.00261
0.50	0.7250			0.964	1.825			
		0.1090	0.1173			0.885	342.73	0.00194
1.00	0.6160			0.846	1.716			
		0.1230	0.1323			0.827	381.02	0.00152
2.00	0.4930			0.714	1.593			
		0.1440	0.1549			0.761	399.38	0.00123
4.00	0.3490			0.559	1.449			
		0.1490	0.1603			0.687	384.05	0.00104
8.00	0.2000			0.399	1.300			
		0.0600	0.0646			0.665		
2.00	0.2600			0.463	1.360			
		0.0450	0.0484			0.691		
0.50	0.3050			0.512	1.405			

LABORATORIUM MEKANIKA TANAH
PT. SUWANDA KARYA MANDIRI
Komp. Bumi Asri Mekar Rahayu Blok II No. B-7, Kopo Bandung (40218)
Telp. (022 - 5417706) Fax. (022 - 5417706)
email : pt_suwanda_karya_mandiri@yahoo.com

KAN Komite Akreditasi Nasional LSSM-045-IDN

CONSOLIDATION

ASTM D 2435

PROJECT	: Pembangunan Stasiun Pengamatan Permukaan Tanah			
LOCATION	: Desa Depok, Kec. Siwalan, Kab. Pekalongan			
BORING NO.	: SPPT-05	Coefficient of Consolidation (Cv)	: 0.00143	cm^2/sec
DEPTH	: 41.00 - 41.55 m	Compression Index (Cc)	: 0.533	
TESTED BY	: Faizal	Swell Index (Cs)	: 0.075	
DATE	: 27/08/2021	Coeff. of Volume Comp. (mv)	: 0.103	cm^2/kg
DESCRIPTION	: -			

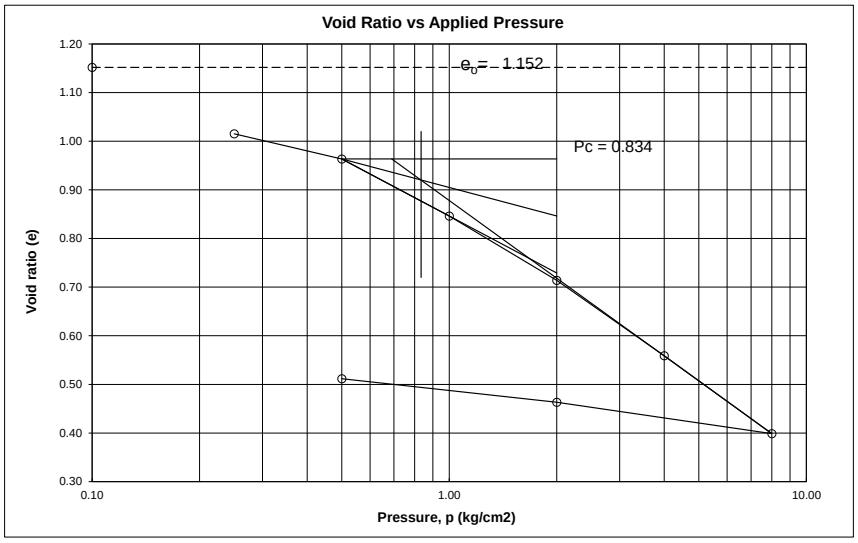

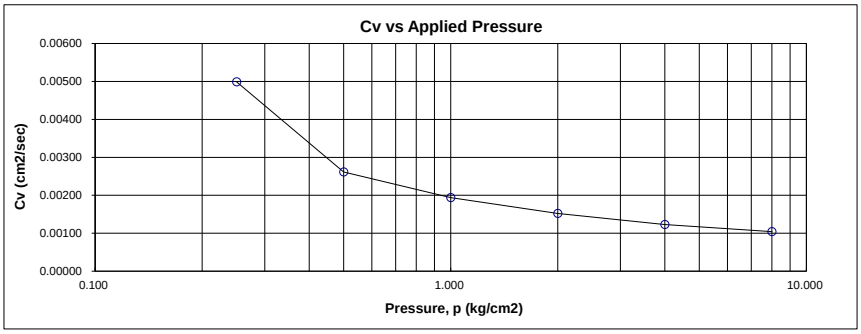

LABORATORIUM MEKANIKA TANAH
PT. SUWANDA KARYA MANDIRI
Komp. Bumi Asri Mekar Rahayu Blok II No. B-7, Kopo Bandung (40218)
Telp. (022 - 5417700) Fax. (022 - 5412700)
email : pt_suwanda_karya_mandiri@yahoo.com

KAN Komite Akreditasi Nasional LSSM-045-IDN

CONSOLIDATION

ASTM D 2435

PROJECT : **Pembangunan Stasiun Pengamatan Permukaan Tanah**
BORING NO. : **SPPT-01**
DEPTH : **11.00 - 11.50 m**

TESTED BY : Faizal
DATE : 20/09/2021

LOCATION : **Kel. Kandang Panjang, Kec. Pekalongan Utara, Kota Pekalongan**
DESCRIPT. : **-**

APPARATUS MEASUREMENTS
CONTAINER HEIGHT : 2.000 cm
CONTAINER DIAMETER : 5.000 cm
CONTAINER AREA (A) : 19.635 cm2

SPECIFIC GRAVITY (Gs) : 2.5970

SOLIDS HEIGHT (Hs) IN cm : 0.616
Hs = Ws/(Gs.γ_w. A)

DEGREE OF SATURATION IN %
TEST START : 72.63
TEST END :

WATER CONTENT

	BEGINNING OF TEST			
CONTAINER NO.	1B			
WT. CONTAINER + WET SOIL IN g	114.450			
WT. CONTAINER IN g	63.290			
WT. WET SOIL IN g	51.160			
WT. DRY SOIL (Ws) IN g	31.428			
WT. WATER (Ww) IN g	19.73			
WATER CONTENT (w) IN %	62.78			

APPLIED PRESSURE kg/cm^2	FINAL DIAL cm	DIAL CHANGE (ΔH) cm	Δe = ΔH/Hs	e = eo - ΣΔe	AVERAGE HEIGHT FOR LOAD cm	H cm	FITTING TIME (t 90) sec	Cv $\frac{0.848\ H^2}{t\ 90}$ cm^2/sec
0.00	0.9000			2.245	2.000			
		0.1900	0.3083			0.953	440.65	0.00175
0.25	0.7100			1.937	1.810			
		0.0980	0.1590			0.881	649.45	0.00101
0.50	0.6120			1.778	1.712			
		0.1010	0.1639			0.831	764.69	0.00077
1.00	0.5110			1.614	1.611			
		0.1240	0.2012			0.775	816.97	0.00062
2.00	0.3870			1.413	1.487			
		0.1370	0.2223			0.709	768.98	0.00055
4.00	0.2500			1.190	1.350			
		0.0330	0.0535			1.696		
2.00	0.2830			1.244	1.383			
		0.0520	0.0844			0.705		
0.50	0.3350			1.328	1.435			

LABORATORIUM MEKANIKA TANAH
PT. SUWANDA KARYA MANDIRI
Komp. Bumi Asri Mekar Rahayu Blok II No. B-7, Kopo Bandung (40218)
Telp. (022 - 5417700) Fax. (022 - 5412700)
email : pt_suwanda_karya_mandiri@yahoo.com

KAN Komite Akreditasi Nasional LSSM-045-IDN

CONSOLIDATION

ASTM D 2435

PROJECT	: Pembangunan Stasiun Pengamatan Permukaan Tanah			
LOCATION	: Kel. Kandang Panjang, Kec. Pekalongan Utara, Kota Pekalongan			
BORING NO.	: SPPT-01	Coefficient of Consolidation (Cv)	: 0.00094	cm^2/sec
DEPTH	: 11.00 - 11.50 m	Compression Index (Cc)	: 0.738	
TESTED BY	: Faizal	Swell Index (Cs)	: 0.092	
DATE	: 20/09/2021	Coeff. of Volume Comp. (mv)	: 0.147	cm^2/kg
DESCRIPTION	: -			

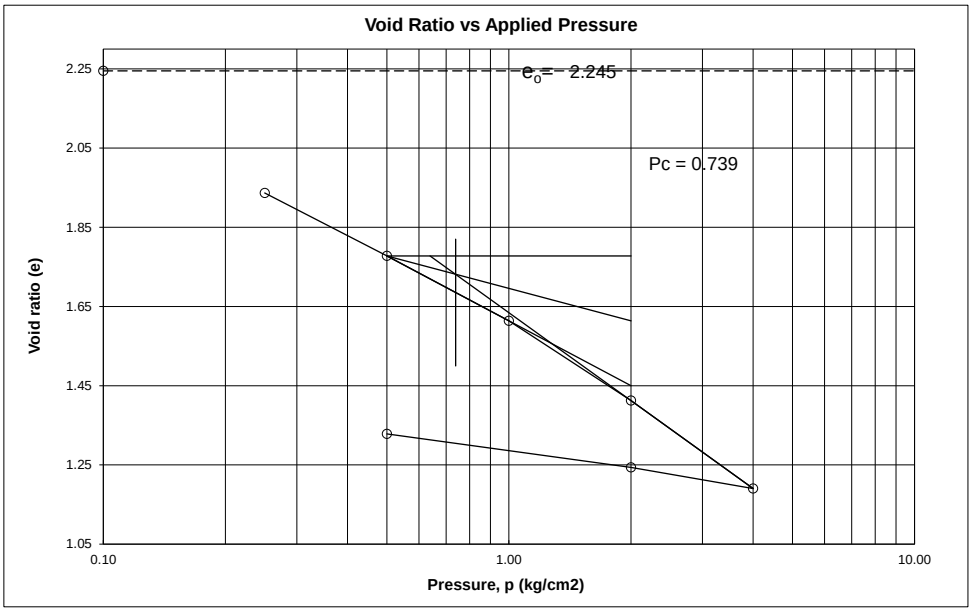

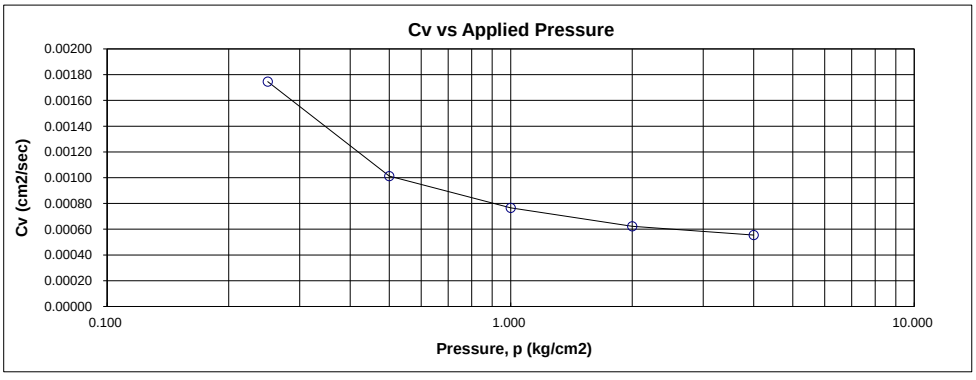

LABORATORIUM MEKANIKA TANAH
PT. SUWANDA KARYA MANDIRI
Komp. Bumi Asri Mekar Rahayu Blok II No. B-7, Kopo Bandung (40218)
Telp. (022 - 5417700) Fax. (022 - 5412700)
email : pt_suwanda_karya_mandiri@yahoo.com

LSSM-045-IDN

CONSOLIDATION

ASTM D 2435

PROJECT : **Pembangunan Stasiun Pengamatan Permukaan Tanah**
BORING NO. : **SPPT-01**
DEPTH : **17.00 - 17.50 m**

TESTED BY : Faizal
DATE : 20/09/2021

LOCATION : **Kel. Kandang Panjang, Kec. Pekalongan Utara, Kota Pekalongan**
DESCRIPT. : **-**

APPARATUS MEASUREMENTS
CONTAINER HEIGHT : 2.000 cm
CONTAINER DIAMETER : 5.000 cm
CONTAINER AREA (A) : 19.635 cm2

SPECIFIC GRAVITY (Gs) : 2.6060

SOLIDS HEIGHT (Hs) IN cm : 0.692
Hs = Ws/(Gs.γ_w. A)

DEGREE OF SATURATION IN %
TEST START : 93.40
TEST END :

WATER CONTENT

	BEGINNING OF TEST		END OF TEST	
CONTAINER NO.	2B			
WT. CONTAINER + WET SOIL IN g	124.780			
WT. CONTAINER IN g	65.400			
WT. WET SOIL IN g	59.380			
WT. DRY SOIL (Ws) IN g	35.384			
WT. WATER (Ww) IN g	24.00			
WATER CONTENT (w) IN %	67.82			

APPLIED PRESSURE kg/cm^2	FINAL DIAL cm	DIAL CHANGE (ΔH) cm	Δe = ΔH/Hs	e = eo - ΣΔe	AVERAGE HEIGHT FOR LOAD cm	H cm	FITTING TIME (t 90) sec	Cv $\frac{0.848\ H^2}{t\ 90}$ cm^2/sec
0.00	0.9000			1.892	2.000			
		0.0250	0.0362			0.994	320.17	0.00262
0.25	0.8750			1.856	1.975			
		0.0410	0.0593			0.977	450.46	0.00180
0.50	0.8340			1.797	1.934			
		0.0750	0.1085			0.948	599.14	0.00127
1.00	0.7590			1.688	1.859			
		0.1530	0.2212			0.891	685.46	0.00098
2.00	0.6060			1.467	1.706			
		0.1590	0.2299			0.813	718.30	0.00078
4.00	0.4470			1.237	1.547			
		0.2220	0.3210			0.718	669.34	0.00065
8.00	0.2250			0.916	1.325			
		0.0550	0.0795			0.676		
2.00	0.2800			0.996	1.380			
		0.0620	0.0897			0.706		
0.50	0.3420			1.085	1.442			

LABORATORIUM MEKANIKA TANAH
PT. SUWANDA KARYA MANDIRI
Komp. Bumi Asri Mekar Rahayu Blok II No. B-7, Kopo Bandung (40218)
Telp. (022 - 5417706) Fax. (022 - 5412706)
email : pt_suwanda_karya_mandiri@yahoo.com

LSSM-045-IDN

CONSOLIDATION

ASTM D 2435

PROJECT	: Pembangunan Stasiun Pengamatan Permukaan Tanah			
LOCATION	: Kel. Kandang Panjang, Kec. Pekalongan Utara, Kota Pekalongan			
BORING NO.	: SPPT-01	Coefficient of Consolidation (Cv)	: 0.00092	cm^2/sec
DEPTH	: 17.00 - 17.50 m	Compression Index (Cc)	: 1.066	
TESTED BY	: Faizal	Swell Index (Cs)	: 0.112	
DATE	: 20/09/2021	Coeff. of Volume Comp. (mv)	: 0.063	cm^2/kg
DESCRIPTION	: -			

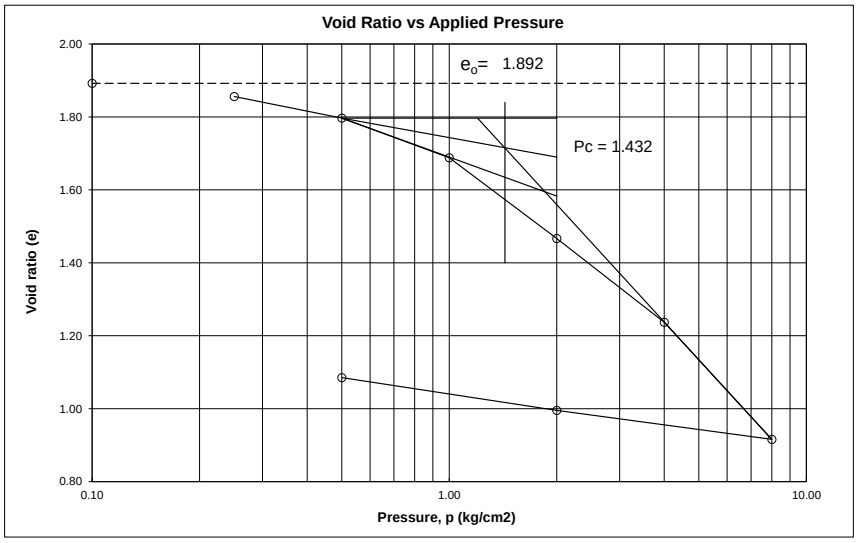

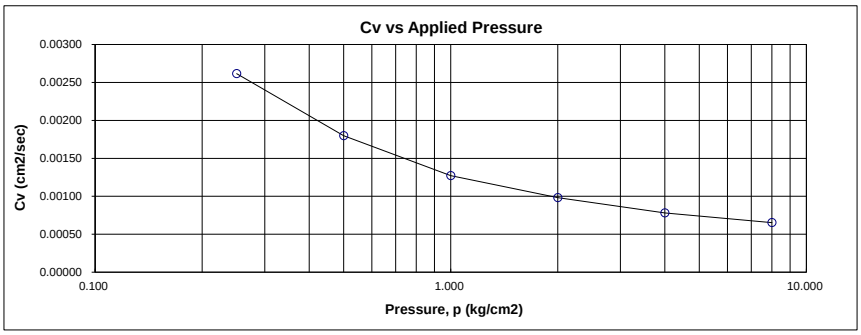

LABORATORIUM MEKANIKA TANAH
PT. SUWANDA KARYA MANDIRI
Komp. Bumi Asri Mekar Rahayu Blok II No. B-7, Kopo Bandung (40218)
Telp. (022 - 5417700) Fax. (022 - 5412700)
email : pt_suwanda_karya_mandiri@yahoo.com

LSSM-045-IDN

CONSOLIDATION

ASTM D 2435

PROJECT : **Pembangunan Stasiun Pengamatan Permukaan Tanah**
BORING NO. : **SPPT-01**
DEPTH : **25.00 - 25.50 m**

TESTED BY : Faizal
DATE : 20/09/2021

LOCATION : **Kel. Kandang Panjang, Kec. Pekalongan Utara, Kota Pekalongan**
DESCRIPT. : **-**

APPARATUS MEASUREMENTS
CONTAINER HEIGHT : 2.000 cm
CONTAINER DIAMETER : 5.000 cm
CONTAINER AREA (A) : 19.635 cm2

SPECIFIC GRAVITY (Gs) : 2.6130
SOLIDS HEIGHT (Hs) IN cm : 0.904
Hs = Ws/(Gs.γ_w. A)

DEGREE OF SATURATION IN %
TEST START : 138.99
TEST END :

WATER CONTENT

	BEGINNING OF TEST		END OF TEST	
CONTAINER NO.	3B			
WT. CONTAINER + WET SOIL IN g	140.160			
WT. CONTAINER IN g	63.870			
WT. WET SOIL IN g	76.290			
WT. DRY SOIL (Ws) IN g	46.376			
WT. WATER (Ww) IN g	29.91			
WATER CONTENT (w) IN %	64.50			

APPLIED PRESSURE kg/cm^2	FINAL DIAL cm	DIAL CHANGE (ΔH) cm	Δe = ΔH/Hs	e = eo - ΣΔe	AVERAGE HEIGHT FOR LOAD cm	H cm	FITTING TIME (t 90) sec	Cv $\frac{0.848\ H^2}{t\ 90}$ cm^2/sec
0.00	0.9000			1.213	2.000			
		0.0170	0.0188			0.996	322.94	0.00260
0.25	0.8830			1.194	1.983			
		0.0250	0.0277			0.985	450.46	0.00183
0.50	0.8580			1.166	1.958			
		0.0270	0.0299			0.972	532.82	0.00150
1.00	0.8310			1.136	1.931			
		0.0500	0.0553			0.953	591.58	0.00130
2.00	0.7810			1.081	1.881			
		0.0630	0.0697			0.925	625.97	0.00116
4.00	0.7180			1.011	1.818			
		0.0990	0.1095			0.884	587.81	0.00113
8.00	0.6190			0.902	1.719			
		0.0320	0.0354			0.868		
2.00	0.6510			0.937	1.751			
		0.0490	0.0542			0.888		
0.50	0.7000			0.991	1.800			

LABORATORIUM MEKANIKA TANAH
PT. SUWANDA KARYA MANDIRI
Komp. Bumi Asri Mekar Rahayu Blok II No. B-7, Kopo Bandung (40218)
Telp. (022 - 5417706) Fax. (022 - 5412706)
email : pt_suwanda_karya_mandiri@yahoo.com

LSSM-045-IDN

CONSOLIDATION

ASTM D 2435

PROJECT	: Pembangunan Stasiun Pengamatan Permukaan Tanah			
LOCATION	: Kel. Kandang Panjang, Kec. Pekalongan Utara, Kota Pekalongan			
BORING NO.	: SPPT-01	Coefficient of Consolidation (Cv)	: 0.00127	cm^2/sec
DEPTH	: 25.00 - 25.50 m	Compression Index (Cc)	: 0.364	
TESTED BY	: Faizal	Swell Index (Cs)	: 0.060	
DATE	: 20/09/2021	Coeff. of Volume Comp. (mv)	: 0.028	cm^2/kg
DESCRIPTION	: -			

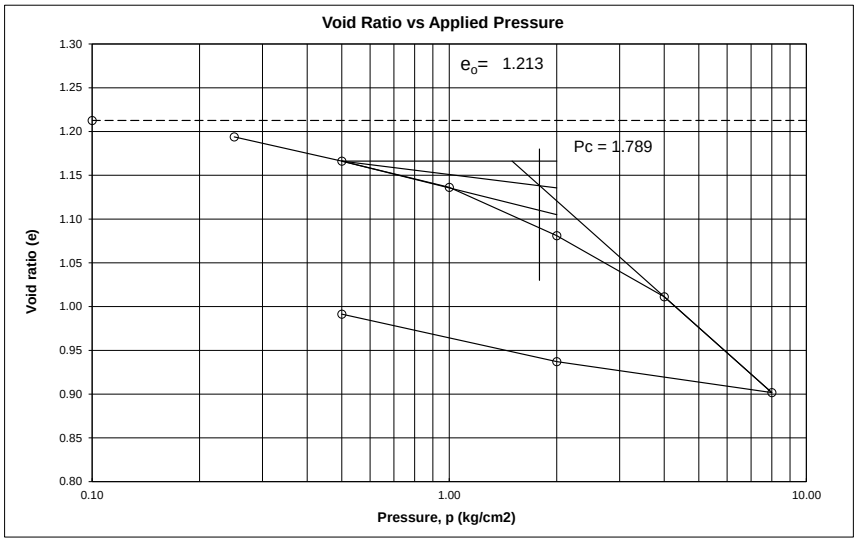

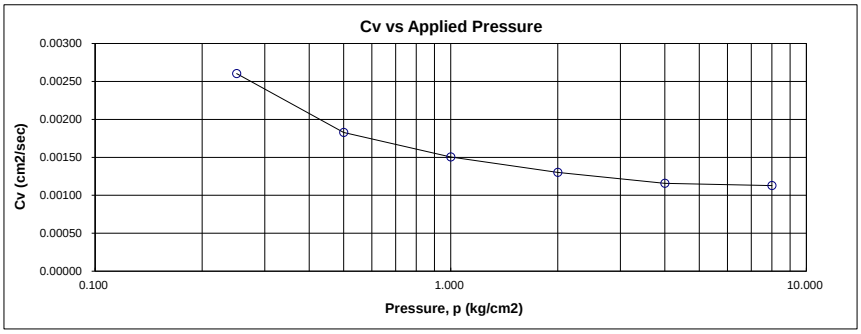

LABORATORIUM MEKANIKA TANAH
PT. SUWANDA KARYA MANDIRI
Komp. Buni Asri Mekar Rahayu Blok II No. B-7, Kopo Bandung (40219)
Telp. (022 - 5417700) Fax. (022 - 5412700)
email : pt_suwanda_karya_mandiri@yahoo.com

KAN Komite Akreditasi Nasional LSSM-045-IDN

CONSOLIDATION TEST

PROJECT : **Pembangunan Stasiun Pengamatan Penurunan Permukaan Tanah**
BORING NO. : **SPPT-08**
DEPTH : **15.00 - 15.50 m**

TESTED BY : Faizal
DATE : 12/08/2021

LOCATION : **Ds. Kepatihan, kec. Wiradesa, kab. Pekalongan**
DESCRIPT. : **UDS**

APPARATUS MEASUREMENTS
CONTAINER HEIGHT : 2.000 cm
CONTAINER DIAMETER : 5.000 cm
CONTAINER AREA (A) : 19.635 cm2

SPECIFIC GRAVITY (Gs) : 2.6121

SOLIDS HEIGHT (Hs) IN cm : 0.594
Hs = Ws/(Gs.γ_w. A)

DEGREE OF SATURATION IN %
TEST START : 94.10
TEST END :

WATER CONTENT	BEGINNING OF TEST		END OF TEST	
CONTAINER NO.	1A			
WT. CONTAINER + WET SOIL IN g	125.150			
WT. CONTAINER IN g	68.690			
WT. WET SOIL IN g	56.460			
WT. DRY SOIL (Ws) IN g	30.490			
WT. WATER (Ww) IN g	25.97			
WATER CONTENT (w) IN %	85.18			

APPLIED PRESSURE kg/cm^2	FINAL DIAL cm	DIAL CHANGE (ΔH) cm	Δe = ΔH/Hs	e = eo - Σ Δe	AVERAGE HEIGHT FOR LOAD cm	H cm	FITTING TIME (t 90) sec	Cv $\frac{0.848\ H^2}{t\ 90}$ cm^2/sec
0.00	0.9000			2.364	2.000			
		0.0660	0.1110			0.984	989.02	0.00083
0.25	0.8340			2.253	1.934			
		0.0640	0.1077			0.951	1423.01	0.00054
0.50	0.7700			2.146	1.870			
		0.0760	0.1278			0.916	1808.41	0.00039
1.00	0.6940			2.018	1.794			
		0.1460	0.2456			0.861	2046.34	0.00031
2.00	0.5480			1.772	1.648			
		0.1690	0.2843			0.782	2081.53	0.00025
4.00	0.3790			1.488	1.479			
		0.2040	0.3432			0.689	2018.40	0.00020
8.00	0.1750			1.145	1.275			
		0.0480	0.0807			0.650		
2.00	0.2230			1.225	1.323			
		0.0670	0.1127			0.678		
0.50	0.2900			1.338	1.390			

LABORATORIUM MEKANIKA TANAH
PT. SUWANDA KARYA MANDIRI
Komp. Bumi Asri Mekar Rahayu Blok II No. B-7, Kopo Bandung (40218)
Telp. (022 - 5417700) Fax. (022 - 5412700)
email : pt_suwanda_karya_mandiri@yahoo.com

CONSOLIDATION TEST

PROJECT	: Pembangunan Stasiun Pengamatan Penurunan Permukaan Tanah			
LOCATION	: Ds. Kepatihan, kec. Wiradesa, kab. Pekalongan			
BORING NO.	: SPPT-08	Coefficient of Consolidation (Cv)	: 0.00029	cm^2/sec
DEPTH	: 15.00 - 15.50 m	Compression Index (Cc)	: 1.140	
TESTED BY	: Faizal	Swell Index (Cs)	: 0.129	
DATE	: 12/08/2021	Coeff. of Volume Comp. (mv)	: 0.085	cm^2/kg
DESCRIPTION	: UDS			

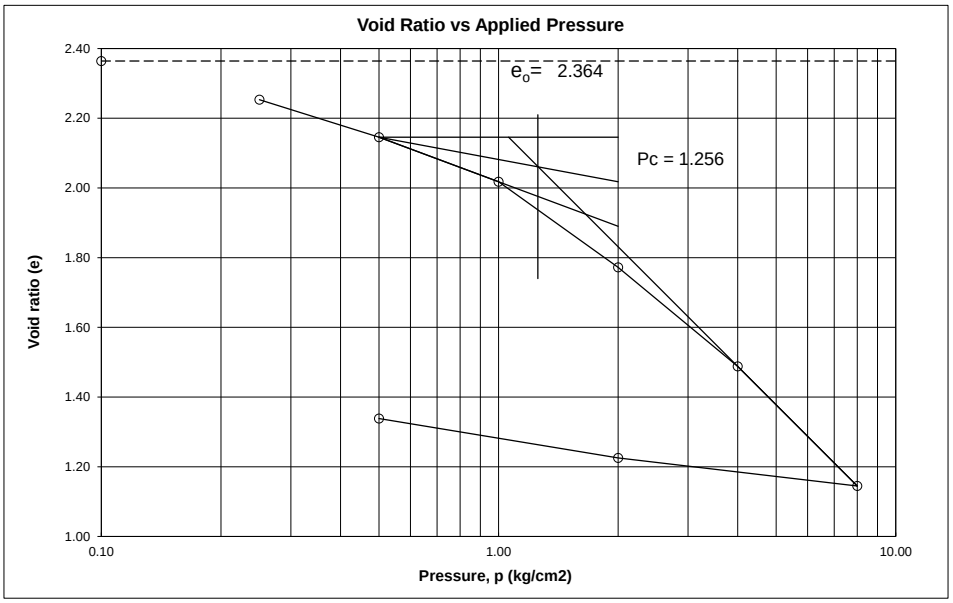

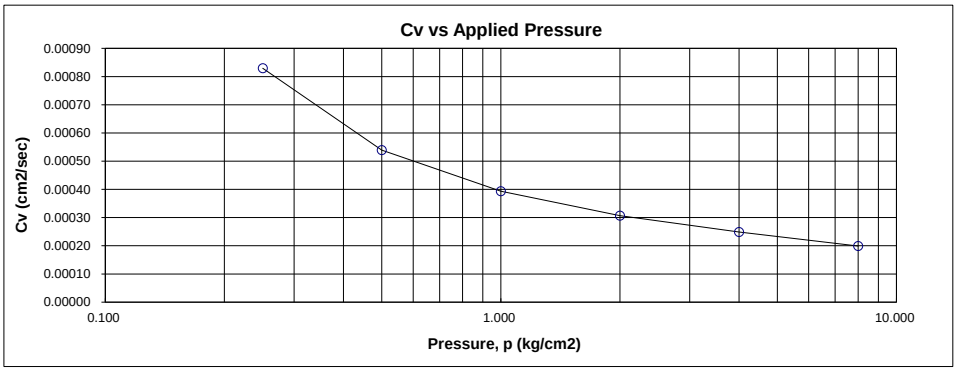

LABORATORIUM MEKANIKA TANAH
PT. SUWANDA KARYA MANDIRI
Komp. Buni Asri Mekar Rahayu Blok II No. B-7, Kopo Bandung (40219)
Telp. (022 - 5417700) Fax. (022 - 5412700)
email : pt_suwanda_karya_mandiri@yahoo.com

CONSOLIDATION TEST

PROJECT : **Pembangunan Stasiun Pengamatan Penurunan Permukaan Tanah**
BORING NO. : **SPPT-08**
DEPTH : **17.00 - 17.50 m**

TESTED BY : Faizal
DATE : 12/08/2021

LOCATION : **Ds. Kepatihan, kec. Wiradesa, kab. Pekalongan**
DESCRIPT. : **UDS**

APPARATUS MEASUREMENTS
CONTAINER HEIGHT : 2.000 cm
CONTAINER DIAMETER : 5.000 cm
CONTAINER AREA (A) : 19.635 cm2

SPECIFIC GRAVITY (Gs) : 2.5952
SOLIDS HEIGHT (Hs) IN cm : 0.867
Hs = Ws/(Gs.γ_w. A)

DEGREE OF SATURATION IN %
TEST START : 157.23
TEST END :

WATER CONTENT	BEGINNING OF TEST	END OF TEST		
CONTAINER NO.	2A			
WT. CONTAINER + WET SOIL IN g	133.640			
WT. CONTAINER IN g	54.490			
WT. WET SOIL IN g	79.150			
WT. DRY SOIL (Ws) IN g	44.160			
WT. WATER (Ww) IN g	34.99			
WATER CONTENT (w) IN %	79.23			

APPLIED PRESSURE kg/cm^2	FINAL DIAL cm	DIAL CHANGE (ΔH) cm	Δe = ΔH/Hs	e = eo - ΣΔe	AVERAGE HEIGHT FOR LOAD cm	H cm	FITTING TIME (t 90) sec	Cv $\frac{0.848\ H^2}{t\ 90}$ cm^2/sec
0.00	0.9000			1.308	2.000			
		0.1610	0.1858			0.960	786.26	0.00099
0.25	0.7390			1.122	1.839			
		0.1010	0.1165			0.894	1156.33	0.00059
0.50	0.6380			1.006	1.738			
		0.0990	0.1142			0.844	1434.73	0.00042
1.00	0.5390			0.891	1.639			
		0.1300	0.1500			0.787	1609.94	0.00033
2.00	0.4090			0.741	1.509			
		0.1400	0.1616			0.720	1679.05	0.00026
4.00	0.2690			0.580	1.369			
		0.1690	0.1950			0.642	1641.17	0.00021
8.00	0.1000			0.385	1.200			
		0.0510	0.0589			0.613		
2.00	0.1510			0.444	1.251			
		0.0640	0.0739			0.642		
0.50	0.2150			0.517	1.315			

LABORATORIUM MEKANIKA TANAH
PT. SUWANDA KARYA MANDIRI
Komp. Bumi Asri Mekar Rahayu Blok II No. B-7, Kopo Bandung (40218)
Telp. (022 - 5417700) Fax. (022 - 5412700)
email : pt_suwanda_karya_mandiri@yahoo.com

CONSOLIDATION TEST

PROJECT	: Pembangunan Stasiun Pengamatan Penurunan Permukaan Tanah			
LOCATION	: Ds. Kepatihan, kec. Wiradesa, kab. Pekalongan			
BORING NO.	: SPPT-08	Coefficient of Consolidation (Cv)	: 0.00031	cm^2/sec
DEPTH	: 17.00 - 17.50 m	Compression Index (Cc)	: 0.648	
TESTED BY	: Faizal	Swell Index (Cs)	: 0.088	
DATE	: 12/08/2021	Coeff. of Volume Comp. (mv)	: 0.135	cm^2/kg
DESCRIPTION	: UDS			

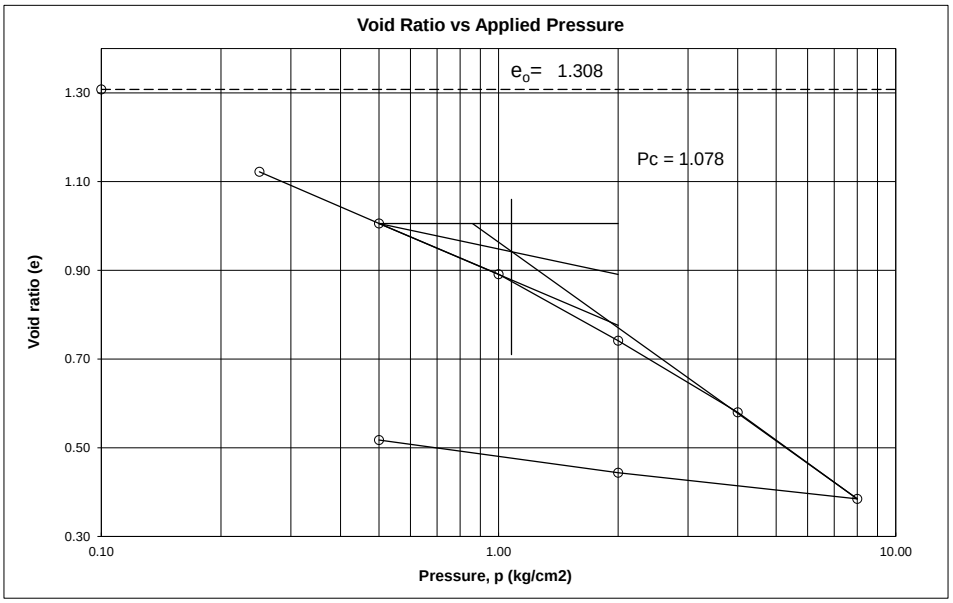

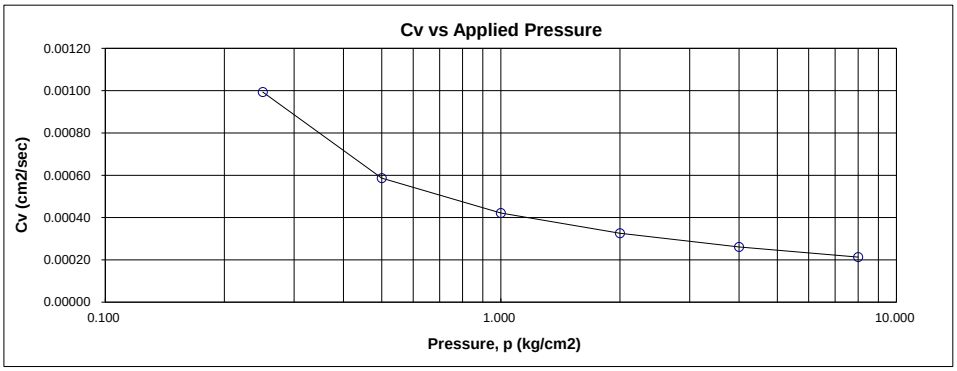

LABORATORIUM MEKANIKA TANAH
PT. SUWANDA KARYA MANDIRI
Komp. Buni Asri Mekar Rahayu Blok II No. B-7, Kopo Bandung (40219)
Telp. (022 - 5417700) Fax. (022 - 5412700)
email : pt_suwanda_karya_mandiri@yahoo.com

KAN Komite Akreditasi Nasional LSSM-045-IDN

CONSOLIDATION TEST

PROJECT : **Pembangunan Stasiun Pengamatan Penurunan Permukaan Tanah**
BORING NO. : **SPPT-08**
DEPTH : **27.00 - 27.50 m**

TESTED BY : Faizal
DATE : 12/08/2021

LOCATION : **Ds. Kepatihan, kec. Wiradesa, kab. Pekalongan**
DESCRIPT. : **UDS**

APPARATUS MEASUREMENTS
CONTAINER HEIGHT : 2.000 cm
CONTAINER DIAMETER : 5.000 cm
CONTAINER AREA (A) : 19.635 cm2

SPECIFIC GRAVITY (Gs) : 2.6216
SOLIDS HEIGHT (Hs) IN cm : 0.824
Hs = Ws/(Gs.γ_w. A)

DEGREE OF SATURATION IN %
TEST START : 98.45
TEST END :

WATER CONTENT	BEGINNING OF TEST	END OF TEST		
CONTAINER NO.	3A			
WT. CONTAINER + WET SOIL IN g	133.640			
WT. CONTAINER IN g	68.480			
WT. WET SOIL IN g	65.160			
WT. DRY SOIL (Ws) IN g	42.433			
WT. WATER (Ww) IN g	22.73			
WATER CONTENT (w) IN %	53.56			

APPLIED PRESSURE kg/cm^2	FINAL DIAL cm	DIAL CHANGE (ΔH) cm	Δe = ΔH/Hs	e = eo - Σ Δe	AVERAGE HEIGHT FOR LOAD cm	H cm	FITTING TIME (t 90) sec	Cv $\frac{0.848\ H^2}{t\ 90}$ cm^2/sec
0.00	0.9000			1.426	2.000			
		0.0720	0.0873			0.982	254.62	0.00321
0.25	0.8280			1.339	1.928			
		0.0260	0.0315			0.958	405.60	0.00192
0.50	0.8020			1.307	1.902			
		0.0370	0.0449			0.942	536.41	0.00140
1.00	0.7650			1.262	1.865			
		0.0570	0.0691			0.918	618.25	0.00116
2.00	0.7080			1.193	1.808			
		0.0760	0.0922			0.885	693.60	0.00096
4.00	0.6320			1.101	1.732			
		0.1050	0.1274			0.840	645.50	0.00093
8.00	0.5270			0.974	1.627			
		0.0290	0.0352			0.821		
2.00	0.5560			1.009	1.656			
		0.0410	0.0497			0.838		
0.50	0.5970			1.059	1.697			

LABORATORIUM MEKANIKA TANAH
PT. SUWANDA KARYA MANDIRI
Komp. Bumi Asri Mekar Rahayu Blok II No. B-7, Kopo Bandung (40218)
Telp. (022 - 5417700) Fax. (022 - 5412700)
email : pt_suwanda_karya_mandiri@yahoo.com

CONSOLIDATION TEST

PROJECT	: Pembangunan Stasiun Pengamatan Penurunan Permukaan Tanah			
LOCATION	: Ds. Kepatihan, kec. Wiradesa, kab. Pekalongan			
BORING NO.	: SPPT-08	Coefficient of Consolidation (Cv)	: 0.00111	cm^2/sec
DEPTH	: 27.00 - 27.50 m	Compression Index (Cc)	: 0.423	
TESTED BY	: Faizal	Swell Index (Cs)	: 0.056	
DATE	: 12/08/2021	Coeff. of Volume Comp. (mv)	: 0.051	cm^2/kg
DESCRIPTION	: UDS			

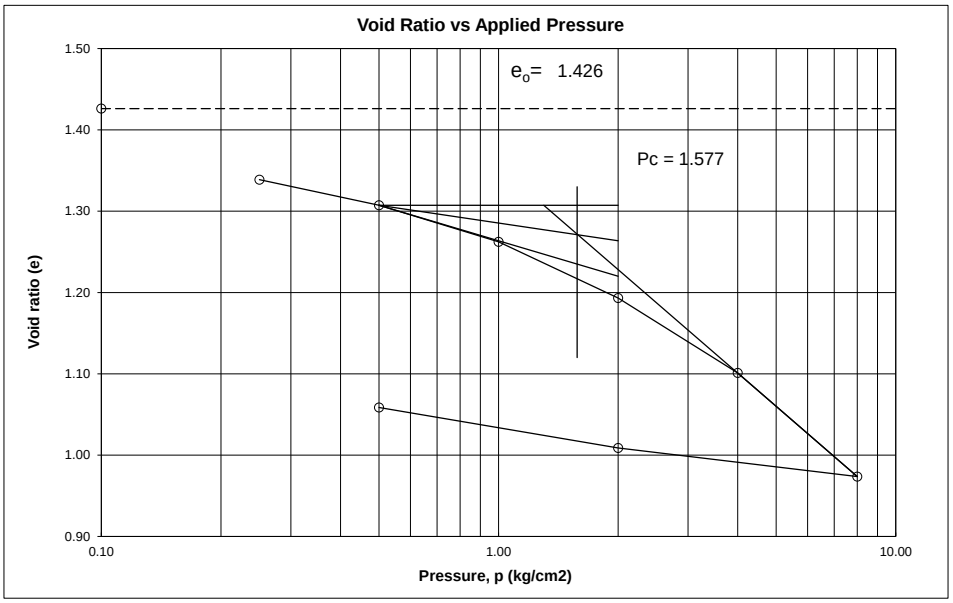

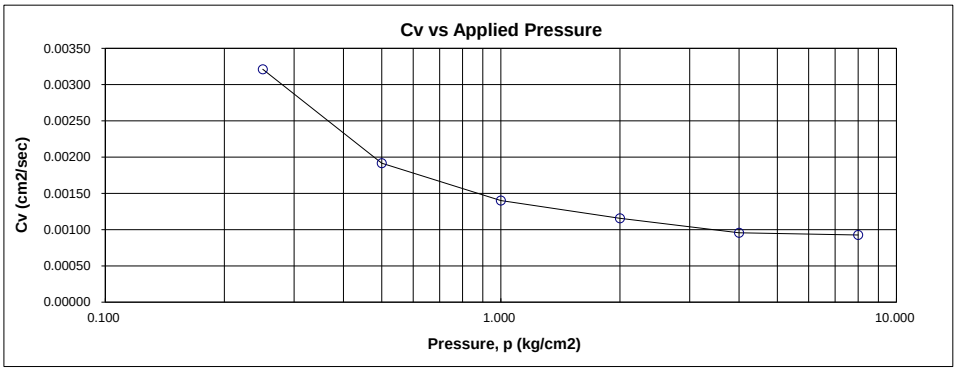

LABORATORIUM MEKANIKA TANAH
PT. SUWANDA KARYA MANDIRI
Komp. Buni Asri Mekar Rahayu Blok II No. B-7, Kopo Bandung (40219)
Telp. (022 - 5417700) Fax. (022 - 5412700)
email : pt_suwanda_karya_mandiri@yahoo.com

LSSM-045-IDN

CONSOLIDATION TEST

PROJECT : **Pembangunan Stasiun Pengamatan Penurunan Permukaan Tanah**
BORING NO. : **SPPT-08**
DEPTH : **31.00 - 31.50 m**

TESTED BY : Faizal
DATE : 12/08/2021

LOCATION : **Ds. Kepatihan, kec. Wiradesa, kab. Pekalongan**
DESCRIPT. : **UDS**

APPARATUS MEASUREMENTS
CONTAINER HEIGHT : 2.000 cm
CONTAINER DIAMETER : 5.000 cm
CONTAINER AREA (A) : 19.635 cm2

SPECIFIC GRAVITY (Gs) : 2.6349

SOLIDS HEIGHT (Hs) IN cm : 0.824
Hs = Ws/(Gs.γ_w. A)

DEGREE OF SATURATION IN %
TEST START : 104.48
TEST END :

WATER CONTENT	BEGINNING OF TEST	END OF TEST		
CONTAINER NO.	4A			
WT. CONTAINER + WET SOIL IN g	129.250			
WT. CONTAINER IN g	62.480			
WT. WET SOIL IN g	66.770			
WT. DRY SOIL (Ws) IN g	42.655			
WT. WATER (Ww) IN g	24.12			
WATER CONTENT (w) IN %	56.53			

APPLIED PRESSURE kg/cm^2	FINAL DIAL cm	DIAL CHANGE (ΔH) cm	Δe = ΔH/Hs	e = eo - ΣΔe	AVERAGE HEIGHT FOR LOAD cm	H cm	FITTING TIME (t 90) sec	Cv $\frac{0.848\ H^2}{t\ 90}$ cm^2/sec
0.00	0.9000			1.426	2.000			
		0.0360	0.0437			0.991	334.18	0.00249
0.25	0.8640			1.382	1.964			
		0.0370	0.0449			0.973	515.09	0.00156
0.50	0.8270			1.337	1.927			
		0.0640	0.0776			0.948	649.45	0.00117
1.00	0.7630			1.260	1.863			
		0.0900	0.1092			0.909	743.42	0.00094
2.00	0.6730			1.150	1.773			
		0.0890	0.1079			0.864	768.98	0.00082
4.00	0.5840			1.043	1.684			
		0.1200	0.1455			0.812	714.15	0.00078
8.00	0.4640			0.897	1.564			
		0.0410	0.0497			0.792		
2.00	0.5050			0.947	1.605			
		0.0470	0.0570			0.814		
0.50	0.5520			1.004	1.652			

LABORATORIUM MEKANIKA TANAH
PT. SUWANDA KARYA MANDIRI
Komp. Bumi Asri Mekar Rahayu Blok II No. B-7, Kopo Bandung (40218)
Telp. (022 - 5417700) Fax. (022 - 5412700)
email : pt_suwanda_karya_mandiri@yahoo.com

CONSOLIDATION TEST

PROJECT	: Pembangunan Stasiun Pengamatan Penurunan Permukaan Tanah			
LOCATION	: Ds. Kepatihan, kec. Wiradesa, kab. Pekalongan			
BORING NO.	: SPPT-08	Coefficient of Consolidation (Cv)	: 0.00093	cm^2/sec
DEPTH	: 31.00 - 31.50 m	Compression Index (Cc)	: 0.483	
TESTED BY	: Faizal	Swell Index (Cs)	: 0.071	
DATE	: 12/08/2021	Coeff. of Volume Comp. (mv)	: 0.051	cm^2/kg
DESCRIPTION	: UDS			

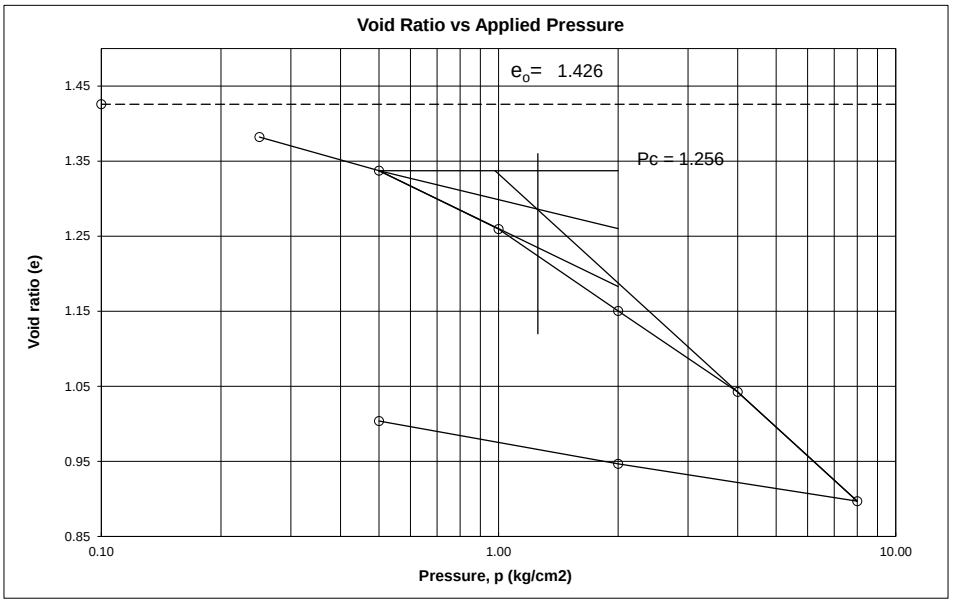

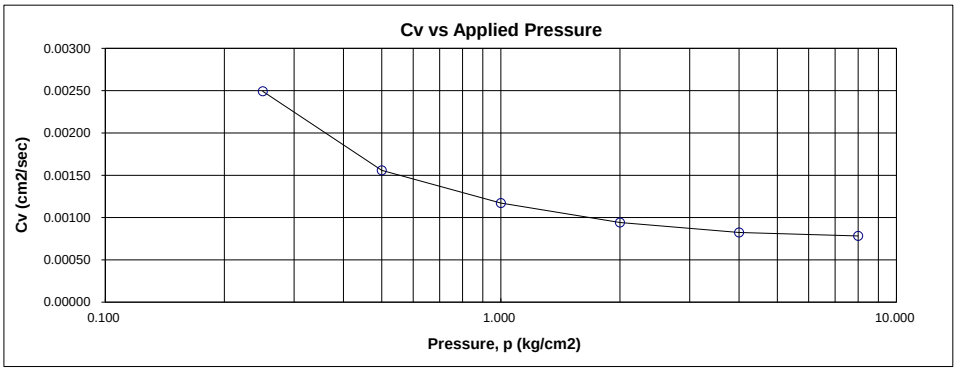

LABORATORIUM MEKANIKA TANAH
PT. SUWANDA KARYA MANDIRI
Komp. Buni Asri Mekar Rahayu Blok II No. B-7, Kopo Bandung (40219)
Telp. (022 - 5417700) Fax. (022 - 5412700)
email : pt_suwanda_karya_mandiri@yahoo.com

LSSM-045-IDN

CONSOLIDATION TEST

PROJECT : **Pembangunan Stasiun Pengamatan Penurunan Permukaan Tanah**
BORING NO. : **SPPT-08**
DEPTH : **39.00 - 39.50 m**

TESTED BY : Faizal
DATE : 15/08/2021

LOCATION : **Ds. Kepatihan, kec. Wiradesa, kab. Pekalongan**
DESCRIPT. : **UDS**

APPARATUS MEASUREMENTS
CONTAINER HEIGHT : 2.000 cm
CONTAINER DIAMETER : 5.000 cm
CONTAINER AREA (A) : 19.635 cm2

SPECIFIC GRAVITY (Gs) : 2.6735
SOLIDS HEIGHT (Hs) IN cm : 0.900
Hs = Ws/(Gs.γ_w. A)

DEGREE OF SATURATION IN %
TEST START : 98.69
TEST END :

WATER CONTENT

	BEGINNING OF TEST			
CONTAINER NO.	4A			
WT. CONTAINER + WET SOIL IN g	131.040			
WT. CONTAINER IN g	62.480			
WT. WET SOIL IN g	68.560			
WT. DRY SOIL (Ws) IN g	47.243			
WT. WATER (Ww) IN g	21.32			
WATER CONTENT (w) IN %	45.12			

APPLIED PRESSURE kg/cm^2	FINAL DIAL cm	DIAL CHANGE (ΔH) cm	Δe = ΔH/Hs	e = eo - Σ Δe	AVERAGE HEIGHT FOR LOAD cm	H cm	FITTING TIME (t 90) sec	Cv $\frac{0.848\ H^2}{t\ 90}$ cm^2/sec
0.00	0.9000			1.222	2.000			
		0.0440	0.0489			0.989	230.50	0.00360
0.25	0.8560			1.173	1.956			
		0.0240	0.0267			0.972	387.10	0.00207
0.50	0.8320			1.147	1.932			
		0.0400	0.0444			0.956	501.13	0.00155
1.00	0.7920			1.102	1.892			
		0.0720	0.0800			0.928	554.50	0.00132
2.00	0.7200			1.022	1.820			
		0.0830	0.0922			0.889	572.89	0.00117
4.00	0.6370			0.930	1.737			
		0.0970	0.1078			0.844	543.61	0.00111
8.00	0.5400			0.822	1.640			
		0.0230	0.0256			0.826		
2.00	0.5630			0.848	1.663			
		0.0270	0.0300			0.838		
0.50	0.5900			0.878	1.690			

LABORATORIUM MEKANIKA TANAH
PT. SUWANDA KARYA MANDIRI
Komp. Bumi Asri Mekar Rahayu Blok II No. B-7, Kopo Bandung (40218)
Telp. (022 - 5417700) Fax. (022 - 5412700)
email : pt_suwanda_karya_mandiri@yahoo.com

CONSOLIDATION TEST

PROJECT	: Pembangunan Stasiun Pengamatan Penurunan Permukaan Tanah			
LOCATION	: Ds. Kepatihan, kec. Wiradesa, kab. Pekalongan			
BORING NO.	: SPPT-08	Coefficient of Consolidation (Cv)	: 0.00129	cm^2/sec
DEPTH	: 39.00 - 39.50 m	Compression Index (Cc)	: 0.358	
TESTED BY	: Faizal	Swell Index (Cs)	: 0.037	
DATE	: 15/08/2021	Coeff. of Volume Comp. (mv)	: 0.042	cm^2/kg
DESCRIPTION	: UDS			

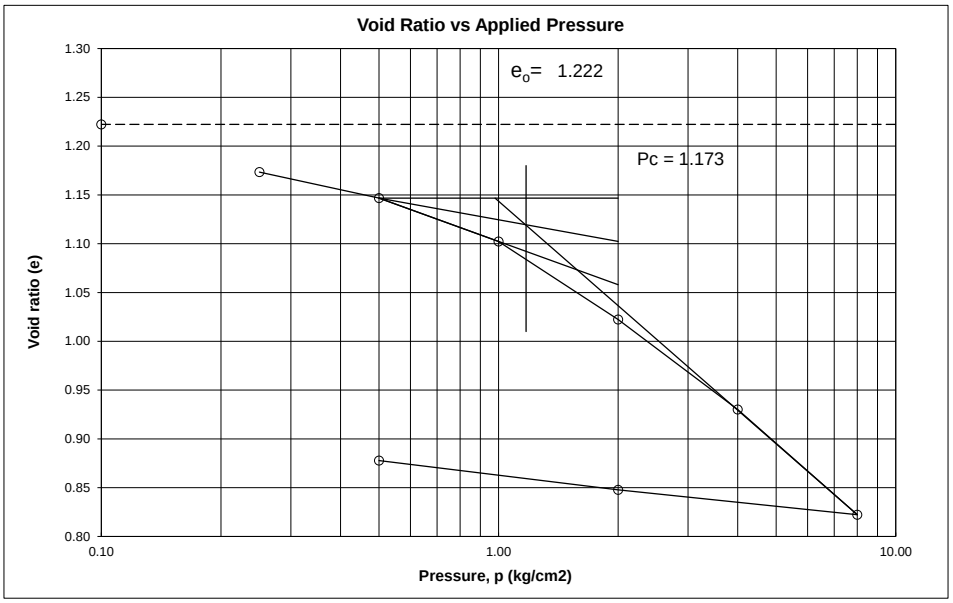

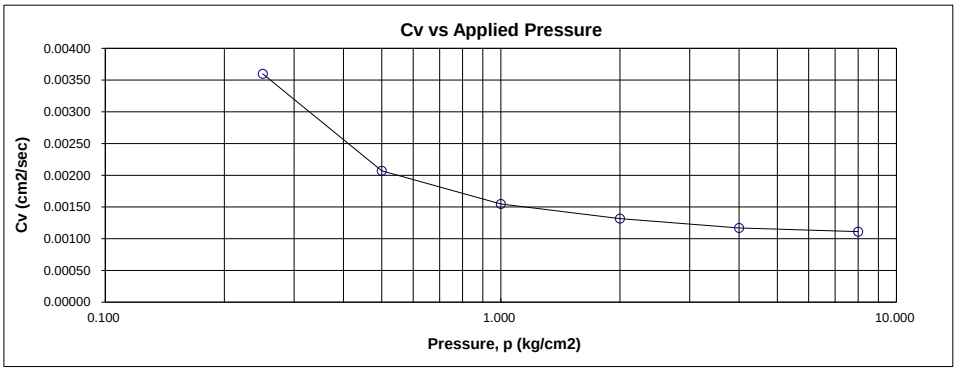

LABORATORIUM MEKANIKA TANAH
PT. SUWANDA KARYA MANDIRI
Komp. Bumi Asri Mekar Rahayu Blok II No. B-7, Kopo Bandung (40218)
Telp. (022 - 5417706) Fax. (022 - 5412706)
email : pt_suwanda_karya_mandiri@yahoo.com

CONSOLIDATION TEST

ASTM D-2435

PROJECT : **Pembangunan Stasiun Pengamatan Penurunan Permukaan Tanah**
BORING NO. : **SPPT-06**
DEPTH : **19.00 - 19.50 m**

TESTED BY : Faizal
DATE : 12/08/2021

LOCATION : **Ds. Siwalan, Kec. Siwalan, Kab. Pekalongan**
DESCRIPT. : **UDS**

APPARATUS MEASUREMENTS
CONTAINER HEIGHT : 2.000 cm
CONTAINER DIAMETER : 5.000 cm
CONTAINER AREA (A) : 19.635 cm2

SPECIFIC GRAVITY (Gs) : 2.5347

SOLIDS HEIGHT (Hs) IN cm : 0.382
Hs = Ws/(Gs.γ_w. A)

DEGREE OF SATURATION IN %
TEST START : 84.39
TEST END :

WATER CONTENT	BEGINNING OF TEST	END OF TEST		
CONTAINER NO.	2C			
WT. CONTAINER + WET SOIL IN g	108.670			
WT. CONTAINER IN g	62.850			
WT. WET SOIL IN g	45.820			
WT. DRY SOIL (Ws) IN g	19.009			
WT. WATER (Ww) IN g	26.81			
WATER CONTENT (w) IN %	141.04			

APPLIED PRESSURE kg/cm^2	FINAL DIAL cm	DIAL CHANGE (ΔH) cm	Δe = ΔH/Hs	e = eo - ΣΔe	AVERAGE HEIGHT FOR LOAD cm	H cm	FITTING TIME (t 90) sec	Cv $\frac{0.848\ H^2}{t\ 90}$ cm^2/sec
0.00	0.9000			4.236	2.000			
		0.0480	0.1257			0.988	1628.65	0.00051
0.25	0.8520			4.111	1.952			
		0.1110	0.2906			0.948	2232.60	0.00034
0.50	0.7410			3.820	1.841			
		0.1410	0.3692			0.885	2741.86	0.00024
1.00	0.6000			3.451	1.700			
		0.2440	0.6388			0.789	2948.41	0.00018
2.00	0.3560			2.812	1.456			
		0.2710	0.7095			0.660	2653.35	0.00014
4.00	0.0850			2.103	1.185			
		0.0410	0.1073			1.492		
2.00	0.1260			2.210	1.226			
		0.1620	0.4241			0.654		
0.50	0.2880			2.634	1.388			

LABORATORIUM MEKANIKA TANAH
PT. SUWANDA KARYA MANDIRI
Komp. Bumi Asri Mekar Rahayu Blok II No. B-7, Kopo Bandung (40218)
Telp. (022 - 5417760) Fax. (022 - 5412700)
email : pt_suwanda_karya_mandiri@yahoo.com

KAN Komite Akreditasi Nasional LSSM-045-IDN

CONSOLIDATION TEST

ASTM D-2435

PROJECT	: Pembangunan Stasiun Pengamatan Penurunan Permukaan Tanah			
LOCATION	: Ds. Siwalan, Kec. Siwalan, Kab. Pekalongan			
BORING NO.	: SPPT-06	Coefficient of Consolidation (Cv)	: 0.00014	cm^2/sec
DEPTH	: 19.00 - 19.50 m	Compression Index (Cc)	: 2.357	
TESTED BY	: Faizal	Swell Index (Cs)	: 0.353	
DATE	: 12/08/2021	Coeff. of Volume Comp. (mv)	: 0.134	cm^2/kg
DESCRIPTION	: UDS			

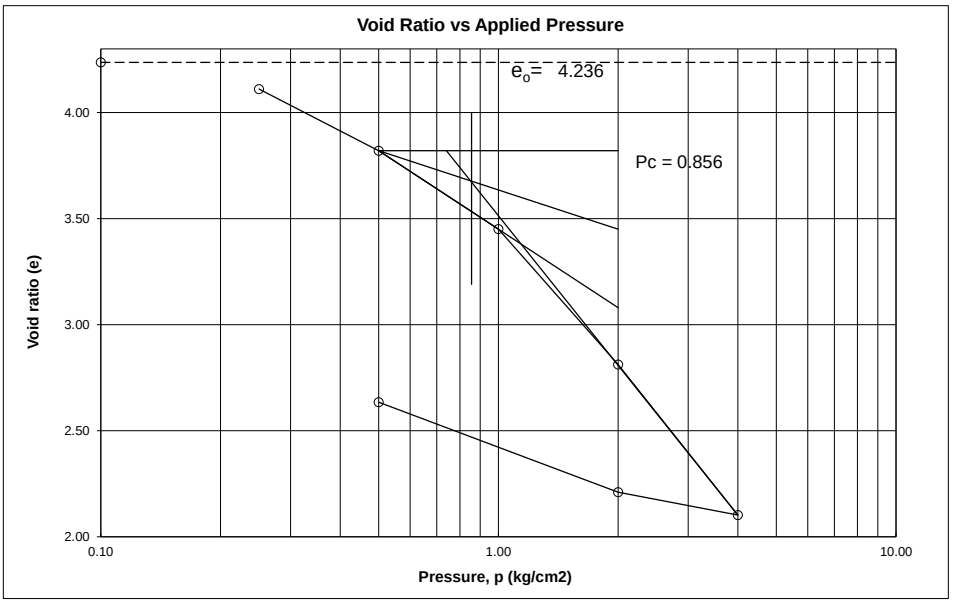

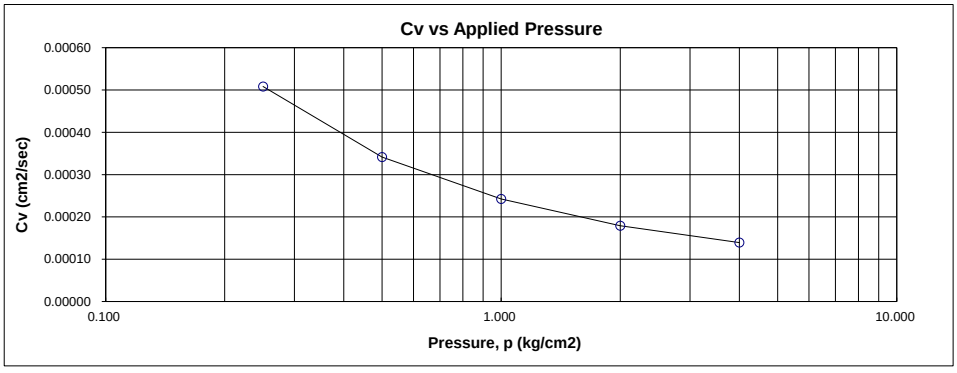

LABORATORIUM MEKANIKA TANAH
PT. SUWANDA KARYA MANDIRI
Komp. Buni Asri Mekar Rahayu Blok II No. B-7, Kopo Bandung (40219)
Telp. (022 - 5417700) Fax. (022 - 5412700)
email : pt_suwanda_karya_mandiri@yahoo.com

CONSOLIDATION TEST

PROJECT : **Pembangunan Stasiun Pengamatan Penurunan Permukaan Tanah**
BORING NO. : **SPPT-06**
DEPTH : **23.00 - 23.50 m**

TESTED BY : Faizal
DATE : 12/08/2021

LOCATION : **Ds. Siwalan, Kec. Siwalan, Kab. Pekalongan**
DESCRIPT. : **UDS**

APPARATUS MEASUREMENTS
CONTAINER HEIGHT : 2.000 cm
CONTAINER DIAMETER : 5.000 cm
CONTAINER AREA (A) : 19.635 cm2

SPECIFIC GRAVITY (Gs) : 2.6365
SOLIDS HEIGHT (Hs) IN cm : 0.865
Hs = Ws/(Gs.γ_w. A)

DEGREE OF SATURATION IN %
TEST START : 100.18
TEST END :

WATER CONTENT	BEGINNING OF TEST	END OF TEST		
CONTAINER NO.	3C			
WT. CONTAINER + WET SOIL IN g	131.420			
WT. CONTAINER IN g	64.320			
WT. WET SOIL IN g	67.100			
WT. DRY SOIL (Ws) IN g	44.770			
WT. WATER (Ww) IN g	22.33			
WATER CONTENT (w) IN %	49.88			

APPLIED PRESSURE kg/cm^2	FINAL DIAL cm	DIAL CHANGE (ΔH) cm	Δe = ΔH/Hs	e = eo - ΣΔe	AVERAGE HEIGHT FOR LOAD cm	H cm	FITTING TIME (t 90) sec	Cv $\frac{0.848\ H^2}{t\ 90}$ cm^2/sec
0.00	0.9000			1.313	2.000			
		0.0340	0.0393			0.992	235.22	0.00354
0.25	0.8660			1.273	1.966			
		0.0210	0.0243			0.978	384.05	0.00211
0.50	0.8450			1.249	1.945			
		0.0320	0.0370			0.965	532.82	0.00148
1.00	0.8130			1.212	1.913			
		0.0530	0.0613			0.943	614.40	0.00123
2.00	0.7600			1.151	1.860			
		0.0590	0.0682			0.915	669.34	0.00106
4.00	0.7010			1.083	1.801			
		0.0840	0.0971			0.880	637.66	0.00103
8.00	0.6170			0.985	1.717			
		0.0210	0.0243			0.864		
2.00	0.6380			1.010	1.738			
		0.0280	0.0324			0.876		
0.50	0.6660			1.042	1.766			

LABORATORIUM MEKANIKA TANAH
PT. SUWANDA KARYA MANDIRI
Komp. Bumi Asri Mekar Rahayu Blok II No. B-7, Kopo Bandung (40218)
Telp. (022 - 5417700) Fax. (022 - 5412700)
email : pt_suwanda_karya_mandiri@yahoo.com

CONSOLIDATION TEST

PROJECT	: Pembangunan Stasiun Pengamatan Penurunan Permukaan Tanah			
LOCATION	: Ds. Siwalan, Kec. Siwalan, Kab. Pekalongan			
BORING NO.	: SPPT-06	Coefficient of Consolidation (Cv)	: 0.00120	cm^2/sec
DEPTH	: 23.00 - 23.50 m	Compression Index (Cc)	: 0.323	
TESTED BY	: Faizal	Swell Index (Cs)	: 0.038	
DATE	: 12/08/2021	Coeff. of Volume Comp. (mv)	: 0.033	cm^2/kg
DESCRIPTION	: UDS			

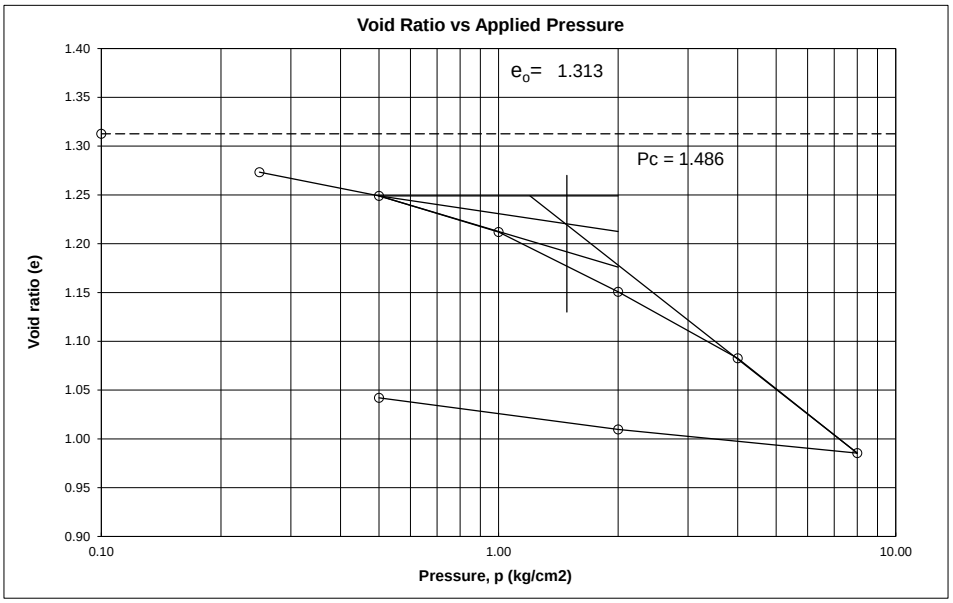

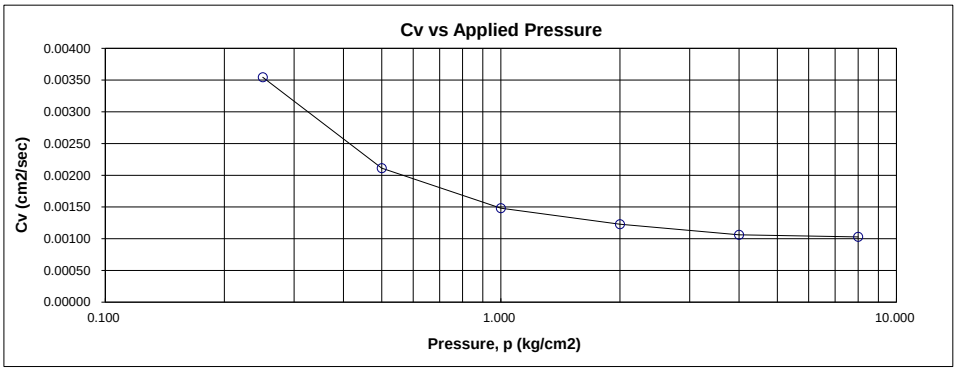

LABORATORIUM MEKANIKA TANAH
PT. SUWANDA KARYA MANDIRI
Komp. Buni Asri Mekar Rahayu Blok II No. B-7, Kopo Bandung (40219)
Telp. (022 - 5417700) Fax. (022 - 5412700)
email : pt_suwanda_karya_mandiri@yahoo.com

CONSOLIDATION TEST

PROJECT : **Pembangunan Stasiun Pengamatan Penurunan Permukaan Tanah**
BORING NO. : **SPPT-06**
DEPTH : **35.00 - 35.50 m**

TESTED BY : Faizal
DATE : 12/08/2021

LOCATION : **Ds. Siwalan, Kec. Siwalan, Kab. Pekalongan**
DESCRIPT. : **UDS**

APPARATUS MEASUREMENTS
CONTAINER HEIGHT : 2.000 cm
CONTAINER DIAMETER : 5.000 cm
CONTAINER AREA (A) : 19.635 cm2

SPECIFIC GRAVITY (Gs) : 2.6265

SOLIDS HEIGHT (Hs) IN cm : 1.172
Hs = Ws/(Gs.γ_w. A)

DEGREE OF SATURATION IN %
TEST START : 98.75
TEST END :

WATER CONTENT	BEGINNING OF TEST	END OF TEST		
CONTAINER NO.	4C			
WT. CONTAINER + WET SOIL IN g	136.370			
WT. CONTAINER IN g	59.890			
WT. WET SOIL IN g	76.480			
WT. DRY SOIL (Ws) IN g	60.416			
WT. WATER (Ww) IN g	16.06			
WATER CONTENT (w) IN %	26.59			

APPLIED PRESSURE kg/cm^2	FINAL DIAL cm	DIAL CHANGE (ΔH) cm	Δe = ΔH/Hs	e = eo - ΣΔe	AVERAGE HEIGHT FOR LOAD cm	H cm	FITTING TIME (t 90) sec	Cv $\frac{0.848\ H^2}{t\ 90}$ cm^2/sec
0.00	0.9000			0.707	2.000			
		0.0830	0.0708			0.979	95.26	0.00854
0.25	0.8170			0.636	1.917			
		0.0420	0.0359			0.948	194.40	0.00392
0.50	0.7750			0.601	1.875			
		0.0500	0.0427			0.925	279.94	0.00259
1.00	0.7250			0.558	1.825			
		0.0630	0.0538			0.897	314.65	0.00217
2.00	0.6620			0.504	1.762			
		0.0620	0.0529			0.866	339.86	0.00187
4.00	0.6000			0.451	1.700			
		0.0850	0.0726			0.829	317.40	0.00183
8.00	0.5150			0.379	1.615			
		0.0270	0.0230			0.814		
2.00	0.5420			0.402	1.642			
		0.0310	0.0265			0.829		
0.50	0.5730			0.428	1.673			

LABORATORIUM MEKANIKA TANAH
PT. SUWANDA KARYA MANDIRI
Komp. Bumi Asri Mekar Rahayu Blok II No. B-7, Kopo Bandung (40218)
Telp. (022 - 5417700) Fax. (022 - 5412700)
email : pt_suwanda_karya_mandiri@yahoo.com

CONSOLIDATION TEST

PROJECT	: Pembangunan Stasiun Pengamatan Penurunan Permukaan Tanah			
LOCATION	: Ds. Siwalan, Kec. Siwalan, Kab. Pekalongan			
BORING NO.	: SPPT-06	Coefficient of Consolidation (Cv)	: 0.00212	cm^2/sec
DEPTH	: 35.00 - 35.50 m	Compression Index (Cc)	: 0.241	
TESTED BY	: Faizal	Swell Index (Cs)	: 0.033	
DATE	: 12/08/2021	Coeff. of Volume Comp. (mv)	: 0.062	cm^2/kg
DESCRIPTION	: UDS			

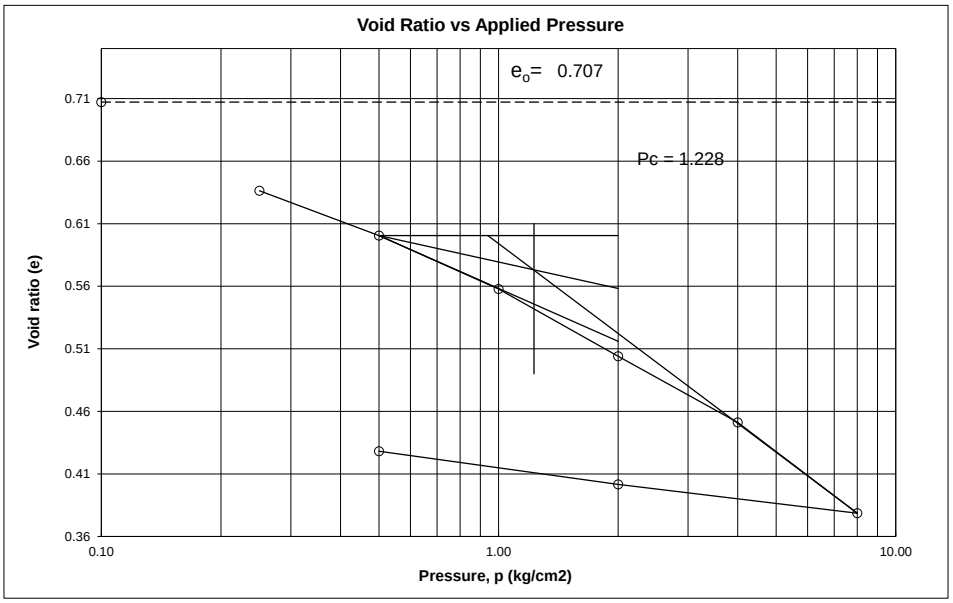

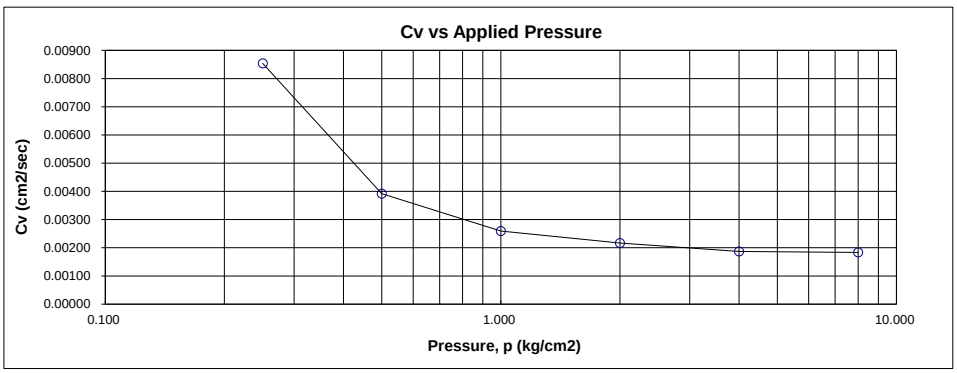

LABORATORIUM MEKANIKA TANAH
PT. SUWANDA KARYA MANDIRI
Komp. Buni Asri Mekar Rahayu Blok II No. B-7, Kopo Bandung (40219)
Telp. (022 - 5417700) Fax. (022 - 5412700)
email : pt_suwanda_karya_mandiri@yahoo.com

CONSOLIDATION TEST

PROJECT : **Pembangunan Stasiun Pengamatan Penurunan Permukaan Tanah**
BORING NO. : **SPPT-06**
DEPTH : **43.00 - 43.50 m**

TESTED BY : Faizal
DATE : 12/08/2021

LOCATION : **Ds. Siwalan, Kec. Siwalan, Kab. Pekalongan**
DESCRIPT. : **DS**

APPARATUS MEASUREMENTS
CONTAINER HEIGHT : 2.000 cm
CONTAINER DIAMETER : 5.000 cm
CONTAINER AREA (A) : 19.635 cm2

SPECIFIC GRAVITY (Gs) : 2.6055
SOLIDS HEIGHT (Hs) IN cm : 0.698
Hs = Ws/(Gs.γ_w. A)

DEGREE OF SATURATION IN %
TEST START : 86.11
TEST END :

WATER CONTENT	BEGINNING OF TEST	END OF TEST		
CONTAINER NO.	1B			
WT. CONTAINER + WET SOIL IN g	121.030			
WT. CONTAINER IN g	63.290			
WT. WET SOIL IN g	57.740			
WT. DRY SOIL (Ws) IN g	35.733			
WT. WATER (Ww) IN g	22.01			
WATER CONTENT (w) IN %	61.59			

APPLIED PRESSURE kg/cm^2	FINAL DIAL cm	DIAL CHANGE (ΔH) cm	Δe = ΔH/Hs	e = eo - ΣΔe	AVERAGE HEIGHT FOR LOAD cm	H cm	FITTING TIME (t 90) sec	Cv $\frac{0.848\ H^2}{t\ 90}$ cm^2/sec
0.00	0.9000			1.863	2.000			
		0.0260	0.0372			0.994	393.22	0.00213
0.25	0.8740			1.826	1.974			
		0.0360	0.0515			0.978	610.57	0.00133
0.50	0.8380			1.775	1.938			
		0.0480	0.0687			0.957	730.81	0.00106
1.00	0.7900			1.706	1.890			
		0.0750	0.1074			0.926	799.35	0.00091
2.00	0.7150			1.599	1.815			
		0.0840	0.1203			0.887	825.85	0.00081
4.00	0.6310			1.478	1.731			
		0.1200	0.1718			0.836	803.74	0.00074
8.00	0.5110			1.306	1.611			
		0.0390	0.0558			0.815		
2.00	0.5500			1.362	1.650			
		0.0470	0.0673			0.837		
0.50	0.5970			1.430	1.697			

LABORATORIUM MEKANIKA TANAH
PT. SUWANDA KARYA MANDIRI
Komp. Bumi Asri Mekar Rahayu Blok II No. B-7, Kopo Bandung (40218)
Telp. (022 - 5417700) Fax. (022 - 5412700)
email : pt_suwanda_karya_mandiri@yahoo.com

CONSOLIDATION TEST

PROJECT	: Pembangunan Stasiun Pengamatan Penurunan Permukaan Tanah			
LOCATION	: Ds. Siwalan, Kec. Siwalan, Kab. Pekalongan			
BORING NO.	: SPPT-06	Coefficient of Consolidation (Cv)	: 0.00088	cm^2/sec
DEPTH	: 43.00 - 43.50 m	Compression Index (Cc)	: 0.571	
TESTED BY	: Faizal	Swell Index (Cs)	: 0.082	
DATE	: 12/08/2021	Coeff. of Volume Comp. (mv)	: 0.042	cm^2/kg
DESCRIPTION	: DS			

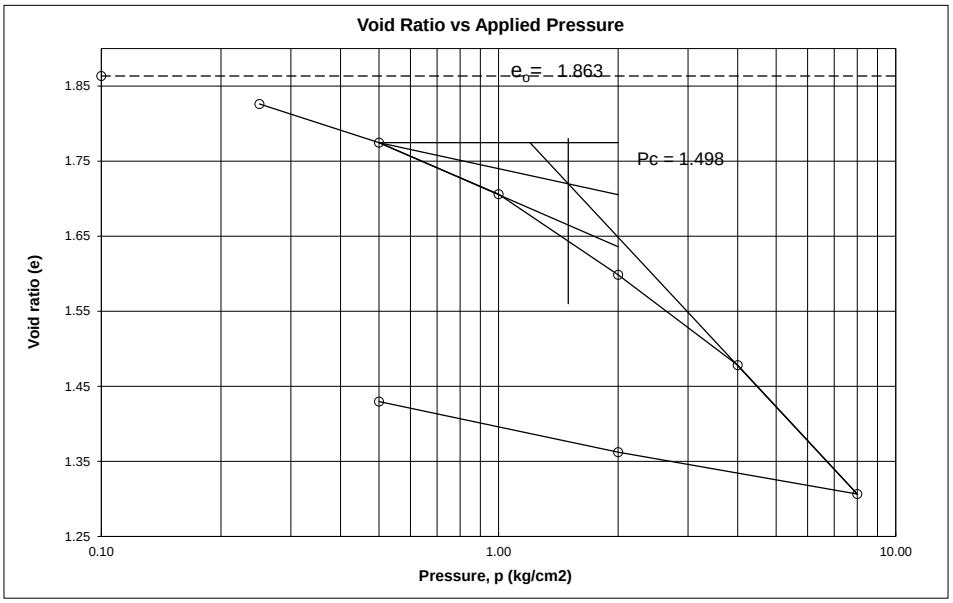

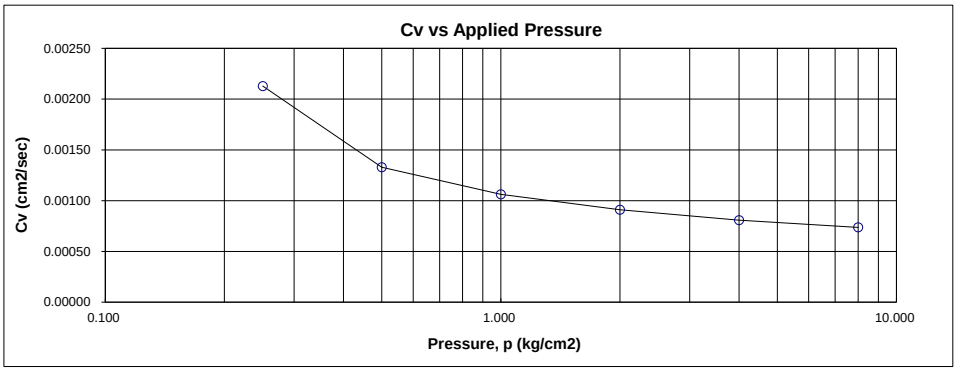

LABORATORIUM MEKANIKA TANAH
PT. SUWANDA KARYA MANDIRI
Komp. Bumi Asri Mekar Rahayu Blok II No. B-7, Kopo Bandung (40218)
Telp. (022 - 5417700) Fax. (022 - 5412700)
email : pt_suwanda_karya_mandiri@yahoo.com

LSSM-045-IDN

CONSOLIDATION

ASTM D 2435

PROJECT : **Pembangunan Stasiun Pengamatan Permukaan Tanah**
BORING NO. : **SPPT-03**
DEPTH : **11.00 - 11.50 m**

TESTED BY : Faizal
DATE : 17/09/2021

LOCATION : **Kel. Tirto, Kec. Pekalongan Barat, Kota Pekalongan**
DESCRIPT. : **-**

APPARATUS MEASUREMENTS
CONTAINER HEIGHT : 2.000 cm
CONTAINER DIAMETER : 5.000 cm
CONTAINER AREA (A) : 19.635 cm2

SPECIFIC GRAVITY (Gs) : 2.5967

SOLIDS HEIGHT (Hs) IN cm : 0.782
Hs = Ws/(Gs.γ_w. A)

DEGREE OF SATURATION IN %
TEST START : 111.39
TEST END :

WATER CONTENT

	BEGINNING OF TEST		END OF TEST	
CONTAINER NO.	1C			
WT. CONTAINER + WET SOIL IN g	132.360			
WT. CONTAINER IN g	65.860			
WT. WET SOIL IN g	66.500			
WT. DRY SOIL (Ws) IN g	39.851			
WT. WATER (Ww) IN g	26.65			
WATER CONTENT (w) IN %	66.87			

APPLIED PRESSURE kg/cm^2	FINAL DIAL cm	DIAL CHANGE (ΔH) cm	Δe = ΔH/Hs	e = eo - ΣΔe	AVERAGE HEIGHT FOR LOAD cm	H cm	FITTING TIME (t 90) sec	Cv $\frac{0.848\ H^2}{t\ 90}$ cm^2/sec
0.00	0.9000			1.559	2.000			
		0.0390	0.0499			0.990	434.17	0.00192
0.25	0.8610			1.509	1.961			
		0.0470	0.0601			0.969	606.74	0.00131
0.50	0.8140			1.449	1.914			
		0.0950	0.1215			0.933	730.81	0.00101
1.00	0.7190			1.327	1.819			
		0.1600	0.2047			0.870	821.40	0.00078
2.00	0.5590			1.123	1.659			
		0.1670	0.2137			0.788	857.30	0.00061
4.00	0.3920			0.909	1.492			
		0.1760	0.2252			0.702	786.26	0.00053
8.00	0.2160			0.684	1.316			
		0.0320	0.0409			0.666		
2.00	0.2480			0.725	1.348			
		0.0610	0.0780			0.689		
0.50	0.3090			0.803	1.409			

LABORATORIUM MEKANIKA TANAH
PT. SUWANDA KARYA MANDIRI
Komp. Bumi Asri Mekar Rahayu Blok II No. B-7, Kopo Bandung (40218)
Telp. (022 - 5417706) Fax. (022 - 5412706)
email : pt_suwanda_karya_mandiri@yahoo.com

LSSM-045-IDN

CONSOLIDATION

ASTM D 2435

PROJECT	: Pembangunan Stasiun Pengamatan Permukaan Tanah			
LOCATION	: Kel. Tirto, Kec. Pekalongan Barat, Kota Pekalongan			
BORING NO.	: SPPT-03	Coefficient of Consolidation (Cv)	: 0.00073	cm^2/sec
DEPTH	: 11.00 - 11.50 m	Compression Index (Cc)	: 0.748	
TESTED BY	: Faizal	Swell Index (Cs)	: 0.079	
DATE	: 17/09/2021	Coeff. of Volume Comp. (mv)	: 0.073	cm^2/kg
DESCRIPTION	: -			

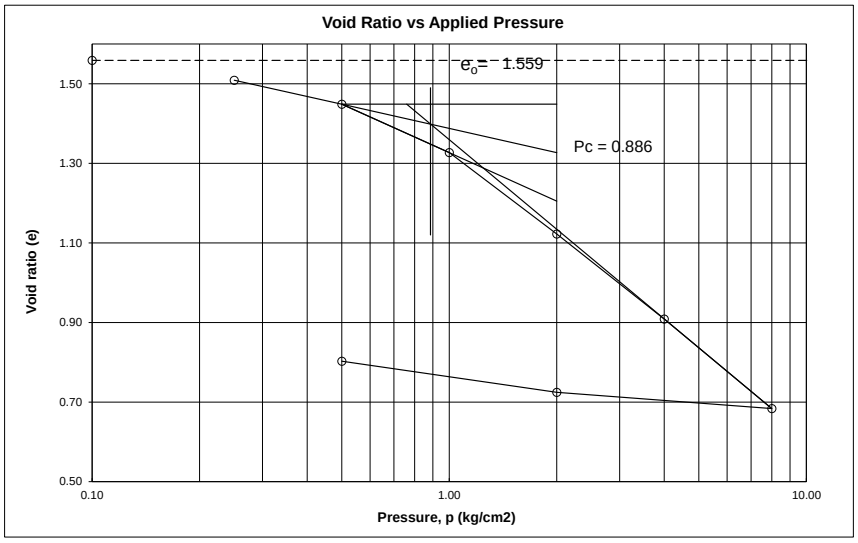

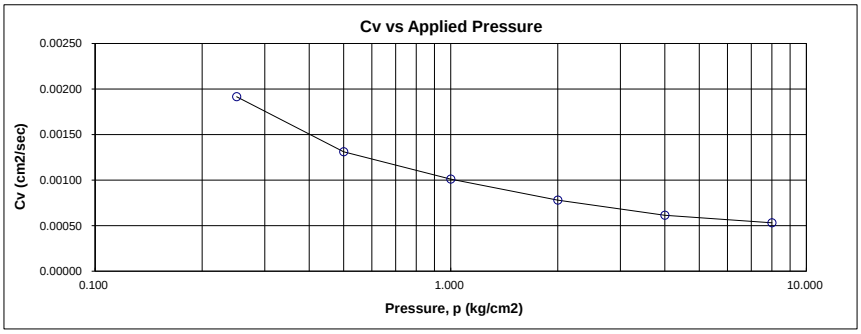

LABORATORIUM MEKANIKA TANAH
PT. SUWANDA KARYA MANDIRI
Komp. Bumi Asri Mekar Rahayu Blok II No. B-7, Kopo Bandung (40218)
Telp. (022 - 5417700) Fax. (022 - 5412700)
email : pt_suwanda_karya_mandiri@yahoo.com

KAN Komite Akreditasi Nasional LSSM-045-IDN

CONSOLIDATION

ASTM D 2435

PROJECT : **Pembangunan Stasiun Pengamatan Permukaan Tanah**
BORING NO. : **SPPT-03**
DEPTH : **15.00 - 15.50 m**

TESTED BY : Faizal
DATE : 17/09/2021

LOCATION : **Kel. Tirto, Kec. Pekalongan Barat, Kota Pekalongan**
DESCRIPT. : **-**

APPARATUS MEASUREMENTS
CONTAINER HEIGHT : 2.000 cm
CONTAINER DIAMETER : 5.000 cm
CONTAINER AREA (A) : 19.635 cm2

SPECIFIC GRAVITY (Gs) : 2.5750

SOLIDS HEIGHT (Hs) IN cm : 0.659
Hs = Ws/(Gs.γ_w. A)

DEGREE OF SATURATION IN %
TEST START : 109.05
TEST END :

WATER CONTENT

	BEGINNING OF TEST			
CONTAINER NO.	2C			
WT. CONTAINER + WET SOIL IN g	124.890			
WT. CONTAINER IN g	62.850			
WT. WET SOIL IN g	62.040			
WT. DRY SOIL (Ws) IN g	33.333			
WT. WATER (Ww) IN g	28.71			
WATER CONTENT (w) IN %	86.12			

APPLIED PRESSURE kg/cm^2	FINAL DIAL cm	DIAL CHANGE (ΔH) cm	Δe = ΔH/Hs	e = eo - ΣΔe	AVERAGE HEIGHT FOR LOAD cm	H cm	FITTING TIME (t 90) sec	Cv $\frac{0.848\ H^2}{t\ 90}$ cm^2/sec
0.00	0.9000			2.034	2.000			
		0.0850	0.1289			0.979	773.29	0.00105
0.25	0.8150			1.905	1.915			
		0.1150	0.1744			0.929	1053.37	0.00069
0.50	0.7000			1.730	1.800			
		0.1240	0.1881			0.869	1204.22	0.00053
1.00	0.5760			1.542	1.676			
		0.1560	0.2366			0.799	1291.78	0.00042
2.00	0.4200			1.306	1.520			
		0.1800	0.2730			0.715	1242.15	0.00035
4.00	0.2400			1.033	1.340			
		0.0200	0.0303			1.680		
2.00	0.2600			1.063	1.360			
		0.0550	0.0834			0.694		
0.50	0.3150			1.146	1.415			

LABORATORIUM MEKANIKA TANAH
PT. SUWANDA KARYA MANDIRI
Komp. Bumi Asri Mekar Rahayu Blok II No. B-7, Kopo Bandung (40218)
Telp. (022 - 5417700) Fax. (022 - 5412700)
email : pt_suwanda_karya_mandiri@yahoo.com

LSSM-045-IDN

CONSOLIDATION

ASTM D 2435

PROJECT	: Pembangunan Stasiun Pengamatan Permukaan Tanah			
LOCATION	: Kel. Tirto, Kec. Pekalongan Barat, Kota Pekalongan			
BORING NO.	: SPPT-03	Coefficient of Consolidation (Cv)	: 0.00061	cm^2/sec
DEPTH	: 15.00 - 15.50 m	Compression Index (Cc)	: 0.907	
TESTED BY	: Faizal	Swell Index (Cs)	: 0.076	
DATE	: 17/09/2021	Coeff. of Volume Comp. (mv)	: 0.127	cm^2/kg
DESCRIPTION	: -			

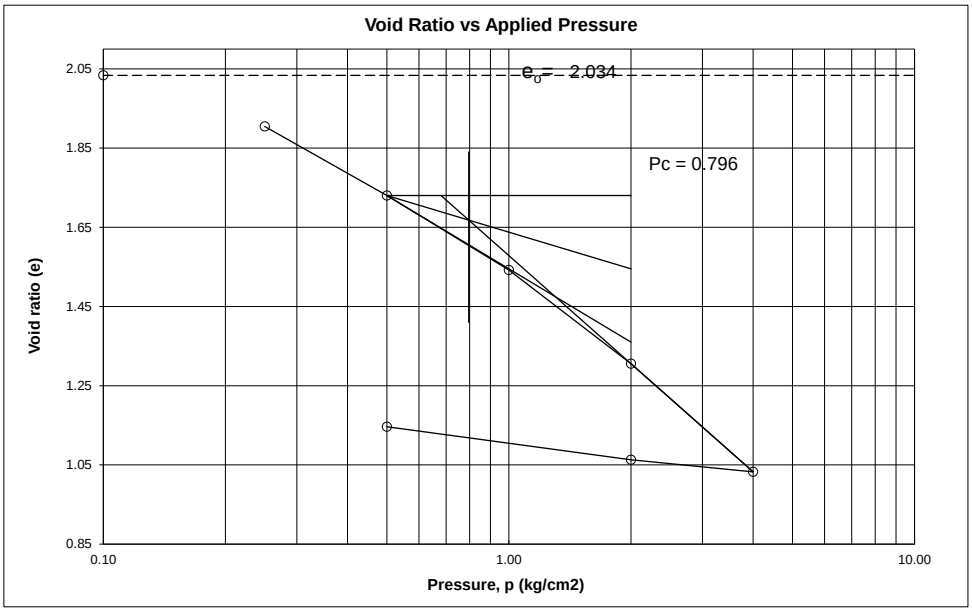

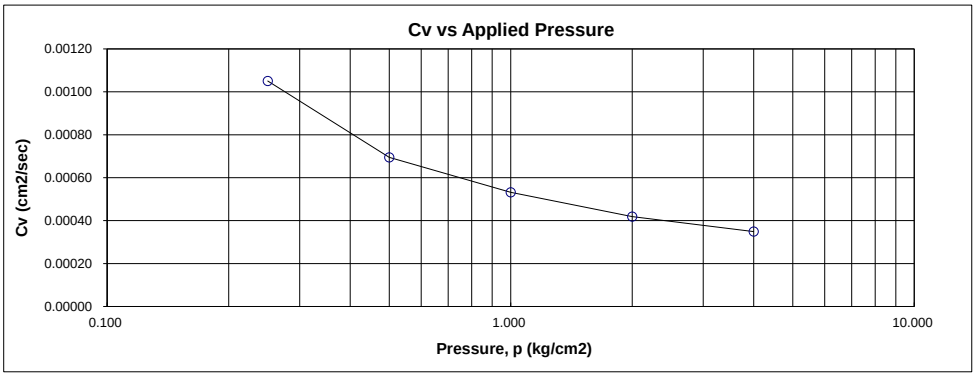

LABORATORIUM MEKANIKA TANAH
PT. SUWANDA KARYA MANDIRI
LSSM-045-IDN

CONSOLIDATION

ASTM D 2435

PROJECT : **Pembangunan Stasiun Pengamatan Permukaan Tanah**
BORING NO. : **SPPT-03**
DEPTH : **27.00 - 27.50 m**

TESTED BY : Faizal
DATE : 17/09/2021

LOCATION : **Kel. Tirto, Kec. Pekalongan Barat, Kota Pekalongan**
DESCRIPT. : **-**

APPARATUS MEASUREMENTS
CONTAINER HEIGHT : 2.000 cm
CONTAINER DIAMETER : 5.000 cm
CONTAINER AREA (A) : 19.635 cm2

SPECIFIC GRAVITY (Gs) : 2.6128
SOLIDS HEIGHT (Hs) IN cm : 0.822
Hs = Ws/(Gs.γ_w. A)

DEGREE OF SATURATION IN %
TEST START : 113.61
TEST END :

WATER CONTENT

	BEGINNING OF TEST		END OF TEST	
CONTAINER NO.	3C			
WT. CONTAINER + WET SOIL IN g	132.760			
WT. CONTAINER IN g	64.320			
WT. WET SOIL IN g	68.440			
WT. DRY SOIL (Ws) IN g	42.158			
WT. WATER (Ww) IN g	26.28			
WATER CONTENT (w) IN %	62.34			

APPLIED PRESSURE kg/cm^2	FINAL DIAL cm	DIAL CHANGE (ΔH) cm	Δe = ΔH/Hs	e = eo - ΣΔe	AVERAGE HEIGHT FOR LOAD cm	H cm	FITTING TIME (t 90) sec	Cv $\frac{0.848\ H^2}{t\ 90}$ cm^2/sec
0.00	0.9000			1.434	2.000			
		0.1190	0.1448			0.970	354.29	0.00225
0.25	0.7810			1.289	1.881			
		0.0660	0.0803			0.924	543.61	0.00133
0.50	0.7150			1.209	1.815			
		0.0740	0.0900			0.889	649.45	0.00103
1.00	0.6410			1.119	1.741			
		0.0860	0.1047			0.849	722.45	0.00085
2.00	0.5550			1.014	1.655			
		0.0770	0.0937			0.808	747.65	0.00074
4.00	0.4780			0.920	1.578			
		0.1090	0.1326			0.762	718.30	0.00069
8.00	0.3690			0.788	1.469			
		0.0400	0.0487			0.745		
2.00	0.4090			0.836	1.509			
		0.0410	0.0499			0.765		
0.50	0.4500			0.886	1.550			

LABORATORIUM MEKANIKA TANAH
PT. SUWANDA KARYA MANDIRI
Komp. Bumi Asri Mekar Rahayu Blok II No. B-7, Kopo Bandung (40218)
Telp. (022 - 5417706) Fax. (022 - 5412706)
email : pt_suwanda_karya_mandiri@yahoo.com

LSSM-045-IDN

CONSOLIDATION

ASTM D 2435

PROJECT	: Pembangunan Stasiun Pengamatan Permukaan Tanah			
LOCATION	: Kel. Tirto, Kec. Pekalongan Barat, Kota Pekalongan			
BORING NO.	: SPPT-03	Coefficient of Consolidation (Cv)	: 0.00083	cm^2/sec
DEPTH	: 27.00 - 27.50 m	Compression Index (Cc)	: 0.441	
TESTED BY	: Faizal	Swell Index (Cs)	: 0.065	
DATE	: 17/09/2021	Coeff. of Volume Comp. (mv)	: 0.092	cm^2/kg
DESCRIPTION	: -			

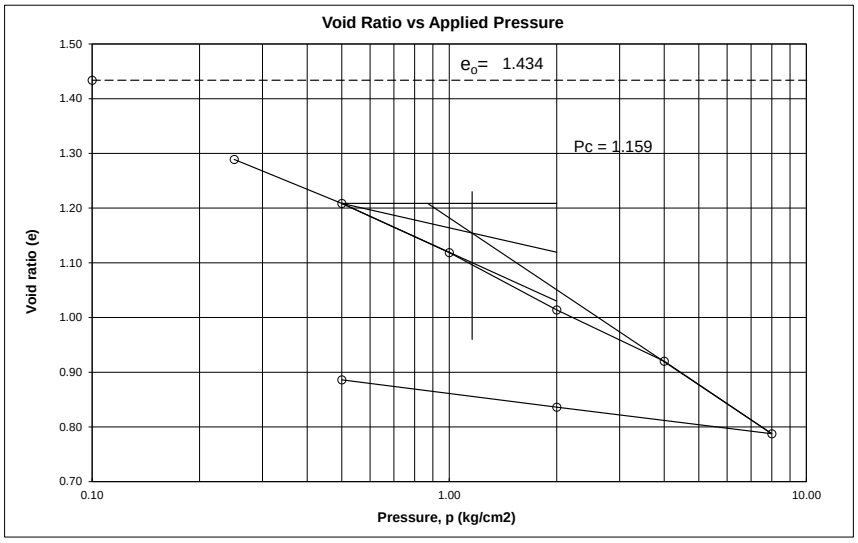

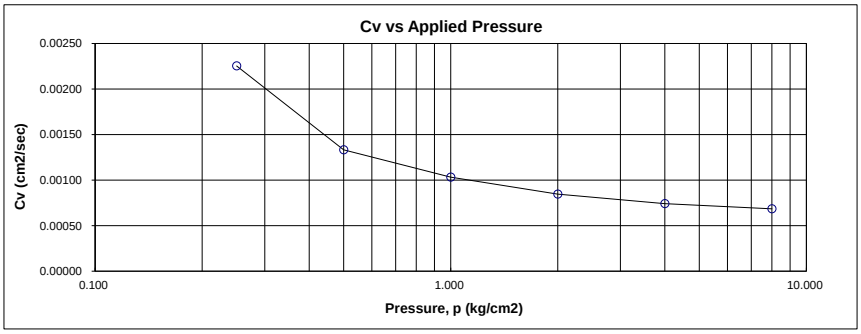

LABORATORIUM MEKANIKA TANAH
PT. SUWANDA KARYA MANDIRI
Komp. Bumi Asri Mekar Rahayu Blok II No. B-7, Kopo Bandung (40218)
Telp. (022 - 5417700) Fax. (022 - 5412700)
email : pt_suwanda_karya_mandiri@yahoo.com

LSSM-045-IDN

CONSOLIDATION

ASTM D 2435

PROJECT : **Pembangunan Stasiun Pengamatan Permukaan Tanah**
BORING NO. : **SPPT-03**
DEPTH : **33.00 - 33.50 m**

TESTED BY : Faizal
DATE : 17/09/2021

LOCATION : **Kel. Tirto, Kec. Pekalongan Barat, Kota Pekalongan**
DESCRIPT. : **-**

APPARATUS MEASUREMENTS
CONTAINER HEIGHT : 2.000 cm
CONTAINER DIAMETER : 5.000 cm
CONTAINER AREA (A) : 19.635 cm2

SPECIFIC GRAVITY (Gs) : 2.6305
SOLIDS HEIGHT (Hs) IN cm : 0.933
Hs = Ws/(Gs.γ_w. A)

DEGREE OF SATURATION IN %
TEST START : 105.04
TEST END :

WATER CONTENT

	BEGINNING OF TEST		END OF TEST	
CONTAINER NO.	4C			
WT. CONTAINER + WET SOIL IN g	130.100			
WT. CONTAINER IN g	59.890			
WT. WET SOIL IN g	70.210			
WT. DRY SOIL (Ws) IN g	48.212			
WT. WATER (Ww) IN g	22.00			
WATER CONTENT (w) IN %	45.63			

APPLIED PRESSURE kg/cm^2	FINAL DIAL cm	DIAL CHANGE (ΔH) cm	Δe = ΔH/Hs	e = eo - ΣΔe	AVERAGE HEIGHT FOR LOAD cm	H cm	FITTING TIME (t 90) sec	Cv $\frac{0.848\ H^2}{t\ 90}$ cm^2/sec
0.00	0.9000			1.143	2.000			
		0.0190	0.0204			0.995	207.58	0.00405
0.25	0.8810			1.122	1.981			
		0.0130	0.0139			0.987	309.17	0.00267
0.50	0.8680			1.108	1.968			
		0.0240	0.0257			0.978	372.01	0.00218
1.00	0.8440			1.083	1.944			
		0.0420	0.0450			0.962	424.54	0.00185
2.00	0.8020			1.038	1.902			
		0.0480	0.0514			0.939	450.46	0.00166
4.00	0.7540			0.986	1.854			
		0.0780	0.0836			0.908	440.65	0.00158
8.00	0.6760			0.903	1.776			
		0.0430	0.0461			0.899		
2.00	0.7190			0.949	1.819			
		0.0480	0.0514			0.922		
0.50	0.7670			1.000	1.867			

LABORATORIUM MEKANIKA TANAH
PT. SUWANDA KARYA MANDIRI
Komp. Bumi Asri Mekar Rahayu Blok II No. B-7, Kopo Bandung (40218)
Telp. (022 - 5417700) Fax. (022 - 5412700)
email : pt_suwanda_karya_mandiri@yahoo.com

LSSM-045-IDN

CONSOLIDATION

ASTM D 2435

PROJECT	: Pembangunan Stasiun Pengamatan Permukaan Tanah			
LOCATION	: Kel. Tirto, Kec. Pekalongan Barat, Kota Pekalongan			
BORING NO.	: SPPT-03	Coefficient of Consolidation (Cv)	: 0.00182	cm^2/sec
DEPTH	: 33.00 - 33.50 m	Compression Index (Cc)	: 0.278	
TESTED BY	: Faizal	Swell Index (Cs)	: 0.065	
DATE	: 17/09/2021	Coeff. of Volume Comp. (mv)	: 0.022	cm^2/kg
DESCRIPTION	: -			

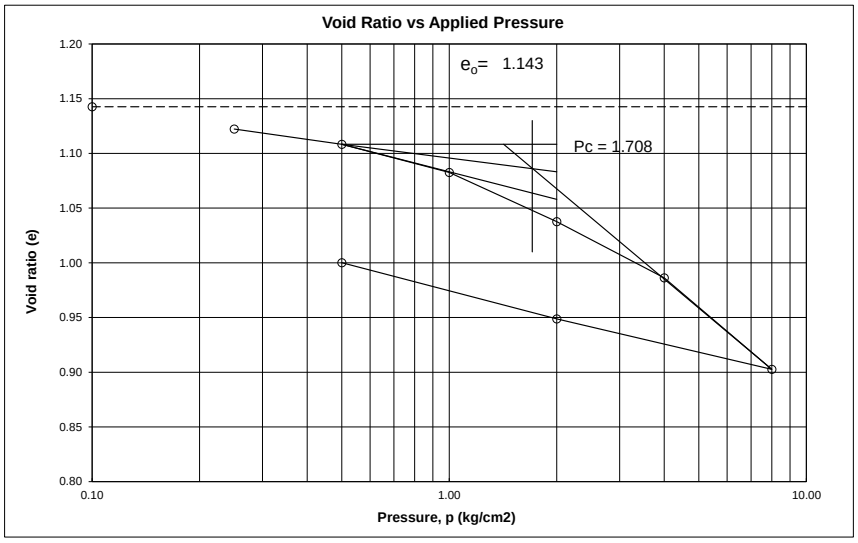

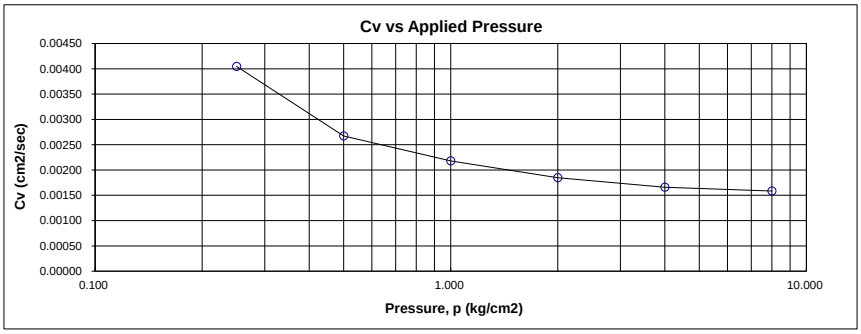

LABORATORIUM MEKANIKA TANAH
PT. SUWANDA KARYA MANDIRI
LSSM-045-IDN

CONSOLIDATION

ASTM D 2435

PROJECT : **Pembangunan Stasiun Pengamatan Permukaan Tanah**
BORING NO. : **SPPT-03**
DEPTH : **41.00 - 41.50 m**

TESTED BY : Faizal
DATE : 17/09/2021

LOCATION : **Kel. Tirto, Kec. Pekalongan Barat, Kota Pekalongan**
DESCRIPT. : **-**

APPARATUS MEASUREMENTS
CONTAINER HEIGHT : 2.000 cm
CONTAINER DIAMETER : 5.000 cm
CONTAINER AREA (A) : 19.635 cm2

SPECIFIC GRAVITY (Gs) : 2.6445
SOLIDS HEIGHT (Hs) IN cm : 1.060
Hs = Ws/(Gs.γ_w. A)

DEGREE OF SATURATION IN %
TEST START : 77.62
TEST END :

WATER CONTENT

	BEGINNING OF TEST		END OF TEST	
CONTAINER NO.	1A			
WT. CONTAINER + WET SOIL IN g	138.070			
WT. CONTAINER IN g	68.690			
WT. WET SOIL IN g	69.380			
WT. DRY SOIL (Ws) IN g	55.058			
WT. WATER (Ww) IN g	14.32			
WATER CONTENT (w) IN %	26.01			

APPLIED PRESSURE kg/cm^2	FINAL DIAL cm	DIAL CHANGE (ΔH) cm	Δe = ΔH/Hs	e = eo - ΣΔe	AVERAGE HEIGHT FOR LOAD cm	H cm	FITTING TIME (t 90) sec	Cv $\frac{0.848\ H^2}{t\ 90}$ cm^2/sec
0.00	0.9000			0.886	2.000			
		0.0840	0.0792			0.979	99.85	0.00814
0.25	0.8160			0.807	1.916			
		0.0500	0.0472			0.946	173.40	0.00437
0.50	0.7660			0.760	1.866			
		0.0750	0.0707			0.914	214.33	0.00331
1.00	0.6910			0.689	1.791			
		0.0910	0.0858			0.873	247.25	0.00261
2.00	0.6000			0.603	1.700			
		0.0840	0.0792			0.829	267.13	0.00218
4.00	0.5160			0.524	1.616			
		0.1020	0.0962			0.783	259.58	0.00200
8.00	0.4140			0.428	1.514			
		0.0310	0.0292			0.765		
2.00	0.4450			0.457	1.545			
		0.0450	0.0424			0.784		
0.50	0.4900			0.500	1.590			

LABORATORIUM MEKANIKA TANAH
PT. SUWANDA KARYA MANDIRI
Komp. Bumi Asri Mekar Rahayu Blok II No. B-7, Kopo Bandung (40218)
Telp. (022 - 5417700) Fax. (022 - 5412700)
email : pt_suwanda_karya_mandiri@yahoo.com

CONSOLIDATION

ASTM D 2435

PROJECT	: Pembangunan Stasiun Pengamatan Permukaan Tanah			
LOCATION	: Kel. Tirto, Kec. Pekalongan Barat, Kota Pekalongan			
BORING NO.	: SPPT-03	Coefficient of Consolidation (Cv)	: 0.00253	cm^2/sec
DEPTH	: 41.00 - 41.50 m	Compression Index (Cc)	: 0.320	
TESTED BY	: Faizal	Swell Index (Cs)	: 0.048	
DATE	: 17/09/2021	Coeff. of Volume Comp. (mv)	: 0.074	cm^2/kg
DESCRIPTION	: -			

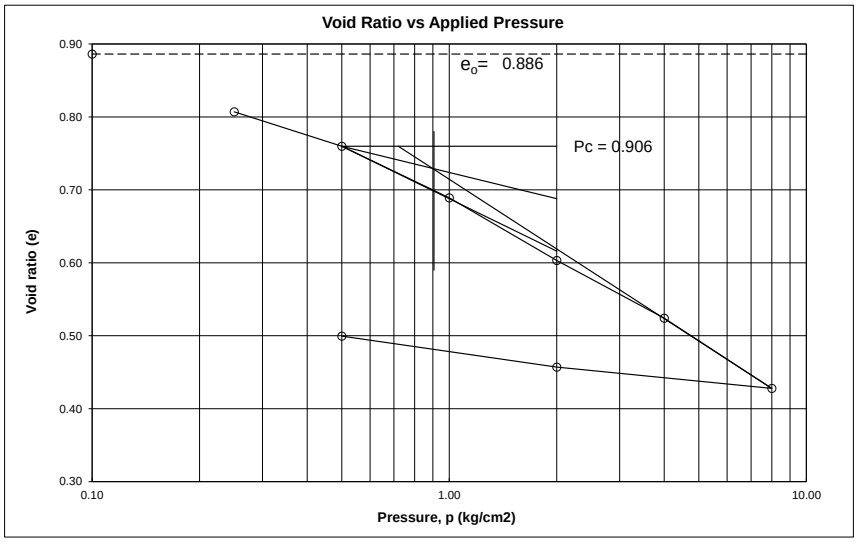

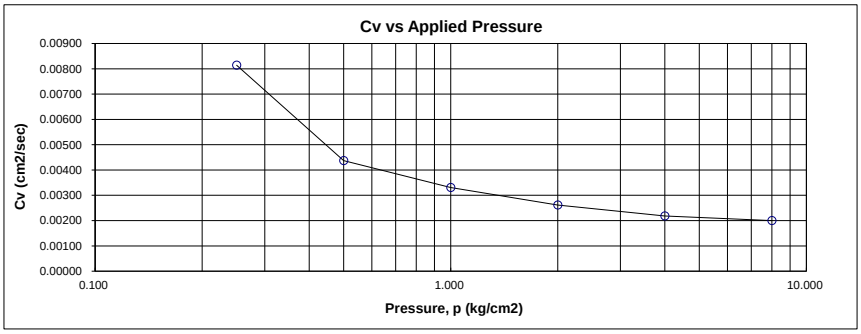

LABORATORIUM MEKANIKA TANAH
PT. SUWANDA KARYA MANDIRI
Komp. Buni Asri Mekar Rahayu Blok II No. B-7, Kopo Bandung (40219)
Telp. (022 - 5417700) Fax. (022 - 5412700)
email : pt_suwanda_karya_mandiri@yahoo.com

CONSOLIDATION TEST

PROJECT : **Pembangunan Stasiun Pengamatan Penurunan Permukaan Tanah**
BORING NO. : **SPPT-07**
DEPTH : **7.00 - 7.50 m**

TESTED BY : Faizal
DATE : 12/08/2021

LOCATION : **Ds. Wonokerto Kulon, Kec. Wonokerto, Kab. Pekalongan**
DESCRIPT. : **UDS**

APPARATUS MEASUREMENTS
CONTAINER HEIGHT : 2.000 cm
CONTAINER DIAMETER : 5.000 cm
CONTAINER AREA (A) : 19.635 cm2

SPECIFIC GRAVITY (Gs) : 2.6316

SOLIDS HEIGHT (Hs) IN cm : 0.798
Hs = Ws/(Gs.γ_w. A)

DEGREE OF SATURATION IN %
TEST START : 111.62
TEST END :

WATER CONTENT

	BEGINNING OF TEST			
CONTAINER NO.	3B			
WT. CONTAINER + WET SOIL IN g	131.460			
WT. CONTAINER IN g	63.870			
WT. WET SOIL IN g	67.590			
WT. DRY SOIL (Ws) IN g	41.258			
WT. WATER (Ww) IN g	26.33			
WATER CONTENT (w) IN %	63.82			

APPLIED PRESSURE kg/cm^2	FINAL DIAL cm	DIAL CHANGE (ΔH) cm	$\Delta e = \Delta H/Hs$	$e = eo - \Sigma\Delta e$	AVERAGE HEIGHT FOR LOAD cm	H cm	FITTING TIME (t 90) sec	Cv $\frac{0.848\ H^2}{t\ 90}$ cm^2/sec
0.00	0.9000			1.505	2.000			
		0.2510	0.3143			0.937	440.65	0.00169
0.25	0.6490			1.190	1.749			
		0.0900	0.1127			0.852	649.45	0.00095
0.50	0.5590			1.078	1.659			
		0.0960	0.1202			0.806	808.13	0.00068
1.00	0.4630			0.957	1.563			
		0.1030	0.1290			0.756	880.13	0.00055
2.00	0.3600			0.828	1.460			
		0.1050	0.1315			0.704	917.29	0.00046
4.00	0.2550			0.697	1.355			
		0.1200	0.1503			0.648	848.26	0.00042
8.00	0.1350			0.547	1.235			
		0.0350	0.0438			0.626		
2.00	0.1700			0.591	1.270			
		0.0450	0.0564			0.646		
0.50	0.2150			0.647	1.315			

LABORATORIUM MEKANIKA TANAH
PT. SUWANDA KARYA MANDIRI
Komp. Bumi Asri Mekar Rahayu Blok II No. B-7, Kopo Bandung (40218)
Telp. (022 - 5417700) Fax. (022 - 5412700)
email : pt_suwanda_karya_mandiri@yahoo.com

CONSOLIDATION TEST

PROJECT	: Pembangunan Stasiun Pengamatan Penurunan Permukaan Tanah			
LOCATION	: Ds. Wonokerto Kulon, Kec. Wonokerto, Kab. Pekalongan			
BORING NO.	: SPPT-07	Coefficient of Consolidation (Cv)	: 0.00053	cm^2/sec
DEPTH	: 7.00 - 7.50 m	Compression Index (Cc)	: 0.499	
TESTED BY	: Faizal	Swell Index (Cs)	: 0.067	
DATE	: 12/08/2021	Coeff. of Volume Comp. (mv)	: 0.158	cm^2/kg
DESCRIPTION	: UDS			

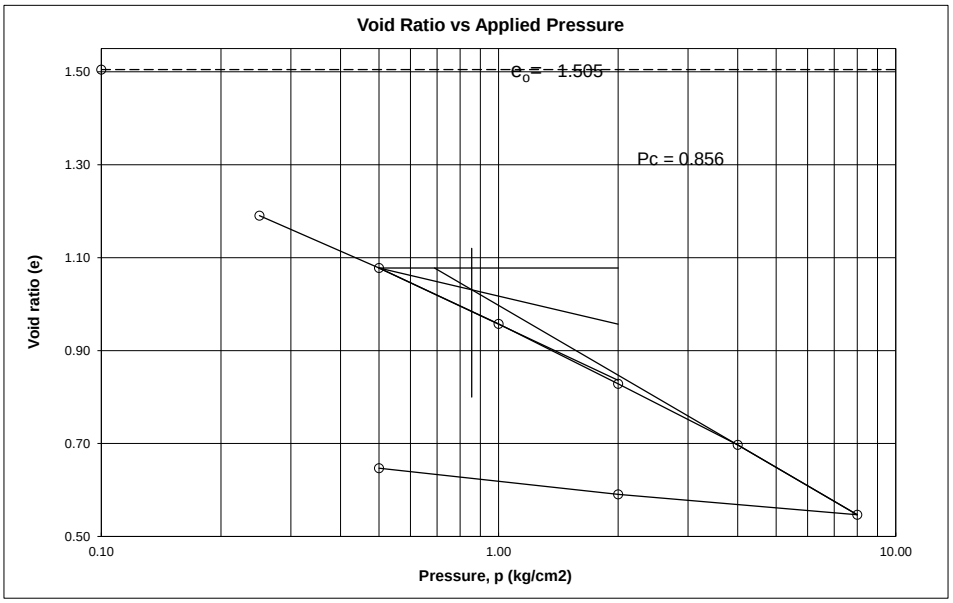

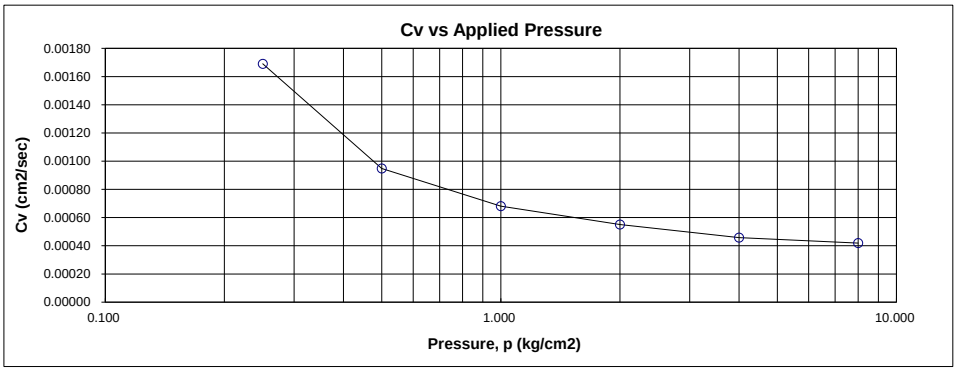

LABORATORIUM MEKANIKA TANAH
PT. SUWANDA KARYA MANDIRI
Komp. Buni Asri Mekar Rahayu Blok II No. B-7, Kopo Bandung (40219)
Telp. (022 - 5417700) Fax. (022 - 5412700)
email : pt_suwanda_karya_mandiri@yahoo.com

CONSOLIDATION TEST

PROJECT : **Pembangunan Stasiun Pengamatan Penurunan Permukaan Tanah**
BORING NO. : **SPPT-07**
DEPTH : **15.00 - 15.50 m**

TESTED BY : Faizal
DATE : 12/08/2021

LOCATION : **Ds. Wonokerto Kulon, Kec. Wonokerto, Kab. Pekalongan**
DESCRIPT. : **UDS**

APPARATUS MEASUREMENTS
CONTAINER HEIGHT : 2.000 cm
CONTAINER DIAMETER : 5.000 cm
CONTAINER AREA (A) : 19.635 cm2

SPECIFIC GRAVITY (Gs) : 2.5870
SOLIDS HEIGHT (Hs) IN cm : 0.651
Hs = Ws/(Gs.γ_w. A)

DEGREE OF SATURATION IN %
TEST START : 107.88
TEST END :

WATER CONTENT	BEGINNING OF TEST	END OF TEST		
CONTAINER NO.	4B			
WT. CONTAINER + WET SOIL IN g	119.310			
WT. CONTAINER IN g	57.670			
WT. WET SOIL IN g	61.640			
WT. DRY SOIL (Ws) IN g	33.066			
WT. WATER (Ww) IN g	28.57			
WATER CONTENT (w) IN %	86.42			

APPLIED PRESSURE kg/cm^2	FINAL DIAL cm	DIAL CHANGE (ΔH) cm	Δe = ΔH/Hs	e = eo - ΣΔe	AVERAGE HEIGHT FOR LOAD cm	H cm	FITTING TIME (t 90) sec	Cv $\frac{0.848\ H^2}{t\ 90}$ cm^2/sec
0.00	0.9000			2.072	2.000			
		0.2370	0.3641			0.941	917.29	0.00082
0.25	0.6630			1.708	1.763			
		0.0860	0.1321			0.860	1308.53	0.00048
0.50	0.5770			1.576	1.677			
		0.1000	0.1536			0.814	1536.22	0.00037
1.00	0.4770			1.423	1.577			
		0.1100	0.1690			0.761	1616.17	0.00030
2.00	0.3670			1.254	1.467			
		0.1010	0.1552			0.708	1616.17	0.00026
4.00	0.2660			1.098	1.366			
		0.1200	0.1843			0.653	1572.86	0.00023
8.00	0.1460			0.914	1.246			
		0.0490	0.0753			0.635		
2.00	0.1950			0.989	1.295			
		0.0540	0.0830			0.661		
0.50	0.2490			1.072	1.349			

LABORATORIUM MEKANIKA TANAH
PT. SUWANDA KARYA MANDIRI
Komp. Bumi Asri Mekar Rahayu Blok II No. B-7, Kopo Bandung (40218)
Telp. (022 - 5417700) Fax. (022 - 5412700)
email : pt_suwanda_karya_mandiri@yahoo.com

CONSOLIDATION TEST

PROJECT	: Pembangunan Stasiun Pengamatan Penurunan Permukaan Tanah			
LOCATION	: Ds. Wonokerto Kulon, Kec. Wonokerto, Kab. Pekalongan			
BORING NO.	: SPPT-07	Coefficient of Consolidation (Cv)	: 0.00029	cm^2/sec
DEPTH	: 15.00 - 15.50 m	Compression Index (Cc)	: 0.612	
TESTED BY	: Faizal	Swell Index (Cs)	: 0.105	
DATE	: 12/08/2021	Coeff. of Volume Comp. (mv)	: 0.152	cm^2/kg
DESCRIPTION	: UDS			

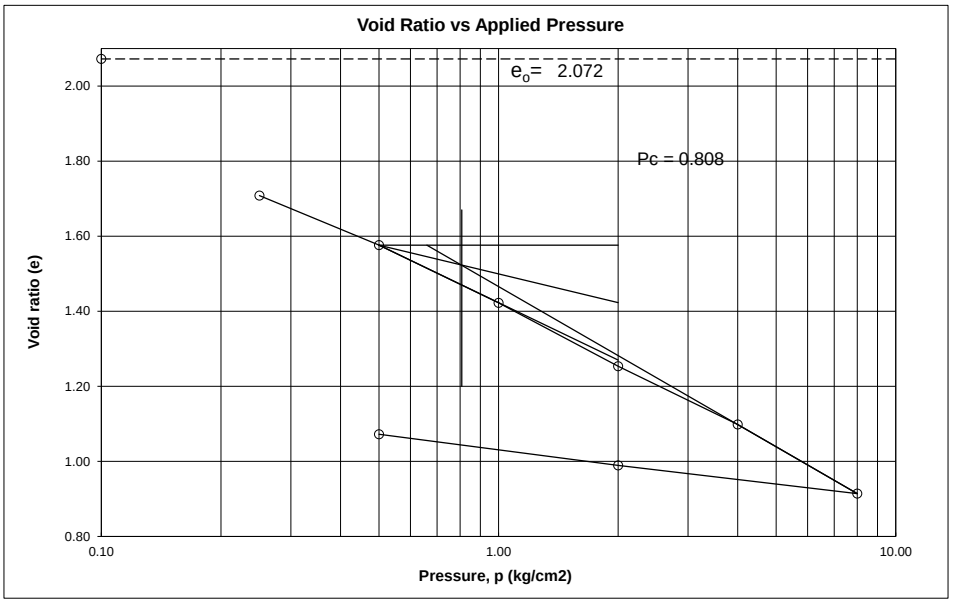

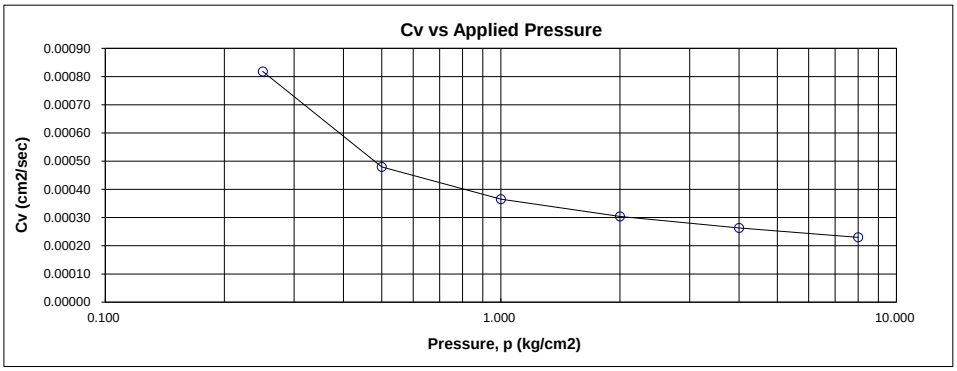

LABORATORIUM MEKANIKA TANAH
PT. SUWANDA KARYA MANDIRI
Komp. Buni Asri Mekar Rahayu Blok II No. B-7, Kopo Bandung (40219)
Telp. (022 - 5417700) Fax. (022 - 5412700)
email : pt_suwanda_karya_mandiri@yahoo.com

LSSM-045-IDN

CONSOLIDATION TEST

PROJECT : **Pembangunan Stasiun Pengamatan Penurunan Permukaan Tanah**
BORING NO. : **SPPT-07**
DEPTH : **23.00 - 23.50 m**

TESTED BY : Faizal
DATE : 12/08/2021

LOCATION : **Ds. Wonokerto Kulon, Kec. Wonokerto, Kab. Pekalongan**
DESCRIPT. : **UDS**

APPARATUS MEASUREMENTS
CONTAINER HEIGHT : 2.000 cm
CONTAINER DIAMETER : 5.000 cm
CONTAINER AREA (A) : 19.635 cm2

SPECIFIC GRAVITY (Gs) : 2.6236

SOLIDS HEIGHT (Hs) IN cm : 0.720
Hs = Ws/(Gs.γ_w. A)

DEGREE OF SATURATION IN %
TEST START : 80.43
TEST END :

WATER CONTENT

	BEGINNING OF TEST			
CONTAINER NO.	1D			
WT. CONTAINER + WET SOIL IN g	123.120			
WT. CONTAINER IN g	65.800			
WT. WET SOIL IN g	57.320			
WT. DRY SOIL (Ws) IN g	37.113			
WT. WATER (Ww) IN g	20.21			
WATER CONTENT (w) IN %	54.45			

APPLIED PRESSURE kg/cm^2	FINAL DIAL cm	DIAL CHANGE (ΔH) cm	Δe = ΔH/Hs	e = eo - ΣΔe	AVERAGE HEIGHT FOR LOAD cm	H cm	FITTING TIME (t 90) sec	Cv $\frac{0.848\ H^2}{t\ 90}$ cm^2/sec
0.00	0.9000			1.776	2.000			
		0.0540	0.0750			0.987	440.65	0.00187
0.25	0.8460			1.701	1.946			
		0.0410	0.0569			0.963	685.46	0.00115
0.50	0.8050			1.644	1.905			
		0.0440	0.0611			0.942	812.54	0.00093
1.00	0.7610			1.583	1.861			
		0.0590	0.0819			0.916	866.40	0.00082
2.00	0.7020			1.501	1.802			
		0.0810	0.1124			0.881	889.35	0.00074
4.00	0.6210			1.389	1.721			
		0.0900	0.1249			0.838	848.26	0.00070
8.00	0.5310			1.264	1.631			
		0.0100	0.0139			0.818		
2.00	0.5410			1.278	1.641			
		0.0260	0.0361			0.827		
0.50	0.5670			1.314	1.667			

LABORATORIUM MEKANIKA TANAH
PT. SUWANDA KARYA MANDIRI
Komp. Bumi Asri Mekar Rahayu Blok II No. B-7, Kopo Bandung (40218)
Telp. (022 - 5417700) Fax. (022 - 5412700)
email : pt_suwanda_karya_mandiri@yahoo.com

CONSOLIDATION TEST

PROJECT	: Pembangunan Stasiun Pengamatan Penurunan Permukaan Tanah			
LOCATION	: Ds. Wonokerto Kulon, Kec. Wonokerto, Kab. Pekalongan			
BORING NO.	: SPPT-07	Coefficient of Consolidation (Cv)	: 0.00080	cm^2/sec
DEPTH	: 23.00 - 23.50 m	Compression Index (Cc)	: 0.415	
TESTED BY	: Faizal	Swell Index (Cs)	: 0.033	
DATE	: 12/08/2021	Coeff. of Volume Comp. (mv)	: 0.051	cm^2/kg
DESCRIPTION	: UDS			

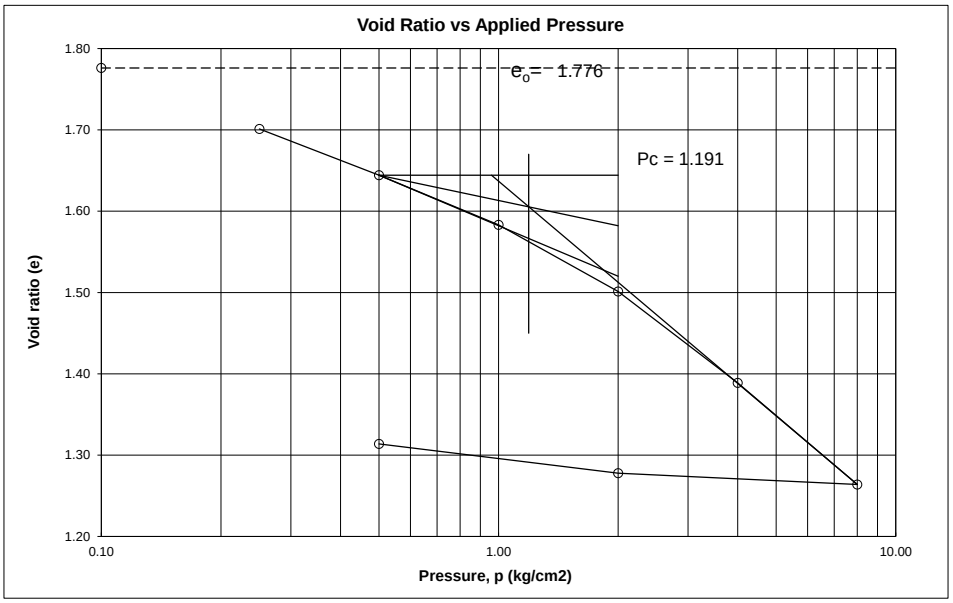

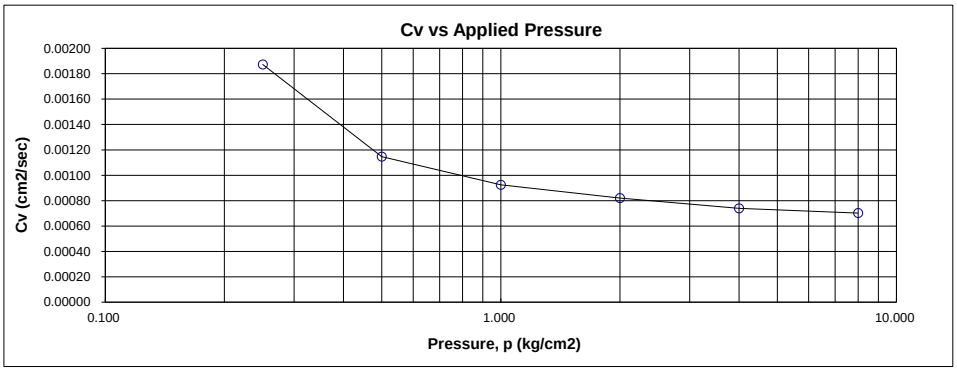

LABORATORIUM MEKANIKA TANAH
PT. SUWANDA KARYA MANDIRI
Komp. Buni Asri Mekar Rahayu Blok II No. B-7, Kopo Bandung (40219)
Telp. (022 - 5417700) Fax. (022 - 5412700)
email : pt_suwanda_karya_mandiri@yahoo.com

CONSOLIDATION TEST

PROJECT : **Pembangunan Stasiun Pengamatan Penurunan Permukaan Tanah**
BORING NO. : **SPPT-07**
DEPTH : **31.00 - 31.50 m**

TESTED BY : Faizal
DATE : 12/08/2021

LOCATION : **Ds. Wonokerto Kulon, Kec. Wonokerto, Kab. Pekalongan**
DESCRIPT. : **UDS**

APPARATUS MEASUREMENTS
CONTAINER HEIGHT : 2.000 cm
CONTAINER DIAMETER : 5.000 cm
CONTAINER AREA (A) : 19.635 cm2

SPECIFIC GRAVITY (Gs) : 2.6217

SOLIDS HEIGHT (Hs) IN cm : 1.031
Hs = Ws/(Gs.γ_w. A)

DEGREE OF SATURATION IN %
TEST START : 141.95
TEST END :

WATER CONTENT	BEGINNING OF TEST	END OF TEST		
CONTAINER NO.	2D			
WT. CONTAINER + WET SOIL IN g	137.120			
WT. CONTAINER IN g	57.040			
WT. WET SOIL IN g	80.080			
WT. DRY SOIL (Ws) IN g	53.072			
WT. WATER (Ww) IN g	27.01			
WATER CONTENT (w) IN %	50.89			

APPLIED PRESSURE kg/cm^2	FINAL DIAL cm	DIAL CHANGE (ΔH) cm	$\Delta e = \Delta H/Hs$	e = eo - $\Sigma\Delta e$	AVERAGE HEIGHT FOR LOAD cm	H cm	FITTING TIME (t 90) sec	Cv $\frac{0.848\ H^2}{t\ 90}$ cm^2/sec
0.00	0.9000			0.940	2.000			
		0.1000	0.0970			0.975	314.65	0.00256
0.25	0.8000			0.843	1.900			
		0.0530	0.0514			0.937	508.09	0.00146
0.50	0.7470			0.791	1.847			
		0.0680	0.0660			0.907	649.45	0.00107
1.00	0.6790			0.726	1.779			
		0.0810	0.0786			0.869	735.00	0.00087
2.00	0.5980			0.647	1.698			
		0.0870	0.0844			0.827	781.93	0.00074
4.00	0.5110			0.563	1.611			
		0.1000	0.0970			0.781	747.65	0.00069
8.00	0.4110			0.466	1.511			
		0.0260	0.0252			0.762		
2.00	0.4370			0.491	1.537			
		0.0350	0.0339			0.777		
0.50	0.4720			0.525	1.572			

LABORATORIUM MEKANIKA TANAH
PT. SUWANDA KARYA MANDIRI
Komp. Bumi Asri Mekar Rahayu Blok II No. B-7, Kopo Bandung (40218)
Telp. (022 - 5417700) Fax. (022 - 5412700)
email : pt_suwanda_karya_mandiri@yahoo.com

CONSOLIDATION TEST

PROJECT	: Pembangunan Stasiun Pengamatan Penurunan Permukaan Tanah			
LOCATION	: Ds. Wonokerto Kulon, Kec. Wonokerto, Kab. Pekalongan			
BORING NO.	: SPPT-07	Coefficient of Consolidation (Cv)	: 0.00084	cm^2/sec
DEPTH	: 31.00 - 31.50 m	Compression Index (Cc)	: 0.322	
TESTED BY	: Faizal	Swell Index (Cs)	: 0.039	
DATE	: 12/08/2021	Coeff. of Volume Comp. (mv)	: 0.079	cm^2/kg
DESCRIPTION	: UDS			

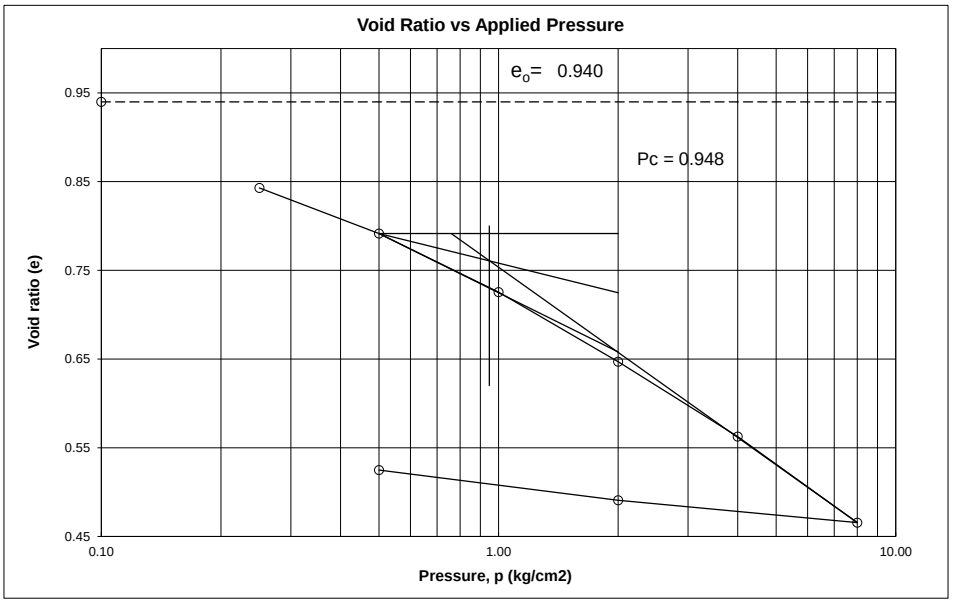

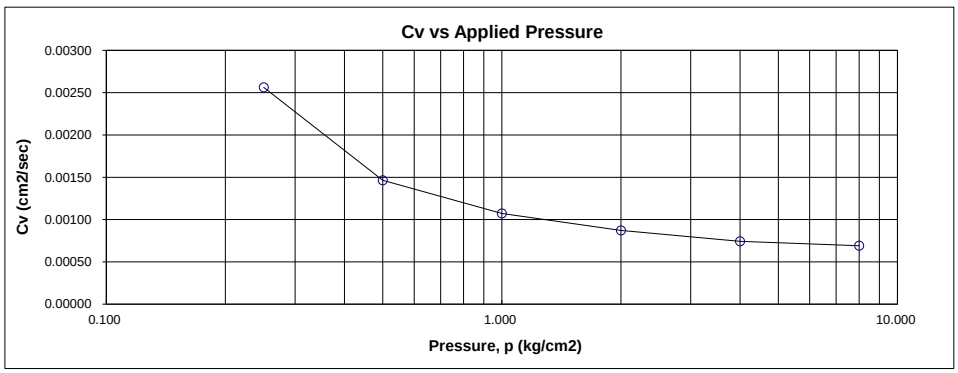

LABORATORIUM MEKANIKA TANAH
PT. SUWANDA KARYA MANDIRI
Komp. Buni Asri Mekar Rahayu Blok II No. B-7, Kopo Bandung (40219)
Telp. (022 - 5417700) Fax. (022 - 5412700)
email : pt_suwanda_karya_mandiri@yahoo.com

LSSM-045-IDN

CONSOLIDATION TEST

PROJECT : **Pembangunan Stasiun Pengamatan Penurunan Permukaan Tanah**
BORING NO. : **SPPT-07**
DEPTH : **39.00 - 39.50 m**

TESTED BY : Faizal
DATE : 12/08/2021

LOCATION : **Ds. Wonokerto Kulon, Kec. Wonokerto, Kab. Pekalongan**
DESCRIPT. : **UDS**

APPARATUS MEASUREMENTS
CONTAINER HEIGHT : 2.000 cm
CONTAINER DIAMETER : 5.000 cm
CONTAINER AREA (A) : 19.635 cm2

SPECIFIC GRAVITY (Gs) : 2.6133

SOLIDS HEIGHT (Hs) IN cm : 0.752
Hs = Ws/(Gs.γ_w. A)

DEGREE OF SATURATION IN %
TEST START : 95.98
TEST END :

WATER CONTENT	BEGINNING OF TEST	END OF TEST		
CONTAINER NO.	3D			
WT. CONTAINER + WET SOIL IN g	124.470			
WT. CONTAINER IN g	62.370			
WT. WET SOIL IN g	62.100			
WT. DRY SOIL (Ws) IN g	38.576			
WT. WATER (Ww) IN g	23.52			
WATER CONTENT (w) IN %	60.98			

APPLIED PRESSURE kg/cm^2	FINAL DIAL cm	DIAL CHANGE (ΔH) cm	Δe = ΔH/Hs	e = eo - ΣΔe	AVERAGE HEIGHT FOR LOAD cm	H cm	FITTING TIME (t 90) sec	Cv $\frac{0.848\ H^2}{t\ 90}$ cm^2/sec
0.00	0.9000			1.660	2.000			
		0.0900	0.1197			0.978	348.49	0.00233
0.25	0.8100			1.541	1.910			
		0.0290	0.0386			0.948	572.89	0.00133
0.50	0.7810			1.502	1.881			
		0.0380	0.0505			0.931	747.65	0.00098
1.00	0.7430			1.451	1.843			
		0.0720	0.0958			0.904	799.35	0.00087
2.00	0.6710			1.356	1.771			
		0.1070	0.1423			0.859	812.54	0.00077
4.00	0.5640			1.213	1.664			
		0.1270	0.1689			0.800	760.42	0.00071
8.00	0.4370			1.044	1.537			
		0.0370	0.0492			0.778		
2.00	0.4740			1.094	1.574			
		0.0230	0.0306			0.793		
0.50	0.4970			1.124	1.597			

LABORATORIUM MEKANIKA TANAH
PT. SUWANDA KARYA MANDIRI
Komp. Bumi Asri Mekar Rahayu Blok II No. B-7, Kopo Bandung (40218)
Telp. (022 - 5417700) Fax. (022 - 5412700)
email : pt_suwanda_karya_mandiri@yahoo.com

CONSOLIDATION TEST

PROJECT	: Pembangunan Stasiun Pengamatan Penurunan Permukaan Tanah			
LOCATION	: Ds. Wonokerto Kulon, Kec. Wonokerto, Kab. Pekalongan			
BORING NO.	: SPPT-07	Coefficient of Consolidation (Cv)	: 0.00083	cm^2/sec
DEPTH	: 39.00 - 39.50 m	Compression Index (Cc)	: 0.561	
TESTED BY	: Faizal	Swell Index (Cs)	: 0.053	
DATE	: 12/08/2021	Coeff. of Volume Comp. (mv)	: 0.062	cm^2/kg
DESCRIPTION	: UDS